Molecular aspects of antibody mediated T cell activation

Sara Hannah Morgan
Linacre College

Thesis submitted for the degree of Doctor of Philosophy
Trinity Term, 2009

Abstract

Molecular aspects of antibody mediated T cell activation

Sara Hannah Morgan, Linacre College
Submitted for the degree of Doctor of Philosophy
Trinity term, 2009

The normal physiological activation of naive T cells requires the engagement of both the T cell receptor (TCR) and the co-stimulatory molecule, CD28. However, a group of monoclonal antibodies (mAbs) have been identified that are able to activate T cells *in vitro* and *in vivo* via CD28 engagement alone. Two defining characteristics found in all CD28 superagonist mAbs are their membrane proximal CD28 epitopes and the requirement for mAb immobilisation. To investigate whether agonistic mAbs to similar cell molecules could be identified based on epitope position alone, mAbs to the inhibitory receptor PD-1 were generated and characterised. Using a drastic mutation-based epitope mapping technique, one mAb was identified with a membrane proximal epitope along with two other mAbs with membrane distal epitopes. These mAbs were tested for triggering activity in a hybridoma stimulation assay. mAb stimulation was observed with all three mAbs but only in cells expressing a PD-1 chimera that associated with the TCR and the strength of activation was dependent on epitope location. Cross-linking of a monomeric PD-1/CD28 chimera with a pair of anti-PD-1 mAbs resulted in signalling in this system, however, suggesting a role for ligand aggregation in addition to epitope position in mAb signalling. To further investigate the role of epitope position in CD28 superagonism, a cell line expressing a chimeric form of CD28 was created wherein the superagonistic mAb epitope was moved to a membrane distal position. When stimulated with a CD28 superagonist mAb signalling was no longer observed. However stimulation with another mAb that had an epitope to a membrane proximal location on the chimera resulted in superagonistic effect. These results show that epitope location is the dominant cause of T cell stimulation observed by CD28 superagonist mAbs and that epitope dependent mAb signalling is possible in other T cell surface molecules. The work described in this thesis has implications for both the development of immune modulating mAb therapeutics and for the general mechanism of triggering of cell surface receptors dependent on extrinsic tyrosine kinases.

Acknowledgements

A thesis cannot be completed without the help of a great number of people.

My first thanks go to Dr. John Young for supplying me with a very interesting monoclonal antibody, which yielded some intriguing results. My thanks also to Neale Banarji for letting me use a number of his proteins as controls for SPR analysis, and for answering my many questions about their construction.

The skills I have learned during my time in the Davis Lab I owe to the great support and help of all members of the lab, both past and present. I have had some great times and made firm friendships. In particular I would like to thank Mai Vuong for her patience in teaching me the ropes in the initial days of my D.Phil, Jan Fennelly, Heather Brouwer and Josh Moorhouse for help with many of my numerous constructs and flow cytometry analysis. Thanks also go to John James and Claire Jessup who gave me enormous support and advice, both while they were in the lab and also from the far flung corners of the world where they now work. Thank you to Ed Evans who taught me all about the wonderful world of BIAcore, and thank you to Dave Sleep for being a wealth of information about all things pure immunology.

To Simon Davis, my supervisor, who gave me the wonderful opportunity to come to Oxford: thank you for the time, support, patience and guidance you have given me. The high standards you set make you a great scientist and I have learned an immense amount from being part of your lab.

My final thanks go to my family and friends. Tom, your love and support has been immeasurable during the hardest times. Thank you with all my heart. To my parents who always supported me throughout the highs and lows and never questioned my ability. To Catrin, my sister, thanks for being down the end of the phone and a good distraction when I needed it. Thanks also go to my many friends, both at Linacre College and The Weatherall Insitiute of Molecular Medicine, with whom I have spent many a happy time.

This thesis was typeset with LaTeX 2_ϵ, using the following packages: amssymb, booktabs, cite, caption, chemarr, color, fancyhdr, graphicx, listings, longtable, lscape, rotating, subfigure and tocbibind. The Palatino®, Optima®, PazoMath and Courier® typefaces are used throughout.

Contents

Abstract i

Acknowledgements ii

Contents iii

List of Figures vii

Abbreviations ix

1 Introduction 1
- 1.1 Overview . . . 1
- 1.2 The adaptive immune response . . . 2
  - 1.2.1 B cell mediated immunity . . . 3
  - 1.2.2 T cell mediated immunity . . . 8
- 1.3 TCR triggering . . . 20
  - 1.3.1 The TCR complex . . . 20
  - 1.3.2 TCR complex signalling . . . 22
- 1.4 The immunological synapse . . . 27
- 1.5 Models of T cell activation . . . 31
  - 1.5.1 Conformational change models . . . 31
  - 1.5.2 Aggregation models . . . 36
  - 1.5.3 Segregation models . . . 39
- 1.6 CD28 . . . 45
  - 1.6.1 CD28 function and structure . . . 46
  - 1.6.2 CD28 signalling . . . 48
  - 1.6.3 CD28 superagonist antibodies . . . 50
- 1.7 PD-1 . . . 55
  - 1.7.1 PD-1 expression . . . 55
  - 1.7.2 PD-1 function . . . 56
  - 1.7.3 PD-1 structure and signalling . . . 59
- 1.8 Aims of this thesis . . . 61
  - 1.8.1 Investigation of epitope dependent mAb signalling by PD-1 . . . 61
  - 1.8.2 Investigation into the mechanism of CD28 superagonism . . . 62

2 General Methods 63
- 2.1 Molecular cloning and vector construction . . . 63
  - 2.1.1 Molecular cloning overview . . . 63
  - 2.1.2 Vectors used in this thesis . . . 63
  - 2.1.3 Molecular biological methods . . . 66
- 2.2 Cell Culture . . . 75

2.2.1 Cell lines used in this thesis . . . 75
2.2.2 General culture techniques . . . 76
2.2.3 Tissue culture media . . . 78
2.3 Protein purification . . . 79
2.3.1 High performance liquid chromatography . . . 79
2.3.2 Polyacrylamide gels . . . 79
2.4 Phenotypic analysis . . . 81
2.4.1 Flow cytometry and analysis . . . 81
2.4.2 Confocal microscopy . . . 82
2.5 Bioluminescence Resonance Energy Transfer . . . 83

3 Characterisation of human PD-1 mAbs 86
3.1 Introduction . . . 86
3.1.1 Epitope location and mitogenic potential of CD28 superagonistic antibodies . . . 86
3.1.2 Superagonism applied to PD-1 . . . 87
3.2 Materials and Methods . . . 89
3.2.1 Anti-human PD-1 mAb hybridoma generation . . . 89
3.2.2 Antibody purification . . . 90
3.2.3 PD-1 ELISA . . . 91
3.2.4 Epitope mapping . . . 92
3.2.5 Surface plasmon resonance . . . 97
3.2.6 Deglycosylation of PD-1/Fc . . . 98
3.2.7 Western blotting . . . 99
3.3 Results . . . 100
3.3.1 Generation of human PD-1 mAbs 10, 19 and 29 . . . 100
3.3.2 Purificiation of PD-1 mAbs 10, 19 and 29 . . . 101
3.3.3 Epitope mapping of human PD-1 mAbs . . . 107
3.3.4 PD-1 mAb binding kinetics . . . 121
3.3.5 Generation and characterisation of PD-1 mAb 2 . . . 123
3.4 Discussion . . . 134
3.4.1 Summary of findings . . . 134
3.4.2 Predictions of superagonism by epitope mapping . . . 135
3.4.3 PD-1 mAb 29 . . . 136
3.4.4 Superagonism and antibody binding affinities . . . 137

4 Superagonistic signalling by PD-1 monoclonal antibodies 138
4.1 Introduction . . . 138
4.1.1 PD-1 superagonistic monoclonal antibodies . . . 138
4.1.2 Assays for superagonism . . . 139
4.2 Materials and methods . . . 140
4.2.1 Generation of chimeric cell lines . . . 140
4.2.2 Construction of hybridoma cell lines . . . 151
4.2.3 BRET analysis . . . 153

4.2.4 Confocal microscopy . . . 153
4.2.5 Antibody stimulation assay . . . 153
4.2.6 IL-2 ELISA . . . 154
4.3 Results . . . 156
4.3.1 CD28 superagonism assay . . . 156
4.3.2 PD-1_{EX}CD$28_{TM/CYT}$ cell line is not triggered by PD-1 mAbs . . . 163
4.3.3 The generation of hPD-1 dimeric constructs . . . 170
4.3.4 PD-1_{EX}CD28_{TM}CD$3\zeta_{CYT}$ chimeras are unresponsive to all mAb stimulation . . . 175
4.3.5 Activation of the PD-1_{EX}CD$3\zeta_{ST/TM}$CD28_{CYT} cell line by PD-1 mAbs 179
4.3.6 PD-1_{EX}CD$3\zeta_{ST/TM/CYT}$ cell lines are not activated by PD-1 mAbs . . 185
4.3.7 Stimulation of the PD-1_{EX}CD$28_{TM/CYT}$ cell line by cross-linking . . 187
4.4 Discussion . . . 190
4.4.1 Summary of findings . . . 190
4.4.2 Applications of the CD28 superagonism assay . . . 191
4.4.3 The identification of correctly processed and presented cell surface proteins . . . 191
4.4.4 Strategies for the formation of dimeric chimeras . . . 192

5 Structural correlates of CD28 superagonism 194
5.1 Introduction . . . 194
5.1.1 The mechanism of CD28 superagonism . . . 194
5.1.2 Methods for the investigation of the mechanism of CD28 superagonism . . . 195
5.2 Materials and methods . . . 196
5.2.1 Generation of constructs . . . 196
5.2.2 Generation of hybridoma cell lines . . . 200
5.2.3 BRET . . . 201
5.2.4 Confocal microscopy . . . 202
5.2.5 Surface plasmon resonance . . . 202
5.2.6 Antibody stimulation assay . . . 203
5.2.7 ELISAs . . . 204
5.3 Results . . . 205
5.3.1 Manipulation of the CD28 stalk region in a rat/mouseCD28 chimera prevents expression . . . 205
5.3.2 Expression of CD28 lengthened by the insertion of a IgG Fc . . . 209
5.3.3 Supergonistic activity of JJ316 is not observed in the rCD28hFc_{EX}m CD$28_{TM/CYT}$ cell line . . . 214
5.3.4 Antibodies to the human IgG1 Fc domain are superagonistic in the rCD28hFc_{EX}mCD$28_{TM/CYT}$ cell line . . . 218
5.3.5 Cross-linking of the A57H mAb does not significantly contribute to its superagonistic properties . . . 227
5.4 Discussion . . . 231
5.4.1 Summary of findings . . . 231

5.4.2 IgG1 Fc mAbs 232
5.4.3 Strategies for the construction of large forms of CD28 233

6 General Discussion **235**
6.1 Current understanding of T cell activation 235
6.2 Results from this thesis 236
6.2.1 The triggering of chimeric receptors in cell lines using human PD-1 mAbs 236
6.2.2 The native PD-1 triggering properties of human PD-1 mAbs . . . 239
6.2.3 The application of PD-1 mAbs as immune modulating therapeutics 240
6.2.4 The mechanism of CD28 superagonism 243
6.3 Implications for T cell function 247
6.3.1 TCR complex signalling 247
6.3.2 CD28 superagonism - Further support for KS-based signalling? . 248

Bibliography **250**

List of Figures

1 Introduction **1**

1.1 Pathways initiated on T cell triggering 23
1.2 Conformational change models of T cell activation 34
1.3 Aggregation models of T cell activation 38
1.4 Segregation models of T cell activation 42
1.5 The mechanism of CD28 superagonism as predicted by the Kinetic Segregation Model 53

2 General Methods **63**

3 Characterisation of human PD-1 mAbs **86**

3.1 Concentration of PD-1 mAb in hybridoma tissue culture supernatants . 102
3.2 SDS page gels of mAb 10 Fractogel® EMD DEAE resin column elutions 103
3.3 Chromatogram and SDS page gel of purified mAb 10 105
3.4 PD-1 mAb binding ELISA 106
3.5 Mutational map of PD-1 108
3.6 PD-1 mAb 10, 19 and 29 flow cytometry epitope mapping assays 110
3.7 Epitopes of human PD-1 mAbs 10 and 19 112
3.8 SPR competition analysis of PD-1 mAbs with indirectly immobilised PD-1/Fc 114
3.9 SPR analysis of PD-1 mAbs binding to directly immobilised PD-1/Fc . 116
3.10 Investigation PD-1 mAb 29 sugar epitope 118
3.11 Western blot analysis of deglycosylated PD-1 with PD-1 monoclonal anitbodies 119
3.12 Human PD-1 mAb kinetics 122
3.13 Comparison of k_{off} and fits of kinetic data collected for mAbs 10, 19 and 29 124
3.14 Western blot of PD-1 mAb hybridoma 2 tissue culture supernatants . . 126
3.15 PD-1 mAb 2 binding ELISA 128
3.16 PD-1 mAb 2 flow cytometry epitope mapping assay 129
3.17 Epitopes of human PD-1 mAbs 2, 10 and 19 130
3.18 PD-1 mAb 2 mAb kinetics 132
3.19 Comparison of k_{off} and fits of kinetic data collected for mAb 2 133

4 Superagonistic signalling by PD-1 monoclonal antibodiese **138**

4.1 Construction and expression of $hCD28_{EX}mCD28_{TM/CYT}$ and $rCD28_{EX}mCD28_{TM/CYT}$ in DO11.10 T cell hybridomas 157
4.2 Confocal microscopy of $hCD28_{EX}mCD28_{TM/CYT}$, $rCD28_{EX}mCD28_{TM/CYT}$, $PD\text{-}1_{EX}CD28_{TM/CYT}$, hCD28 and hCTLA-4 expression in HEK 293T cells 158

4.3 BRET analysis of chimeric CD28 constructs . . . 160
4.4 CD28 superagonism . . . 161
4.5 CD28 co-stimulation . . . 162
4.6 PD-1_{EX}CD$28_{TM/CYT}$ expression . . . 165
4.7 PD-1_{EX}CD$28_{TM/CYT}$ surface expression . . . 166
4.8 PD-1_{EX}CD$28_{TM/CYT}$ superagonism and co-stimulation testing . . . 167
4.9 BRET analysis of the chimeric PD-1 construct . . . 168
4.10 Dimer construct diagrams . . . 169
4.11 Dimer construct expression . . . 173
4.12 BRET analysis of hPD-1/mCD28 chimeric dimers . . . 174
4.13 Dimer construct cell line expression and stimulation . . . 176
4.14 Constructs containing CD3ζ elements . . . 178
4.15 CD3ζ construct diagrams . . . 180
4.16 CD3ζ construct expression . . . 182
4.17 PD-1 mAb stimulation of CD3ζ constructs . . . 183
4.18 BRET analysis of CD3ζ containing PD-1 chimeras . . . 186
4.19 Cross-linking of the PD-1_{EX}CD$28_{TM/CYT}$ cell line . . . 189

5 Structural correlates of CD28 superagonism 194
5.1 rCD28_{EX}mCD$28_{TM/CYT}$L#Xconstruction . . . 206
5.2 Expression of CD28 extended stalk constructs . . . 208
5.3 Construction and expression of rCD28hFc_{EX}mCD$28_{TM/CYT}$ . . . 210
5.4 Expression of rCD28hFc_{EX}mCD$28_{TM/CYT}$ . . . 212
5.5 BRET analysis of rCD28hFc_{EX}mCD$28_{TM/CYT}$ . . . 213
5.6 CD28 superagonism KO in rCD28hFc_{EX}mCD$28_{TM/CYT}$ . . . 215
5.7 JJ316 is co-stimulatory in the rCD28hFc_{EX}mCD$28_{TM/CYT}$ cell line . . . 217
5.8 Rat CD28 and Human Fc specific mAb binding . . . 219
5.9 rmCD28Ig mAb binding . . . 222
5.10 Competition analysis of anti-human IgG1 mAb binding to directly immobilised BAFFR-Fc . . . 223
5.11 Superagonism observed with a titration of hIgG1 Fc mAbs A57H and F890 in the rCD28hFc_{EX}mCD$28_{TM/CYT}$ cell line . . . 225
5.12 A57H, HP6091 and F890 are co-stimulatory for the rCD28hFc_{EX}mCD$28_{TM/CYT}$ cell line . . . 226
5.13 Donkey anti-mouse IgG antibody also binds mouse IgM . . . 229
5.14 A57H is only superagonistic when immobilised . . . 230

6 General Discussion 235

Abbreviations

α-GalCer	α-galactosylceramide
ABTS	2,2′-azino-bis(3-ethylbenzthiazoline-6-sulphonic acid)
ADAP	Adhesion and Degranulation-promoting Adapter Protein
APC	Antigen Presenting Cell
BCR	B Cell Antigen Receptor
BRET	Bioluminescence Resonance Energy Transfer
CLIP	Class II-associated Invariant-chain Peptide
CMV	Cytomegalovirus
CTLA-4	Cytotoxic T Lymphocyte Antigen-4
Csk	C-terminus Src kinase
cSMAC	central SMAC
Da	Dalton
DAG	Diacylglycerol
DAPI	4′,6-diamidino-2-phenylindole
DNA	deoxyribonucleic Acid
dSMAC	distal SMAC
EAE	Experimental Autoimmune Encephalomyelitis
ELISA	Enzyme-Linked Immunosorbant Assay
emGFP	emerald GFP
ER	Endoplasmic Reticulum
F-actin	Filamentous actin
FACS	Fluorescence-activated Cell Sorting
FcR	Fc Antibody Receptor
FCS	Foetal Calf Serum
FPLC	Fast Performance Liquid Chromatography
FU	Fluorescence Units
Gads	GRB2-related Adaptor Downstream of Shc
GFP^2	Green Fluorescent Protein
GPCR	G-Protein Coupled Receptor
GRB-2	Growth actor Receptor-Bound protein 2
HCV	Hepatitis C Virus
HEK	Human Endothelial Kidney
HIV	Human Immunodeficiency Virus
HPK1	Hematopoietic Progenitor Kinase 1
ICOS	Inducible T cell Co-Stimulator
IE	Immediate Early
IEL	Intraepithelial Lymphocytes
IFN-γ	Interferon-γ
Ig	Immunoglobulin
IgSF	Immunoglobulin-domain Superfamily

Ii	Invarient Chain
IL	Interleukin
IP_3	Inositol 1,4,5-triphosphate
IRES	Internal Ribosome Entry Site
IS	Immunological Synapse
ITAM	Immunoreceptor Tyrosine based Activation Motif
ITIM	Immunoreceptor Tyrosine based Inhibitory Motif
ITSM	Immunoreceptor Tyrosine based Switch Motif
ItK	IL-2 induced Tyrosine Kinase
IVS	Intervening Sequence
JNK	c-Jun Kinase
K_d	Dissociation Constant
KS	Kinetic Segregation
LB broth	Luria Bertani broth
LAT	Linker for Activation of T Cells
Lck	Lymphocyte-specific Tyrosine Kinase
LCMV	Lymphocytic Choriomeningitis Virus
LTR	Long Terminal Repeat
LU	Luminescence Units
Luc	*Renilla* Luciferase
mAb	Monoclonal Antibody
MAPK	MAP Kinase
MEM	Minimal Essential Medium
MHC	Major Histocompatibility Complex
Nck1	Non-catalytic Region of Tyrosine Kinase Adaptor Protein 1
NF-κB	Nuclear Factor-κB
NK cell	Natural Killer cell
NKT cell	Natural Killer T cell
NOD	Non-obese Diabetic
pAPC	Professional APC
PAGE	Polyacrylamide Gel Electrophoresis
PBS	Phosphate-buffered Saline solution
PI3K	Phosphoinositide 3-Kinase
PIP_2	Phospholipid phophatidylinositol 4,5-bisphosphate
PKB	Protein Kinase B
PLCγ1	Phospholipase C γ1
p:MHC	Peptide-complexed Major Histocompatibility Complex
pSMAC	peripheral SMAC
Rac1	Ras related C3 botulinum toxin substrate 1
RasGRP	Ras Guanine Releasing Protein
RFU	Relative Fluorescence Units
RLU	Relative Luminescence Units
SDS	Sodium Dodecyl Sulphate
SFFV	Spleen Focus Forming Virus

SH2	Src Homology Domain 2
SLP-76	SH2 Domain-containing Leukocyte Protein, 76kDa
SMAC	Supramolecular Activation Cluster
SOS	Son Of Sevenless
SPR	Surface Plasmon Resonance
SV40	Simian vacuolating Virus 40
TAP	Transporters Associated With Antigen Processing
TBE	Tris-Borate EDTA
T_C cell	Cytotoxic T cell
TCR	T Cell Antigen Receptor
TEMED	N,N,N′,N′-tetramethylethylenediamine
T_H cell	Helper T cell
TIRFM	Total Internal Reflection Fluorescence Microscopy
TNF-α	Tumor Necrosis Factor-α
T_{reg} cell	Regulatory T cell
TSS	Transformation and Storage Solution
VSV-G	Vesicular Stomatitis Virus Envelope Protein G
WASp	Wiskott-Aldrich Syndrome protein
WPRE	Woodchuck hepatitis virus Post-transcriptional Regulatory Element
ZAP-70	ζ-chain Associated Protein, 70kDa

Chapter 1

Introduction

1.1 Overview

For the immune system to fullfill its function of protecting a host from disease, it must be able to detect disease causing agents and trigger an appropriate response. The many effector cells of the immune system that eliminate identified pathogens are specifically triggered by membrane bound receptors that have specificity for a pathogen antigen. While the majority of receptors involved in the initial activation and subsequent regulation of immune effector cells have been characterised, we are still elucidating the signalling pathways these immune receptors activate and the mechanisms by which they are initiated. By understanding these processes we will gain insight into the broader interactions of components of the immune system and also identify targets for therapeutics that modulate these systems.

This thesis looks at how monoclonal antibodies (mAbs) can be used to stimulate T cells in the absence of native immune ligands. Triggering mAbs have been used as reagents to investigate many aspects of T cell function *in vitro* and *in vivo*, and their triggering abilities have been harnessed by therapeutics for the treatment of a number of diseases. However the precise way these mAbs are able to trigger T cell surface receptors is unclear. In this thesis we investigate the mechanism of a specific group of T cell stimulatory mAbs, and see if our proposed mechanism of action can be applied

to other T cell surface signalling molecules.

In this introductory chapter the adaptive immune response will be reviewed, looking in particular at the important role T cells play in mediating cell based immunity, and key molecules that modulate and control their activity. It will also review the current models and theories of T cell activation and introduce two key molecules involved in T cell activation and control, CD28 and PD-1, which are the focus of investigation in this thesis.

1.2 The adaptive immune response

The various defence systems that are orchestrated by the immune system of higher vertebrates depend on the capacity to identify and respond to pathogens. In response to the diverse range of infectious agents that challenge the immune system, it has evolved two distinct but interconnecting arms. The first arm, the innate immune system, provides the early stages of the immune response and is generally non-specific. It depends on genetically pre-determined recognition receptors that recognise common pathogen antigens. While the broad pathogen killing mechanisms employed by the innate immune system are highly effective, the non-specific pathogen receptors it employs are unable to identify all infectious agents and adapt upon re-infection.

This role is filled by the second arm, the adaptive immune system. Using highly diversified receptors selected by specificity for a distinct pathogen antigen at the time of exposure, it is able to produce an immune response to novel pathogens. A successful response to a pathogen by the adaptive immune system results in the development

of immunological memory, which leads to an accelerated response upon re-exposure. However, with the highly diverse specificity to pathogen antigen shown by the adaptive immune system comes the potential development of immunity to self antigens. Although the adaptive immune system has several self regulatory mechanisms to prevent autoimmunity, when this regulation breaks down it can have profound results for the host. There are two main functional types of cells that are responsible for mediating adaptive immunity, the B cell and the T cell.

1.2.1 B cell mediated immunity

The primary role of B cells is to produce antibodies. Antibodies are globular plasma proteins that bind to the specific pathogen molecules and once bound, they engage effector mechanisms that destroy the pathogen.

Antibodies consist of two heavy chain and two light chain proteins chains that are joined by disulphide bonds to form a "Y" glycoprotein. The tip of the "arms" of an antibody constitute the variable antigen recognition regions, whilst the rest of the molecule forms a constant region specific to the initiation of different immune effector functions [1]. The diversity of the variable region of an antibody is down to somatic recombination, a specialised process where germline antibody DNA is assembled by joining a number of gene segments. Three component segments, variable (V), diversity (D) and joining (J) gene segments, are drawn from a pool of genes and are recombined to form the variable region of the antibody heavy chain [2]. The variable region of the light chain is generated by a similar method, except no D segment is included. This process creates B cells which produce antibodies with a wide repertoire of specificities.

The diversity of antibodies generated is further increased during B cell maturation when recombination of the heavy chain can lead to a variable region being partnered with a different constant region in a process called isotype switching [3]. The five different forms of the constant region allow antibody with a specific variable region to be expressed as different "isotypes", leading to the production of antibodies with the same antigen specificity but different effector functions.

B cell activation and development

B cells are activated through the B cell receptor (BCR) which is a membrane-bound antibody splice variant. The BCR alone has no signalling ability and so it is in complex with the proteins CD79a and CD79b that have signalling motifs in their cytoplasmic domains [4]. B cells initially develop from hematopoietic stem cells in the bone marrow and it is here that they undergo somatic gene rearrangement, which gives each B cell a surface immunoglobulin with a single specificity. The bone marrow is also the site where the specificity of a B cell BCR is first tested for recognition of self antigen. If a BCR binds multivalently to a self antigen, apoptotic signals are triggered and the B cell undergoes cell death, thus eliminating the cell from the B cell population [5]. This was originally thought to be the only fate of B cells with a strong affinity for self antigen, however, some B cells undergo receptor editing, where the light chain of the auto-antibody is replaced thus changing their specificity [6]. Also if a B cell binds soluble self antigen univalently, it is rendered unresponsive or anergic to that antigen, which prevents its effective function. Only B cells that do not react to antigen in the bone marrow, go on to develop to maturity and are released into the peripheral

lymphoid tissues.

The surface immunoglobulin contained within the BCR has two functions upon antigen engagement. First, it initiates a direct signal to the interior of the cell. Secondly, the BCR is internalised on antigen binding, delivering the immunoglobulin bound antigen to intracellular sites where it is degraded and the peptide fragments returned to the cell surface and bound to the MHC class II complex, discussed below 1.2.2. The presentation of this peptide in the context of the p:MHC complex is recognised by a T cell subset, T helper cells (T_H cells), which in turn produce soluble and membrane bound factors that trigger a second signal in the B cell that causes the cell to proliferate and differentiate into an antibody secreting cell. For a B cell to be engaged by a T_H cell, the T cell must first be activated through antigen recognition on a professional antigen presenting cell. In addition, a T_H cell must also recognise the same antigen as a B cell, however, the epitope specificity of each cell may be different. The binding of B cell presented peptide by a T_H cell triggers the expression of CD40 ligand and the secretion of IL-4 and other cytokines [7]. It is these factors that initiate activation of the B cell. However, it is important to note that certain B cells can be activated without the second signal triggered through the engagement of these T_H cells, as B cells specific to certain microbial antigens can be activated through the binding of antigen alone [8].

The dependence of the majority of B cells on T_H cells for activation means that the most B cell activation occurs in the T cell areas of lymphoid tissues where T_H cells become activated. Upon activation, B cells migrate to the thymus or spleen where

they engage with dendritic cells and form germinal centres. Within the germinal centres three important processes take place: affinity maturation, class switching and proliferation. Affinity maturation is an additional somatic hypermution process of the variable region genes. Through interaction with follicular dendritic cells, the BCR affinity for an antigen is increased through the selective expansion of high affinity B cells [9]. During class switching the constant domain of the antibody secreted by the B cell may be altered. Prior to this stage, mature naive B cells express IgM and IgD at the cell surface but via cytokine stimulus from a stimulating T cell, the isotype secreted by the B cell is modified [3]. The resultant B cells released into the periphery after the successful completion of these processes, are mature plasma cells, which are able to secrete large amounts of high affinity antibody.

The humoral immune response

The antibodies produced by mature plasma cells do not directly cause the destruction of pathogens, but instead bind to a pathogen and attract the attention of a number of immune effector mechanisms from the innate immune system. By binding directly to antigen at high levels, a specific antibody may target a pathogen for destruction by recruiting phagocytic cells directly, in a process called opsonisation. Phagocytes recognise a motif in the constant domain of the antibody coating a pathogen through Fc receptors (FcR), which signal to the phagocyte that the pathogen is to be ingested and destroyed (reviewed here [10]). FcRs expressed on other cells also enable them to bind to opsonised cells. By binding antibody Fc regions, Natural Killer (NK) cells directly kill antibody labelled pathogens using a process called antibody-dependent

cell-mediated cytotoxicity [11]. An antibody labelled pathogen can also activate a system of serum proteins called the complement system. Complement is a biochemical cascade that can attack extracellular pathogens by coating them in proteins that either facilitate their removal by phagocytosis or kill them directly.

Antibodies activate the classical pathway of complement, however an alternative pathways exists that can be initiated by complement binding directly to pathogen associated molecular patterns or mannose binding lectins on a pathogen surface. The early events in all the complement initiating pathways culminate in the formation of C3 convertase, which binds to the pathogen surface. Through its serine protease activity, C3 convertase cleaves the complement protein C3 into various cleavage fragments that direct subsequent complement effector function. The cleavage fragment C3b opsonises the pathogen labelling it for removal by macrophages and neutrophils. These phagocytes bind to the opsonised pathogen by their complement binding receptors which leads to pathogen engulfment and destruction. C3b also allows late stage complement proteins to form a "membrane attack complex" on the surface of the pathogen, which damages its membrane leading to lysis. Smaller cleavage products of C3 convertase, C3a and C5a, function as cytokines that recruit phagocytes to the site of infection and can direct neutrophils to neutralise ingested pathogens. C3a and C5a also act as anaphylatoxins, soluble signalling molecules that can trigger the release of immune mediators from mast cells (a more detailed review of the complement system can be found here [12]).

An additional way that antibodies aid host defence is via direct neutralisation.

Through antigen binding, an antibody can inhibit a pathogen by directly blocking receptors that bacteria or viruses use to target a host cell. This antibody neutralisation mechanism is also used to identify and eradicate soluble toxins. By subsequent opsonisation of a pathogen or toxin, it can be labelled for elimination by cellular immune effectors.

1.2.2 T cell mediated immunity

While the diffuse nature of antibodies allows them to penetrate the tissues and extracellular spaces of a host to identify and eliminate pathogens, not all pathogens that infect a host are accessible to antibodies. Some parasites, bacterial pathogens and all viruses enter host cells where they can multiply safely shielded from antibody identification. T cells are a lymphocyte population that has evolved to operate against host cells which contain intracellular organisms. Unlike B cells that produce antibodies to mediate pathogen elimination, the T cell immune response is cell mediated. Two main subsets of T cells carry out this immune response, cytotoxic T cells (T_C cells), which can directly kill virus infected cells, and helper T cells (T_H cells), which activate macrophages and B cells. Both types of T cell also secrete a variety of cytokines that can recruit and modify other arms of the immune system in response to pathogen identification.

T cell antigen recognition

The cell mediated immune response depends on not only the recognition of pathogenic antigen but also a host surface marker, which informs the T cell of its engagement with

another host cell. These cell markers are a group of cell surface proteins called the major histocompatibility complex (MHC). The MHC displays peptide fragments, transported from intracellular compartments, in a groove of their extracellular domain. A T cell is able to recognise a peptide:MHC (p:MHC) displayed by cells through its antigen specific receptor, the T cell receptor (TCR). Peptides are presented on two distinct classes of MHC, which each present antigen to only one of the main T cell subsets. T_H cells, which activate B cells and macrophages recognise MHC class II, whereas T_C cells,which kill pathogen infected cells, recognise MHC class I. The two main T cell subsets are aided in their identification of MHC class by distinct co-receptors, which along with TCR binds one of the two MHC classes. T_H cells express CD4 and T_C cells express CD8. The antigens that stimulate each type of T cell come from different sources within the cell, and this is reflected in the peptide specificity of the two classes of MHC.

MHC class I binds and presents peptides from cytosolic pathogens such as viruses and some bacteria. It consists of the α-polypeptide chain that is arranged into three large globular domains (α_1, α_2 and α_3) that non-covalently associate with a second chain, the invariant β_2-microglobulin [13]. The α_1 and α_2 domains form the peptide-binding groove and are located at the top of the molecule, above α_3 from which a hydrophobic section of the chain anchors the whole molecule to the cell surface. The nature of the MHC class I groove is such that it can only bind short peptides of 8 - 9 residues long. These peptide fragments are loaded into the MHC class I cleft by a specific mechanism [14]. Cytosolic proteins are degraded by the proteosome into

short peptide sequences. These are then actively transported into the endoplasmic reticulum (ER) by the transporter associated with antigen processing (TAP) protein complex, where under the influence of the TAP transporters and other chaperone proteins the nascent MHC class I is loaded with the peptide. The resultant peptide in complex with MHC (p:MHC) makes its way through the Golgi system and is then presented at the cell surface.

MHC class II is predominately expressed on professional antigen presenting cells (pAPC). They present antigens derived from proteins degraded by acidified endocytic vesicles. As such, the peptides presented can originate from intracellular bacteria or parasites that replicate in macrophage vesicles and other opsonised or endocytosed pathogens that originated from the extracellular environment and were eliminated by the innate immune response. MHC class II also presents antigen internalised by the BCR during B cell activation (1.2.1). Similarly to MHC class I, MHC class II is made up of two peptide chains, but unlike MHC class I, both chains contribute to the peptide groove and both provide attachment to the membrane [15]. The two chains each form two globular domains (α_1, α_2, and β_1 and β_2), of which the α_1 and β_1 domains form the peptide groove that shows striking similarity to that of MHC class I. However, the groove does differ in that it presents peptides of at least 12 amino acids in length due to the open configuration of the end of its groove. When the MHC class II is assembled in the ER, its peptide groove is loaded with an endosomal pathway targeting chaperone protein called the invariant chain (Ii or CD74), which blocks the groove from undirected peptide binding. The acidic conditions of the peptide contain-

ing late endosome, which fuses with the MHC class II-Ii containing vesicle, cause the cleavage of Ii leaving the Ii fragment CLIP (class II-associated invariant-chain peptide) within the peptide groove. Pathogen derived peptides are then substituted for CLIP, chaperoned by an MHC related molecule, HLA-DM (reviewed in [16]).

T cell development and diversity

While the presentation of antigen to T cells is mediated by MHC molecules, the recognition of specific peptides is mediated by the TCR. As well as displaying peptides from intracellular pathogens, the MHC can also present fragments of the host cells own proteins. Therefore, not only must a host's TCR repertoire be able to identify a diverse range of pathogen antigens, but also be educated for tolerance to self. Both T cells and B cells are derived from a common progenitor, the hematopoietic stem cell, but while B cells spend time in the bone marrow maturing, T cells are defined by the site of their maturation, the thymus. In the thymus, immature T cells undergo a series of developmental stages that are accompanied by changes in the expression of cell surface proteins. The initial stage of T cell development is an intense period of proliferation, however, only 3% of the T cells generated in the thymus will be released into the periphery [17]. This is due to the high level of cell death induced as developing T cells undergo screening for MHC restriction and self tolerance.

The process of T cell receptor gene rearrangement in many ways is similar to the process that occurs in B cells. The variable region of the two main peptide chains which make up the TCR (the α and β chains) are also encoded by gene fragments that generate receptor diversity by recombination. The β chain is constructed from TCR

specific V, D and J gene segments, whereas the α TCR chain is encoded by the V and J gene segments. Both chains are also recombined with a constant domain segment, encoding the remainder of the TCR including the transmembrane region required for cell surface attachment. Like the sequential rearrangement of immunoglobulin heavy and light chain genes in B cell development (1.2.1), the β-chain gene segments rearrange first and only after the successful expression of a β-chain at the cell surface can α-chain gene rearrangement begin [18]. However, the β-chain cannot be expressed at the cell surface alone, so a newly formed β-chain is expressed with a surrogate pre-Tα TCR chain [19]. Effective β-chain recombination and therefore expression, also triggers the down regulation of the surrogate chain, so that the subsequent expression of a mature TCR only occurs after the successful recombination of both TCR chains. Expression of the co-receptors CD4 and CD8 accompany the expression of the nascent TCR, and the presence of both on early T cells signals the expression of a functional $\alpha\beta$ TCR.

The next stage of T cell development is guided by the interaction of double positive T cells ($CD4^+/CD8^+$) with thymic cortex epithelial cells. Here the T cells are positively selected for expression of TCR that is capable of recognising self-MHC molecules. The cortical epithelial cells present MHC class I or MHC class II molecules loaded with self peptides from the thymic environment to T cells. Only T cells which bind a p:MHC with sufficient affinity receive a survival signal [20]. Developing T cells that are unable to bind die by apoptosis, as without an affinity for self-MHC molecules they could not fulfil their immune function. The subclass of a developing T cell is also decided during

positive selection, as the co-receptor expressed by a mature cell is determined by the class of MHC to which the TCR binds [20]. A cell expressing a TCR that binds to MHC class I will express CD8, and a TCR that binds to class II will express CD4. While the immature T cells that enter the single positive stage of development have been selected for ability to identify host MHC, the positive selection process does not remove cells that may cause autoimmunity by binding to p:MHC containing host peptide. These cells are removed in the next stage of development, negative selection.

Progression to this final stage of development is accompanied by the migration of T cells from the thymic cortex to the thymic medulla. Here they come into contact with pAPCs, such as macrophages and dendritic cells, which present self peptides in complex with MHC molecules. The peptides presented by the pAPCs are generally representative of the self peptides a mature T cell will encounter in the host periphery. In an opposite process to positive selection, cells that express TCRs with a strong affinity for self p:MHC are eliminated from the population by apoptosis, thus preventing the release of self-reactive T cells to the periphery [21]. The vast majority of all developing T cells are eliminated during negative selection, leaving the remaining T cells, reactive only to non-self peptides presented on self MHC molecules, free to be released from the thymus into the periphery as mature naive T cells.

The processes of positive and negative selection, whilst in practice, is able to select for self MHC restriction and against self peptide restriction, in theory, creates a paradox. The removal of T cells that are not specific to host MHC and the subsequent removal of cells that are specific to host peptide could result in the death of all devel-

oping T cells. However, two theories have been developed to explain this discrepancy between theory and practice. The differential avidity hypothesis suggests that T cells are eliminated if they possess receptors that have very low or very high affinity for self antigens [22]. It suggests that the outcome of TCR/p:MHC binding depends on the signal strength initiated by the TCR upon binding, which in turn is dependent on the TCR affinity for a p:MHC and the density of bound p:MHC. Therefore during positive selection, cells whose TCR has a very low affinity are eliminated at the positive selection stage whereas cells with TCR of a very high affinity for p:MHC undergo cell death during negative selection. Those TCRs with medium affinity receive a signal to mature and so progress to negative selection. Because there will be more cells with medium affinity TCRs than very high or low affinities, more T cells will be selected by positive selection than are eliminated by negative selection. An alternative hypothesis is the theory of differential signalling [23]. This hypothesis suggests that the nature of the signals initiated by the TCR during positive and negative selection are qualitatively different, and therefore are not solely dependent on the number or receptors engaged or strength of signal.

T cell activation and effector function

The activation of naive T cells in the periphery requires the recognition of foreign peptides displayed as p:MHC by the TCR, but this alone is not enough to drive full activation and the subsequent clonal expansion of the T cell and its development into an effector cell. A second signal, in addition to that initiated by TCR/p:MHC ligation is required, which is triggered via co-stimulatory molecules [24]. Only pAPCs are

able to co-express both classes of MHC and co-stimulatory molecules, so therefore a naive T cell can only be triggered by a pAPC. While all pAPCs, such as dendritic cells and macrophages and B cells, endocytose antigen and present it to the external environment on MHC class I and II molecules, each has a distinct function in eliciting a T cell response. Dentritic cells perform the primary peptide presentation to naive T cells. Once mature they migrate to the lymph nodes where they express high levels of MHC class I and II molecules with co-stimulatory and adhesion molecules, which facilitate their role as primary naive T cell stimulators [25]. Lymphoid dendritic cells are particularly efficient at presenting viral peptides [26]. Macrophages endocytose both dead cells and cell debris as well as pathogens, therefore only when they encounter pathogenic material do they express co-stimulatory molecules, preventing inappropriate activation of naive T cells [27]. Finally, B cells are able to present antigen to which their antibody is directed and trigger activation with the co-expression of co-stimulatory molecules [28].

Naive T cells circulate between the blood and the lymph nodes, crossing between each area through high endothelial venules [29]. During their migration through the lymph nodes, naive T cells come into contact with pAPCs that are scanned for specific antigen. Naive T cells first engage APCs through the binding of low affinity cell surface adhesion molecules that allow T cells to scan the large number of p:MHC presented by APCs. Once a naive T cell identifies its specific p:MHC, a signal is initiated in the cell that stops further cell migration and initiates the stabilisation of interactions between the cell and the APC. Without the co-ligation of a co-stimulatory

molecule, T cells cannot progress to the next stage of activation and fall into a state of inactivation called anergy [30]. This response to TCR/p:MHC ligation alone, prevents inappropriate activation of naive T cells in the periphery by non-professional APCs. The signals induced by the co-ligation of the costimulatory receptor CD28 and the TCR on the naive T cell to the costimulatory molecule CD86 and the p:MHC on the APC triggers the T cell to enter the G1 phase of the cell cycle and express the cytokine IL-2 and the high affinity IL-2 receptor (CD25) [31]. By binding the IL-2 it expresses upon activation, an activated T cell progresses through the rest of the cell cycle over several days leading to the production of high numbers of T cells that all bear an identical antigen receptor [31]. At a late stage in this proliferative response, the activated T cells develop into effector cells. Effector T cells have the capacity to produce and use specialised effector molecules upon host cells presenting specific antigen in the absence of co-stimulatory molecules. They circulate through the blood, scanning host cells for presented antigen in a similar manner to that of naive cells and can also be recruited to the site of inflammation or infection by specific cytokines and chemokines.

The role of T_c cells is to kill cells infected with intracellular pathogen upon identification through a specific p:MHC. They are able to kill infected cells in a number of ways. Firstly, T_c cells can kill cells by damaging the cell surface by the secretion of perforin and cytotoxins. Perforin polymerises on the target cell surface and forms membrane pores that allow water, salts and cytotoxins, such as granzymes to enter the cell, thus killing it [32]. Secondly, they induce apoptosis through the engagement of Fas ligand on the T_c surface with Fas, which can be expressed by some infected

cells [33]. Thirdly T_C effector cells secrete cytokines such as IFN-γ, TNF-α and TNF-β upon TCR ligation. These cytokines play a variety of roles in the elimination of infected cells. They can aid the host defence by activating and recruiting macrophages, mobilise phagocytes and professional APCs to the site of infection, inhibit intracellular viral replication and promote viral antigen presentation by MHC class I in infected cells.

While naive CD8 T cells leaving the thymus are predestined to become T_C effector cells upon activation in the periphery, the route of development of CD4 T_H as effector cells is more complex. Upon activation T_H cells can differentiate into different subtypes of effector cells. Traditionally, two main subtypes have been considered: T_H1 and T_H2 cells. However, more recently other subtypes of $CD4^+$ T cells have been identified: Regulatory T cells (T_{reg} cells) and T_H17 cells. Each subset can be identified by the cytokines they produce, but more importantly they co-ordinate different sections of the immune response.

The induction of T_H1 effectors at a site of infection invokes cell mediated immunity by acting as specialised macrophage activators and encouraging the proliferation of T_C cells [34]. They also secrete IFN-γ that acts to suppress T_H2 responses as well as having anti-viral properties. T_H2 cells are B cell stimulators and so invoke the humoral immune system (1.2.1) [35]. They express CD40 ligand, which is essential in B cell activation and also secrete specific B cell growth factors that play roles in B cell activation and differentiation [36].

The recently described T_H17 cells are characterised by the production of interleukin

17 (IL-17) and interleukin 22 (IL-22) [37,38]. T_H17 cells develop independently of the T_H1 and T_H2 lineage and their development is directly inhibited by the presence of the T_H1 and T_H2 cytokines IFN-γ and IL-4 [37]. The T_H17 cell subtype is thought to be an important part of the adaptive immune system's response to extracellular bacteria and fungi [39,40] and also some studies have also linked T_H17 cells to some chronic autoinflammatory diseases [41,42].

The T_{reg} subgroup of T cells, identified by expression of CD4, CD25 and the transcriptional regulator Foxp3, control pathogenic auto-reactive immune responses, therefore playing an important role in the tolerance of self-antigens (reviewed in [43,44]). All the directing mediators of the different T_H cell differentiation paths are still unclear, however, the local cytokine environment and the type of co-stimulatory signals at the time of activation are known to influence the path of differentiation. For example, IFN-γ and interleukin 12 (IL-12) has been shown to promote T_H1 differentiation, whereas IL-4 is known to drive T_H2 differentiation [45,46]. Evidence has also shown that the development of T_{reg} cells can take place in the periphery as well as the thymus, however the factors which induce peripheral T_{reg} cell development are unclear [47].

The large numbers of effector T cells that are created in response to a pathogen antigen do not remain in the host indefinitely. Post infection, most cells undergo deletion but some remain and persist at low levels, circulating within the host as "memory" of the immune systems response to a specific pathogen. These cells are able to respond and proliferate more quickly to antigen than naive T cells and are maintained at a level above the initial naive T cell frequency. How these memory T cells develop

and are maintained within the immune system is a matter of debate (reviewed in [48]). However, it is known that they have distinct gene expression profiles that control cell survival and express patterns of cell surface proteins distinct from naive and effector T cells.

Other T cell subtypes

While the majority of circulating T cells can be defined as $CD4^+$ or $CD8^+$, there are also additional T cell subtypes that also play roles in the adaptive immune response.

One of these alternative T cell populations express a TCR composed of a δ and a γ chain instead of the $\alpha\beta$ TCR, which is expressed on the majority of circulating T cells. $\delta\gamma$ T cells are less prevalent in the periphery than $\alpha\beta$ T cells, but they are found at higher levels in gut mucosa as intraepithelial lymphocytes (IEL). The genetic recombination of the $\delta\gamma$ and $\alpha\beta$ TCR genes are thought to occur simultaneously in the same T cell precursor, however the factors which contribute to the commitment of a T cell to either lineage is unclear (reviewed in [49]). Their overall role in T cell mediated immunity is still not fully known as are the target antigens that act as their ligands. But some differences in the composition and activation of the $\delta\gamma$ TCR have been noted. Some $\delta\gamma$ T cells do not require MHC to bind foreign antigen and also the TCR complex formed by $\delta\gamma$ T cells does not contain a component found in the $\alpha\beta$ TCR, the CD3γ chain [50, 51].

Natural killer T cells (NKT cells) are a subset of T cells that express both an $\alpha\beta$ TCR and NK cell markers like CD161 and CD94. They bear TCRs specific for glycolipid ligand that is presented by CD1d, a MHC class 1 like glycoprotein [52]. CD1d has

a binding cleft specifically tailored to presenting lipid antigen due to the presence of a large hydrophobic pocket at their presenting surface. NKT cells are classified as invariant NKT cells (type I NKT cells) or type II NKT cells based on their specificity for the experimental glycolipid antigen α-galactosylceramide (α-GalCer) [53]. Type I NKT cells bind and react to CD1d presented α-GalCer, but have a very restricted repertoire, where as type II NKT cells express TCR with a far greater diversity and therefore are not α-GalCer restricted. NKT cells can be activated by both exogenous and self lipid ligand and on activation are able to secret large amounts of both the T_H1 and T_H2 cytokines IFN-γ, TNF-α, IL-2 and IL-4 [54] [55]. They only make up 0.2% of the total T cells in the peripheral blood, however, their rapid cytokine response suggests an innate immune like role within the adaptive immune system [56, 57]. NKT cells are thought to play a role in the immunity of a number of viral infections, including hepatitis B [58]. NKT cell activity has also been observed as an aggravating factor in autoimmune disorders such as allergic asthma, atherosclerosis and diabetes (reviewed in [57]).

1.3 TCR triggering

1.3.1 The TCR complex

With the responsibility for recognising foreign antigen and initiating powerful T cell effector functions, the T cell antigen receptor plays the central role in T cell triggering. As described previously (1.2.2), the majority of T cells express TCRα and TCRβ chains that are expressed at the cell surface as a heterodimer, joined by a disulphide bond.

Each TCR chain is comprised of two IgSF domains [59]. The N-terminal domains of each chain, as encoded by the V, (D) and J gene segments (1.2.2), comprise the variable region of the receptor and form a single p:MHC binding epitope. The second, membrane proximal domain is encoded by the constant gene segment that also encodes the C-terminal transmembrane domain and short intracellular domain.

Like the B cell receptor, the TCR does not contain any signalling domains, but associates with the invariant cell surface molecules CD3γ, CD3δ, CD3ϵ and CD3ζ (CD247), which all contain intracellular Immunoreceptor Tyrosine based Activation Motifs (ITAMs). In association with the TCRα and β chains, they form the TCR complex [60]. When in complex with the TCR, the CD3 chains form two heterodimers, CD3$\gamma\epsilon$, CD3$\delta\epsilon$, and a homodimer CD3$\zeta\zeta$. Co-expression with CD3$\gamma\epsilon$ and CD3$\delta\epsilon$ is essential for TCR expression at the cell surface [61–63]. However, a low level of TCR expression is observed in the absence of CD3$\zeta\zeta$ [63]. The complex assembles in the endoplasmic reticulum, with the association of each of the CD3 dimers with the $\alpha\beta$TCR being governed by three basic residues in the $\alpha\beta$TCR transmembrane domain and a pair of acidic residues in the centre of each of the CD3 membrane spanning segments [64]. CD3γ, CD3δ and CD3ϵ all have IgSF extracellular domains [65, 66], and one cytoplasmic ITAM each. CD3ζ differs from the rest of the CD3 chains in that its extracellular domain consists of only a few residues, but it possesses three ITAMs on its intracellular domain.

Upon TCR/p:MHC ligation the tyrosine residues within the ITAM motifs, [*DE*]xx**Y**x x[*LI*]$_{6\text{-}12}$**Y**xx[*LI*], become phosphorylated making them targets for a number of intracel-

lular signalling molecules with SH2 domains. The initial ITAM phosphorylation is the first step in an intracellular signalling cascade that results in the changes in gene and protein expression that characterise T cell activation. While we understand the structure of the extracellular domains of each individual component of the TCR complex via crystallographic structural data [59, 65, 66], as of yet, the complete structure of the TCR complex is unsolved. However, mutagenesis of possible interacting extracellular surfaces within the complex, using methods like those used in a recent study [67], may yield more information on the overall structure of the $\alpha\beta$TCR complex.

1.3.2 TCR complex signalling

While the process by which TCR/p:MHC ligation initiates signal transduction is still unclear (1.5), many of the major intracellular signalling pathways that are initiated by this event are well studied (reviewed in [68]). However, as more pathways are investigated the signalling outcome of T cell activation gets evermore complex, therefore this section will give a brief overview of the main signalling pathways initiated by the TCR and their effects. Figure 1.1 illustrates some of the protein interactions and signalling pathways that occur after TCR ligation as discussed in this section.

As mentioned above, the phosphorylation of CD3 ITAMs is the initiation point of all signalling pathways triggered by TCR ligation. This phosphorylation is mediated by two Src-family kinases, Lck and Fyn, and the activation of these phosphotyrosine kinases (PTK) is one of the earliest detectable events following TCR engagement [68, 69]. Lck is involved in CD3 ITAM phosphorylation, its recruitment being aided by its constitutive association with the cytoplasmic domain of the co-receptors CD4 and

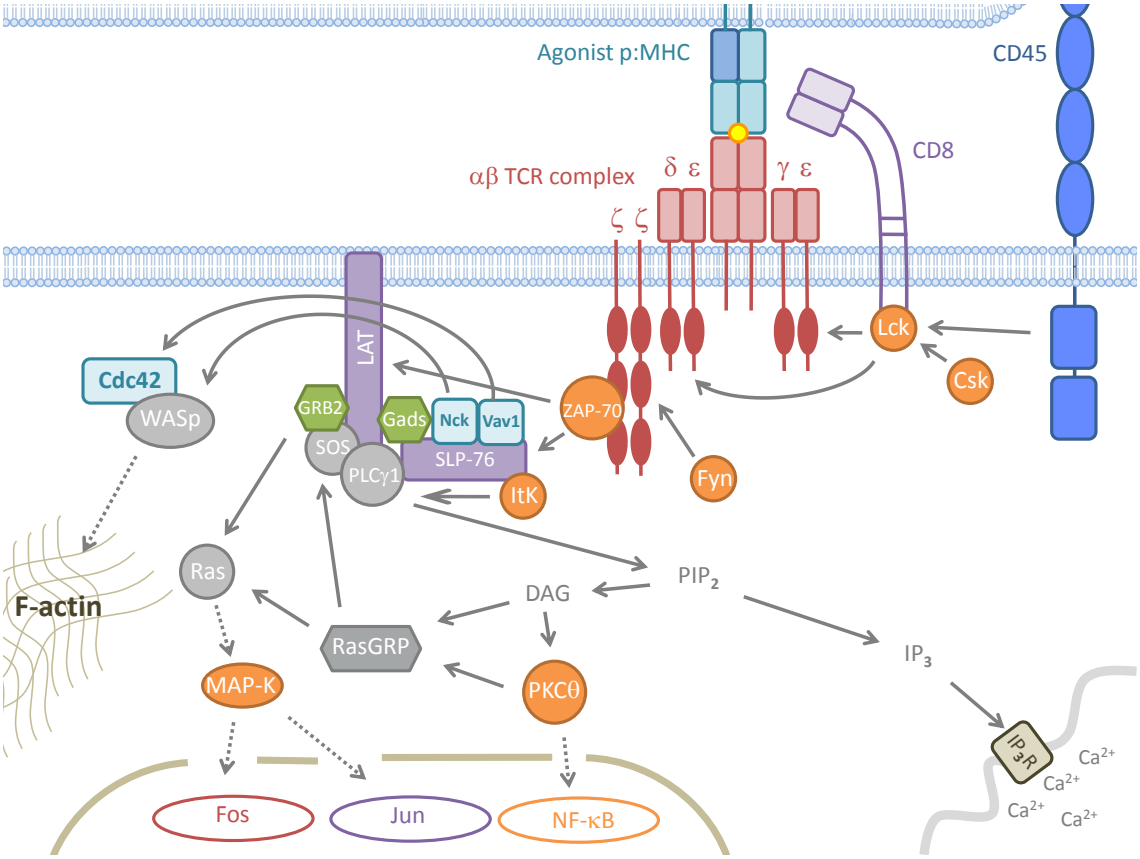


Figure 1.1: Some of the signalling pathways initiated on T cell triggering. Solid lines represent protein interactions, whereas dotted lines represent interactions via further signalling pathways not described here. After agonist p:MHC/TCR ligation one of the earliest signalling events is the phosphorylation of CD3 chain ITAMs by Lck or Fyn. Lck is constitutively associated with the co-receptors CD8 (shown here) and CD4. The activity of Lck is regulated by Csk and CD45. Upon CD3ζ homodimer phosphorylation, ZAP-70 is recruited to the TCR and is also phosphorylated by Lck. Active ZAP-70 then phosphorylates LAT, which recruits both SLP-76 and Gads. ZAP-70 phosphorylation of SLP-76 results in the further recruitment of Nck, Vav1, Itk and PLCγ1. Itk and ZAP-70 phosphorylate and activate PLCγ1, which hydrolyses PIP_2 producing DAG and IP_3. IP_3 directly activates IP_3R that releases calcium from the ER into the cytoplasm. DAG binds PKCθ, which is a regulator of the transcription factor NF-κB. DAG also recruits RasGRP that is phosphorylated by PKCθ. SOS bound to GRB2, activates RAS that is required for the activation of the MAPK pathway, which contributes to the activation of the transcription factors Jun and Fos. RasGRP can also activate Ras and SOS. WASp is recruited to the surface by SLP-76 bound Nck, where it is activated by Vav1 dependent stimulation by Cdc42. Activated WASp activates a pathway that leads to F-actin accumulation at the site of activation.

CD8. Fyn, the second PTK, associates with the cytoplasmic domains of CD3ϵ and CD3ζ following TCR engagement. Phosphorylation of the CD3ζ ITAMs leads to the recruitment of the Syk family tyrosine kinase, ζ associated protein, 70kDa (ZAP-70), which associates with Src kinase phosphorylated CD3ζ ITAMs by its SH2 domains [70].

The phosphorylation of membrane proximal signalling molecules by Src kinases is essential for the inital steps of T cell activation, therefore the regulators of Src kinase activity also have an important role. Activity of these kinases is regulated by the phosphorylation state of tyrosine residues contained in the C-terminus and the kinase domain. Phosphorylation of the tyrosine within the kinase domain results in activation [71], but the phosphorylation of the C-terminus by C-terminus Src kinase (Csk) results in kinase inhibition [72]. CD45, is a membrane bound phosphatase, which is required for receptor signalling in lymphocytes. It counteracts the inhibitory effects of Csk by maintaining the dephosphorylated state of the C-terminus tyrosine and therefore ensures an active Src kinase state [73, 74]. Thus, the balance between Csk and CD45 influences the signalling role played by the Src kinase family in T cells. However, CD45 also dephosphorylates many other of the key signalling molecules involved in the membrane proximal steps of the TCR activation cascade, which are substrates for Lck [75,76]. Therefore CD45 has both an important activating and inhibitory role in T cell activation.

Active ZAP-70 bound to the CD3ζ ITAMs in turn recruits and phosphorylates the key adaptor protein, Linker for Activation of T cells (LAT) [77]. The recruitment of

this protein to the TCR is a stage from which multiple signalling pathways are initiated, with the LAT adapter protein containing multiple binding sites that encourages the formation of a multimolecular signalling complex. The nine tyrosine residues contained on LAT act as a scaffold for a variety of SH2-domain-containing signalling intermediates. These include Phospholipase C $\gamma 1$ (PLC$\gamma 1$), Growth factor Receptor-Bound protein 2 (GRB-2) and GRB2-related adaptor downstream of Shc (Gads) [78]. SH2 domain-containing Leukocyte Phosphoprotein, 76kDa (SLP-76) is recruited to LAT and phosphorylated by ZAP-70 where it forms a trimeric complex with LAT and associated Gads [79, 80]. Once bound, SLP-76 itself acts as a signalling scaffold, binding further SH2-domain-containing proteins such as Vav1, Nck, IL-2 induced tyrosine Kinase (ItK), PLC$\gamma 1$, Adhesion and Degranulation-promoting Adapter Protein (ADAP) and Hematopoietic Progenitor Kinase 1 (HPK1) [81].

Each one of the molecules which binds to LAT and SLP-76 activates or influences pathways that drive the phenotypic effects that can be observed in a T cell post TCR ligation. These pathways are vast and our knowledge of them is ever growing, so the following passages briefly describes the roles and interactions of just some of the molecules mentioned above.

PLC$\gamma 1$ is activated through phosphorylation by ZAP-70 and ItK complexed with LAT. Once active, it hydrolyses the membrane lipid phospholipid phosphatidylinositol 4,5-bisphosphate (PIP_2) into the secondary messengers inositol 1,4,5-triphosphate (IP_3) and Diacylglycerol (DAG). IP_3 triggers the calcium signalling pathway by directly stimulating ICa^{2+} permeable ion channel receptors (P_3R) on the ER, which release Ca^{2+}

from the ER into the cytoplasm (reviewed in [82]). DAG activates Protein Kinase C θ (PKCθ), a regulator of Nuclear Factor κ-light-chain-enhancer of activated B cells (NF-κB) activation, which controls DNA transcription (reviewed in [83]). DAG also has an additional role in Ras activation, by recruiting Ras Guanine Releasing Protein (RasGRP) to the membrane where it is phosphorylated by PKCθ [84,85].

Ras activation is also controlled by GRB2. Ras is member of a family of GTPases that lie upstream of the MAP kinase (MAPK) signalling pathway [86]. The MAPK pathway controls several important transcription factors such as Fos and Jun, which have roles in the expression of IL-2 (reviewed in [87]). The guanine nucleotide exchange factor Son of Sevenless (SOS), is constitutively bound to GRB2, and on TCR stimulation when GRB2 is recruited to LAT, SOS is also brought into the membrane proximal signalling complex. Here, as well as its association with LAT, it is also brought into association with RasGRP, which catalyses the SOS action of Ras-GTPases therefore forming a positive feedback loop for T cell induced Ras activation [88,89].

When associated with SLP-76, the adaptor protein Nck recruits Wiskott-Aldrich Syndrome protein (WASp), which is activated by Vav-1-dependent stimulation of the Rho family GTPase Cell division cycle 42 (Cdc42) [90]. WASp is an activator of a pathway that leads to the accumulation of filamentous actin (F-actin) at the TCR/APC interface in response to TCR triggering. Itk and Vav-1 co-association with SLP-76 has been shown to be required for correct Vav-1 function within this context [91].

This represents just some of the signalling pathways that are activated upon TCR ligation. They do not account for the signal enhancing influence of co-stimulatory

molecules like CD28 (1.6) or the inhibitory co-stimulators like CTLA-4 (CD152) or PD-1 (CD279) (1.7), which modulate the response to TCR engagement in activated T cells. However, these examples do show how through the use of adaptor proteins such as LAT and SLP-76, multiple signalling cascades with diverse effects can result from phosphorylation of the ITAM motifs of the TCR complex.

1.4 The immunological synapse

The term immunological synapse (IS) is used for the organised congregation of molecules that form at the contact site between an APC and a lymphocyte. The use of the word synapse in the context of immunological junctions was first used by Norcross in 1984 [92], who suggested that there was "a similarity between the T cell recognition-activation process and the cell communication processes found in other organ systems, especially the nervous system". Early studies showed that upon APC engagement lymphocytes undergo secretory apparatus polarisation [93] and cytoskeleton reorganisation [94], however it was the development of cellular imaging techniques that allowed a more organised definition of the IS to be proposed. Size segregation of cell surface molecules at the stable TCR/MHC interface was then observed by Dustin *et al* (1998) and others [95, 96], and from this a more structured proposal of the T cell immunological synapse was proposed [95,96].

The immunological synapse is arranged in two concentric rings termed supramolecular activation clusters (SMAC). The TCR rich inner spatial domain is the central SMAC (cSMAC), while the outer ring containing the integrin LFA-1, is the peripheral

SMAC (pSMAC) [96,97]. The formation of the synapse is F-actin dependent, indicating that its formation is an active process [96].

Initially, it was proposed that the cSMAC enhanced receptor engagement and stabilised transduction through the TCR due to the concentration of receptors [96, 98]. Although the formation of the IS correlates well with full activation and this full activation is inhibited by the disruption of cytoskeleton movement [96, 97], it is now thought that the formation of the IS occurs after TCR triggering [99]. The evidence supporting this comes from experiments that show that the levels of phosphorylation in the cSMAC are low and prior to cSMAC formation, higher phosphorylation levels are observed accompanying TCR ligation and signalling [99]. Lck and ZAP-70 phosphorylation occur well before the formation of the mature synapse [99], and Ca^{2+} signalling peaks at 30 seconds. This is a significant period of time before the formation of the mature IS, a process that takes a couple of minutes [96].

Current evidence suggests that the initiation of a TCR signal occurs in TCR microclusters that arise before IS formation. The clusters are formed on ligation of TCR/p:MHC and have associated intracellular complexes of the signalling molecules LAT and SLP-76, that initiate activating signalling pathways, such as Ca^{2+} signalling [100–102]. These clusters then coalesce to form the cSMAC over a period of 2 minutes [103, 104]. Whilst F-actin plays a role in the formation of the mature IS, it has been also shown to be involved in the formation of these microclusters when initiated by either CD3 antibody or p:MHC [102, 105].

Recently, the cSMAC has been further refined into the cSMACa and the cSMACb,

and a further spatial domain defined beyond the pSMAC called the distal SMAC (dSMAC) [104]. The characterisation of the cSMACa and cSMACb is based on the visualisation of the segregation of CD28 from the TCR, following the migration of microclusters to form the cSMAC [106,107], with the TCR/MHC segregated to the cSMACa and CD28/CD80 and PKCθ enriching the cSMACb. This shows a distinct segregation of CD28 and its associated signalling molecules, suggesting a co-stimulatory signal transduction role for the cSMAC, but as of yet the full role of this organisation, signalling or otherwise is unknown. The dSMAC was first described as a region containing high levels of both CD45 and CD4 [108], however visualisation of the IS on lipid bilayers using total internal reflection fluorescence microscopy (TIRFM) does not consistently show this segregation. CD45 has been observed throughout the synapse, although it has been seen to be excluded from small areas of TCR within clustering in the cSMAC [102]. The term "dSMAC" is now used to describe the area of radial lamellipodium that forms the IS, which contains cytoskeletal elements that support the central structures of the dSMAC and cSMAC [104].

So what is the role of the IS? The IS appears to play some role in the directed delivery of T cell effector molecules upon activation. In T_c cells, secretory granules are deposited via the cSMAC, into the synapses formed between two interacting cells. Large adhesion molecules, which form the pSMAC, seem to prevent the diffusion of cytotoxic granule content beyond the IS, and so reduce the cytotoxic affects on bystander cells [109,110]. This delivery role of the IS is supported by evidence of a method of cell-cell communication in activated T cells as observed by Sabatos *et al*

2008 [111]. They describe the formation of an integrin based synapse-like structure that mediated IL-2 secretion and targeted delivery to adjoining cells.

Lee *et al.* (2002) [99] suggest that the clustering of the TCR within the IS allows for its down regulation and eventual endocytosis. Endocytosis as a method of manipulating TCR expression in the TCR enriched environment of the IS has been suggested as a method of amplifying weak agonist TCR signals [112], and also suggested as a negative regulatory mechanism of T cell signalling [113].

A third potential role of the IS could be its use as a structure to which accessory or regulatory molecules are recruited, and that through the interaction with ligands presented on the APC a T cells fate could be determined or modified. As previously described, the segregation of CD28 and signalling molecules from the TCR in the cSMAC suggests that the cSMAC may be important for co-stimulatory signalling [106, 107]. Also Linsley *et al.* [114], show that internal vesicles of the inhibitory molecule CTLA-4 (CD152), which is expressed post activation, are directly targeted to the APC contact site. As well as a site for the initiation of T cell activation modulating signals, some reports have proposed a role for the IS in the mechanism of T cell differentiation. Maldonado *et al.* (2004) [115], show that the interferon-γ receptor co-localises with the TCR in the synapse of naive T_H cells and that IL-4 prevents this co-localisation. This suggests a role for the IS in the differention pathways of both T_H1 and T_H2 cells.

While a better understanding of the structure and function of the IS will help us understand the processes that occur post T cell activation, it is clear that the initial TCR triggering event occurs prior to IS formation and thus is caused by another

mechanism.

1.5 Models of T cell activation

In the fifteen years since the discovery that the CD3 cytoplasmic domain ITAMs are responsible for the transduction of the signals resulting from TCR ligation, much research has been performed to understand the divergent signalling pathways that result from this event (1.3.2). However the exact mechanism of how TCR signal transduction is initiated by the ligation of TCR to p:MHC is still unclear. The ability of the TCR to identify a complementary p:MHC while also being able to maintain interactions with non-specific p:MHC when scanning for specific peptide on the surface of APCs, results in the relatively low range of affinities of the TCR/p:MHC interactions [116]. Any mechanism that explains the triggering of T cells must be able to account for the discriminatory abilities of the TCR/p:MHC interactions and the early changes observed in T cells upon TCR ligation. Many models of T cell activation have been proposed and they can be roughly grouped based on their underlying mechanisms of action.

1.5.1 Conformational change models

The basic tenet behind any conformational change model of TCR triggering is that the ligation of an agonist p:MHC alters the tertiary or quaternary structure of the TCR, CD3 associated chains or the TCR complex as a whole. And it is these changes that result in CD3 ITAM phosphorylation.

Models based on conformational change are attractive as they can easily explain

the T cell triggering that is observed at low levels of agonist p:MHC. It is also a mechanism by which other receptor molecules are activated on the cell surface. Conformational changes have been described in the activation of nicotinic acetylcholine receptors and proteins in the G-protein coupled receptor (GPCR) superfamily [117,118]. In these instances, ligand binding induced conformational changes are transmitted through the length of the molecule to alter the arrangement of multiple pass transmembrane domains, which then initiates signalling. However the TCR contains a single transmembrane domain and a very small intracellular domain that does not contain any signalling motifs or structures with enzymatic activity. Also within the TCR structure there is no functional structure through which a signal like this could be transmitted. Therefore it is hard to imagine how a mechanism such as this could work for the TCR.

Until recently it was also thought that the structural diversity in the TCR variable regions would mean a conformational change mechanism through the TCR alone was unlikely due to the lack of conservation between TCR ligand binding regions. This view was supported by lack of crystallographic data for such changes [119]. However a recent report of a change within the A-B loop of the α chain constant region of the TCR on ligation with agonist pMHC [120], raises the possibility that a conformational change could occur within the more conserved TCR constant region. This change was observed in the same region of two different p:MHC TCRs, but it is unclear if this change constitutes an evolutionary conserved mechanism of TCR triggering or is only a property of certain TCRs. Also, whether this structural change is found upon

p:MHC ligation of $\delta\gamma$TCRs is also unknown.

Several conformational change mechanisms suggest that changes within the structure of the TCR can be transmitted to or "sensed" by the associated CD3 chains [121–124]. The receptor deformation model, as proposed by Ma *et al.* 2008 [122], suggests that a conformational change within the TCR complex is caused by the mechanical forces caused by the T cell as it travels across the surface of an APC (Figure 1.2). In itself, the interaction of a TCR with p:MHC does not cause triggering, but the force exerted by a T cell that detatches it from the APC surface is felt by the bound TCR/p:MHC. If the interaction of the ligated molecules is strong enough, this force will deform the conformation or configuration of the TCR complex and this initiates signalling. Weak TCR/p:MHC interactions will be detached more easily by this force and therefore the change within the TCR will not occur and no signalling observed. In a similar theory, some have suggested that parts of the TCR complex are pressed down perpendicular to the membrane in a "piston-like" movement when bound to agonist p:MHC [125] (Figure 1.2). This is caused by the force of the T cell/APC membrane interaction and results in the availability of activating residues on the cytoplasmic domains of the CD3 chains [125]. This activity is proposed to be mediated through the rigid dimeric structure of the CD3$\epsilon\gamma$ heterodimer and is suggested to perform the piston role in a similar effect to the aspartate receptor [126]. However, neither of these theories account for the antigen independent triggering that occurs by ligation of antibodies to CD3 in solution. Also in the mechanisms involving a "piston-like" movement of the TCR, is it conceivable that any other non-specific force should be

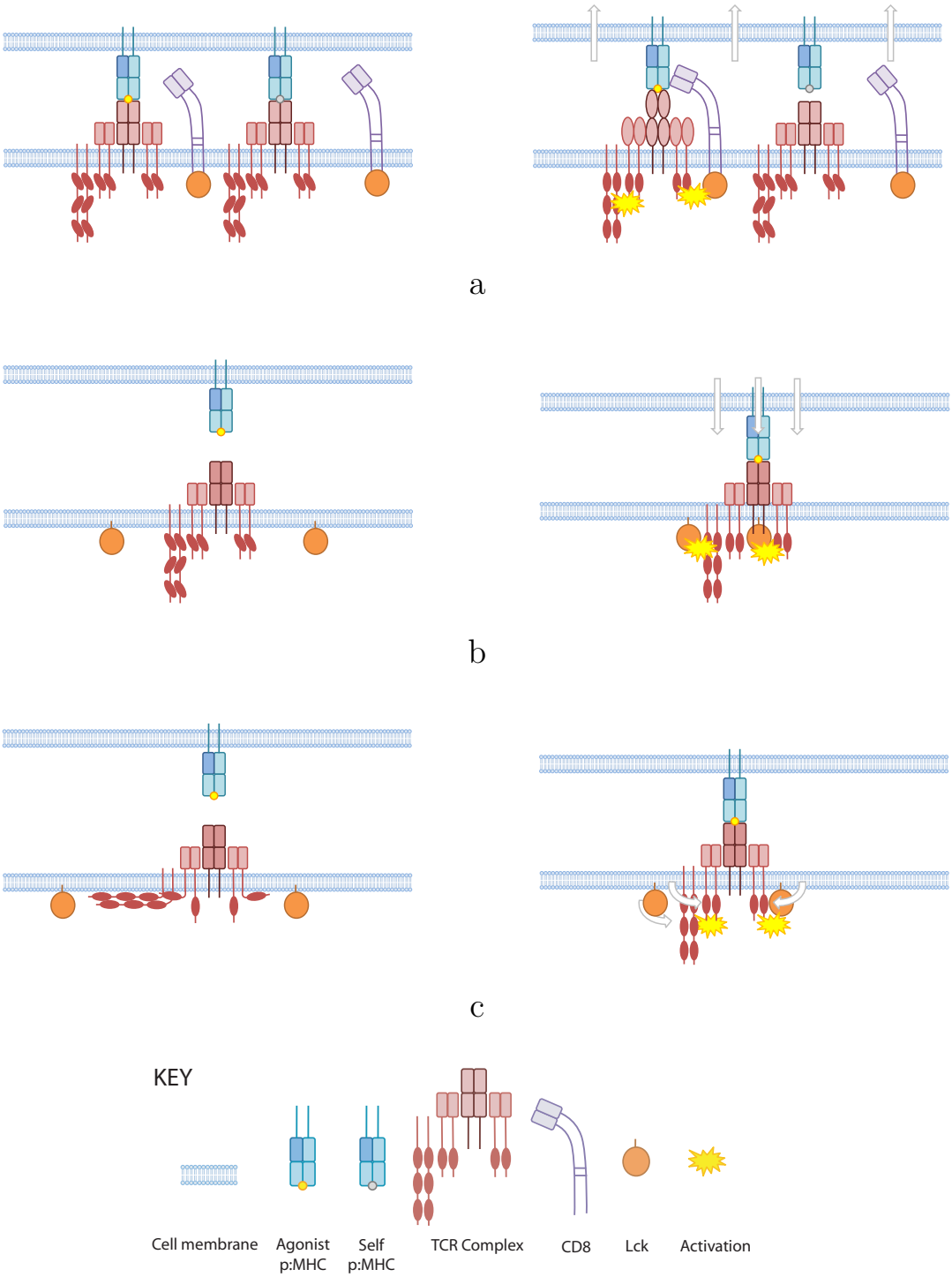


Figure 1.2: Conformational change models of T cell activation. (a) The receptor deformation model. (b) The "piston" model. (c) The CD3 cytoplasmic domain conformational change model, as proposed by Xu *et al.* 2008 [124]

able to trigger the TCR through placing pressure on the TCR, but this is not the case.

If a clear conformational change is shown to transmit the TCR binding event across the membrane, what are the changes in the intracellular environment that initiate signalling? Two mechanisms propose that a conformational change occurs within the CD3 cytoplasmic domain on agonist p:MHC ligation [123, 124]. The first theory is based on a conformational change that occurs in the cytoplasmic chain of CD3ζ independently of ITAM phosphorylation, which regulates cytoplasmic domain association with the cell membrane [127]. Xu *et al.* 2008 [124] further examined change of this type and suggested that CD3ϵ ITAM displacement from the cell membrane plays a role in the initiation of triggering and that charged motifs found on each CD3ϵ ITAM are responsible for their association with the lipid bilayer (Figure 1.2). The regulation of this association is attributed to changes in the lipid composition of the cell membrane, although how TCR ligation is able to achieve these changes is unknown. A second model involves a conformational change in the structure of the cytoplasmic domain of CD3ϵ that has been observed upon both agonist p:MHC engagement and binding of certain monoclonal antibodies [123, 128]. This change, which is said to occur prior to tyrosine phosphorylation, forms a "cryptic epitope" that allows the binding of Nck [128], acting as a key step in the initiation of triggering. The conformational change in CD3ϵ again has been proposed to be caused by a "piston-like" effect on the TCR complex as proposed in other triggering mechanisms [125, 126, 129]. However, dependence of this theory on a role for Nck in the first stages of T cell activation is at odds with our current knowledge of its role in later stages of triggering where it

associates with SLP-76 [90]. Also removal of the CD3ϵ proline-rich sequence to which Nck binds has been found not to affect either T cell function or development [130].

1.5.2 Aggregation models

Another group of models used to explain the triggering of T cells involves the aggregation of the T cell receptor. The method of receptor oligomerisation to initiate signalling is a mechanism that has been observed in many other receptor signalling systems including those of interferon γ [131], human growth factor [132], epidermal growth factor [133] and fibroblast growth factor [134]. In many of these cases by bringing two or more receptors into close proximity, intrinsic kinase activity is invoked or inhibited. Also some of the ligands for these receptors are dimeric or bivalent, which facilitates the oligomerisation of the receptors. However this is not the case for the TCR, as all kinase activity is performed extrinsically and as part of a large TCR-CD3 complex, also there is little evidence that the p:MHC occur naturally as dimers.

The proposal that aggregation plays a role in the initiation of TCR triggering is popular due to the observation that under experimental conditions TCR triggering can be initiated by soluble multimeric p:MHC or antibody. This assertion is supported by many despite the observation that single agonist p:MHCs are also able to trigger T cell signalling when membrane bound [135, 136]. The extremely low amount of p:MHC required to trigger a T cell [137,138] combined with the relatively low affinity of TCR/p:MHC interactions suggest that the formation of oligomerised clusters is very unlikely. Also it is very possible that a TCR/pMHC will have dissociated before it is joined by another complementary TCR/p:MHC on the cell surface.

To overcome some of these issues, alternative models of TCR aggregation have been put forward as mechanisms of T cell triggering. The model of co-receptor heterodimerisation requires that a CD8 or CD4 co-receptor must bind to p:MHC along with complementary TCR for the initiation of signalling [139] (Figure 1.3). The association of CD4 and CD8 with the kinase Lck and its subsequent association with the ITAMs of the TCR complex suggests a plausible role for co-receptors in signal initiation. The inhibition of monomeric soluble p:MHC $CD8^+$ cell triggering by the inhibition of CD8/p:MHC binding is also strong evidence for this theory [140]. However, *in vivo* TCR triggering can proceed in the absence of CD4 and CD8, showing co-receptor binding is not an essential factor of TCR stimulation [141, 142]. A modification of this model is the mechanism of pseudodimerisation [135, 143]. Through the recruitment of a second TCR by an agonist TCR/p:MHC complex and its associated CD4, a stable pseudodimer complex is formed when the second TCR binds to endogenous p:MHC. This causes phosphorylation of the CD3 ITAMs by proximity to CD4 associated Lck or alternately conformational change (Figure 1.3). This theory explains how TCR/p:MHC dimers could occur even at low agonist p:MHC concentrations and trigger activation, and supporting this, Krogsgaard *et al.* (2005) [143] found that if the CD4 binding site on soluble agonist/endogenous p:MHC heterodimers was disrupted no signalling was observed. However, triggering was not observed equally with all endogenous peptides, suggesting that a T cell would have to scan for and engage with two p:MHCs with different affinities to initiate signalling. Also, as with the co-receptor heterodimerisation model, a clear co-receptor role is defined for triggering

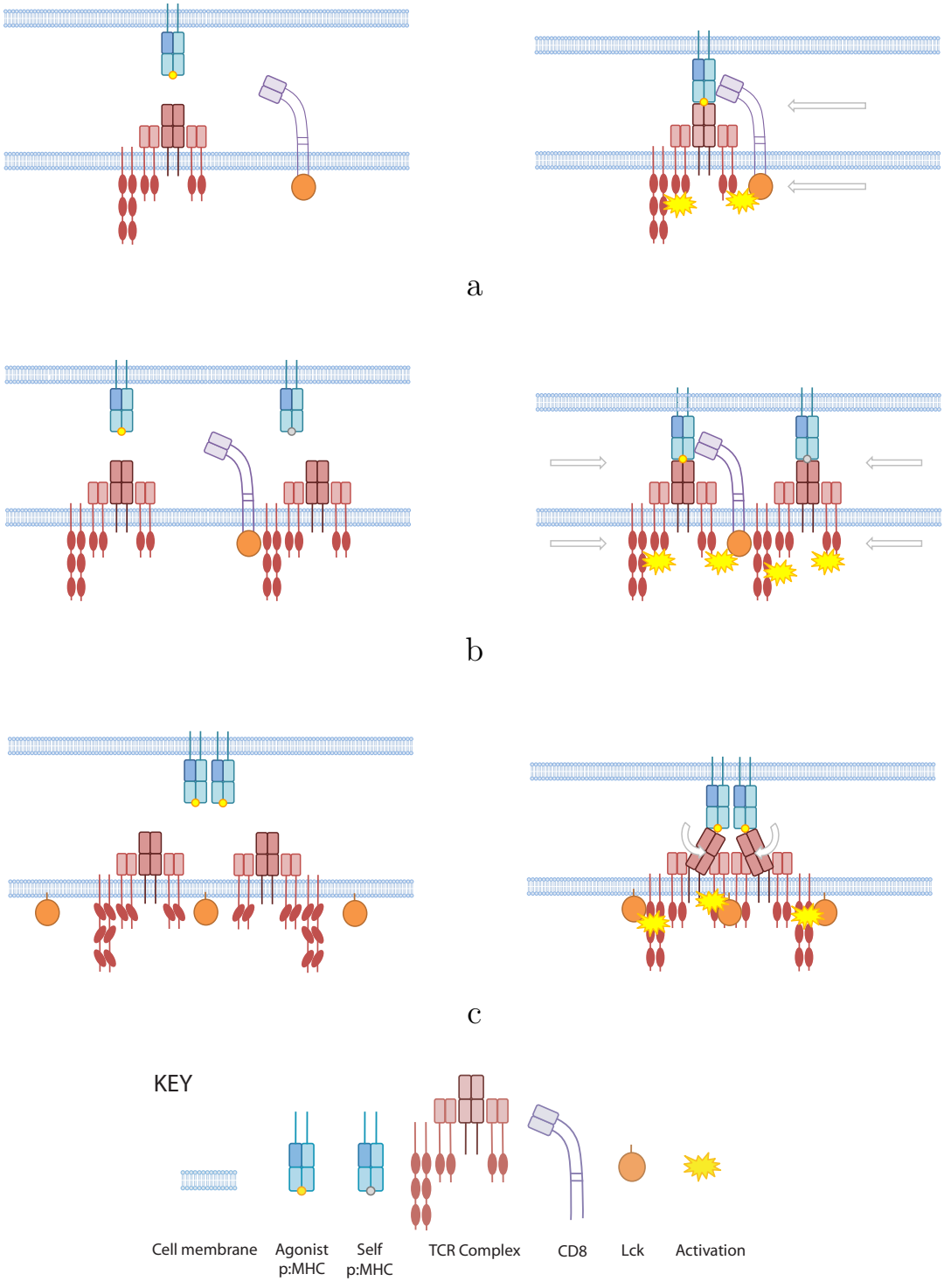


Figure 1.3: Aggregation models of T cell activation (a) The heterodimerisation model. (b) The pseudodimerisation model. (c) The permissive geometry model.

initiation even when evidence shows that T cells can signal in their absence [141,142].

It is perhaps possible that signalling is initiated by a combination of both of aggregation and conformational change effects. One model which suggests this is the permissive geometry theory [144]. The binding of the TCR to dimeric p:MHC is suggested to induce a rotational conformational change in the TCR that exposes the CD3 chain ITAMs for kinase phosphorylation [144,145]. This rotation is proposed to occur in both single TCR and multiple TCR configurations, pivoting around the transmembrane domain (Figure 1.3). Evidence presented in support of this theory is the diagonal orientations at which the $\alpha\beta$TCR binds p:MHC [146,147] and some studies where MHC molecules appear clustered at the cell surface [148,149]. However this mechanism does not address how CD3 antibody is able to achieve this rotation of the TCR or indicate how single agonist p:MHC is able to trigger T cells [135,136].

1.5.3 Segregation models

While both the aggregation and conformational change models discussed above address many of effects observed upon successful T cell activation, they cannot explain a key observation by Mustelin *et al.* (1995) [76]. They found that massive TCR triggering could be observed by treating T cells with pervanadate alone. Pervanadate inhibits cellular phosphatase activity and its effect in T cells shows that a resting T cell may be activated in the complete absence of TCR ligation indicating that it has no intrinsic function within T cell signalling. Many of the above models also do not address the experimental observations that efficient T cell activation requires ligand or antibody immobilisation. Whilst it is possible to activate T cells with soluble mul-

timeric p:MHC or antibody [143, 150], the stimulation achieved is poor compared to the activation seen with p:MHC or antibody presented to T cells on plates or by cells and beads [150–152]. Also is the triggering mechanism T cell activation via the TCR unique in evolution? There are many other signalling receptors at the T cell surface, which like the TCR, require external kinase activity on cytoplasmic tyrosine motifs for signal initiation [153]. While conformational change and aggregation models can explain signalling events at the TCR they so far have not been applied to these other receptors, which may have evolved a common method of signal initiation.

The models reviewed in this section that all propose that T cell triggering is initiated by the segregation or redistribution of the TCR complex from other T cell surface molecules.

The kinetic-segregation (KS) model, proposed by Davis and van der Merwe (1996) [154], builds on an observation by Springer (1990) [155]. He speculated that many of the major TCR signalling molecules in complex with their ligands are significantly smaller than the membrane bound tyrosine phosphatases, such as CD45 and CD148, and cellular adhesion molecules, like LFA-1 (Lymphocyte Function-associated Antigen 1) and ICAM-1 (Inter-Cellular Adhesion Molecule 1), which have large glycosylated extracellular domains. On the binding of these signalling receptors to their ligands on an APC, he proposed that these large molecules would be excluded from the cell-cell contact area on account of their size. This phosphatase exclusion, Springer further postulated, may have an effect on signalling. Another observation that led to the formation of the KS model is the fact that the ITAMs of the TCR complex are

constitutively phosphorylated, as shown by the massive induction of phosphorylation observed in resting T cells when treated with pervanadate, a phosphatase inhibitor [156]. By removing phosphatase activity from the T cell surface environment, the constant equilibrium of tyrosine kinase and phosphatase activity is disrupted in favour of kinases. These observations and those of the interactions of the adhesion molecules CD2/CD58, which are similar in size to TCR/p:MHC, were the basis for the development of the KS model.

It suggests that ligation of agonist p:MHC to TCR forms close contact zones between the membranes of the TCR and APC. Large tyrosine phosphatases, primarily CD45 [157, 158], are excluded from these close contact zones, disrupting the balance of phosphorylation and thus initiating signalling (Figure 1.4). Cognate TCR/p:MHC stable in these zones are triggered due to the extended half-life of the phosphorylated ITAMs, and the resultant recruitment of the cytoplasmic membrane proximal signalling complex, in the absence of phosphatase activity. Non-specific TCRs within these zones are also phosphorylated but without an association with specific p:MHC, they diffuse out of the zone where they are dephosphorylated, preventing full signalling.

In the thirteen years since the proposal of the KS model many of its predictions have been tested in key experiments. The role of the large extracellular domains of tyrosine phosphatases were tested by Irles *et al.* (2003) [159]. By introducing a CD45 chimera containing a smaller extracellular domains of CD45 into CD45 deficient T cells, it was possible to knock out TCR signalling. In the same experiment where a

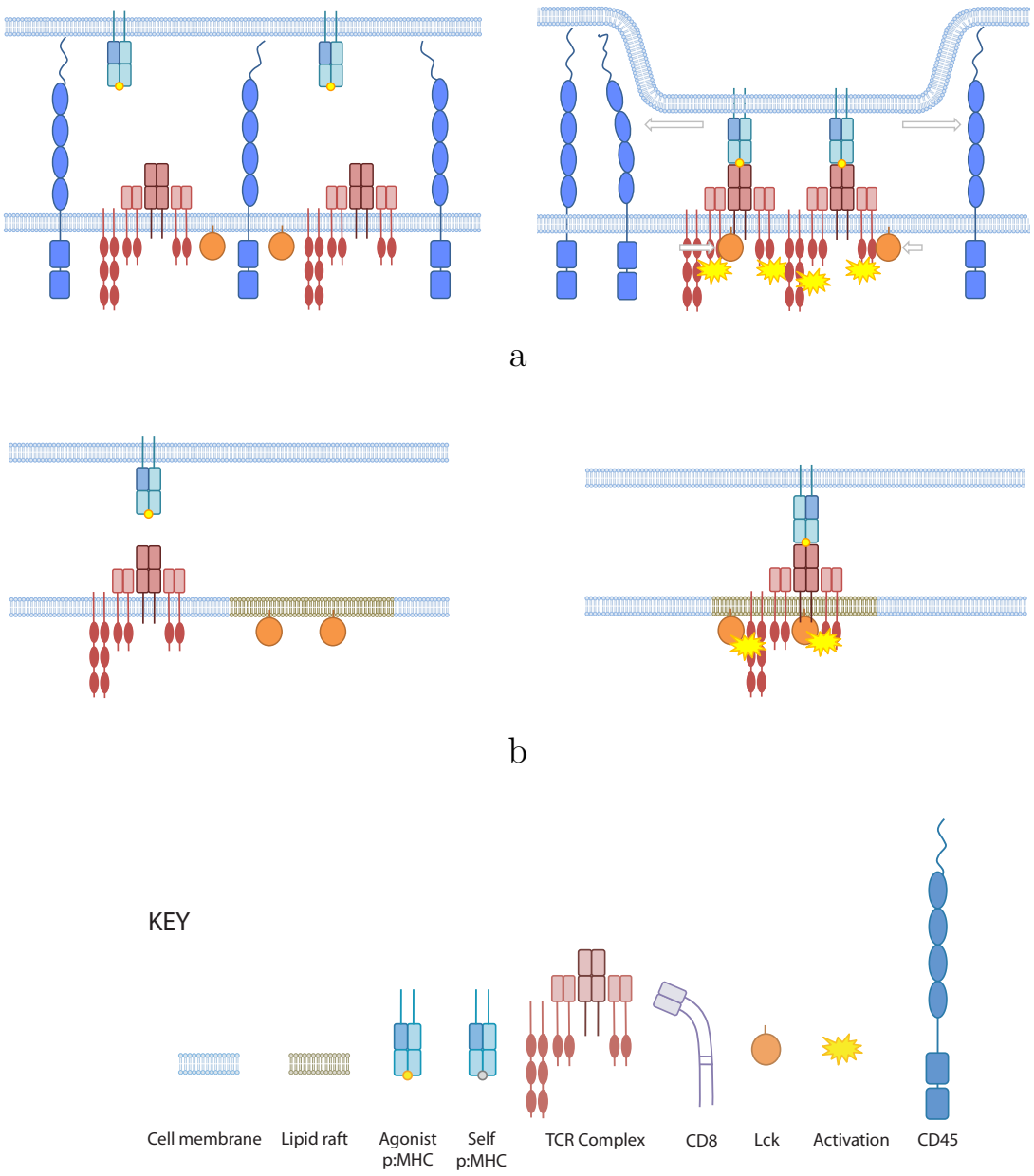


Figure 1.4: Segregation models of T cell activation. (a) The kinetic segregation model. (b) The lipid raft model.

CD45 chimera containing the large extracellular domain of CD43 was introduced, signalling was restored. While this result is supportive of the proposed size exclusion of CD45 in the KS model, the positive regulatory role CD45 plays in the control of Lck (1.3.2) may also be affected by the size of its extracellular domain. To investigate this, similar experiments were performed with CD148, a phosphatase with no Lck regulatory function. In these experiments, like observed with CD45, truncated CD148 inhibited TCR induced activation [160]. The KS model suggests that initial segregation is in principle, solely due to the size of molecules. Therefore by increasing the size of signalling molecules the distance between membranes will increase and they will be exposed to greater phosphatase activity, thus affecting signalling. This prediction was tested by extending the extracellular domain of p:MHC, and thus increasing the dimensions of the TCR/p:MHC interaction [161]. This modification of the p:MHC had no effect on TCR ligation, but did however decrease the level of TCR triggering. The difference in inter-membrane distance caused by the p:MHC size increase was directly observed by electron microscopy. Evidence was also shown in the same study that the ligation of chimeric signalling molecules with the same dimensions as the TCR/p:MHC could also initiate signalling, showing that the segregation from phosphatases alone could cause triggering in signalling molecules.

As described earlier in this chapter, CD45 can be found in the cSMAC [108]. When the cSMAC was initially though to be the site of TCR signal initiation, this evidence contradicted the KS model. However, the initiation of signalling is thought to occur in microclusters that preceded the formation of the cSMAC and from which CD45 is

excluded [102]. More evidence for the exclusion of CD45 from the site of signal initiation has been shown in monoclonal antibody triggering where CD45 is also observed to be excluded from the focal site of TCR activation [100].

While the KS model currently is able to address much of the evidence presented for the initiation of T cell triggering, and be applied to other T cell signalling molecules [153], it can only account for signalling initiated by traditional tyrosine phosphorylation. There is some evidence (reviewed in [162]) that in some instances TCR triggering may occur via alternative pathways and these pathways also should be accounted for by any proposed triggering mechanism.

An adaptation of the KS model is the diffusion trapping model, as proposed by Varma (2008) [163]. In a similar way to the KS model, the diffusion trapping model predicts that signalling is initiated in close contact zones that contain TCR/p:MHC. However, the trapping interactions of TCR/p:MHC within these zones is dependent on the affinity and valency of TCR/p:MHC interactions and the diffusion co-efficient of p:MHC on the APC surface. In this way, this model is able to accommodate aggregation and conformational changes that have been proposed in other models of T cell activation.

The apparent association of many key T cell signalling molecules with lipid rafts suggests a possible role for them in the initiation of T cell signalling [164] (Figure 1.4). Evidence suggests that TCR signalling occurs in areas of the plasma membrane with a distinct cholesterol and glycerophospholipid composition [165], and some theories already described, suggest a role for membrane lipid composition in the conformational

changes of CD3 cytoplasmic domains [124]. Also the apparent association of the co-stimulatory molecule CD28 with lipid rafts and IL-2 production [166] have led some to propose a key role for lipid rafts in T cell co-stimulation [167]. However, the field of lipid rafts remains controversial [168,169], and a mechanism has yet to be proposed that successfully details how TCR ligation causes association with lipid rafts and its role in the initiation of TCR signalling.

As models described in this section show, T cell activation is one of the most studied fields of immunology, but also one where key mechanisms are still not fully understood. Further investigation of the protein interactions involved in T cell activation using new techniques, such as TIRFM, and by investigating triggering in similar signalling molecules, such as the BCR and CD28, will hopefully yield evidence that will give use greater insight into the process of T cell activation.

1.6 CD28

As described previously(1.2.2), the ligation of the TCR to cognate p:MHC is the initiating factor in the activation of T cells. However, this signal is not sufficient to fully activate a naive T cell. For this a second signal is required, a co-stimulatory signal, and this signal is initiated via the co-stimulatory molecules. This two signal model was proposed by Lafferty *et al* (1980) [24], and was confirmed by experimental evidence that showed that the absence of a co-stimulatory signal upon TCR mediated activation of naive T cells resulted in a state of T cell anergy, which was characterised by an inability to respond upon subsequent antigen exposure [30, 170]. The key role

of co-stimulation is to prevent inappropriate T cell activation and this has made it an important area of immunological research. CD28 was the first T cell co-stimulatory receptor to be identified [171], and its identification was soon followed by the discovery of a related receptor CTLA-4 [172] (reviewed in [173]). However, while both CD28 and CTLA-4 bind the same ligands [174,175], evidence suggested that instead of having a stimulatory effect like CD28, CTLA-4 has an inhibitory function [176,177]. This was the first example of such receptors delivering inhibitory as well as activating second signals.

Since the identification of CD28 and CTLA-4, more co-stimulatory and inhibitory receptors, ligands and pathways have been discovered, including further members of the CD28 family, members of the tumour necrosis family and their receptors, and proteins from the TIM gene family (reviewed in [178]).

1.6.1 CD28 function and structure

CD28 was first identified in 1985 as a 44kD disulphide bonded polypeptide dimer, which was an antigen for antibodies that, along with phorbol 12-myristate 13-acetate (PMA), could induce T cell activation and increase IL-2 expression [179]. The human form of CD28 is encoded on chromosome 2q33 [180] and is constitutively expressed on $CD4^+$ T cells and approximately 50% of CD8 T cells [181–183]. At the cell surface, CD28 has a single IgSF V-set domain connected to cell surface by a single transmembrane domain and is expressed as a disulphide linked covalent homodimer [184]. CD28 has no intrinsic enzymatic activity, but mediates its signalling by binding intracellular signalling proteins via the phosphorylation of cytoplasmic tyrosines, which bind the SH2

domains of other signalling molecules. Proline based motifs in the CD28 cytoplasmic domain also play a role in the signalling induced by binding the SH3 domains of other signalling proteins.

CD28 co-stimulation boosts and sustains the effects of TCR signalling by promoting cell survival and the secretion of a variety of cytokines. CD28 especially promotes the production of IL-2 [183, 185–187]. In *Cd28*$^{-/-}$ mice the development of T cells is normal and cytotoxic cells could still be induced to perform cellular killing. However, T cells from these mice generally have a lower sensitivity to decreased antigen and are unable to sustain immune responses [182, 183], illustrating the key co-stimulatory role of CD28. Another proposed role of CD28 co-stimulation is as a factor directing T_H cell differentiation. The observed decrease in T_H cell activity in *Cd28*$^{-/-}$ mice and the absence of IL-4 production in splenic T cells when CD28/B7 interactions were blocked [188, 189], supports this theory. Also naive T cells are biased towards T_H1 differentiation in the absence of CD28 signalling, suggesting CD28 signalling directly influences T_H2 differentiation [181]. A role for CD28 in IL-4 production and therefore T_H differentiation has more recently been highlighted by the identification of a motif in the CD28 cytoplasmic domain, which can influence IL-4 production [190].

The ligands of CD28 are CD80 (B7-1) and CD86 (B7-2), members of the B7 family of molecules [174, 175]. CD80 and CD86 each consist of two IgSF domains, a receptor binding V-set domain, and a membrane proximal C1-set domain [181, 191]. Consistent with their roles in preventing inappropriate T cell activation, the co-stimulatory ligands are only expressed on pAPCs. CD86 is expressed constitutively at low levels

and is rapidly upregulated upon APC activation but CD80 expression is only induced after activation occurs [175, 192]. As mentioned above, CD28 shares its ligands with the inhibitory molecule CTLA-4. Unlike CD28, CTLA-4 is only expressed after T cell activation, when it is trafficked from intracellular compartments to the site of ligation [114]. The inhibitory action of CTLA-4 dampens a T cell response, protecting against the development of autoimmune and auto-proliferative diseases (reviewed in [193–195]). Both CD28 and CTLA-4 are similar in structure [184] and both bind to the B7 ligands via a conserved FG loop in their V-set IgSF domain [196]. Surface plasmon resonance analysis has shown that CD28 dimers are monovalent for B7 ligand binding compared to the bivalent CTLA-4 [197]. This difference is thought to be is caused by steric interference from the occupation of one binding site an another [184]. The precise binding motif of the ligands was identified as the MYPPPY sequence (amino acids 99-104), which was identified by mutational analysis [196]. Despite the similar binding domains, the binding affinities of CD28 and CTLA-4 for each ligand are different. The affinity of CD80 for CD28 is 80% stronger than that of CD86 and the overall affinities for CTLA-4 are ten times stronger than for CD28 [197,198]. These affinity differences relative to CTLA-4, have been cited as a reason for the differential expression of the B7 molecules and a proposed inhibitory role for CD80 [184,197].

1.6.2 CD28 signalling

During early investigations into CD28 signalling, it was unclear if the signalling pathways initiated by B7 ligation turned on a distinct set genes or merely modified the gene regulation resulting from TCR and cognate p:MHC binding. The function of

CD28 signalling was elucidated by profiling gene expression upon co-stimulation, which showed that CD28 signalling amplifies the transcriptional effects of TCR triggering [199,200]. The presence of tyrosine and proline motifs specific for the binding of SH2 and SH3 domains within the CD28 cytoplasmic domain suggests triggering of CD28 can initiate a number of signalling cascades. Although the full extent of signalling initiated by co-stimulation is still being discovered, some of the more well investigated pathways are detailed below.

Upon the initiation of a co-stimulatory signal the CD28 cytoplasmic domain tyrosine motif YMNM undergoes phosphorylation, which then allows the binding of the SH2 domain containing molecules PI3K (phosphoinositide 3-kinase) and Grb2 [201,202]. Like the phosphorylation of the ITAMs of the TCR associated CD3 chains, this phosphorylation is thought to be mediated by Lck and Fyn [203]. PI3K, through the production of a number of lipids activates both Phosphoinositide-Dependent protein Kinase 1 (PDK1) and Protein Kinase B (PKB)/AKT. Multiple pathways that regulate cell survival, glucose metabolism and protein synthesis are then activated by the kinase activity of these proteins [193,204,205].

Grb2, a linker molecule, contains a SH2 domains and two SH3 domains, and as observed in TCR signalling (1.3.2), the exchange factor SOS binds to Grb2 and thus initiates the Ras and MAPK signalling pathways. Grb2 binding of CD28 is also needed for the phosphorylation and activation of Vav-1 [206]. Once phosphorylated, Vav-1 plays many roles. CD28 induced phosphorylation of Vav-1, like that seen in TCR signalling, can activate Cdc42 and trigger a pathway that results in the accumulation

of actin at the site of activation [207]. There is indirect evidence that through the CD28 directed activation of c-Jun Kinase (JNK), Vav-1 can also activate Ras-related C3 botulinum toxin substrate 1 (Rac1) resulting in increased IL-2 promoter activity [206, 208, 209].

In studies of the murine CD28 cytoplasmic domain, a mutation of the residue Y188, found in the tyrosine motif YMNM, has been shown to diminish CD28 mediated NF-κB activation [210]. Recent evidence suggests that CD28 is able to initiate NF-κB activation via a pathway involving PKCθ and Grb2, independently of the TCR [211]. It is unknown how this tyrosine residue may interact with this proposed pathway, but evidence does suggest that CD28 engagement plays an important role in the activation of the NF-κB transcription factor [212].

Two proline motifs (PRRPGP and PYAP) lie downstream of the YMNM tyrosine region. A member of the Tec family kinases, Itk, has been observed binding to the PRRPGP region via its SH3 domain [203, 206], but the role of this binding is unclear [173]. The PYAP motif within the CD28 cytoplasmic domain has a suggested role in the localisation of CD28 to the cSMAC. PKCθ binds to the PYAP motif and some reports suggest that it is joined by an actin-binding scaffold protein, FLNA, which allows PKCθ and CD28 migration to the cSMAC via "lipid rafts" [106, 210, 213, 214].

1.6.3 CD28 superagonist antibodies

As stated by the two signal hypothesis, is not possible to activate the T cell through CD28 ligation alone, as only in conjunction with TCR stimulation will successful activation of a T cell be achieved. This activation is not only possible using natu-

ral ligands [215], but also monoclonal antibodies (mAbs) to the TCR complex and CD28 [179]. However, certain mAbs specific to CD28 have been shown to be able to activate T cells in the absence of any other stimulus both *in vitro* and *in vivo* [216,217]. These stimulatory mAbs have been termed "superagonist" mAbs [218]. Through characterisation of rat, human and mouse CD28 superagonist mAbs, a link has been established between the stimulatory activity of these mAbs and their CD28 epitope. Binding of CD28 mAbs that can activate T cells in a superagonistic manner is disrupted by mutations in the C″D loop of CD28, which is located in a membrane proximal position and at opposite ends of the molecule to the ligand binding MYPPPY motif [218,219]. Further investigations showed that CD28 mAbs that could only stimulate CD28 under co-stimulatory conditions, bound to a more membrane distal epitope, specifically the MYPPPY motif [218]. The other key characteristic of these superagonistic mAbs is that they are not active in solution and must be immobilised to induce T cell activation [218]. Several explanations for this epitope-function relationship have been proposed. One, is that co-stimulatory mAbs mimic the monovalency of B7 binding to CD28, whereas superagonist mAbs bivalently bind CD28, causing the formation of a cross-linked network of CD28 and mAb that initiates signalling [219]. However, this proposal is unlikely as at least one co-stimulatory mAb has been seen to cross-link CD28 [184]. A second mechanism of action proposed for CD28 superagonists is based on the KS model of T cell triggering. Combining the epitope topology dependent activation seen in superagonists and the requirement for immobilisation for their activity, it is proposed that the binding of CD28 mAbs brings the CD28 containing cell

membrane and the immobilising surface close together. The differences in epitope distance from the membrane between superagonist and co-stimulatory mAb means that superagonist binding brings the two surfaces close enough together to sufficiently exclude large cell surface phosphatases and initiate signalling. Co-stimulatory mAb binding, while still bringing the cell and immobilising surface close together, results in sufficient distance between the surfaces so that some phosphatases can access the zone of CD28 signalling reducing the strength of this signal so that activation requires additional stimulation through the TCR [153,184] (Figure 1.5).

In vitro, CD28 superagonists induce $CD4^+$ and $CD8^+$ T cell proliferation and high levels of IL-2 secretion [217]. The impact of CD28 superagonist mAb *in vivo* stimulation was first shown in rat, where treatment with a CD28 superagonist resulted in splenomegaly and lymphadenopathy [217]. Further *in vitro* and *in vivo* investigations suggested that these mAbs could stimulate the expansion of the $CD4^+CD25^+$ T cell subset, known as regulatory T cells (T_{reg} cells) [160]. This subset of T cells, identified by expression of CD4, CD25 and the transcriptional regulator Foxp3, control pathogenic auto-reactive immune responses and play an important role in the tolerance of self-antigens (see). Based on this T_{reg} cell proliferative activity, the effect of CD28 superagonists in animal auto-immune disease models was also tested. CD28 superagonist induced expansion of T_{reg} cells prevented the rejection of rat cardio allografts [220] and also alleviated the symptoms of experimental autoimmune neuritis within Lewis rats [221,222].

The successful treatment of autoimmune diseases in animal models with CD28 su-

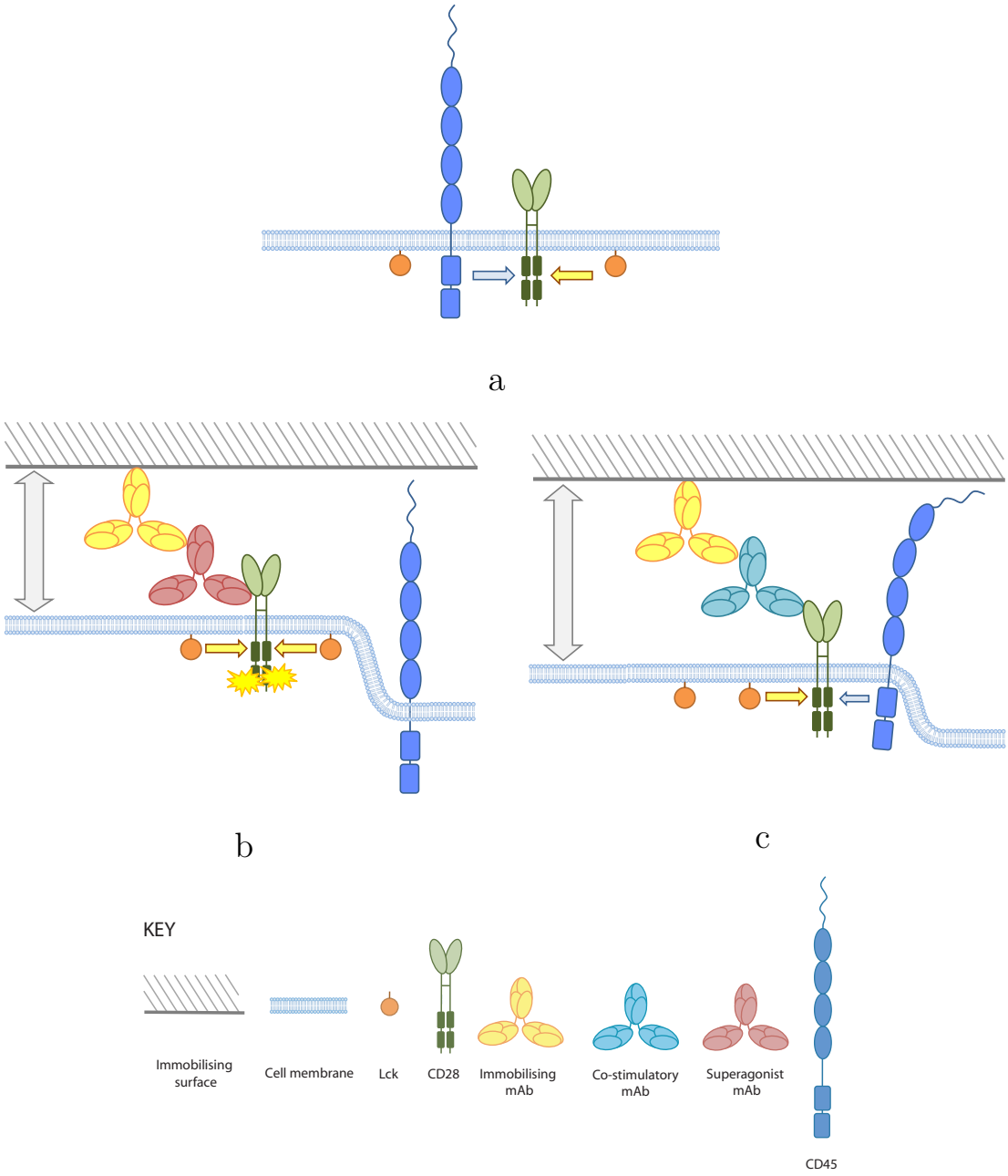


Figure 1.5: The mechanism of CD28 superagonism as predicted by the Kinetic Segregation Model. (a) On a resting T cell CD28 is in a state of phosphorylation equilibrium, being able to be both phosphorylated by intracellular kinases like Lck and dephosphorylated by phosphatases such as CD45. (b) When stimulated with immobilised superagonist mAb, the distance between the cell and immobilising surface are such that large phosphatases are excluded from the binding area. The absence of CD45 allows kinases to fully phosphorylated CD28 and so signalling is initiated. (c) In the same conditions when stimulated with a co-stimulatory mAb, the more membrane distal epitope of the mAb means that the distance between the cell and immobilising surfaces is greater. This increase in distance allows CD45 some access to the binding region allowing some dephosphorylation of CD28. The reduction in phosphorylation state of CD28 within the area of binding means that a second signal via the TCR is required for full activation.

peragonists led to the possibility that these mAbs would have some therapeutic effects in humans. However, the phase I clinical trial of human CD28 superagonist TGN1412, showed that the relatively benign behavior of CD28 superagonist mAbs observed in animal models does not occur in humans. Clinical trial participants suffered a life threatening cytokine storm that led to multiple organ failure [223]. In the aftermath of this disaster, much research was put into the causes of the vastly different human immune modulatory response, but the reasons for the human response are still not completely clear [224–226]. However, the massive stimulatory effects observed do indicate that these antibodies are able to stimulate the immune system via CD28 in a novel manner and require more research.

Subsequent research investigating the signalling pathways initiated by CD28 superagonists has confirmed earlier work that showed superagonist mAbs could induce pathways that were distinct from those initiated by CD28 mediated co-stimulatory signalling. No engagement of the co-stimulatory Ras/P13K/PKB pathways are observed [227, 228] in superagonist signalling, but the SLP-76 signalosome is shown to be active and seems to play an important role in the superagonist signalling outcome [227, 229, 230]. Also while there is no evidence to suggest superagonist signalling involves the phosphorylation of the TCR complex, CD28 superagonistic T cell activation can only be observed in cells expressing functional TCR, CD3 chains and ZAP-70 [227, 230, 231].

1.7 PD-1

As exemplified by CTLA-4, additional signalling receptors on T cells can not only provide the crucial second signal to initiate and sustain activation of T cells, but they can also contribute a negative second signal that modulates and inhibits T cell function. As mentioned above, the CD28/CTLA-4 CD80/CD86 pathways are the best characterised of the ligand/receptor interactions modulating TCR signalling. However, other members of the CD28 and B7 family have been identified that have broadened our knowledge of the pathways that control T cell activity.

1.7.1 PD-1 expression

One such additional member of this family is Programmed cell death 1 (PD-1, PCDC-1, CD279), first identified by subtractive hybridisation of genes expressed in two T cell hybridoma lines undergoing programmed cell death [232]. However, its function as a molecule important in immune regulation was identified through the *Pdcd1*$^{-/-}$ mouse, which suffers an autoimmune phenotype, resulting in cardiomyopathy, lupus like arthritis and glomerulonephritis [233, 234]. This phenotype suggests an immune inhibitory role for PD-1, like that of CTLA-4. However, the phenotype of the *Pdcd1*$^{-/-}$ mouse is vastly different from the *CTLA-4*$^{-/-}$ mouse, which suffers from a massive lymphoproliferative disorder that occurs within weeks of birth [176]. Although both molecules have immune inhibitory roles, PD-1 deficiency leads to autoimmune diseases associated with immune dysfunction observed in later life, suggesting a role in the maintainence of peripheral tolerance to self.

PD-1 is expressed on T cells, B cells, NKT cells, activated monocytes and dendritic cells [235–237]. Expression is not constitutive, as PD-1 is not expressed on resting T cells, but is only expressed after activation through the TCR (or after BCR induced activation on B cells) [238, 239]. Upon TCR ligation, surface expression is observed within 24 hours and there is some evidence to suggest that, in certain T cell subsets, PD-1 is stored in intracellular vesicles in a similar manner to that observed with CTLA-4, before trafficking to the synapse upon T cell activation [240]. The ligands for PD-1 are PD-L1 (B7-H1, CD274) [241, 242] and PD-L2 (B7-DC, CD273) [243, 244], each of which have distinct expression patterns. PD-L1 is constitutively expressed on murine T and B cells, macrophages, dendritic cells, bone marrow cultured stem mast and mesenchymal stem cells [245, 246]. It is also widely expressed on a variety of non-haematopoetic cell types from the brain to lungs and muscle cells, as well as being expressed at sites of immune privilege such as the eye and placenta [235, 236]. PD-L2 has a more restricted expression profile, being only inducibly expressed on dendritic cells, macrophages and cultured bone marrow derived mast cells [235, 236].

1.7.2 PD-1 function

Since the PD-1 - PD-L pathways were identified, its role in inducing and maintaining peripheral tolerance has been confirmed. In addition, a recent discovery that the expression of PD-1 is an important factor in the immune response to viral infection [247], has broadened our understanding of the wider roles that this inhibitory molecule has within the immune system.

The role of PD-1 in the induction of tolerance has been shown to start in the thymus

where it can be found on maturing thymocytes. It is expressed on $CD4^{-}CD8^{-}$ double negative T cells where it is required for developmental progression post TCRβ gene rearrangement [248]. PD-1 expression is then upregulated at the $CD4^{+}CD8^{+}$ double positive stage of development, when interaction with PD-L1 influences the successful outcomes of functional TCR expression, as well as contributing to positive and negative thymocyte selection signals [248–250]. From this initial influential role in central tolerance, the expression of PD-1 and its ligands also act as regulators of peripheral tolerance.

In tissues with immune privilege such as the placenta and the eye, the PD-1 - PD-L pathway is thought to protect these sites from the immune response. PD-L1 and PD-L2 can be found expressed within the placenta and the presence of blocking PD-L1 antibody has been shown to lead to increased placental T cell infiltration and fetus abortion rate [251–253]. Constitutive expression of PD-L1 in many parts of the eye also suggest a tolerance role, which was confirmed in studies showing that the rejection of corneal allografts was accelerated by administering blocking PD-1 or PD-L1 antibodies [254].

A large body of evidence has emerged on the roles of PD-1 in peripheral tolerance through the study of the expression and interactions of this molecule and its ligands in mouse models of autoimmune disease. Experiments involving the non-obese diabetic (NOD) murine model of diabetes have shown that blockade of PD-1 and PD-L1 causes rapid onset diabetes and the emergence of high levels of islet antigen specific T cells from the spleen [255]. In a model of therapeutic remission in NOD mice, Fife

et al (2006) [256], showed that the PD-1 - PD-L1 interaction was essential for the reduction of antigen specific T cell proliferation and inflammatory cytokine production. Experimental autoimmune encephalomyelitis (EAE) is used to model the human demyelinating disease, multiple sclerosis [257,258]. In this model, PD-1 blockade results in the acceleration of EAE onset, an increase in antigen specific interferon-γ producing T cells and antigen specific antibodies [259]. The control of the self reactive T cells in this model was found to be due to PD-1 - PD-L1 interactions but not interactions with PD-L2 [260].

With the clear role PD-1 plays in the regulation of autoimmune diseases, it is not surprising that single nucleotide polymorphisms in PD-1 have been shown to be associated with several human autoimmune diseases. These include rheumatoid arthritis, Grave's disease, type I diabetes and systemic lupus erythematosis (reviewed in [261]). The majority of the polymorphisms that correlate to disease are found in PD-1 intronic sequences that are thought to cause mRNA instability and poor PD-1 expression [261].

Other roles for the PD-1 - PD-L pathways have been found in both tumour and transplantation immunity (reviewed in [262]). PD-L1 expression can be found on many tumour types and there is evidence that tumour lymphocyte infiltrates have increased levels of PD-1 expression, aiding tumour cell tolerance [248]. Both PD-1 and PD-L1 are also up-regulated on alloreactive T cells post transplant, with additional PD-L1 upregulation on the allografts themselves [263,264]. This suggests a role for PD-1 in both the control of the host immune response to transplanted tissue and the down

regulation of the T cell response to tumours that may lead to tumour progression.

An important, more recent discovery has been the role of PD-1 - PD-L interactions in the immune response to chronic viral infection. T cells in individuals suffering from long term viral infectious diseases, such as human immunodeficiency virus (HIV) or hepatitis C virus (HCV) often show an "exhausted" phenotype, where T cells no longer have effector function. This state can often result in T cell death [247]. This process aids the progression of such diseases, as it prevents an effective ongoing immune response and the prospect of viral control and clearance. As described above, PD-1 is up regulated on T cell activation and in chronic viral infection, $CD8^+$ specific T cells continue to express high levels of PD-1. This was first seen in a mouse lymphocytic choriomeningitis virus (LCMV) model [247], where a comparison with an LCMV strain that could be effectively cleared, showed that the dysfunctional T cell phenotype in a chronic infection was due to PD-1 expression. In the same study, it was also found that by blocking the PD-1 - PD-L1 interaction it was possible to restore T cell function and reduce viral load. These effects have since been observed in the immune response to many other chronic viral infections such as HIV, HCV and hepatitis B virus (HBV) [265–267].

1.7.3 PD-1 structure and signalling

PD-1 is expressed at the cell surface as a monomer, with an extracellular IgSF V-set domain, transmembrane domain and an intracellular domain containing an immunoreceptor tyrosine based inhibitory motif (ITIM) and a immunoreceptor tyrosine based switch motif (ITSM) [268,269]. Although it is grouped in the same family as CD28, it

only shares 23% protein sequence homology with CD28 and unlike other members of the CD28 family, such as CTLA-4 and inducible T cell co-stimulator (ICOS), it lacks an extracellular disulphide bond that induces dimerisation [194].

Like other co-signalling molecules, the effects of signalling through PD-1 are only seen when engaged simultaneously with the TCR or BCR. On ligand binding, the two tyrosine motifs of the PD-1 cytoplasmic tail are phosphorylated and then recruit phosphatases which modulate antigen receptor signalling. The signal pathway of PD-1 directly influences the signals transduced through the TCR or BCR, by altering the phosphorylation state of key intermediates on these pathways . The effects of PD-1 ligation are strongest in T cells when the TCR signal is weak, and PD-1 inhibition is abrogated by CD28 or IL-2 signalling [242, 270]. While both PD-1 tyrosine motifs are phosphorylated upon signal initiation, it is thought that signalling via the ITSM motif is responsible for inhibitory function, as mutation of the ITSM, but not ITIM, results in loss of inhibitory function [271]. Two phosphatases bind phosphorylated PD-1, SH2-domain containing tyrosine phosphatase 1 (SHP-1) and SH2-domain containing tyrosine phosphatase 2 (SHP-2), however SHP-2 associates only with the ITIM whereas both SHP-1 and 2 bind the ITSM motif [272]. Evidence that ligation of PD-1 must occur in close proximity to the area of antigen receptor ligation, suggests that inhibition by PD-1 is mediated through the recruitment of the PD-1-associated phosphatases to the site of the antigen receptor signalling complex [262]. PD-1 ligation affects some of most membrane proximal TCR signalling events as well as suppressing the PI3K pathway, which is regulated by CD28. Phosphorylated PD-1 associated

SHP phosphatases inhibit the phosphorylation of CD3ζ, ZAP-70 and PKCθ [273] while the inhibition of the PI3K pathway results in the downstream inhibition of the kinase Akt, which regulates glucose metabolism and cell survival. The inhibition of Akt is a mechanism also used by CTLA-4 to modulate T cell activation [273]. However the way Akt inhibition is achieved is different, which goes some way to explain the differences in their inhibitory activity. By targeting Akt directly, CTLA-4 only inhibits IL-2 cytokine production, thus preventing cell cycle progression, whereas the inhibition of PI3K by PD-1 further up the signalling chain similarily inhibits IL-2 production, but also glucose metabolism and production of Bcl-xL, a protein key for cell survival .

1.8 Aims of this thesis

1.8.1 Investigation of epitope dependent mAb signalling by PD-1

The effects of superagonistic CD28 mAbs *in vitro* and both in animal models and humans has provided new insights into the varied effects of immune modulating mAbs, as well as highlighting new information on the function and signalling of CD28. The ability of superagonist mAbs to trigger T cells directly through CD28 in the absence of conventional activating signals has been linked both to their epitope location and their functional requirement for immobilisation.

An interpretation of these key characteristics using the KS model of T cell triggering suggests that the activating ability of CD28 superagonists is due principally to epitope location. This prediction, coupled with the knowledge that many of the signalling and functional characteristics of CD28 are not characteristic of it alone, sug-

gests that mAbs capable of triggering other T cell signalling molecules in a similar fashion could be produced. Such antibodies could not only be used to enhance the study of such signalling molecules, but also, due to their novel triggering abilities, be developed into immunomodulatory therapeutics.

This thesis investigates the characteristics and signalling properties of mAbs raised against an inhibitory member of the CD28 family of molecules, PD-1. In particular this thesis aims to investigate the role of epitope location of PD-1 mAbs and identify any mAbs with characteristics suggestive of superagonist-like agonist activity. Once identified, a further aim of this work is to evaluate the activity of these antibodies for activation of PD-1 signalling using an *in vitro* method that allows direct comparison between CD28 and PD-1 mAb superagonistic stimulation.

1.8.2 Investigation into the mechanism of CD28 superagonism

These studies of mAb-induced triggering of PD-1 suggested that mAb cross-linking may play a role in the mechanism of action of stimulatory mAbs with a membrane proximal epitope. Further work in this thesis therefore returns to the CD28 model to investigate the factors in the triggering mechanism of CD28 superagonism. This was achieved using assays for superagonism established previously in the thesis to directly investigate the influence of mAb epitope location on their activating ability. The ultimate aim of this thesis is to fully understand the mechanism of antibody superagonism, which may increase our understanding of how the phenomenon could be utilized therapeutically and may give some insight into how T cell signalling molecules are triggered.

Chapter 2

General Methods

2.1 Molecular cloning and vector construction

2.1.1 Molecular cloning overview

To create vectors that allowed the specific protein expression in the appropriate cell lines, standard molecular biological techniques were used [274]. In overview, the genes of interest were amplified from a template sequence by polymerase chain reaction using specific oligonucleotide primers. The amplified genes were purified and inserted into the pCR®4-TOPO® using the TOPO® reaction. The gene of interest was then digested out of pCR®4-TOPO®using specific restriction sites contained in the 5′ and 3′ oligonucleotide primers used to amplify the genes, and ligated into a specific expression vector. The vectors were transformed into *E.coli* and colonies containing the correctly orientated gene were selected using antibiotic selection and polymerase chain reaction. After the sequence of the gene of interest was confirmed, large stocks of the vectors were prepared for use in further applications.

2.1.2 Vectors used in this thesis

pCR®4-TOPO® This is a sequencing vector that allows direct insertion of fresh *Taq* amplified DNA using a topoisomerase reaction. *Taq* polymerase adds a single deoxyadenosine (A) to the 3′ end of amplified DNA. Linearised pCR®4-TOPO®vector has a single thymidine (T) overhang and a covalently bound topoisomerase I. When

this vector is added to a reaction containing the freshly amplified DNA the isomerase ligation activity results in a one stage cloning reaction. The vector contains M13 forward and reverse priming sites for either side of the cloning site which allows the use of common sequencing oligonucleotides independent of inserted DNA sequence. The backbone of the vector contains both ampicillin (*bla*) and kanamycin resistance genes allowing bacterial selection of transformed vectors.

pHR-SIN-BX-IRES-EM pHR vectors are based on the HIV genome and allow the production of non-replicating lentiviral particles which can be used to stably infect target cells [275]. Long terminal repeats (LTR) flank the inserted cloned gene. The distal LTR contains the δU3 mutation that abolishes the transcriptional activity of the LTR and means the virus produced is self inactivated. The vector also contains the Spleen focus forming virus (SFFV) viral promoter and an additional Woodchuck hepatitis virus post-transcriptional regulatory element (WPRE) enhancer at the $3'$-end. An internal ribosome entry site (IRES) downstream of the cloned gene allows for translational initiation of a emerald GFP (emGFP) after the cloned gene in the mRNA that allows confirmation of the insertion of the vector into the host cell genome on expression. The vector confers resistance to ampicillin in bacterial cells.

p8.91 The p8.91 vector is used in conjuction with pHR-SIN-BX-IRES-EM and contains the structural proteins and enzymes needed to generate an infectious viral particle [275]. The proteins gag, pol, tat, and rev are under the control of a Cytomegalovirus immediate-early (CMV-IE) promoter and the plasmid also encodes an ampicillin re-

sistance gene.

pMDG The pMDG vector contains viral coat proteins which used with p8.91 and pHR-SIN-BX-IRES-EM allows the expression of an functional non-replicating infectious virus [275]. It encodes the Vesicular stomatitis virus envelope protein gene (VSV-G) that acts as a pseudotyped coat protein for the virus. VSV-G is promiscuous in the glycosylation motifs it binds to, allowing the produced virus entry into a variety of mammalian cells. An upstream CMV IE promoter and β-globulin intervening sequence sequence (IVS) promotes efficient expression of VSV-G and the vector confers ampicillin resistance in bacterial cells.

pGFP^2-N3 The Bioluminescence Resonance Energy Transfer (BRET) assay is used to detect protein-protein interactions at the cell surface. The vector pGFP^2-N3 is used in conjunction with prLuc-N3 in this assay. A multiple cloning site upstream of the GFP^2 gene allows a cloned gene to be fused to the GFP^2 fluorophore in the N3 reading frame. The genes are under the control of the CMV-IE promoter which causes constitutively high expression. GFP^2 is a variant of GFP which is excited by light at a wavelength of 405nm and emits light at 515nm. The vectors also carries a gene for zeocin resistance that allows selection in both mammalian and bacterial cells.

pRluc-N3 The pRluc-N3 vector is similar in structure to the pGFP^2-N3 expression vector. It has a similar cloning region which allows the fusion of a *Renilla* luciferase to an inserted cloned gene. *Renilla* luciferase is a bioluminescent protein from the

sea pansy *Renilla reniformis*, which has a maximal emission wavelength of 480nm in the presence of a specific substrate, coelenterazine. It carries a neomycin resistance gene for selection in mammalian cells and a kanamycin resistance gene for selection in bacteria.

2.1.3 Molecular biological methods

Polymerase chain reation

Polymerase chain reaction was used to amplify genes of interest for insertion into expression vectors. Sequence specific oligo nucleotide primers were designed for the 5′ and 3′ ends of the amplified DNA and contained specific restriction endonuclease sites to enable insertion into the applicable vectors. The details of the specific primer sequences and digestion sites used can be found in the appropriate chapters. The following general PCR mix was used for amplifying genes from template plasmid or cDNA.

	Company	Concⁿ	Volume
Polymerase Buffer	Roche	10 ×	4.0 μl
dNTP	Bioline	10 mM	0.5 μl
ddH_2O	Sigma	—	32.4 μl
Primer 1	Sigma-Genosys	10 μM	0.8 μl
Primer 2	Sigma-Genosys	10 μM	0.8 μl
Template	—	100 ng/μl	1.0 μl
DNA Polymerase	Roche	5 U/μl	0.5 μl

All PCR reactions were performed using a Tetrad DNA Engine (RJ Research). To ensure accurate amplification, FastStart High Fidelity Enzyme blend (Roche) was used in all initial PCR reactions. It contains a hot start Taq DNA polymerase and a thermostable proofreading protein which enables accurate amplification up to 5kb.

For PCR reactions using plasmid template DNA the following standard cycling programme was used.

	Step	Temp.(°C)	Time
1	Initialisation	95	2 min
2	Denaturation	94	30 s
3	Annealing	55	30 s
4	Extension	72	1 min/kb
	Repeat 2→4		29 ×
5	Final Extension	72	10 min
6	Cooling	4	∞

For genes amplified from cDNA, the following touchdown cycling programme was used to increase specificity.

	Step	Temp.(°C)	Time
1	Initialisation	95	2 min
2	Denaturation	94	30 s
3	Annealing	64	30 s
4	Extension	72	1 min/kb
	Repeat 2→4		5 ×
5	Denaturation	94	30 s
6	Annealing	58	30 s
7	Extension	72	1 min/kb
	Repeat 5→7		5 ×
8	Denaturation	94	30 s
9	Annealing	53	30 s
10	Extension	72	1 min/kb
	Repeat 8→10		25 ×
11	Final Extension	72	10 min
12	Cooling	4	∞

Many proteins were created that contained the sequences of two or more different genes. To generate this DNA sequence a chimeric PCR was used. In the first part of the process a standard PCR reaction and conditions were used to amplify the two different genes that are to be fused. This was performed using standard external

primers but internal overlapping primers (∼20 nucleotides) at the intersection of the two genes. The resultant gene fragments with complementary internal sequences where then added as a template to a second reaction with external 5′ and 3′ primers. The PCR reaction for the chimeric PCR is as follows.

	Company	Concⁿ.	Volume
Polymerase Buffer	Roche	10 ×	4.0 μl
dNTP	Bioline	10 mM	0.5 μl
Primer 1	Sigma-Genosys	10 μM	0.8 μl
Primer 2	Sigma-Genosys	10 μM	0.8 μl
Gene A template DNA	—	—	5.0 μl
Gene B template DNA	—	—	5.0 μl
DNA Polymerase	Roche	5 U/μl	0.5 μl
ddH_2O	Sigma	—	33.5 μl

The number of cycles were decreased in the chimeric PCR reaction due to the high concentration of template that is incorporated into the final amplified product.

	Step	Temp.(°C)	Time
1	Initialisation	95	2 min
2	Denaturation	94	30 s
3	Annealing	55	30 s
4	Extension	72	1 min/kb
	Repeat 2→4		15 ×
5	Final Extension	72	10 min
6	Cooling	4	∞

PCR was also used to screen bacterial colonies for the correct insertion of genes in expression vectors. The oligonucleotide primers used are described in the appropriate chapters. A less accurate Taq polymerase was used in these reactions as accurate proof reading activity was not required for the PCR screening reactions. This also meant a different PCR mix was used.

	Company	Concⁿ.	Volume
Polymerase Buffer	New England Biolabs	10 ×	1.5 μl
dNTP	Bioline	10 mM	0.2 μl
ddH_2O	Sigma	—	12.5 μl
Primer 1	Sigma-Genosys	10 μM	0.3 μl
Primer 2	Sigma-Genosys	10 μM	0.3 μl
Colony sample	—		
DNA Polymerase	New England Biolabs	5 U/μl	0.2 μl

The screening process involved spiking bacterial colonies from LB agar plates directly into the PCR reactions, so an additional bacterial lysis step was added into the PCR programme as follows.

	Step	Temp.(°C)	Time
1	Bacterial lysis & initialisation	95	10 min
2	Denaturation	94	30 s
3	Annealing	55	30 s
4	Extension	72	1 min/kb
	Repeat 2→4		34 ×
5	Final Extension	72	10 min
6	Cooling	4	∞

Agarose gel DNA separation

To resolve and quantify DNA produced from PCR amplification and other downstream processes, agarose gels were used. For general resolution 1% (w/v) high-quality agarose (SeaKem LE Agarose, BioWhittaker) was disolved in Tris-borate EDTA (TBE) (Sigma). The agarose was melted in the microwave for 90 seconds and ethidium bromide added to a concentration of 0.5μg/ml. 50ml of the agarose was then poured into a gel tank containing the appropriate gel combs. For a higher resolution of DNA 1.5% (w/v) agarose gels were cast. Prior to loading, DNA samples were mixed with

loading buffer (40% (w/v) sucrose, bromophenol blue/xylene cyanol), then loaded and the gels run at 70mA for 60 minutes with a PowerPac 300 (BioRad). DNA bands were resolved via UV illumination and DNA bands excised using a clean scalpel. For general use, DNA samples were purified from agarose gel using QIAquick Gel extraction kit (Qiagen). For use in TOPO cloning reactions GenElute® agarose spin columns (Sigma) were used.

DNA restriction endonuclease digestion

DNA was cleaved at specific sites using DNA restriction endonuclease digestion. Purified DNA was added to the following digestion mix and incubated for 1 hour at the enzymes optimum activity temperature (in most cases 37°C).

	Company	Conc^{n}.	Volume
Restriction buffer	New England Biolabs	10 ×	5.0 μl
BSA	New England Biolabs	10 ×	5.0 μl
ddH_2O	Sigma	—	8.0 μl
DNA	—	—	30.0 μl
Restriction enzyme	New England Biolabs	10 U/μl	2.0 μl

In cases where DNA was digested with more than one restriction endonuclease the enzymes were used together in the same reaction as long as both worked efficiently in the same restriction buffer. Where two enzymes required different buffers, sequential digests were performed purifying the DNA between each reaction using QIAquick PCR purification kit (Qiagen).

Alkaline phosphatase treatment of vectors

To ensure that digested vectors in ligation reactions remain linearised and to allow efficient ligation with inserts, the $5'$ phosphate groups were removed from cleaved DNA using calf intestine alkaline phosphatase (New England Biolabs). The restriction digestion reactions were not purified, and added directly to the alkaline phosphatase reactions that were incubated for 1 hour at 37°C.

	Company	Concⁿ	Volume
Phosphatase buffer	New England Biolabs	10 ×	10.0 μl
Alkaline phosphatase	New England Biolabs	10 U/μl	2.0 μl
ddH_2O	Sigma	—	38.0 μl
Digested DNA	—	—	50.0 μl

All alkaline phosphatase reactions were run on a agarose gel to visualise digested vector and purified to ensure that no undigested vector would contaminate subsequent ligations.

Insert ligation into vectors

Digested DNA inserts were ligated into digested and alkaline phosphatased vector using the following ligation reaction mix.

	Company	Concⁿ	Volume
Ligase buffer	New England Biolabs	10 ×	2.0 μl
Insert DNA	—	Various	10.0 μl
Vector DNA	—	100 ng	5.0 μl
ddH_2O	Sigma	—	2.0 μl
T4 DNA ligase	New England Biolabs	400 U/μl	1.0 μl

To check the efficiency of ligations, control reactions were performed containing prepared vector without insert and prepared vector in the absence of ligase. All reactions were incubated at 16°C overnight.

Chemical transformation of chemically competent *E.coli*

E.coli for use in the chemical transformation of vectors and ligations were prepared by innoculating 5ml sterile Luria Bertani broth (LB broth) with TOP10 *E.coli* (Invitrogen). This was incubated overnight at 37°C at 225rpm. 1ml of this culture was used to innoculate 30ml LB broth incubated for 2.5 hours at 37°C, 225rpm. The optical density of the culture at 600nm was checked to be between 0.3 and 0.6nm and the cells were centrifuged for 15 minutes at 2000g and resuspended in ice cold transformation and storage solution (TSS), the recipe for which is as follows.

	Company	Conc^{n}.	Amount
DMSO	Sigma	100 %	5.0 ml
Polyethylene glycol 6000	Sigma	—	10.0 g
$MgCl_2$	Sigma	1 M	5.0 ml
LB broth	Sigma	—	90.0 ml

100μl of the chemically competent cells were aliquoted into 1.6ml eppendorf tubes on ice. To these cells 10μl of a ligation reaction was added or 5μl of undigested supercoiled vector (10ng/μl) and mixed gently by flicking the tube. The reactions were incubated on ice for 15 minutes before being heat shocked at 37°C for 5 minutes. After the heat shock, the cells were briefly incubated on ice, whilst 400μl LB broth was added to each reaction. They then were incubated at 37°C for one hour before plating

out. Antibiotic at the appropriate concentration was added to molten agar (Sigma, prepared from agar tablets and autoclaved) and poured into 90mm petri dishes (Sterilin) to set and dry at 37°C for 1 hour. The transformed cells (300μl) were spread out on the plates using a ethanol sterilised glass spreader. The petri dishes were incubated at 37°C overnight (approximately 16 hours) and the resultant colonies counted and PCR screened for correct gene insert and orientation.

TOPO® TA Cloning®

DNA sequences were cloned directly into the pCR®4-TOPO® vector for DNA sequencing and sub-cloning into specific expression vectors. In brief, freshly amplified DNA was gel purified using GenElute® agarose spin columns (Sigma). The purified DNA was then added to the TOPO® TA cloning® reaction (Invitrogen).

Reagent	Amount
PCR product	2.0 μl
Salt Solution	1.0 μl
Water	1.0 μl
TOPO®vector	1.0 μl

The reaction was mixed gently and incubated for 5 minutes at room temperature. 2μl of the cloning reaction was added to a vial of One Shot® Chemically Competent *E.coli* (Invtrogen) and mixed gently. After a 5 minute incubation on ice, the cells were heat shocked for 40 seconds at 42°C, placed back on ice and 250μl SOC added to the cells. The cells are then shaken horizontally (200rpm) at 37°C for 1 hour. The transformed cells (300μl) were spread out on plates using an ethanol sterilised glass

spreader. The petri dishes were incubated at 37°C overnight (approximately 16 hours) and the resultant colonies counted and PCR screened for correct insert and orientation.

Vector purification

Expression vectors were purified for DNA sequencing and other downstream processes from overnight bacterial cultures using the appropriate antibiotic selection. Small scale purifications were carried out using PureLink® HiPure Plasmid Miniprep kit (Invitrogen), purifying plasmid from 5ml bacterial cultures. Larger extractions from 100ml bacterial cultures were performed using QIAGEN Plasmid Midi Kit (Qiagen). Both purification methods use a modified alkaline lysis procedure, followed by the binding of plasmid DNA to an anion-exchange resin under low pH and salt conditions. DNA remains bound to the resin whilst RNA, proteins, carbohydrates and other impurities are washed away with a medium-salt wash. Plasmid DNA is eluted under high salt conditions, precipitated using propan-2-ol and pelleted by centrifugation. The resultant pellet is washed with 70% ethanol to remove salt residues and resuspended in TE buffer (10nM Tris-HCl, 1mM EDTA, pH 8.0) to an appropriate concentration. The DNA concentration was measured by UV spectrophotometry. DNA was diluted 1 in 20 and its absorbancy measured at 260nm. To ascertain the quality of the extracted DNA, absorbancy at 280nm was also recorded. Only DNA with a OD-260nm/OD-280nm ratio between 1.8 and 2.0 was used in further applications.

DNA sequencing and analysis

DNA sequencing was carried out at the Weatherall Institute of Molecular Medicine (Oxford University) sequencing core on a capillary ABI-3730 DNA analyser using Applied Biosystems BigDye Terminator v3.1 chemistry or by Geneservice Ltd. Oxford.

Storage of transformed bacteria

Transformed bacteria containing correctly sequenced expression vectors were stored as gycerol stocks. 800μl of fresh overnight bacterial culture was mixed with 200μl (80% v/v) filter sterile glycerol and stored at -80°C. Bacteria were re-cultured from these stocks by innoculating LB broth containing the correct selecting antibiotic with a pipette tip stab from the frozen glycerol stock and culturing overnight at 37°C.

2.2 Cell Culture

2.2.1 Cell lines used in this thesis

HEK-293T cells The adherent HEK-293T cells are a variant of the transformed human embryonic kidney (HEK) cells that contains the SV40 large T-antigen that allows episomal replication of transfected plasmids containing the Simian vacuolating Virus 40 (SV40) origin of replication [276]. This makes the cell line excellent for extended temporal expression of most mammalian genes under the control of the CMV promoter.

B cell hybridomas B cells were cultured to harvest the secreted monoclonal they produced. Creation of these cells are described elsewhere (see Chapter 3).

DO11.10 T cell Hybridomas This T cell hybridoma cell line is derived from BALB/C mice [277]. It is specific for a peptide fragment of chicken ovalbumin and restricted by the H-2 class II molecule, 1-A^d [278,279].

2.2.2 General culture techniques

All tissue culture was performed using standard aseptic technique in HEPA filtered cell culture cabinets to maintain sterility. Cells were grown at 37°C in a 5% CO_2 atmosphere.

Freezing and thawing cells

To thaw cells from gas phase liquid nitrogen storage, they were quickly thawed completely at 37°C, then diluted in 50ml media pre-warmed to 37°C. The cells were pelleted at 1,300rpm for 5 minutes before resuspension in 10ml media. Cells were checked for viability and incubated at 37°C 5% CO_2 for 24 hours. Cells to be frozen were counted, pelleted by centrifuagtion at 1,300rpm for 5 minutes, then resuspended in 1ml freezing solution (10% (v/v) dimethyl sulfoxide (Sigma) in foetal calf serum) and transfered to a 1.5ml cryovial (Nunc). The vial was immediately placed in a freezing chamber which was them placed at -80°C. The freezing chamber containing propan-2-ol which allows the tubes to reach -80°C at a slow and regulated rate. After storage at -80°C for 24 hours the vials were transfered to gas phase liquid nitrogen

storage.

Cell viability and counting

A haemocytometer was used to visually check cell viability and ascertain total cell counts. 50μl of cell suspension was mixed thoroughly with 50μl of Trypan blue (Sigma). 50μl of this mix was then transfered to a chamber of a haemocytometer, and the cells were microscopically observed and counted.

Cell passage

HEK-293T cells are adherent cells which were sub-cultured when they reached 70-90% confluency. The media was first removed and the cells washed with 10ml sterile cold phosphate buffered saline solution (PBS). The cells were detatched from the flask surface by adding 5ml 10% (v/v) trypsin/PBS and placing the cells at 37°C for 5 minutes. After this incubation, the flask was gently shaken to ensure all the cells were completely detatched. To inactivate the trypsin enzyme activity, the cells were then diluted with 15ml of media. The cells were pelleted by centrifugation at 1,300rpm for 5 minutes, then resuspended in 10ml of media. The cell viability and density was checked as outlined above and then an appropriate volume of cells was transfered to a fresh 75cm^2 flask and topped up to 20ml using fresh media. When sub-culturing HEK-293T cells into 6 well plates for transfections, the cells were diluted to a concentration which would allow them to reach between 60 - 80% confluency in 24 hours. T cell and B cell hybridomas grow in suspension. They were passaged by first calculating

their cell viability and cell density, and then transfering some of the culture to a clean tissue culture flask and diluting it with fresh media. This left the subcultured cells at an appropriate density to enable them to grow back to confluency. In general culture DO11.10 T cell hybridomas were cultured at between 1×10^5 and 1×10^6 cells/ml.

2.2.3 Tissue culture media

T-DMEM – Media for HEK-293T cells

	Company	Cat.No	Amount
DMEM	Sigma	D5796	500.0 ml
Foetal Calf Serum	PAA	A15-114	50.0 ml
L-Glutamine (200mM)	Sigma	G7513	10.0 ml
Antibiotics (Pen/Strep/Neo)	Sigma	P4083	5.0 ml

JMEM – Media for DO11.10 cells

	Company	Cat.No	Amount
RPMI-1640	Gibco	21875-034	500.0 ml
Foetal Calf Serum	PAA	A15-114	50.0 ml
HEPES (1M)	Sigma	H0887	5.0 ml
Sodium Pyruvate (100mM)	Gibco	11360-039	5.0 ml
Antibiotics (Pen/Strep/Neo)	Sigma	P4083	5.0 ml

BMEM – Media for B cell hybridoma cells

	Company	Cat.No	Amount
RPMI-1640	Gibco	21875-034	500.0 ml
IgG stripped Foetal Calf Serum	PAA	A15-106	100.0 ml
HEPES (1M)	Sigma	H0887	5.0 ml
Sodium Pyruvate (100mM)	Gibco	11360-039	5.0 ml
HT Supplement (50x)	Gibco	41065-012	5.0 ml
Antibiotics (Pen/Strep/Neo)	Sigma	P4083	5.0 ml

2.3 Protein purification

2.3.1 High performance liquid chromatography

A gel filtration chromatography system was used to separate proteins on the basis of size. It removed misfolded protein or contaminants from initial monoclonal antibody purification fractions and proteins used in Surface Plasmon Resonance (SPR) analysis. Proteins were run over a Superdex 200 HR column using a ÄKTA FPLC system which can resolve proteins of 10-600kDa in size. Proteins were first concentrated to a volume of 500μl using Vivaspin 20 columns (Sartorius Stedim Biotech) which concentrate proteins larger than 5kDa. Proteins were not gel filtrated at concentration greater than 20mg/ml, therefore protein concentration was determined spectrophotometrically at 280nm prior to loading and adjusted if necessary. Samples were also centrifuged for 13,000rpm for 10 minutes to pellet any precipitation or impurities before loading. The column was first washed with one column volume using a HEPES-buffered saline solution (150mM NaCl, 10mM HEPES, 0.5% NaN_3) then the protein was injected into the column. One column volume was eluted and the 500μl fractions collected after elution of the column dead volume. The concentration of all elutions were recorded and pure fractions were pooled to create stock protein.

2.3.2 Polyacrylamide gels

To separate digested protein and check the purity of proteins, samples were run on 12% polyacrylamide gels. Gels were prepared in pre-cleaned glass plates using Mini-

protean II gel apparatus (BioRad). Resolving gels were poured first, over layed with distilled water and allowed to polymerase for 10 minutes. The water was drained off and then the stacking gel containing the appropriate well comb were layered on top.

Resolving Gel	Company	Conc^{n}.	Amount
dH_2O	—	—	3.5 ml
ProtoGel® Resolving buffer (1.5M Tris-HCl, 0.4% SDS, pH 8.8)	National Diagnostics	4 ×	2.5 ml
Acrylamide:Bis-acrylamide (37.5:1)	National Diagnostics	30 %	4.0 ml
Ammonium persulphate	Sigma	10 %	50.0 μl
TEMED	Sigma	—	20.0 μl

Stacking Gel	Company	Conc^{n}.	Amount
dH_2O	—	—	3.1 ml
ProtoGel® Stacking buffer (0.5M Tris-HCl, 0.4% SDS, pH 6.8)	National Diagnostics	4 ×	1.25 ml
Acrylamide:Bis-acrylamide (37.5:1)	National Diagnostics	30 %	650.0 μl
Ammonium persulphate	Sigma	10 %	25.0 μl
TEMED	Sigma	—	10.0 μl

Protein samples were loaded on the polyacrylamide gels with both non-reducing (125mM Tris-HCl, 20% w/v glycerol, 4% SDS, 0.05% bromophenol blue) and reducing (as with non-reducing buffer but with 10% β-mercaptoethanol) loading buffer. The protein samples were mixed with buffers and boiled for 1 minute. The gels were immersed with running buffer (25mM Tris-HCl, 0.1 w/v SDS, 192mM glycine) and the samples loaded. The gels were run for 60 minutes at 150V using a PowerPack 300 (BioRad). To visualise the proteins the gels were carefully removed from the gel plates, stained for 15 minutes with coomassie stain (45% methanol, 92% acetic acid, 0.125% coomassie blue) and then placed in de-stain buffer (12 methanol, 10% acetic acid) for 2 hours.

2.4 Phenotypic analysis

2.4.1 Flow cytometry and analysis

Flow cytometry was used to examine the expression of cell surface proteins. Approximately 5×10^5 cells were washed with 3ml fluorescence-activated cell sorting buffer (FACS buffer) (2% FBS in PBS) and spun at 13,000 rpm in polypropylene FACS tubes. Specific monoclonal antibodies that were directly or indirectly conjugated to fluorophores were used to label surface protein targets. Many of the cell surface proteins were expressed along with or tagged with GFP, therefore the fluorophore used to check surface expression was chosen so that there was a minimal fluorescent overlap. The antibodies were diluted to a working volume in FACS buffer, added to the cells and incubated at 4°C for 30 minutes. The cells were again pelleted at 13,000rpm and washed with 3ml FACS buffer. If the primary antibody was not conjugated with a fluorophore, the antibody incubation was repeated with a secondary antibody conjugate. The antibody labelled cells were analysed on a Cyan APP (Dako) FACS cytometer. Cells were gated for forward and side scatter and the fluorescence of viable cells recorded. Final fluorescence emission was calulated after channel compensation based on labelled controls if appropriate.

Cells were fluorescence-activated cell sorted (FACS) for cell surface protein expression after being labeled with monoclonal antibodies as above. Cells were sorted using appropriate gates on a MoFlow®cytometry system (Dako) at the FACS facility of the Weatherall Institute of Molecular Medicine, Oxford University. Post sorting, cells were

centrifuged at 1,300rpm for 5 minutes then resuspended in fresh media. The cells were cultured at 37°C, 5% CO_2 until the cells reached a confluence that allowed a FACS to be repeated to check expression.

2.4.2 Confocal microscopy

For cellular visualisation of GFP tagged proteins, transfected cells were grown on sterile cover slips. Hek-293T cells were grown in a 6 well plate containing a sterile coverslip to 60-80% confluency. A transfection mix consisting of 1μg/ml vector and 200μl transfection media were mixed carefully and transfection complexes left to form for 30 minutes. Transfection media was prepared 10 minutes prior to the addition of DNA by adding of 3μl GeneJuice transfection reagent (Novagen, Merck) to 100μl DMEM (without FCS) per transfection. Transfection volumes were then added dropwise to the 6 well plates containing the HEK-293T cells, rocking the cells gently to ensure even mixing of the transfection reaction, then incubated at 37°C, 5% CO_2 for 24 hours. The transfected cells were washed with chilled PBS and fixed with 2% paraformaldehyde. Cover slips were mounted on slides using Vectashield mounting medium with 4',6-diamidino-2-phenylindole (DAPI) (Vector Laboratories). A BioRad Radiance 2000 confocal microscope, excited coverslip bound cells at 488nm, and were examined through an oil immersed 60x objective by light filtered in a channel from 515$\pm$15nm. Fluorescence was collected using Laser Sharp 2000 software (Zeiss) and used with minimal manipulation to optimise signal:noise ratio.

2.5 Bioluminescence Resonance Energy Transfer

Bioluminescence resonance energy transfer (BRET) is a method which uses nonradiative energy transfer between donor and acceptor fluorophores for analysing interactions of cell surface molecules [72]. Luciferase (a 35 kDa protein from *Renilla reniformis*) is a bioluminescent protein which releases photons when it oxidises its substrate, coelenterazine. If another appropriate fluorophore is within 100Å, it can be excited to a higher energetic state, emitting photons with longer wavelengths. Proteins to be assayed are expressed in target cells fused to both GFP^2 and Renilla luciferase (Rluc). The ratio of GFP^2 to Rluc and BRET$_{eff}$, the signal surface density of the proteins, can be used to differentiate between random interactions and oligomerisation at the cell surface [280].

Hek-293T cells were grown in a 6 well plate to 60-80% confluency. DNA stocks of GFP^2 and Rluc constructs were made to 0.05μg/μl and aliquoted into the following ratios.

Ratio	pGFP^2(μl)	pRluc (μl)
2:1	6.7	13.3
1:1	10.0	10.0
1:3	15.0	15.0
1:6	17.1	2.9
1.9	18.0	2.0
1:12	18.5	1.5
1:15	18.75	1.25
1.39	19.5	0.5

After mixing, the DNA was added drop-wise to transfection media, mixed carefully by flicking and left at room temperature for 30 minutes for the transfection complexes to form. For a positive control 6μl BRET^2 vector at 0.2μg/μl was added

to transfection media. Transfection media was made 10 minutes prior to addition of DNA by adding 3μl GeneJuice transfection reagent (Novagen, Merck) to 100μl DMEM per transfection reaction and gently mixed. Each transfection volume was then added dropwise to a 6 well plate well and the plate then rocked gently to ensure even mixing of the transfection reaction. The plates were incubated (37°C, 5% CO_2) for 24 hours.

Transfected cells were washed by first removing the media from each well and washing the cells with 1ml 4°C PBS, and harvested by pipetting 1ml 4°C PBS over the cells to detach them from the well surface. Cells were centrifuged at 3000rpm for 3 minutes in a microfuge, then the supernatant removed from the cell pellet with a syringe. The pellet was resuspended in 400μl 4°C PBS and stored on ice.

To assay GFP^2 expression, 100μl of transfected cells were excited at 420nm in a 96-well OptiPlate® (PerkinElmer) using a Fusion microplate analyser (PerkinElmer). The emission was recorded 3 times for 1 second at 515$\pm$15nm and recorded as the total expressed fluorescent units (FU). Rluc expression was assayed using the same cells but with 10μM coenterazine-*h* for two minutes before reading the total emissions as for GFP^2. This was recorded as the total expressed luminescent units (LU). To perform the BRET^2 assay, DeepBlueC (to a final concentration of 10μM) was added to 100μl transfected cells. The collected light emissions at 515$\pm$15nm (BRET-A) and 410$\pm$40nm (BRET-B) were collected three times for 1 second at each wavelength range.

BRET values were calculated as described by James *et al.* (2006) [280]. In brief, acceptor/donor ratio (FU/LU) was converted to concentrations ([GFP]/[Luc]) and plotted against the BRET efficiency ($BRET_{eff}$). ($BRET_{eff}$) is the ratio of GFP emission to

that of Luc emission dependent on the inverse sixth-power of the mean separation of donor and acceptor. This is calculated using BRET-A and BRET-B. The $BRET_{eff}$ for each ([GFP]/[Luc]) were plotted against each other to estimate the level of oligomerisation. The Origin®7.5 (Originlab) software was used to fit the data using the equations 2.1 and 2.2.

$$\frac{BRET_{eff}}{BRET_{max}} = 1 - \frac{1}{(1+f)^{n-1}} \tag{2.1}$$

$$BRET_{eff} = c \qquad \text{for } [GFP]/[Luc] > 2 \tag{2.2}$$

Equation 2.1 was used to fit data from oligomeric molecules, where f is the acceptor:donor ratio and n is the stoichiometry of the oligomer. Monomeric molecules that are predicted to have random cell surface interactions. $BRET_{eff}$ values for monomers are independent of the [GFP]/[Luc] ratio beyond a value of 2 [280]. Therefore monomeric data was fitted to a constant value for points with [GFP]/[Luc]>2 (equation 2.2).

Chapter 3

Characterisation of human PD-1 mAbs

3.1 Introduction

3.1.1 Epitope location and mitogenic potential of CD28 superagonistic antibodies

Superagonistic antibodies to CD28 are characterised by their ability to activate T cells in a TCR independent manner when immobilised. This is compared to "conventional" CD28 antibodies which require an additional TCR stimulus to co-stimulate T cells. A distinguishing feature of all CD28 superagonistic antibodies characterised to date is their binding topology. Whilst the epitopes of conventional CD28 antibodies are located close to the binding site of the natural CD28 ligands, CD80 and CD86, superagonists bind a distinct exposed lateral loop [218]. The important distinction between these epitopes is that the CD28 ligand binding region is in a membrane distal region of CD28 whereas the superagonist epitope is membrane proximal.

Structural studies showing human superagonists binding the membrane proximal epitope of CD28 have been used to explain their potency using the kinetic segregation model [184]. The application of the kinetic segregation model to CD28 superagonists suggests that an immobilised CD28 antibody binding to a lower epitope is more

effective at excluding large phosphatases (CD45 and CD148) from accessing CD28. This allows greater phosphorylation of CD28 by cytoplasmic tyrosine kinases, which are not excluded from the area. The resultant net increase in phosphorylation of the cytoplasmic domain of CD28 initiates signalling.

CD28 is one of many T cell surface molecules that has cytoplasmic tyrosine signalling motifs which are dependent on intracellular kinases and large membrane bound phosphatases to regulate their phosphorylation [153]. If CD28 superagonistic antibodies are able to activate T cells through the exclusion of large cell bound phosphatases and this ability can be attributed to the membrane proximal epitope of the antibody alone, it may be inferred that any signalling molecule phosphorylated by extrinsic tyrosine kinases may be induced to signal by an antibody binding close to the membrane.

3.1.2 Superagonism applied to PD-1

PD-1 is an inhibitory molecule that can be inducibly expressed on the cell surface post TCR stimulation [239, 271] and has an important role in autoimmunity and tolerance [194]. Two cytoplasmic signalling domains have been identified on the intracellular region of PD-1, an ITIM and an ITSM domain (1.7.3). While these domains of PD-1 are thought to initiate pathways that have an inhibitory effect on T cells, they are similar to the activating motifs found on CD28 in that they are tyrosine based, and the phosphorylation of these tyrosines on ligand engagement is a key initiator in their signalling pathways (1.6.2-1.7.3). Because of these signalling similarities, it is

proposed that PD-1, like CD28, could also be induced to signal by antibodies in an epitope dependent manner.

Although as of yet, the application of superagonistic antibodies to CD28 in a therapeutic setting has not, and may never be successful [223], the potential to use the signalling abilities of such antibodies with other T cell signalling molecules is great. They not only could be used to modulate the signalling of activating receptors like CD28, but inhibitory receptors also. Such antibodies could be used to independently initiate PD-1 signalling and therefore, due to the important role PD-1 plays in the maintenance of immune tolerance [262], have applications in many autoimmune diseases. The similarities between PD-1 and CD28 both in structure and signalling would also make agonistic mAbs to PD-1 a good target molecule for further investigation into the mechanism of antibodies with epitope dependent activating activity. The observation of epitope dependent mAb signalling in a T cell molecule other than CD28 would further confirm the role of phosphatase exclusion in their mechanism of action.

The work in this chapter details the characterisation of four mAbs generated against human PD-1. To identify PD-1 mAbs with potentially agonistic epitope locations, the antibodies were fully characterised. First, residue mutational analysis was performed to identify antibody epitopes. Then the binding antibody binding affinities were investigated and compared using SPR analysis.

3.2 Materials and Methods

3.2.1 Anti-human PD-1 mAb hybridoma generation

The generation of hybridoma cell lines producing mAbs against PD-1 was performed by BioGenes GmbH (Berlin). In brief, 8 week old BALB/C mice were immunised with a human PD1/mouse Fc fusion protein (PD-1/Fc) (Heather Walsh, Human Immunology Unit, Weatherall Institute of Molecular Medicine, Oxford University). The fusion protein consisted of the extracellular domain of human PD-1 (amino acids 1 to 147 of the mature peptide) fused with the mouse IgG1 Fc domain (amino acids 98 to 324 of mature secreted peptide, cysteine residues found at 102, 104, 107 and 109 were substituted with serine to prevent interchain formation). To allow purification, a 8x histidine tag was added to the C-terminus of the Fc. The junction between human PD-1 and mouse Fc also contained a thrombin cleavage site (LVPRGS) which enabled the cleavage of Fc for other uses.

An alum precipitate of PD-1/Fc was administered intraperitoneally to BALB/C, female, 8 week old mice over 60 days, initially immunising with 50μg protein and then boosting with 25μg. The spleens of the immunised mice were harvested, and a spleen cell suspension produced. The suspension was fused with the SP2/0-Ag14 myeloma cell line and incubated for 10 days. Tissue culture supernatants were screened for IgG by ELISA, and wells that had an OD_{405nm} that was two fold higher than the average plate value were selected as positive. After further culture, IgG producing positive fusions were screened to select PD-1 specific hybridomas. First a PD-1/Fc ELISA was

carried out to identify mAbs specific to PD-1/Fc, then a second ELISA was performed using human PD-1 cleaved of mouse Fc to identify fusions producing mAb specific to human PD-1. Positive fusions underwent two rounds of limiting dilution cloning to ensure pure populations of anti-PD-1 mAb producing hybridomas. The cloned hybridoma was certified mycoplasma free and the antibody produced by the hybridomas isotyped.

3.2.2 Antibody purification

To allow the harvesting of anti-human PD-1 mAbs from tissue culture supernatant, hybridomas were grown in BMEM media (Section 2.2.3) in CELLine CL 1000 bioreactors (IBS Integra Biosciences). Harvested tissue culture supernatant in 100ml volumes was dialysed with 6L low salt buffer (25mM Tris HCl, 0.05M NaCl, pH7.4), until tissue culture supernatant reached a pH of 7.4. Bovine serum albumin was removed from dialysed tissue culture supernatant using ion exchange chromatography. Supernatant was passed across a Fragtogel® EMD DEAE resin (Merck) column followed by two column volumes of low salt buffer. All elutions were collected and samples of the elutions were run on reducing and non-reducing SDS-PAGE gels (Section 2.3.2) to ensure the removal of Bovine serum albumin. Elutions still containing bovine serum albumin were purified with the ion exchange chromatography column for a second time. Bovine serum albumin free elutions were pooled and concentrated using a Vivaspin 20 (Sartorius Stedim Biotech) and then run over a Superdex 200 HR column using a ÄKTA FPLC system (Section 2.3.1). Elutions containing pure IgG were pooled and

their concentration recorded before aliquoting and storage at -80°C.

3.2.3 PD-1 ELISA

96-well flat bottomed plates (Costar EIA/RIA plates) were coated overnight at 4°C with PD-1 target protein at a concentration of 10μg/ml in sterile coating buffer (15mM Na_2CO_3, 35mM $NaHCO_3$, pH 9.6). Coating buffer was removed and the plate washed with 150μl wash buffer (Sterile PBS, 0.05% Tween®20 (Sigma), at 4°C) and repeated a further two times. Plates were blocked with 200μl block buffer (1% Casein (Sigma) in PBS with 0.05% NaN_3) at room temperature for 30 minutes. Plates were then washed three times with 150μl wash buffer. 50μl of PD-1 mAb 2, 10, 19 and 29 and IgG1 isotype control OX-7 (Alistair Waugh , University of Oxford) were titrated from 100μg/ml to 0.0001μg/ml into wells and incubated at 4°C for 2 hours. Antibodies were discarded and the plates washed three times with 150μl wash buffer. 50μl secondary IgG anti-Fab specific horseradish peroxidase conjugated antibody (Sigma) was added diluted at 1 in 2000 with block buffer and incubated on the plate for 1 hour at 4°C. The secondary antibody was discarded and washed three times with 150μl wash buffer. 100μl substrate 2,2'-Azino-bis(3-ethylbenzothiazoline-6-sulphonic acid) diammonium salt (ABTS) (Sigma) dissolved in 100ml 0.05M phosphate-citrate buffer (0.2M dibasic sodium phosphate, 0.1M citric acid, pH 5.0)) was added and plates were incubated at room temperature for 20 minutes in the dark to develop. Colour intensity of wells was recorded by a Fusion microplate analyser (PerkinElmer) at 425nm.

3.2.4 Epitope mapping

Generation of wild type and mutant PD-1_{EX}CD$28_{TM/CYT}$

The chimera PD-1_{EX}CD$28_{TM/CYT}$ was created through the fusion of the human PD-1 extracellular domain (amino acids 1 to 148 of the mature peptide) to the mouse transmembrane and intracellular domain of CD28 (amino acids 132 to 198 of the mature peptide). Details of all the oligonucleotides used in the construction of the following constructs can be found in Tables 3.1-3.3. The oligonucleotide 989 containing a *Eco*RI restriction site, rat ribosomal binding site and the human PD-1 signal peptide was used in a PCR along with the oligonucleotide 991, which fuses the last 7 residues of the human PD-1 extracellular domain with the first 8 residues of the mouse CD28 transmembrane domain. This first human PD-1 PCR product was amplified from human cDNA. The complementary oligonucleotide of 991, 990 was used to amplify the mouse transmembrane and intracellular domain with the oligonucleotide 1018, which contains the last 7 residues of mouse CD28 and an *Bam*HI restriction site. Mouse CD28 was amplified from DO11.10 mouse cDNA. The products from these two PCR reactions were used as templates for a chimeric PCR reaction using the oligonucleotides 1017 and 1018. The resultant PD-1_{EX}CD$28_{TM/CYT}$ chimera was digested with *Bam*HI and *Eco*RI and ligated into the pGFP^2-N3 vector.

Construct	Oligo Name	Number	Primer Sequence	Restriction
PD-1_{EX}CD$28_{TM/CYT}$	hPD1/mCD28 5′	989	TAGTAGGATTCCTCAAGCAGGCCACCCTGCAGA	*Eco*RI
	hPD1/mCD28 int 5′	990	GCCAGCCGGCCAGTTGGAAACCTTTTGGGCACTGGTCGTG GTTGCT	–
	hPD1/mCD28 int 3′	991	AGCAACCACGACCAGTGCCCAAAAGGTTTCCAACTGGCCG GCTGGC	–
	mCD28 3	1018	CTACTAGGATCCGGGGCGGTACGCTGC	*Bam*HI
PD-1_{EX}CD$28_{TM/CYT}$-mutants	EcoRI rCD4-5′	1017	TAGTAGGAATTCCTCAAGCAGGCCACC	*Eco*RI
PD-1_{EX}CD$28_{TM/CYT}$-T11E	hPD1-T11Ef	452	CAGGCCCTGGAACCCCCCCGAGTTCTCCCCAGCCCTGCTC	–
	hPD1-T11Er	453	GAGCAGGGCTGGGGAGAACTCGGGGGGGTTCCAGGGCCTG	–
PD-1_{EX}CD$28_{TM/CYT}$-F13E	hPD-1-F13E-F	1053	CTGGAACCCCCCCACCTTCGAGCCAGCCCTGCTCGTGGTG	–
	hPD-1-F13E-R	1054	CACCACGAGCAGGGCTGGCTCGAAGGTGGGGGGGTTCCAG	–
PD-1_{EX}CD$28_{TM/CYT}$-A15R	hPD1-A15R 5′	2228	CCACCTTCTCCCCACGCCTGCTCGTGGT	–
	hPD1-A15R 3′	2229	ACCACGAGCAGGCGTGGGGAGAAGGTGG	–
PD-1_{EX}CD$28_{TM/CYT}$-L16R	hPD1-L16Rf	1218	CCCACCTTCTCCCCAGCCAGGCTCGTGGTGACCGAAGGG	–
	hPD1-L16Rr	1219	CCCTTCGGTCACCACGAGCCTGGCTGGGGAGAAGGTGGG	–
PD-1_{EX}CD$28_{TM/CYT}$-V18R	hPD1-V18Rf		TTCTCCCCAGCCCTGCTCCGGGTGACCGAAGGGGACAAC	–
	hPD1-V18Rr		GTTGTCCCCTTCGGTCACCCGGAGCAGGGCTGGGGAGAA	–
PD-1_{EX}CD$28_{TM/CYT}$-T20E	hPD1-T20Ef	1220	CCAGCCCTGCTCGTGGTGGAGGAAGGGGACAACGCCACC	–
	hPD1-T20Er	1221	GGTGGCGTTGTCCCCTTCCTCCACCACGAGCAGGGCTGG	–
PD-1_{EX}CD$28_{TM/CYT}$-S32E	hPD1-S32Ef	1222	ACCTTCACCTGCAGCTTCGAGAACACATCGGAGAGCTTC	–
	hPD1-S32Er	1223	GAAGCTCTCCGATGTGTTCTCGAAGCTGCAGGTGAAGGT	–
PD-1_{EX}CD$28_{TM/CYT}$-E36R	hPD1-E36Rf	1224	AGCTTCTCCAACACATCGAGGAGCTTCGTGCTAAACTGG	–
	hPD1-E36Rr	1225	CCAGTTTAGCACGAAGCTCCTCGATGTGTTGGAGAAGCT	–
PD-1_{EX}CD$28_{TM/CYT}$-N41K	hPD1-N41Kf	1226	TCGGAGAGCTTCGTGCTAAAATGGTACCGCATGAGCCCC	–
	hPD1-N41Kr	1227	GGGGCTCATGCGGTACCATTTTAGCACGAAGCTCTCCGA	–
PD-1_{EX}CD$28_{TM/CYT}$-Y43R	hPD1-Y43R 5′	2232	CTTCGTGCTAAACTGGCGCCGCATGAGCCCCAGC	–
	hPD1-Y43R 3′	2233	GCTGGGGCTCATGCGGCGCCAGTTTAGCACGAAG	–
PD-1_{EX}CD$28_{TM/CYT}$-S48R	hPD1-S48R 5′	2234	GCATGAGCCCCAGGAACCAGGACGGACA	–
	hPD1-S48R 3′	2235	TGTCCGTCCTGGTTCCTGGGGCTCATGC	–

Table 3.1: Oligonucleotide primers used to produce the constructs detailed in this chapter

Construct	Oligo Name	Number	Primer Sequence	Restriction
PD-1_{EX}CD$28_{TM/CYT}$-D52K	hPD-1-D52K-F	1055	GACGGGCAGCAACCAGACGAAAAAGCTGGCCGCCTTCCCC	–
	hPD-1-D52K-R	1056	GGGGAAGGCGGCCAGCTTTTTCGTCTGGTTGCTGCCCGTC	–
PD-1_{EX}CD$28_{TM/CYT}$-K53E	hPD1-K53E 5′	2236	CAACCAGACGGACGAGCTGGCCGCCTT	–
	hPD1-K53E 3′	2237	AAGGCGGCCAGCTCGTCCGTCTGGTTG	–
PD-1_{EX}CD$28_{TM/CYT}$-A56R	hPD1-A56R 5′	2238	GGACAAGCTGGCCCGCTTCCCCGAGGAC	–
	hPD1-A56R 3′	2239	GTCCTCGGGGAAGCGGGCCAGCTTGTCC	–
PD-1_{EX}CD$28_{TM/CYT}$-E59K	hPD1-E59Kf	1240	AAGCTGGCCGCCTTCCCCAAGGACCGCAGCCAGCCCGGCCA	–
	hPD1-E59Kr	1240	TGGCCGGGCTGGCTGCGGTCCTTGGGGAAGGCGGCCAGCTT	–
PD-1_{EX}CD$28_{TM/CYT}$-Q63R	hPD-1-Q63R-F	1057	CTTCCCCGAGGACCGCAGCAGGCCCGGCCAGGACTGCCGC	–
	hPD-1-Q63R-R	1058	GCGGCAGTCCTGGCCGGGCCTGCTGCGGTCCTCGGGGAAG	–
PD-1_{EX}CD$28_{TM/CYT}$-Q66R	hPD-1-Q66R-F	1059	GGACCGCAGCCAGCCCGGCAGGGACTGCCGCTTCCGTGTC	–
	hPD-1-Q66R-R	1060	GACACGGAAGCGGCAGTCCCTGCCGGGCTGGCTGCGGTCC	–
PD-1_{EX}CD$28_{TM/CYT}$-C68H	hPD1-C68Hf	1228	AGCCAGCCCGGCCAGGACCACCGCTTCCGTGTCACACAA	–
	hPD1-C68Hr	1229	TTGTGTGACACGGAAGCGGTGGTCCTGGCCGGGCTGGCT	–
PD-1_{EX}CD$28_{TM/CYT}$-R71D	hPD-1-R71D-F	1061	CGGCCAGGACTGCCGCTTCGATGTCACACAACTGCCCAAC	–
	hPD-1-R71D-R	1062	GTTGGGCAGTTGTGTGACATCGAAGCGGCAGTCCTGGCCG	–
PD-1_{EX}CD$28_{TM/CYT}$-T73R	hPD1-T73Rf	1230	GACTGCCGCTTCCGTGTCCGACAACTGCCCAACGGGCGT	–
	hPD1-T73Rr	1231	ACGCCCGTTGGGCAGTTGTCGGACACGGAAGCGGCAGTC	–
PD-1_{EX}CD$28_{TM/CYT}$-Q74K	hPD1-Q74Kf	1239	TGCCGCTTCCGTGTCACAAAACTGCCCAACGGGCGTGACT	–
	hPD1-Q74Kr	1232	AGTCACGCCCGTTGGGCAGTTTTGTGACACGGAAGCGGCA	–
PD-1_{EX}CD$28_{TM/CYT}$-G78R	hPD-1-G78R-F	1063	TGTCACACAACTGCCCAACCGGCGTGACTTCCACATGAGC	–
	hPD-1-G78R-R	1064	GCTCATGTGGAAGTCACGCCGGTTGGGCAGTTGTGTGACA	–
PD-1_{EX}CD$28_{TM/CYT}$-D80R	hPD1-D80R 5′	2240	TGCCCAACGGGCGTCGCTTCCACATGAGCG	–
	hPD1-D80R 3′	2241	CGCTCATGTGGAAGCGACGCCCGTTGGGCA	–
PD-1_{EX}CD$28_{TM/CYT}$-H82D	hPD-1-H82D-F	1065	CTGCCCAACGGGCGTGACTTCGACATGAGCGTGGTCAGGG	–
	hPD-1-H82D-R	1066	CCCTGACCACGCTCATGTCGAAGTCACGCCCGTTGGGCAG	–

Table 3.2: Oligonucleotide primers used to produce the constructs detailed in this chapter

Construct	Oligo Name	Number	Primer Sequence	Restriction
PD-1_{EX}CD$28_{TM/CYT}$-R87D	hPD-1-R87D-F	1067	CTTCCACATGAGCGTGGTCGATGCCCGGCGCAATGACAGC	–
	hPD-1-R87D-R	1068	GCTGTCATTGCGCCGGGCATCGACCACGCTCATGTGGAAG	–
PD-1_{EX}CD$28_{TM/CYT}$-R90E	hPD1-R90Ef	1233	AGCGTGGTCAGGGCCCGGGAAAATGACAGCGGCACCTAC	–
	hPD1-R90Er	1234	GTAGGTGCCGCTGTCATTTTCCCGGGCCCTGACCACGCT	–
PD-1_{EX}CD$28_{TM/CYT}$-T95K	hPD-1-T95K-F	1077	CCCGGCGCAATGACAGCGGCAAATACCTCTGTGGGGCCATC	–
	hPD-1-T95K-R	1078	GATGGCCCCACAGAGGTATTTGCCGCTGTCATTGCGCCGGG	–
PD-1_{EX}CD$28_{TM/CYT}$-I101D	hPD1-I101Df	1457	ACCTACCTCTGTGGGGCCGACTCCCTGGCCCCCAAGGCG	–
	hPD1-I101Dr	1458	CGCCTTGGGGGCCAGGGAGTCGGCCCCACAGAGGTAGGT	–
PD-1_{EX}CD$28_{TM/CYT}$-L103E	hPD-1-L103E-F	1079	CCTCTGTGGGGCCATCTCCGAGGCCCCCAAGGCGCAGATCA	–
	hPD-1-L103E-R	1080	TGATCTGCGCCTTGGGGGCCTCGGAGATGGCCCCACAGAGG	–
PD-1_{EX}CD$28_{TM/CYT}$-A104R	hPD1-A104R 5′	2242	CTGCGCCTTGGGGCGCAGGGAGATGGCC	–
	hPD1-A104R 3′	2243	GGCCATCTCCCTGCGCCCCAAGGCGCAG	–
PD-1_{EX}CD$28_{TM/CYT}$-K106E	hPD1-K106Ef	1235	GCCATCTCCCTGGCCCCCGAAGCGCAGATCAAAGAGAGCC	–
	hPD1-K106Er	1236	GGCTCTCTTTGATCTGCGCTTCGGGGGCCAGGGAGATGGC	–
PD-1_{EX}CD$28_{TM/CYT}$-A107R	hPD1-A107R 5′	2244	TCCCTGGCCCCCAAGAGGCAGATCAAAGAGAG	–
	hPD1-A107R 3′	2245	CTCTCTTTGATCTGCCTCTTGGGGGCCAGGGA	–
PD-1_{EX}CD$28_{TM/CYT}$-I109D	hPD-1-I109D-F	1069	CCTGGCCCCCAAGGCGCAGGACAAAGAGAGCCTGCGGGCA	–
	hPD-1-I109D-R	1070	TGCCCGCAGGCTCTCTTTGTCCTGCGCCTTGGGGGCCAGG	–
PD-1_{EX}CD$28_{TM/CYT}$-E111R	hPD1-E111Rf	1237	CCCAAGGCGCAGATCAAACGCAGCCTGCGGGCAGAGCTCA	–
	hPD1-E111Rr	1238	TGAGCTCTGCCCGCAGGCTGCGTTTGATCTGCGCCTTGGG	–
PD-1_{EX}CD$28_{TM/CYT}$-E116R	hPD1-E116Rf	1459	AAAGAGAGCCTGCGGGCACGGCTCAGGGTGACAGAGAGAAGG	–
	hPD1-E116Rr	1460	CCTTCTCTCTGTCACCCTGAGCCGTGCCCGCAGGCTCTCTTT	–
PD-1_{EX}CD$28_{TM/CYT}$-R118D	hPD-1-R118D-F	1071	TGCCCTTCTCTCTGTCACATCGAGCTCTGCCCGCAGGCTC	–
	hPD-1-R118D-R	1072	GAGCCTGCGGGCAGAGCTCGATGTGACAGAGAGAAGGGCA	–
PD-1_{EX}CD$28_{TM/CYT}$-T120R	hPD1-T120R 5′	2246	GGCAGAGCTCAGGGTGAGAGAGAGAAGG	–
	hPD1-T120R 3′	2247	CCTTCTCTCTCTCACCCTGAGCTCTGCC	–

Table 3.3: Oligonucleotide primers used to produce the constructs detailed in this chapter

Thirty seven PD-1_{EX}CD$28_{TM/CYT}$ constructs containing single amino acid mutations of PD-1 were created by chimeric PCR, using PD-1_{EX}CD$28_{TM/CYT}$ as a template. First a PCR using the oligonucleotide 1017, encoding a *Eco*RI site and a rat ribosomal binding site was used with an internal PD-1 oligonucleotide encoding the single amino acid substitution to create a $5'$ mutation template. The second PCR was performed with an oligonucleotide complementary to the internal PD-1 mutation used in the first reaction and oligonucleotide 1017, creating the $3'$ mutation template. These two PCR products were used as template in a chimeric PCR using the oligonucletides 1017 and 1018. All mutant sequences were digested with *Bam*HI and *Eco*RI and ligated into the pGFP²-N3 vector. After sequence verification vector stocks were prepared for use in transfection reactions. Details of all methods used in construction of these vectors can be found in Section 2.1.

Flow cytometry epitope mapping assay

Mutant pGFP²-N3-PD-1_{EX}CD$28_{TM/CYT}$ constructs and the wild type pGFP²-N3-hCD28_{EX} mCD$28_{TM/CYT}$ and pGFP²-N3-hCD28_{EX}mCD$28_{TM/CYT}$ (For construction of PD-1_{EX} CD$28_{TM/CYT}$ see Chapter 4) control constructs were transiently transfected into HEK-293T cells. Transfection media was prepared by adding 3μl GeneJuice® transfection reagent (Novagen, Merck) to 100μl DMEM (Sigma) per reaction, mixed gently and left at room temperature for 10 minutes. 1μg/ml vector DNA was added dropwise to 100μl transfection media per reaction. The DNA was mixed gently with the transfection media and incubated at room temperature for 30 minutes. The transfection volume was then

added dropwise to HEK-293T cells at 60-80% confluency in a 6 well plate. Plates were incubated (37°C, 5% CO_2) for 24 hours. Cells were washed with 1ml chilled PBS and harvested by pipetting 1ml chilled PBS over the cells to detach them from the plate.

Transfected cells were adjusted to the appropriate concentration (1×10^5 cells/sample) for incubation with PD-1 mAbs 2, 10, 19 and 29 at 5μg/ml at 4°C for 20 minutes. MOPC-21 at 5μg/ml was used as an IgG1 isotype control (Mr Alistair Waugh, Human Immunology Unit, Weatherall Institute of Molecular Medicine, University of Oxford). After staining with PD-1 antibodies, cells were washed twice with 1ml chilled PBS containing 5% FCS. AlexaFluor®647 conjugated Donkey anti-mouse (Molecular Probes, Invitrogen) antibody was added to the cells at 5μgml and incubated at 4°C for 20 minutes. Cells were washed twice with 1ml chilled PBS containing 5% FCS and resuspended in PBS containing 5% FCS, 2% paraformaldehyde before being analysed by flow cytometry. For more information about the methods used in flow cytometry see Section 2.4.1.

3.2.5 Surface plasmon resonance

All surface plasmon resonance (SPR) experiments were performed using a BIACORE 3000® machine, BIAcore software and reagents (GE Healthcare UK Ltd.).

Experiments were performed using CM5 sensor chips (research grade) at 25°C in the running buffer HBS (10mM HEPES ph4.7, 150mM NaCl, 2mM EDTA, 0.005% surficant P-20, buffer premixed from BIAcore (GE Healthcare UK Ltd.)). All proteins were attached to chips using an amine coupling method [281]. To determine the

optimum conditions for protein coupling, a pre-concentration reaction was performed. Protein was diluted to a concentration of 0.2mg/ml in pH 5.5, 5.0, 4.5 and 4.0 10mM acetate. 30μl of these samples were injected over a single flow cell sequentially. The buffer with the highest pH at which protein readily concentrated at the chip surface electrostatically was chosen to use in protein coupling.

In brief, amine coupling was performed as follows. First, chip flow cells were activated by injecting 100μl 1-ethyl-3-(3-dimethylaminopropyl) carbodiimide (EDC) (0.4M) mixed 1:1 with N-hydroxysuccinimide (NHS) (0.1M) over the chips before injecting protein at 20-50μg/ml in the buffer determined by pre-concentration. When the required amount of protein was bound, the chip was deactivated by injecting 100μl ethanolamine/HCl (1M, pH 8.0). To wash the chip and determine the final amount of protein coupled, 30μl glycine (pH 2.5) was injected. Results were recorded using BIAcore Control Software version 3.1.1 (GE Healthcare UK Ltd.). Binding kinetics were analysed using BIAevaluation software (GE healthcare UK Ltd.).

3.2.6 Deglycosylation of PD-1/Fc

The Fc domain of PD-1/Fc was removed using thrombin to cleave PD-1 from Fc using an engineered site at their fusion junction. The protein was incubated with thrombin (Sigma) at 5 units/mg in HBS overnight, shaking at room temperature. To remove the cleaved Fc region (containing a 8x histidine tag) from the protein mixture, Ni-NTA magnetic agarose beads (Qiagen) in PBS pH 8.0 were mixed with the digested protein and incubated at room temperature, shaking for 3 hours. The reaction was

then centrifuged at 100rpm for 5 minutes and the supernatant, which only contained cleaved PD-1, was removed and retained. To test for the full removal of Fc, PD-1 supernatant was run on a SDS-PAGE gel under reducing and non-reducing conditions.

PD-1 was deglycosylated with either Endoglycosidse H (Endo H) or Peptide: N-Glycosidase F (PNGase F). The deglycosylation reaction using Endo H was carried out as follows.

	Company	Concⁿ	Volume
G5 reaction buffer	New England Biolabs	10 ×	10.0μl
Endo H	New England Biolabs	500 U/μl	5.0μl
ddH_2O	Sigma	—	5.0μl
PD-1	—	0 25μg/ml	80.0μl

Reactions were incubated at 37°C for 3 hours. PD-1 was deglycosylated by PNGase F in the following reaction.

	Company	Concⁿ	Volume
G7 reaction buffer	New England Biolabs	10 ×	11.0μl
PNGase F	New England Biolabs	500 U/μl	5.0μl
NP40	Merck	10%	11.0μl
ddH_2O	Sigma	—	4.0μl
PD-1	—	0 25μg/ml	80.0μl

The reaction containing PNGase F was incubated for 3 hours at 37°C. To visualise digested protein, samples of the reactions were run on reducing and non-reducing SDS-PAGE gels (For SDS-PAGE method see Section 2.3.2).

3.2.7 Western blotting

All western blotting was performed using mini Trans-Blot® cells (Bio-Rad). SDS-PAGE gels were blotted in Tris/glycine buffer (EC-880, National Diagnostics) on to Hybond® ECL® nitrocellulose membrane (Amersham GE Healthcare) at 100V for 45

minutes. Western blot membranes were blocked for 30 minutes in blocking buffer (PBS with 1% w/v casein, 0.05% NaN_3), before washing the blot three times for 5 minutes in wash buffer (0.05% Tween®20 in PBS with 0.05% NaN_3). Blots were probed with PD-1 mAbs at 0.2μg/ml in blocking buffer for 45 minutes on ice and the wash step repeated. The blots were probed with goat anti-mouse Fc horseradish peroxidase conjugate (Sigma) or goat anti-mouse FAB horseradish peroxidase conjugate (Sigma) at 0.2μg/ml in blocking buffer for 30 minutes on ice. After a further wash step, blots were visualised with ECL western blot substrate (Pierce).

3.3 Results

To enable the investigation of stimulatory activities of PD-1 mAbs and the effects of epitope position on antibody stimulatory activity, the generation of mAbs against human PD-1 was first required. To this end PD-1 mAbs were generated against the extracellular domain of human PD-1. Two rounds of antibody generation were performed to produce a total of four human PD-1 specific mAbs. The first round produced the human PD-1 mAbs 10, 19 and 29.

3.3.1 Generation of human PD-1 mAbs 10, 19 and 29

In the generation of human PD-1 mAbs 10, 19 and 29, a chimeric PD-1/Fc protein was used as the PD-1 protein antigen in the generation of human PD-1 mAbs. All mouse PD-1/Fc immunisations, mouse harvesting, hybridoma generation and screening was performed by BioGenes GmbH, Berlin, Germany and for further details see Section

3.2.1. Initial characterisation of the PD-1 mAbs, produced by the three hybridoma clones identified, showed them to be of an IgG1 isotype.

When cultured, the human PD-1 mAb hybridoma clones secreted high levels of mAb into tissue culture supernatant (Figure 3.1). The three PD-1 mAbs are resolved between 97 kDa and 220 kDa; this is consistent with the $\sim$ 140kDa molecular weight of mouse IgG. By comparing the intensity of the control 19A/Fc bands observed at $\sim$40kDa to those of the PD-1 mAbs the relative concentration of the antibodies can be estimated. The mAb bands in the PD-1 mAb hybridoma tissue culture supernatant are all of an equal or greater intensity than the control protein 19A/Fc, therefore the mAbs are in tissue culture supernatant at a concentration of 0.4mg/ml or above.

3.3.2 Purificiation of PD-1 mAbs 10, 19 and 29

During the mAb purification process, using weak anion exchange chromatography as outlined in 3.2.2, all elutions were collected and run on reducing and non-reducing SDS-PAGE gels to check for the presence of mAbs in low or high salt buffer elutions. Figure 3.2 shows the reducing and non-reducing SDS-PAGE gels of PD-1 mAb 10 ion exchange column elutions. This figure is representative of elutions obtained during the purification of all PD-1 mAbs.

The figure shows that the majority of the mAb (resolving in non-reducing conditions at $\sim$140 kDa and in reducing conditions as the $\sim$50 kDa IgG heavy chain and the $\sim$25 kDa IgG light chain) is eluted in elutions 2 to 4 with a small amount being observed in elution 5. A small amount of BSA (resolved in reducing and non-reducing

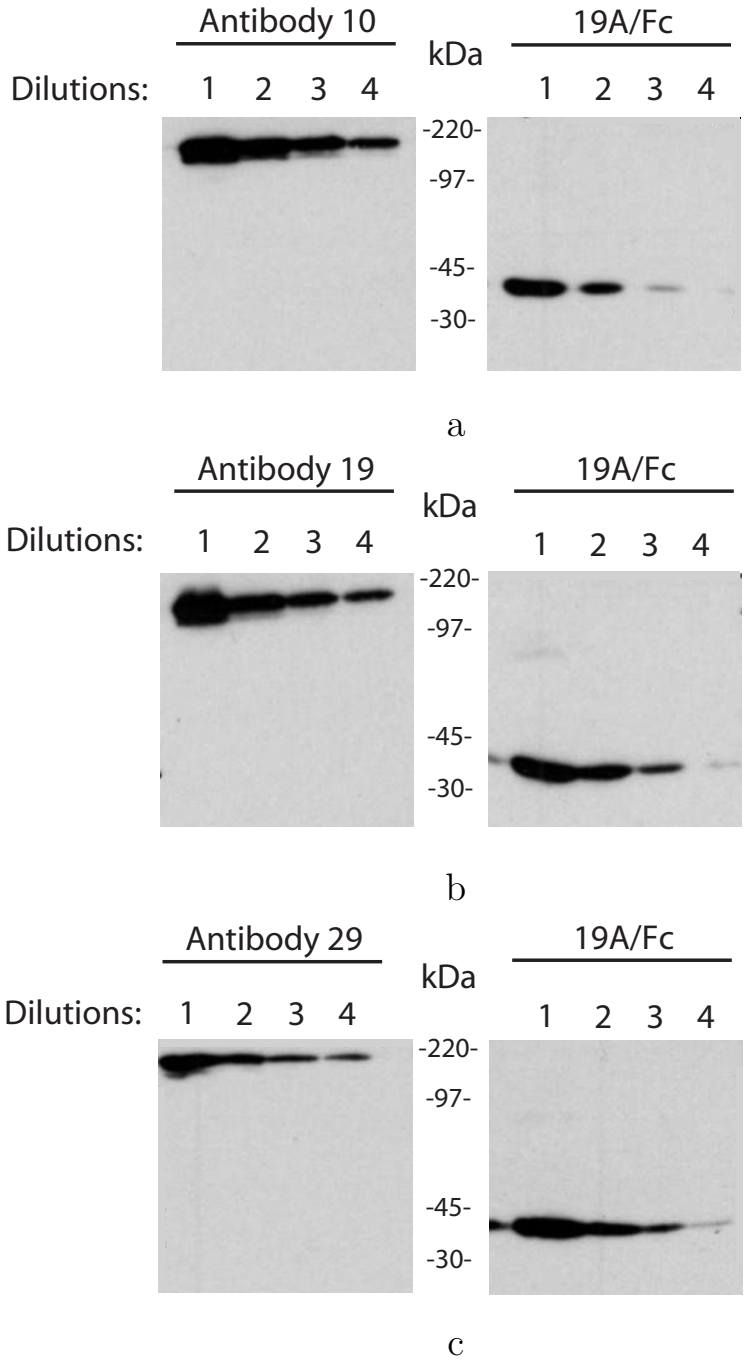
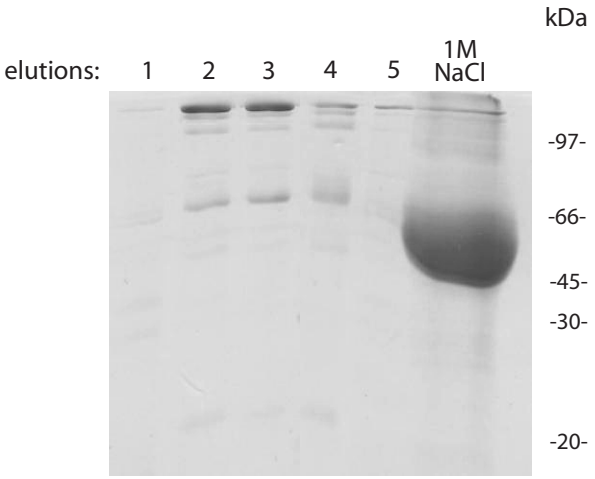
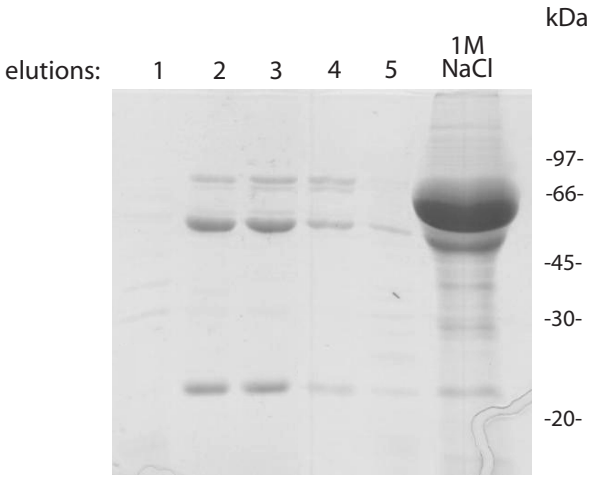


Figure 3.1: Tissue culture supernatants from PD-1 mAb hybridoma clone cultures (a) 10, (b) 19 and (c) 29 were diluted at 1/10, 1/30, 1/90 and 1/270 with BMEM media and run on 12% non-reducing SDS-PAGE gels. 19A/Fc chimeric protein at 0.4 mg/ml was run in the same dilution series alongside the PD-1 supernatants as a positive control to enable concentration estimation. Western blots of the gels were probed with a anti-mouse Fc HRP conjugate at 0.2μg/ml.

.



a



b

Figure 3.2: (A) Non-reducing and (B) reducing SDS-PAGE gels of PD-1 mAb 10 Fractogel® EMD DEAE resin column elutions. Dialysed tissue culture supernatant from PD-1 mAb hybridoma 10 was loaded on to a Fractogel® EMD DEAE resin column. mAb was eluted with 5 x 20ml column volumes of 0.05M NaCl TRIS-HCl buffer. To elute column bound BSA, 1 x 20ml column volume of 1M NaCl TRIS-HCl buffer was passed over the column before regeneration of the ion exchange media with 3 x 20ml column volumes of 0.05M NaCl TRIS-HCl buffer. 15μl samples of elutions one to five and the BSA elution were run on a 12% reducing and non-reducing SDS-Page gels to visualise BSA and PD-1 mAb 10.

conditions at 66 kDa) can be seen in elutions 2 to 4, but the majority of BSA is eluted from the column in the high salt buffer elution. The high levels of BSA seen eluted from the column during this elution is consistent with the high capacity of the column resin (100 mg BSA/ml resin). A small amount of mAb is present in the high salt elution, indicating a small amount of non-specific binding. Any high salt elutions containing significant amounts of mAb were pooled, re-dialysed and passed again over the ion exchange column.

To remove the remaining BSA from the low salt buffer elutions containing human PD-1 mAbs and to also remove any protein aggregations, antibody elutions were pooled, concentrated and passed over a size exclusion column. Samples of the elutions were run on reducing and non-reducing SDS-PAGE gels. Figure 3.3 shows the chromatogram of PD-1 mAb 10 eluting from a size exclusion column and a reducing and non-reducing SDS-PAGE gel of the elutions. The 140, 50 and 25 kDa bands on the reducing and non-reducing SDS-PAGE gels show that PD-1 mAb elutes from the column at approximately 64ml whereas the remaining BSA in the anion exchange purified mAb eluted at 74ml, shown on the reducing and non-reducing gel as 66 kDa bands. Pure mAb fractions were pooled, the concentration recorded and the antibody stored at -80°C for further use.

The post purification activity of all three PD-1 mAbs was tested by titration against PD-1 in an ELISA (Figure 3.4). mAbs 10, 19 and 29 all bound to plate bound PD-1 at high concentrations, although in titration, the mAbs 10 and 29 had different binding profiles to that of 19. At 100μg/ml mAb 29 binds to PD-1 at half of the level of mAb

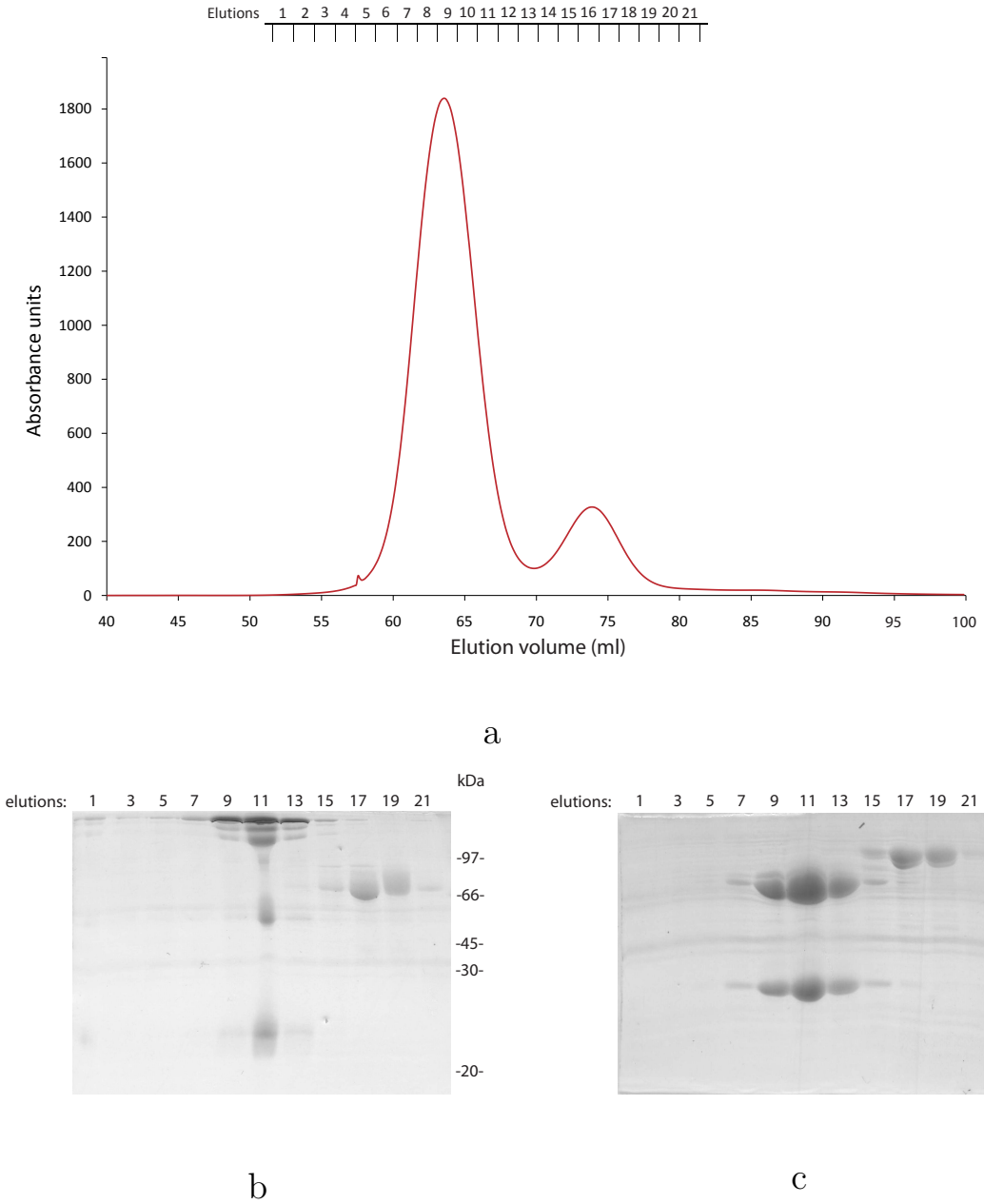


Figure 3.3: (a) Chromatogram of size exclusion chromatography purified PD-1 mAb 10. Concentrated anion exchange chromatography purified tissue culture supernatant containing PD-1 mAb 10 was passed over a Superdex 200 HR column size exclusion column at 0.5ml/min using a HPLC system. Antibody was eluted in HBS buffer in 1.5 ml elutions. (b) Non-reducing and (c) reducing SDS-PAGE gels of PD-1 mAb 10 size exclusion column elutions. 15μl samples of the elutions collected from the size exclusion column were run on reducing and non-reducing 12% SDS-PAGE gels.

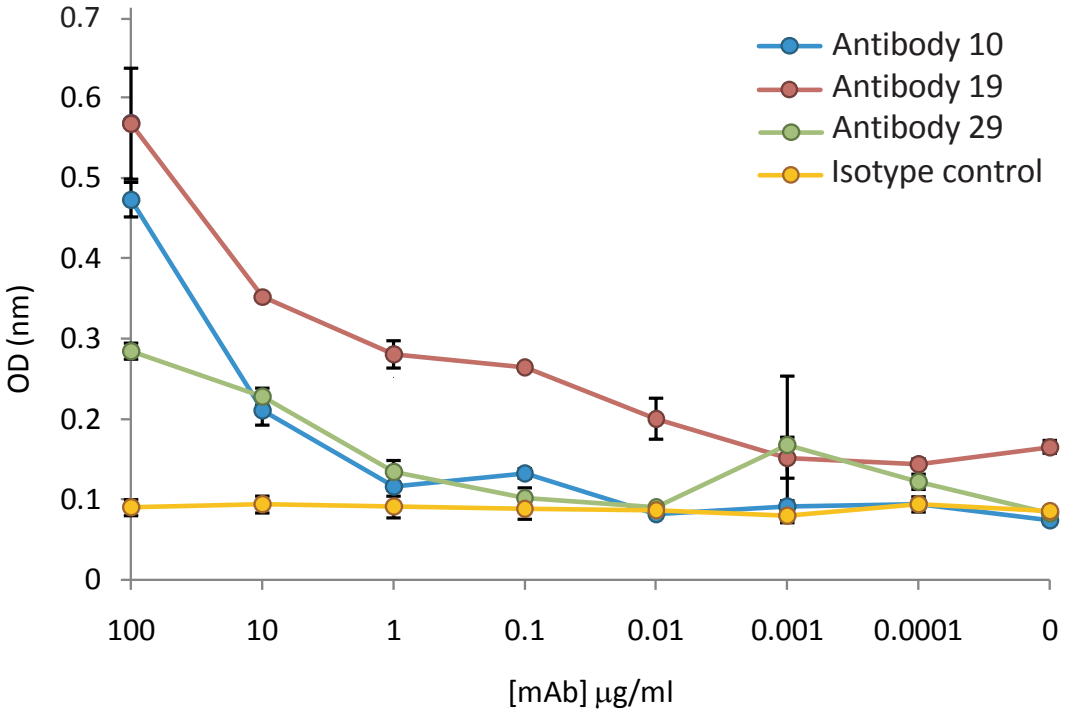


Figure 3.4: PD-1 mAb ELISA. Purified PD-1 mAbs 10, 19, 29 and OX7 isotype control were titrated from 100μg/ml to 0.0001μg/ml against human PD-1 plate immobilised target at 10μg/ml.Human PD-1 was prepared from thrombin cleaved PD-1/Fc purified of its Fc by Ni affinity chromatography. A secondary IgG anti-Fab specific horseradish peroxidase conjugated antibody and ABTS substrate was used to develop the ELISA, reading substrate colour intensity at 425mn.

19 at higher concentrations until a concentration of 0.001μg/ml. At this concentration the binding of all the mAbs was reduced to background levels. In comparison mAb 10 binds PD-1 at an equivalent level to 19 at 100μg/ml but then its binding drops rapidly to levels of mAb 29. These results suggest that the PD-1 antibodies produced have differing binding affinities. Although the concentrations of the PD-1 mAbs were titrated to relatively high levels, none of the antibodies reached saturation. mAb 29 is the only antibody which looks to be reaching saturation at 100μg/ml.

3.3.3 Epitope mapping of human PD-1 mAbs

Based on the crystal structure of murine PD-1 [269] thirty seven human PD-1 mutants were designed to map the epitopes of the human PD-1 mAbs (for details of mutations see Tables 3.1-3.3 and Figure 3.5). To ensure the maximum disruption of mAb epitopes, drastic residue changes were made: small residues were changed to large residues, e.g. alanine 56 was mutated to arginine, and uncharged residues were substituted with charged residues, e.g. asparagine 41 mutated to lysine. This strategy was used to saturate the surface of human PD-1 with mutations with the aim of disrupting the epitopes of human PD-1 mAbs 10, 19 and 29. Residues with externally facing side chains according to the crystal structure were chosen for mutation, and asparagine residues were not mutated if thought to be involved in the glycosylation of PD-1. By mutating selected residues drastically, if any residues important in the structural stability of PD-1 were chosen for mutation, their drastic mutation would lead to the resultant protein not being expressed, so reducing the amount of false

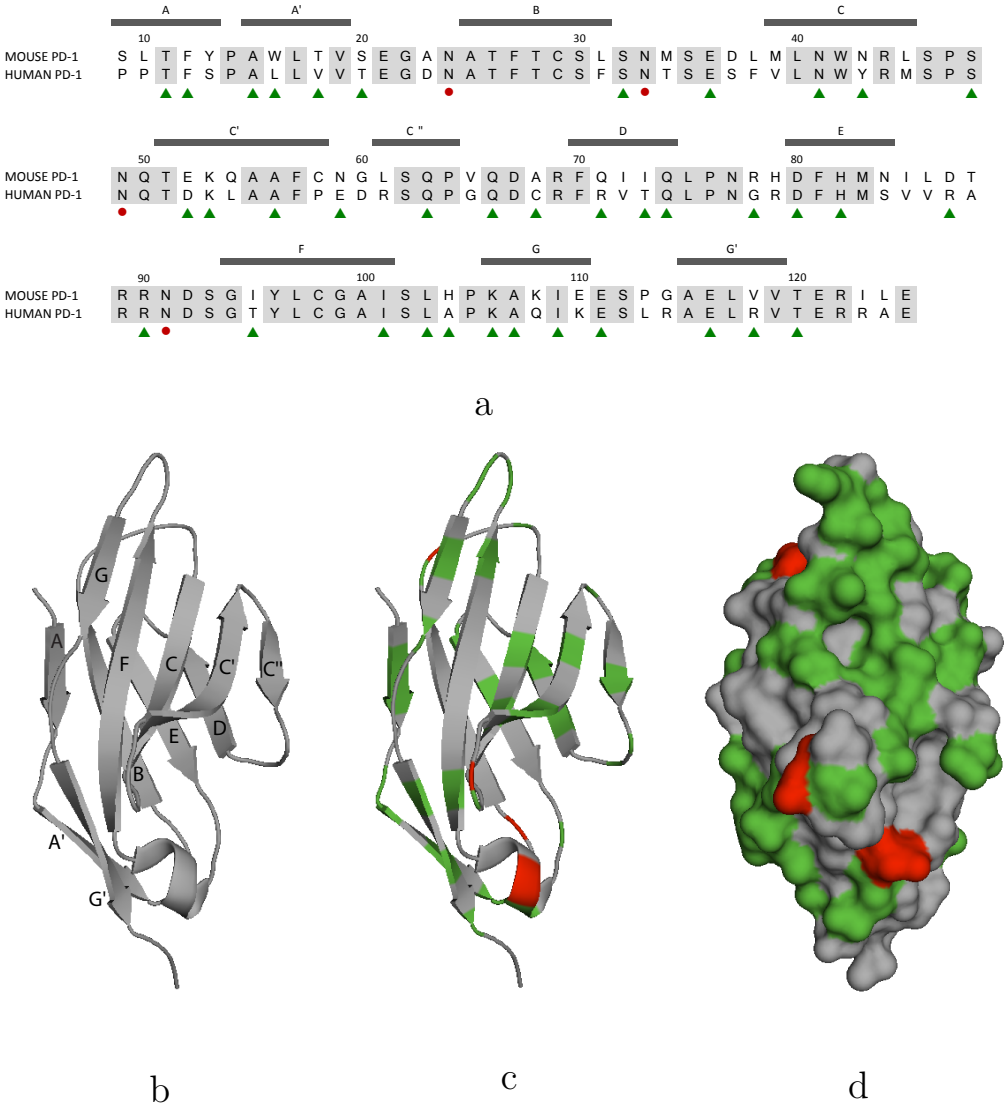


Figure 3.5: Sequences, structure and mutations of PD-1. (a) Sequence alignment of human and mouse PD-1. Residues which form the β strands in the PD-1 Ig V-set domain are indicated by the labelled dark grey bars. Conserved residues between human and mouse PD-1 are highlighted grey. Residues in human PD-1 selected for mutation are indicated by closed green triangles. The four potential N-linked glycosylation sites are identified by closed red circles. (b) Ribbon diagram of the Ig V-type domain of mouse PD-1. (c) and (d) Ribbon diagram and surface representation of the mouse PD-1 structure. Equivalent residues mutated in human PD-1 are coloured green. Putative N-linked glycosylation sites are coloured red.

negatives. The epitopes of the human PD-1 mAbs were investigated by determining the level that the PD-1 mAbs bind to PD-1 mutants using flow cytometry. All PD-1 mutants were expressed in the pGFP^2-N3 vector, which fuses a GFP^2 to the C-terminus of the PD-1 mutant constructs. This allows the localisation of expressed PD-1 to be visualised with UV microscopy when transiently expressed in HEK 293T cells. All of the PD-1 mutants showed the same expression as wild type PD-1_{EX}CD$28_{TM/CYT}$ and localised to the cell surface with no significant observed intracellular localisation. The similar behavior shown by the wild type and mutant PD-1 constructs imply that all the PD-1 mutant proteins were correctly folded and processed to the cell surface. In preparation for flow cytometry analysis, transfected cells were harvested and incubated with PD-1 mAb 10, 19, 29 and an IgG1 isotype control before staining with a secondary anti-mouse IgG AlexaFluor®647 secondary. The binding of each mAb to mutant PD-1_{EX}CD$28_{TM/CYT}$ was expressed as the percentage of GFP^2 positive cells which were negative for mAb binding. Figure 3.6 shows that through screening with the thirty seven PD-1 mutants, residues were identified which when mutated affected the binding of PD-1 mAbs 10 and 19, and from these data their epitopes were identified.

PD-1 mAb 10 epitope

A total of five mutations of PD-1 affected the binding of mAb 10 (Figure 3.6). mAb 10 binding is completely abolished by PD-1 mutation K53E, whereas mutations L103E, N41K, A56R and Y43R reduced mAb 10 binding by ∼75% ∼45% ∼30% and ∼17% respectively. Residues N41K, K53E, A56R and Y43R are clustered together across the

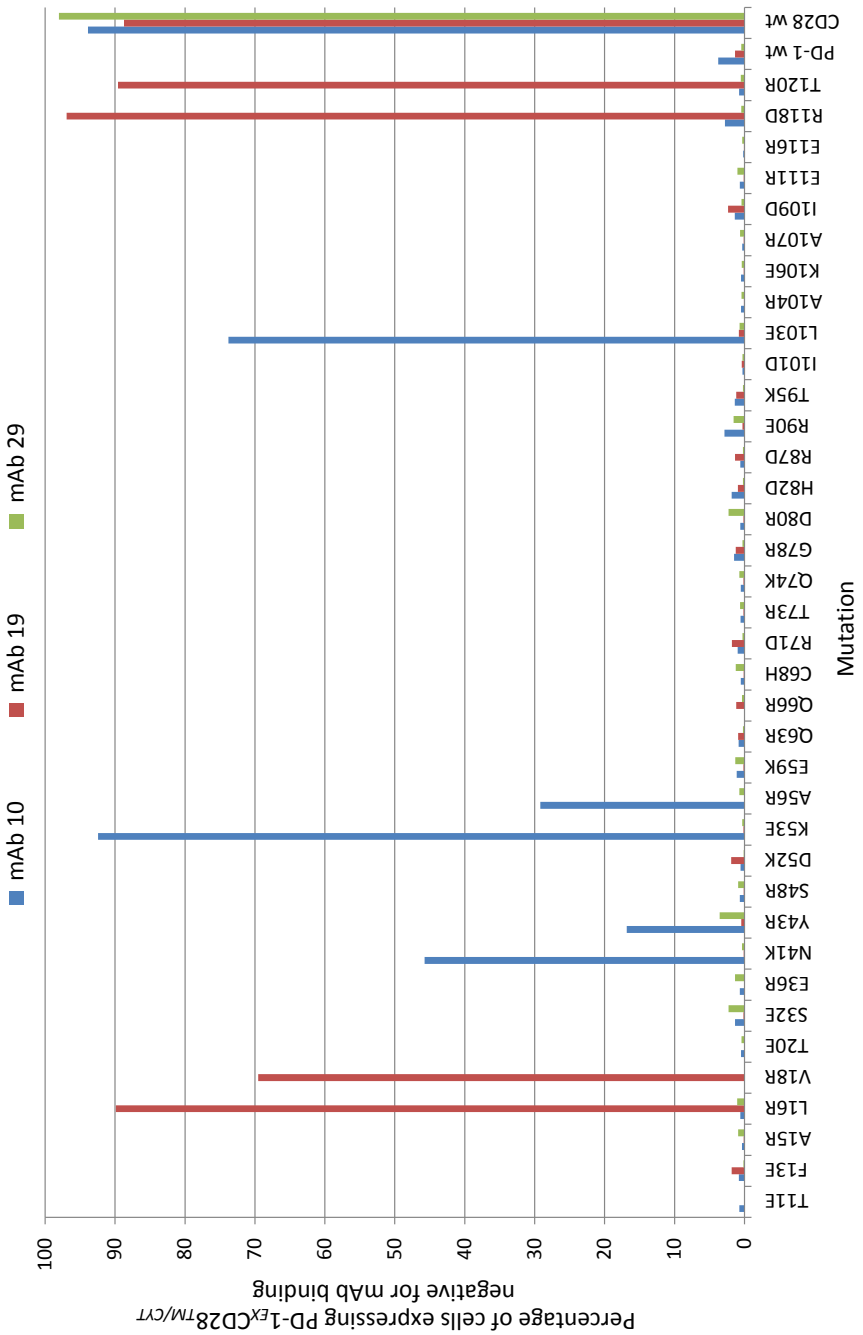


Figure 3.6: Human PD-1 mAb epitope mapping. Mutant PD-1_{EX}CD$28_{TM/CYT}$ GFP^2 fusion constructs were transiently transfected into HEK-293T cells. After 24 hours, cells were harvested and the binding of PD-1 antibodies 10, 19 and 29 was assayed by flow cytometry. Cells were stained with 5μg/ml PD-1 antibody before staining with donkey anti-mouse AlexaFluor®647 secondary conjugate at 5μg/ml. Successfully transfected cells were identified by gating for GFP expression and transfected cells positive for PD-1 antibody binding were recorded by gating for AlexaFluor®647 positive cells. To identify residues of which mutations affected mAb binding data is expressed as the percentage of PD-1_{EX}CD$28_{TM/CYT}$ positive cells that are negative for mAb binding.

C and C′ strands of PD-1, which suggests that this region may form the core of the epitope (Figure 3.7). Mutation L103E has a significant effect on mAb 10 binding but is situated on the loop between the F and G strands, which is away from the C/C ′ location of the other four clustered residues which appear to form the core of the mAb 10 epitope. Although other residues found on and around the FG loop were mutated, only mutation L103E elicited an effect on mAb 10 binding. The FG loop is common to the structure of the CD28 protein family of which PD-1 is a member [194]. But unlike the CD28 and CTLA-4 FG loop which has the rigid MYPPPY motif, the FG loop of PD-1 is thought to be highly flexible. This is suggested by its crystal structure and protein sequence [269]. The flexible nature of the PD-1 FG loop may allow the involvement of residue L103E in the mAb 10 epitope despite its distance from the other clustered residues in the C/C ′ area. L103E may be directly part of an mAb 10 epitope which stretches across the top of PD-1 or indirectly influence the structure of an epitope of mAb 10 which is centered on the C and C ′ strands.

PD-1 mAB 19 epitope

Four mutations of PD-1 greatly affected PD-1 mAb 19 binding. Mutations L16R, R118D and T120R completely eliminated mAb 19 binding, and mutation V18R reduced binding by $\sim$ 70% (Figure 3.6). These mutations are found clustered on a membrane proximal region of the A′ and G′ strands of human PD-1. This orientates the mAb 19 epitope diagonally opposite to the epitope of mAb 10 which is on a more membrane distal position of PD-1 (Figure 3.7).

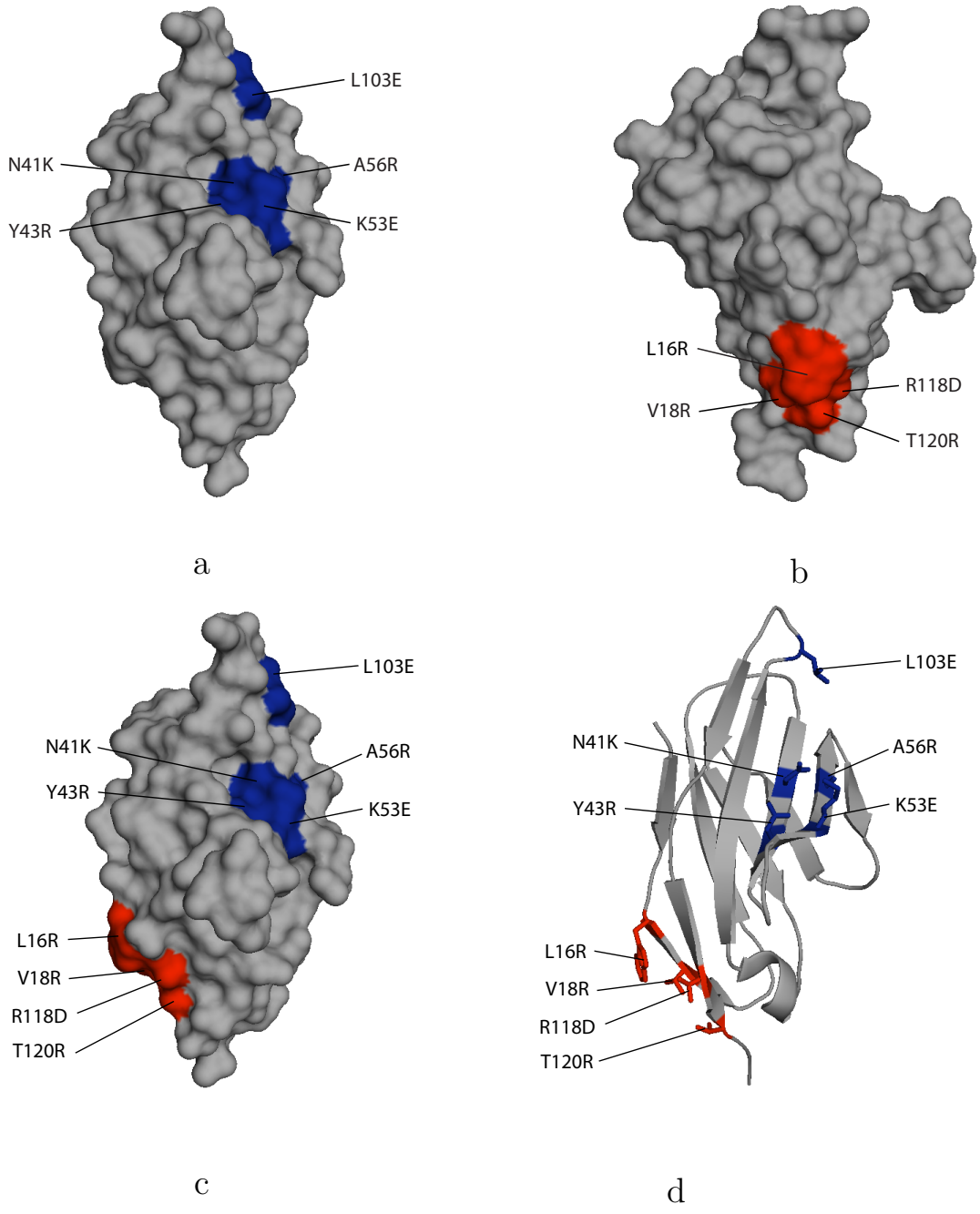


Figure 3.7: Epitopes of human PD-1 mAbs 10 and 19. The molecular surface of PD-1 highlighted with residues whose mutations resulted in reduced or abolished PD-1 mAb binding. (a) Residues involved in the mAb 10 epitope are labelled in blue. (b) The molecular surface of PD-1 rotated 90° to show the residues involved in the mAb 19 epitope (red). (c) The molecular surface of PD-1 showing the epitopes of both PD-1mAb 10 and 19. (d) A ribbon diagram of PD-1 showing the epitopes of both PD-1 mAbs 10 and 19.

PD-1 mAb 29 epitope

The epitope mapping that was employed to identify the epitopes of mAbs 10 and 19 was unable to identify the epitope of mAb 29. The thirty seven mutated PD-1 residues were chosen to cover the accessible surface of human PD-1, but none of the mutations affected the binding of PD-1 mAb 29 (Figure 3.6).

Because the epitopes of mAb 10 and 19 were identified through mutational epitope mapping, we were able to investigate if these two regions of PD-1 were involved with the mAb 29 epitope and whether each of the three PD-1 mAbs has a distinct epitope. An SPR competition binding assay was performed in which each individual human PD-1 mAb was successively injected over immobilised hPD-1/Fc (injections of mAb 29, 19 and 10 respectively) (Figure 3.8). If mAb 29 shared epitope residues with or bound to PD-1 in the same region as mAb 19 or 10, by binding first to PD-1 it would prevent the binding of mAbs 19 and 10 to hPD-1/Fc.

The rat anti-mouse IgG1 used to immobilise the hPD-1/Fc is also able to bind directly to the mouse derived human PD-1 mAbs. To minimise the amount of PD-1 mAbs 19 and 10 binding to the rat anti-mouse IgG1 in subsequent injections, three successive injections of mAb 29 were made to ensure complete saturation of PD-1/Fc and any free rat anti-mouse IgG1. mAbs 10 and 19 bound successfully to immobilised PD-1 after mAb 29 saturation, suggesting that the epitope of mAb 29 is in a different region to the epitopes of mAbs 10 and 19.

To investigate the extent to which the method of hPD-1/Fc immobilisation influenced the results of the SPR competition experiment, amine coupling was used to

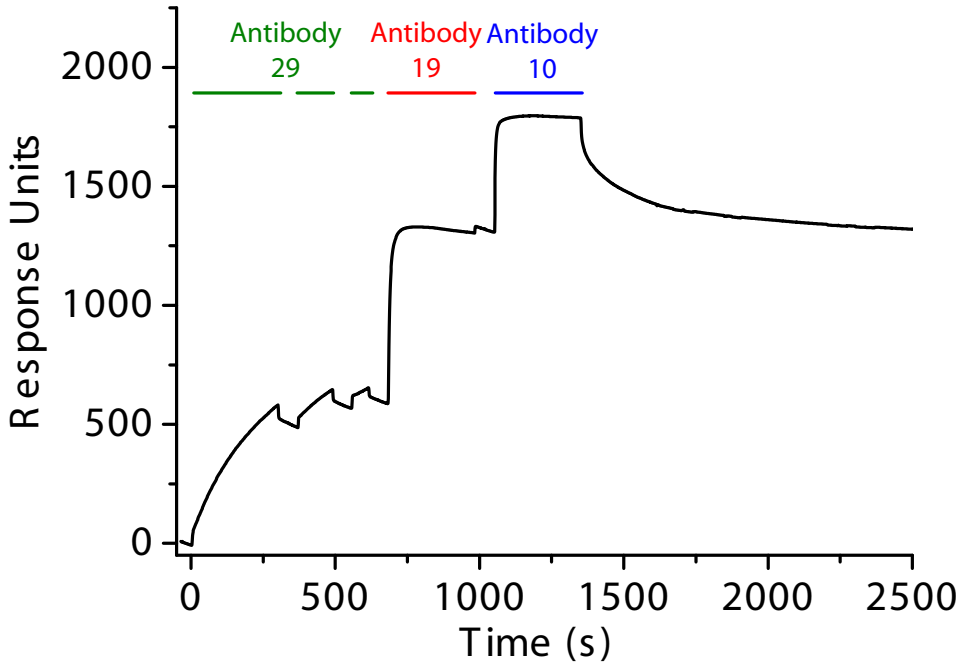
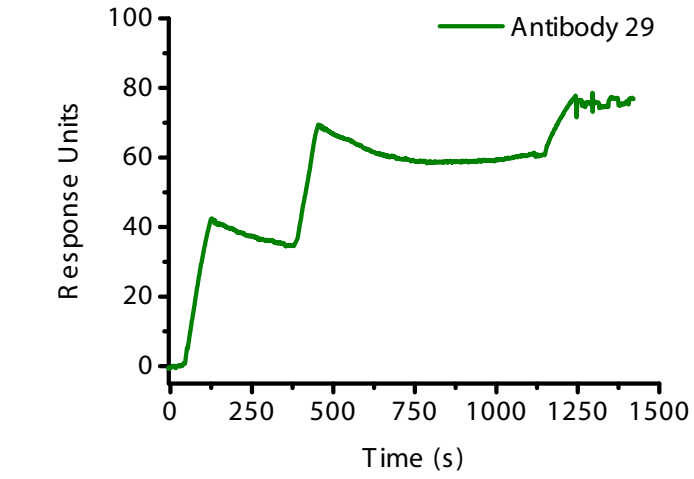


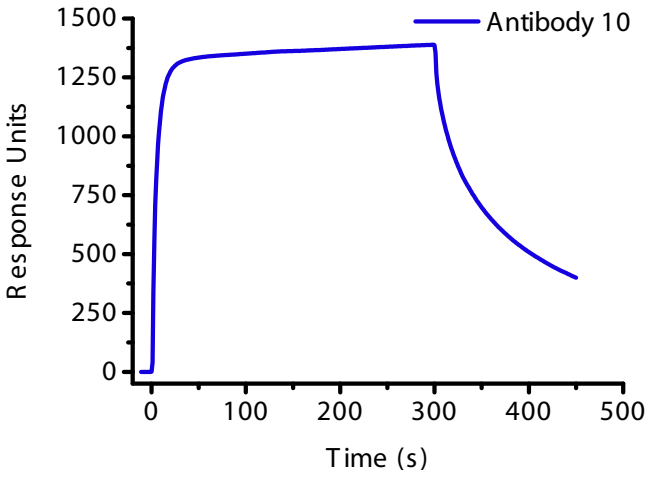
Figure 3.8: Competition binding of human PD-1 mAbs to indirectly immobilised PD-1/Fc. ∼5100 RU of rat anti-mouse IgG1 was directly immobilised by amine coupling in pH 4.0 acetate to a CM5 BIAcore sensor chip. This was used to indirecly immobilise ∼1000 RU of PD-1/Fc. Three successive injections of PD-1 mAb 29 at 200μg/ml of 50μl, 20μl and 5μl were made over the immobilised PD-1/Fc at 30μl/min at 25°C. This was followed by 50μl injections of PD-1 mAb 19 (200μg/ml) and 10 (200μg/ml).

directly immobilise the hPD-1/Fc opposed to the previous method of indirect immobilisation with rat anti-mouse IgG1 (Figure 3.9). Initial observations suggested that no PD-1 mAb 29 bound to the directly immobilised PD-1/Fc. But after the subtraction of control protein (CTLA-4/Fc) sensogram data collected concurrently with the PD-1/Fc binding, it emerged that PD-1 mAb 29 does bind to directly immobilised PD-1/Fc but at a greatly reduced level. When ∼2000 RU of PD-1/Fc is directly immobilised on the chip, mAb 29 approaches saturation at only ∼100 RU. This is compared to the saturation of indirectly immobilised PD-1/Fc with <500 RU mAb 29 at only half the level of immobilised PD-1/Fc. To confirm that the conformational integrity of the immobilised PD-1/Fc, PD-1 mAb 10 was injected over directly immobilised PD-1/Fc. PD-1 mAb 10 bound to the PD-1/Fc at high levels (1659 RU). This binding suggests that, when directly immobilised on the chip, the PD-1/Fc mAb 10 epitope retains a level of conformational stability. This indicates that the direct immobilisation process does not completely alter the tertiary structure of PD-1/Fc.

Protein glycosylation is important in the correct folding and stabilisation of proteins [282]. Human PD-1 has four N-linked glycosylation sites at residues 24, 33, 49 and 91. The presence of these glycans leads to the possibility that mAb 29 binds to a sugar epitope. To investigate the possibility of a sugar epitope or an epitope influenced by glycosylation, wild type PD-1_{EX}CD$28_{TM/CYT}$ in the pGFP^2-N3 vector was transiently expressed in HEK 293S cells. These are a GnTI$^{-/-}$ deficient form of the HEK 293T cell line [283] that lack N-acetylglucosaminyltransferase I and so cannot produce complex N-linked glycans. These cells expressing PD-1_{EX}CD$28_{TM/CYT}$ were



a



b

Figure 3.9: Binding of human PD-1 mAb 29 and 10 to directly immobilised PD-1/Fc. 2100RU of hPD-1/Fc at 200μg/ml was directly immobilised in pH 4.5 sodium acetate by amine coupling on a CM5 BIAcore sensor chip. As a control protein 2500RU of CTLA-4/Fc was directly immobilised in pH 4.5 sodium acetate by amine coupling on one flow cell. (a) Three 20μl injections of PD-1 mAb 29 at 200μg/ml were made over immobilised PD-1/Fc and CTLA-4/Fc at 30μl/min at 25°C. Sensogram data obtained for the CTLA-4 flow cell was subtracted from that of the PD-1/Fc flow cell to create sensogram shown. (b) 50μl PD-1 mAb at 200μg/ml was injected over directly immobilised hPD-1/Fc at 30μl/min at 25°C.

studied by flow cytometry analysis using mAb 29 (Figure 3.10). The levels of mAb 29 binding observed by flow cytometry analysis were expressed as the percentage of PD-1_{EX}CD$28_{TM/CYT}$ positive cells that were also positive for PD-1 mAb binding. mAb 29 bound to PD-1_{EX}CD$28_{TM/CYT}$ processed in GnTI$^{-/-}$ HEK 293S cells to a similar degree as PD-1 expressed in HEK 293T cells. This indicates that complex glycans are not involved in creating the epitope of mAb 29.

To investigate how drastic changes in PD-1 glycans affect mAb 29 binding, PD-1 was cleaved of its complex sugars and probed for mAb 29 binding (Figure 3.11). This was achived by treating PD-1 with PNGase F or Endo H. PNGase F is an amidase which cleaves N-linked glycoproteins between the innermost N-acetylglucosamine and asparagine residues of high mannose, hybrid, and complex oligosaccharides [284]. The recombinant glycosidase Endo H cleaves within the chitobiose core of high mannose and some hybrid oligosaccharides from N-linked glycoproteins [284]. mAb 19 was used as a positive control in this experiment due to its compact, well characterised protein dependent epitope which is unlikely to be influenced by PD-1 glycans. As figure 3.11 shows, untreated human PD-1 resolves at ∼30kDa. Endo H cleaves all four glycan residues from PD-1, leaving the completely deglycosylated form of PD-1 at ∼15kDa which is close to its calculated molecular weight of 16895 Da. The Western blot shows that the digestion of PD-1 with PNGase F did not go to completion. Fully glycosylated PD-1 is still present along with three partially deglycosylated forms of PD-1 (at ∼27kDa, ∼23kDa and ∼20kDa) and PD-1 cleaved of all four of its complex sugars (∼17kDa). The Western blot probed with PD-1 mAb 19 shows that the mAb

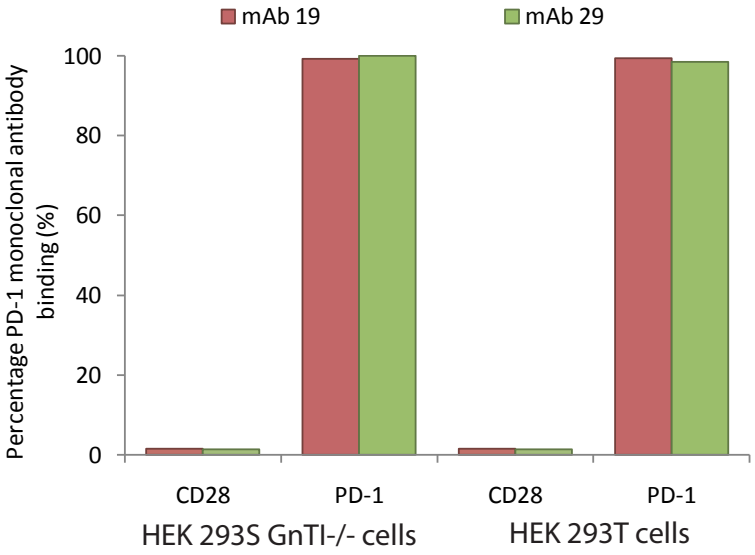


Figure 3.10: Investigation of the effect of complex N-linked glycans on the binding of PD-1 mAb 29 on PD-$1_{EX}CD28_{TM/CYT}$ expressed in HEK 293S GnTI$^{-/-}$. Binding of PD-1 mAbs 29 and 19 to PD-$1_{EX}CD28_{TM/CYT}$ and $hCD28_{EX}mCD28_{TM/CYT}$ transiently expressed on HEK 293T and HEK 293S GnTI$^{-/-}$ cells. Cells were transiently transfected with PD-$1_{EX}CD28_{TM/CYT}$ or $hCD28_{EX}mCD28_{TM/CYT}$in pGFP^2-N3 for 24 hours before staining with either 5μg/ml PD-1 mAb 19 (red) or 29 (green) followed by secondary staining with AlexaFluor®647 conjugated donkey anti-mouse antibody at 5μg/ml. Cells were analysed using flow cytometry. Successfully transfected cells were selected by gating for GFP expression and the transfected cells positive for PD-1 mAb binding were recorded by gating for AlexaFluor®647 positive cells.

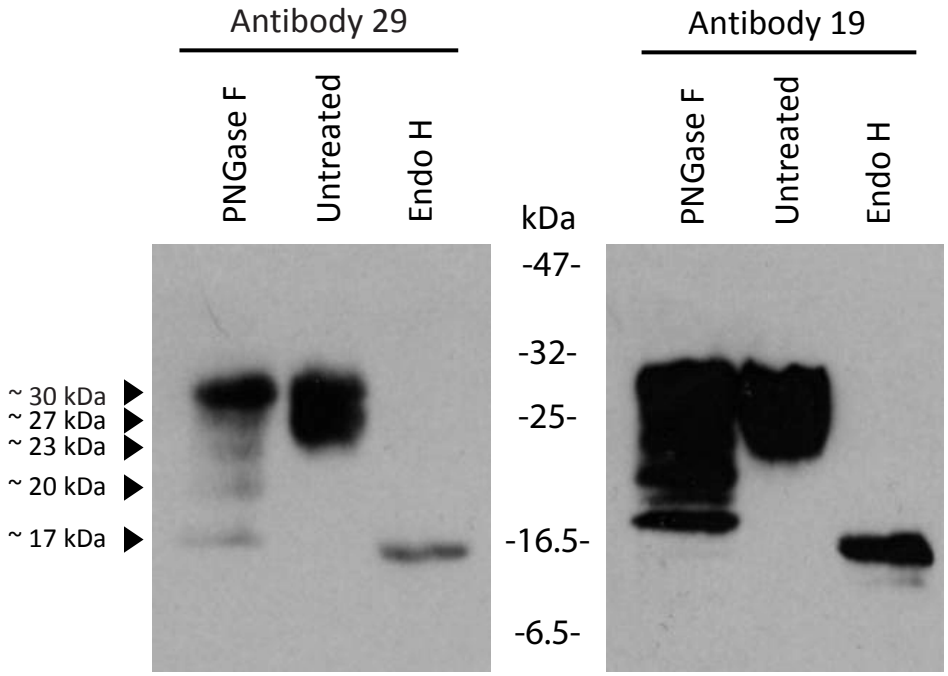


Figure 3.11: Investigation of the effect of deglycosylation of PD-1 on the binding of PD-1 mAb 29. PD-1/Fc was cleaved of Fc by thrombin cleavage and purified from the Fc domain using nickel affinity chromatography. PD-1 was incubated for 3 hours at 37°C with PNGase F or Endo H. Deglycosylated PD-1 was run on SDS-PAGE gel alongside untreated PD-1 and western blotted. Blots were probed with PD-1 mAbs 29 or 19 at 0.2μg/ml and goat anti-mouse FAB horseradish peroxidase conjugate at 0.2μg/ml secondary antibody.

binds to all deglycosylated forms of PD-1. This confirms that the epitope of mAb 19 is not influenced by the glycans present on PD-1. The mAb 29 probed Western blot shows that mAb 29 was significantly poorer at binding deglycosylated forms of PD-1 compared to mAb 19. When compared to untreated PD-1, mAb 29 binds to all four forms of PNGase F treated PD-1 and Endo H treated PD-1, but at a much reduced level. These results suggest that PD-1 mAb 29 has an epitope which is directly influenced by PD-1 glycans, but the observed binding of mAb 29 to completely deglycosylated PD-1 shows that it is not a solely sugar epitope. By removing the sugars from PD-1, the mAb 29 epitope may be structurally destabilised, only leaving a small proportion of PD-1 with an epitope which the mAb can effectively bind to.

Whilst developing the Western blots described here, it was observed that mAb 29 was poor as a probing mAb. Both mAbs were used at a concentration of 0.2μg/ml diluted in a casein based buffer, but during the exposure, the length of time needed to resolve the mAb 19 and 29 Western blots were significantly different. Western blots probed with PD-1 mAb 19 required an exposure of only 20 seconds to be able to visualise PD-1, whereas mAb 29 blots required an exposure of 5 minutes before PD-1 bands became visible. Whilst evidence suggests that the epitope of mAb 29 may be influenced by the sugar residues of PD-1, this addition experimental evidence illustrates that mAb 29 is a poor antibody that seems to bind weakly to PD-1.

3.3.4 PD-1 mAb binding kinetics

Having identified the epitope of PD-1 mAb 10 at a membrane distal position and the epitope of mAb 19 at a membrane proximal location on PD-1, it is possible to make a prediction on their agonist properties. However, to be able to compare the stimulatory abilities of these two mAbs and draw conclusions based on epitope position, the binding kinetics of the two mAbs have to be similar. If the binding affinities of the mAbs are not comparable any difference in stimulatory activity could be attributed to binding affinity and not epitope location. To better understand the affinities of each mAb the binding kinetics of mAb 10, 19 and 29 were investigated using SPR analysis.

Figure 3.12 shows the sensorgrams obtained from injections of PD-1 over directly immobilised PD-1 mAbs 10, 19 and 29. The PD-1 used in the kinetic injections was the same PD-1/Fc protein that was used in the generation of PD-1 mAbs, cleaved of its Fc using thrombin protease. To ensure that only monomeric PD-1 was used in the injections, other impurities and aggregated proteins were removed by passing PD-1 through a Superdex 75 gel filtration column immediately prior to injection. Initial observations of the three sensorgrams generated show that mAbs 10, 19 and 29 have very different kinetics. Data obtained from passing 8.8μM PD-1 over PD-1 mAb 10 shows that the sensorgram returns to baseline less than fifty seconds post PD-1 injection whereas in flow cells containing mAbs 19 and 29, PD-1 is still associated with the mAbs after 15 minutes. This difference in dissociation time suggests that mAb 10 has a mush faster off rate than mAb 19 or 29.

A comparison of the dissociation phase data of the PD-1 mAbs is shown in Fig-

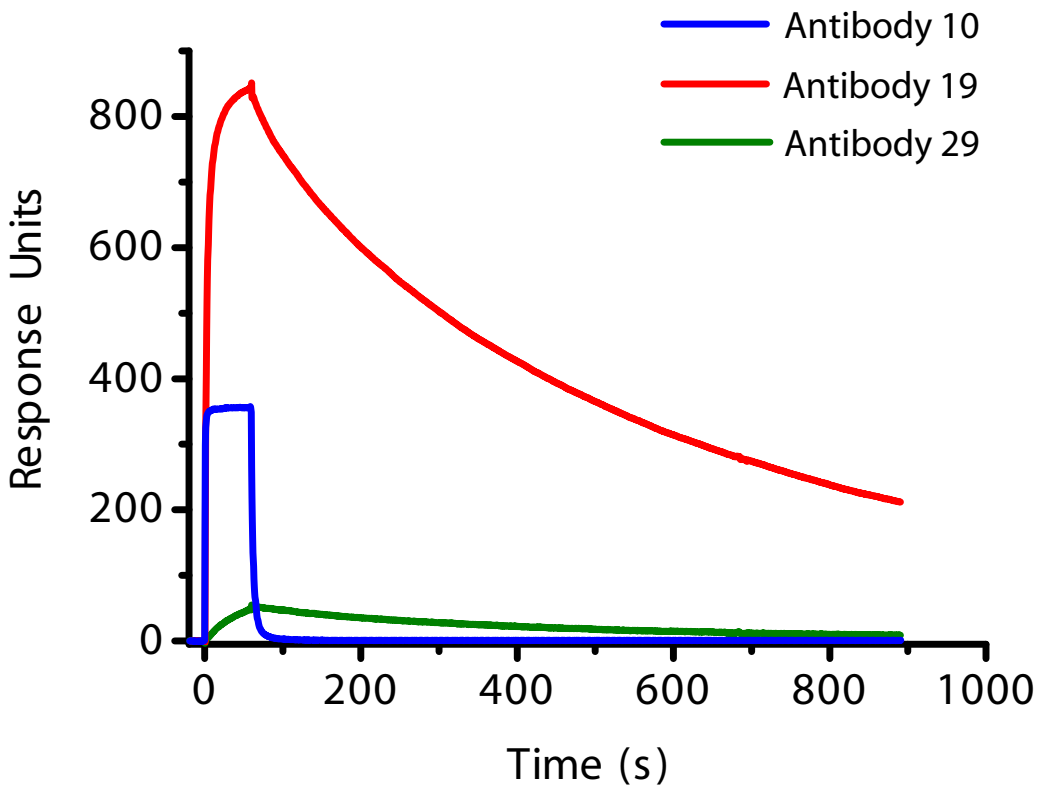


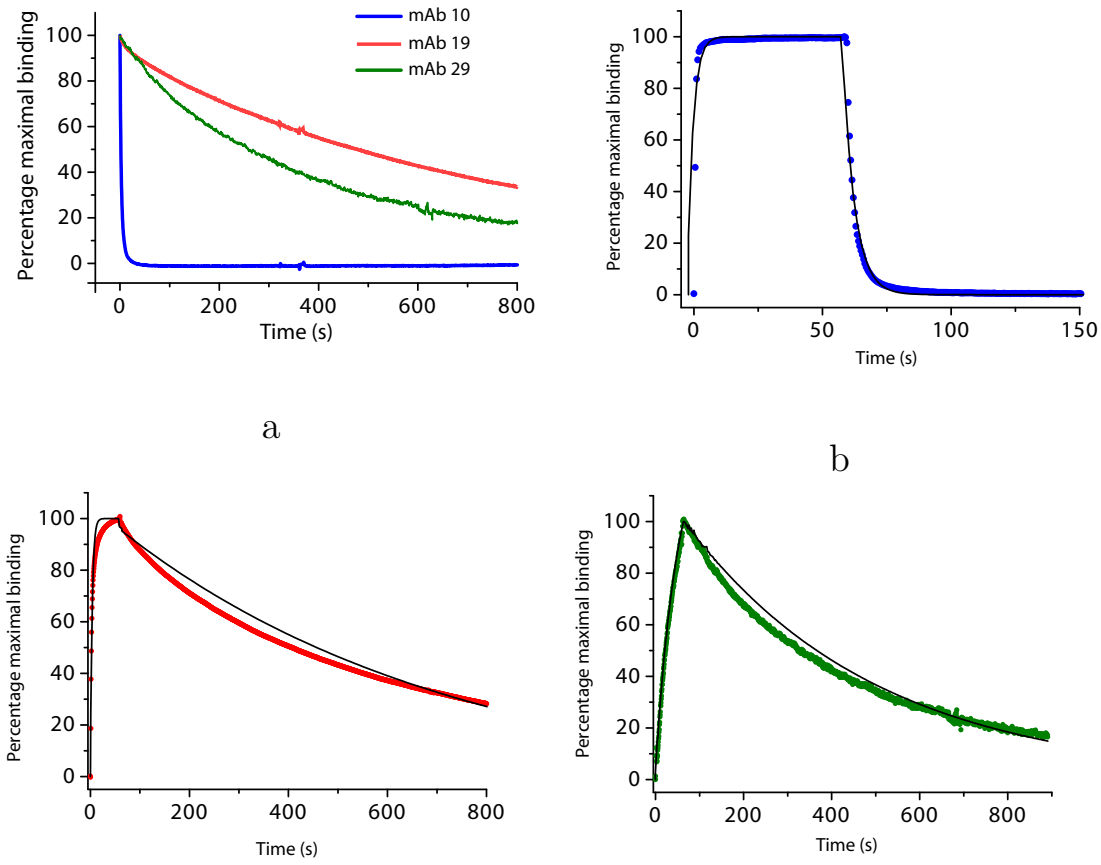
Figure 3.12: Sensorgram of human PD-1 binding to PD-1 mAbs 10, 19 and 29. 8.8 μM monomeric PD-1 was kinetically injected directly over directly immobilised PD-1 mAbs 10 (4695 RU), 19 (4255 RU) and 29 (4052 RU) and control mouse IgG1 (4764 RU) at 30μl/min at 25°C. PD-1 mAbs were directly immobilised by amine coupling. Data was recorded for 15 minutes. Sensorgram data recorded for the control mouse IgG1 was subtracted from PD-1 mAb data to account for background non-specific protein interactions and buffer effects.

ure 3.13. The association rate (k_{on}), dissociation rate (k_{off}) and dissociation constant (K_d) were simultaneously calculated using the sensorgram data generated using a 1:1 Langmuir binding model (Figure 3.12). The k_{off} values (Figure 3.13) show that the k_{off} for mAb 29 binding to PD-1 (2.31×10^{-3} s^{-1}) is double that for mAb 19 (1.17×10^{-3} s^{-1}), but both dissociation rates are significantly lower than the k_{off} for mAb 10 (2.31×10^{-3} s^{-1}). The association rate (k_{on}) and dissociation constant (K_d) were calculated using the calculated k_{off} and sensorgram data generated using a 1:1 Langmuir binding model (Figure 3.12). The k_{on} values calculated reflect what can be observed from the sensorgram data, i.e. that mAb 29 has a slow k_{on} (2.01×10^{3} $M^{-1}s^{-1}$). This k_{on} is 10 times slower than mAbs 10 (2.69×10^{4} $M^{-1}s^{-1}$) and 19 (3.22×10^{4} $M^{-1}s^{-1}$), which both have similar association rates.

Despite the similar association rates calculated for mAbs 10 and 19, their dissociation constants differ significantly resulting in K_d values of 8.03×10^{-6} M for mAb 10 and 5.32×10^{-8} M for mAb 19. This 66 fold difference in affinity can be accounted for by the very fast dissociation rate of mAb 10. Similarly the k_{off} for mAb 19 and mAb 29 are both relatively similar but the slow association rate of mAb 29 leads to the 462 fold difference in dissociation constant (K_d at 1.15×10^{-6}M).

3.3.5 Generation and characterisation of PD-1 mAb 2

The characterisation of the three PD-1 mAbs generated show that mAb 19 has a membrane proximal epitope whereas mAb 10 has a membrane distal epitope. Through the successful identification of two PD-1 mAbs with membrane proximal and distal



PD-1 antibody	K_{off} (s^{-1})	K_{on} (m^{-1} s^{-1})	K_d (M)
10	2.16×10^{-1}	2.69×10^{4}	8.03×10^{-6}
19	1.17×10^{-3}	3.22×10^{4}	5.32×10^{-8}
29	2.31×10^{-3}	2.01×10^{3}	1.15×10^{-6}

e

Figure 3.13: Comparison of kinetic data of PD-1 mAbs 10, 19 and 29. (a) A comparison of PD-1 mAb off rates. Percentage maximal binding was calculated from the dissociation phase data collected in Figure 3.12. Antibody dissociation data was divided by the maximal PD-1 binding value for that antibody and expressed as a percentage. (b-d) Binding data collected in Figure 3.12 was fitted with a 1:1 Langmuir binding model to calculate an association rate (k_{on}), dissociation rate (k_{off}) and dissociation constant (K_d) for mAbs 10 (b), 19 (c) and 29 (d). Values calculated are shown in (e).

epitopes, it is hoped that downstream testing for stimulatory activity may show a link between stimulatory strength and epitope position. But the effects of stimulatory antibodies may also be attributed to antibody binding affinity as well as epitope location [262]. The significant differences in the binding kinetics of mAb 10 and 19 shown, would make it impossible to attribute any stimulatory differences observed to epitope position alone. With this in mind a second round of human PD-1 mAb generation was undertaken, with a view to generating PD-1 mAbs with similar binding affinities which could be used to investigate epitope dependent stimulatory activity.

Generation and Purification of PD-1 mAb 2

The same method which was used to generate PD-1 mAbs 10, 19 and 29 was used in the second round of human PD-1 mAb generation. PD-1/Fc mouse immunisation, mouse harvesting, cell fusions and hybridoma selections were all performed by BioGenes GmbH, Berlin, Germany as outlined in Section 3.2.1. From the hybridomas produced by the cell fusion process only one hybridoma clone was found to be specific to human PD-1. This was PD-1 mAb hybridoma clone 2. The antibody produced by hybridoma clone 2 was found to be isotype IgG1. To ascertain how much mAb was produced by hybridoma clone 2, tissue culture supernatants were run on a non-reducing SDS-PAGE gel and then Western blotted using a mouse Fc specific mAb (Figure 3.14).

Purified PD-1 mAb 19 was run in the same dilution series alongside the supernatant from hybridoma clone 2 to allow estimation of the concentration of mAb 2 in

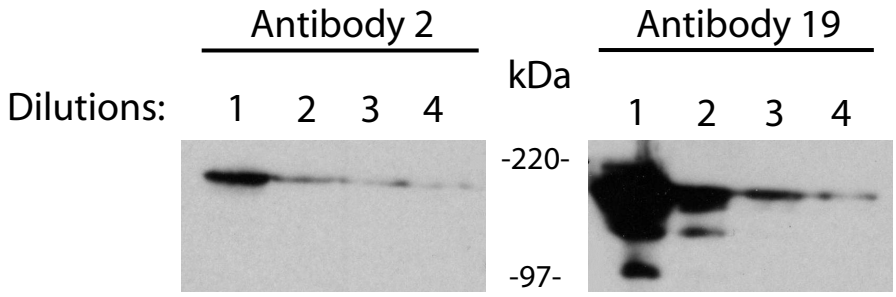


Figure 3.14: Tissue culture supernatant from PD-1 mAb hybridoma clone 2 was diluted at well 2- 1/10, well 3- 1/100 and well 4- 1/250 with BMEM media. Well 1 contained undiluted tissue culture supernatant. Samples were run on 12% non-reducing SDS-PAGE gels. Purified PD-1 mAb 19 at 1mg/ml was run in the same dilution series alongside the clone 2 PD-1 supernatant as a positive control to enable concentration estimation. Western blots of the gels were probed with a anti-mouse Fc HRP conjugate at 0.2μg/ml.

tissue culture supernatant. The undiluted tissue culture supernatant from hybridoma clone 2 band in well 1 is of an equal intensity to the 1/10 dilution of PD-1 mAb 19. From this, mAb 2 can be estimated to be present in the tissue culture supernatant at a concentration of $\sim$10 μg/ml. This level of antibody production by this hybridoma is 40x lower than the $\sim$400 μg/ml mAb observed in the supernatants of antibody hybridomas 10, 19 and 29. PD-1 mAb 2 was purified from tissue culture supernatant using ion exhange and size exclusion chromatography (see Section 3.3.2). To check the activity of the mAb post purification, mAb 2 was titrated by ELISA against PD-1 (Figure 3.15). mAb 2 binds to plate bound PD-1 at high concentrations and has a very similar binding profile to that of the positive control, mAb 19. Like mAb 19, mAb 2 does not reach saturation point at 100μg/ml and mAb binding drops to non-specific levels at $\sim$0.001μg/ml. Although no quantitative kinetic data can be derived from this experiment, there are close similarities in the titration curves of mAbs 19 and 2 which suggest similar binding affinities.

Epitope mapping of PD-1 mAb 2

The method of drastically mutating residues of PD-1 to affect mAb binding which was used to successfully map the epitopes of PD-1 mAbs 10 and 19 (Section 3.3.3) was used to map the mAb 2 epitope. Figure 3.16 shows that a total of three mutations of PD-1 affected the binding of mAb 2. Mutation A56R completely abolished binding, whereas the mutations K53E and N41K reduced binding of mAb 2 to PD-1 by only approximately 25-35%. The position of these mutated amino acid residues place the epitope of mAb 2 on the upper part of the C and C $'$ strands of PD-1 (Figure 3.17).

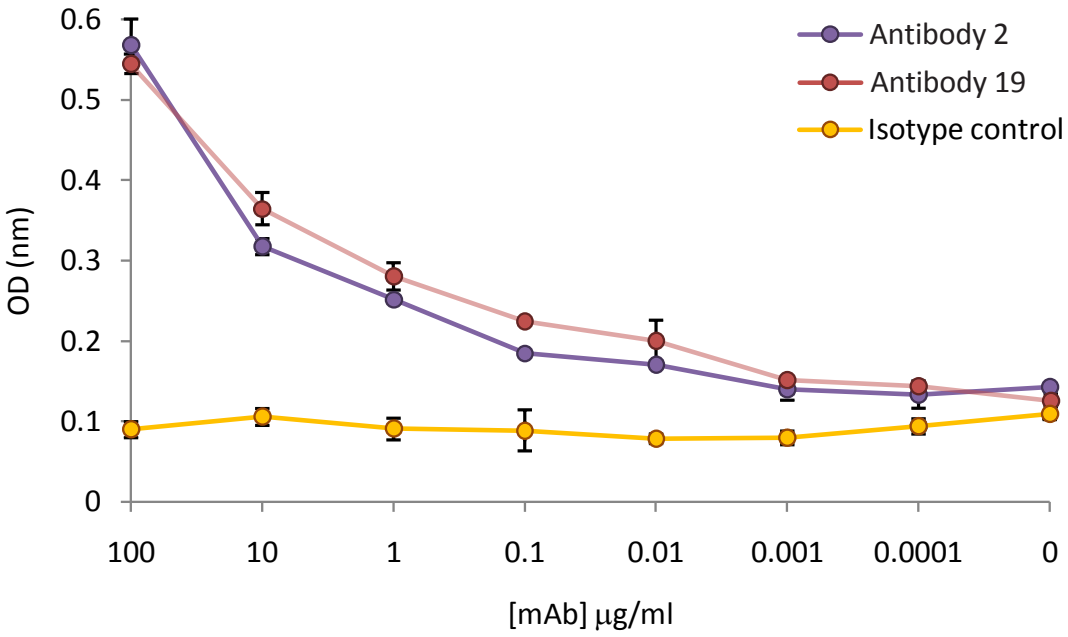


Figure 3.15: PD-1 mAb ELISA. Purified PD-1 mAb 2, 19 and an IgG1 isotype control (OX-7) was titrated from 100μg/ml to 0.0001μg/ml against a PD-1 plate immobilised target at 10μg/ml. PD-1 was prepared from thrombin cleaved PD-1/Fc purified of its Fc by Ni affinity chromatography. A secondary IgG Fab specific horseradish peroxidase conjugated antibody and ABTS substrate was used to develop the ELISA, reading substrate colour intensity at 425mn.

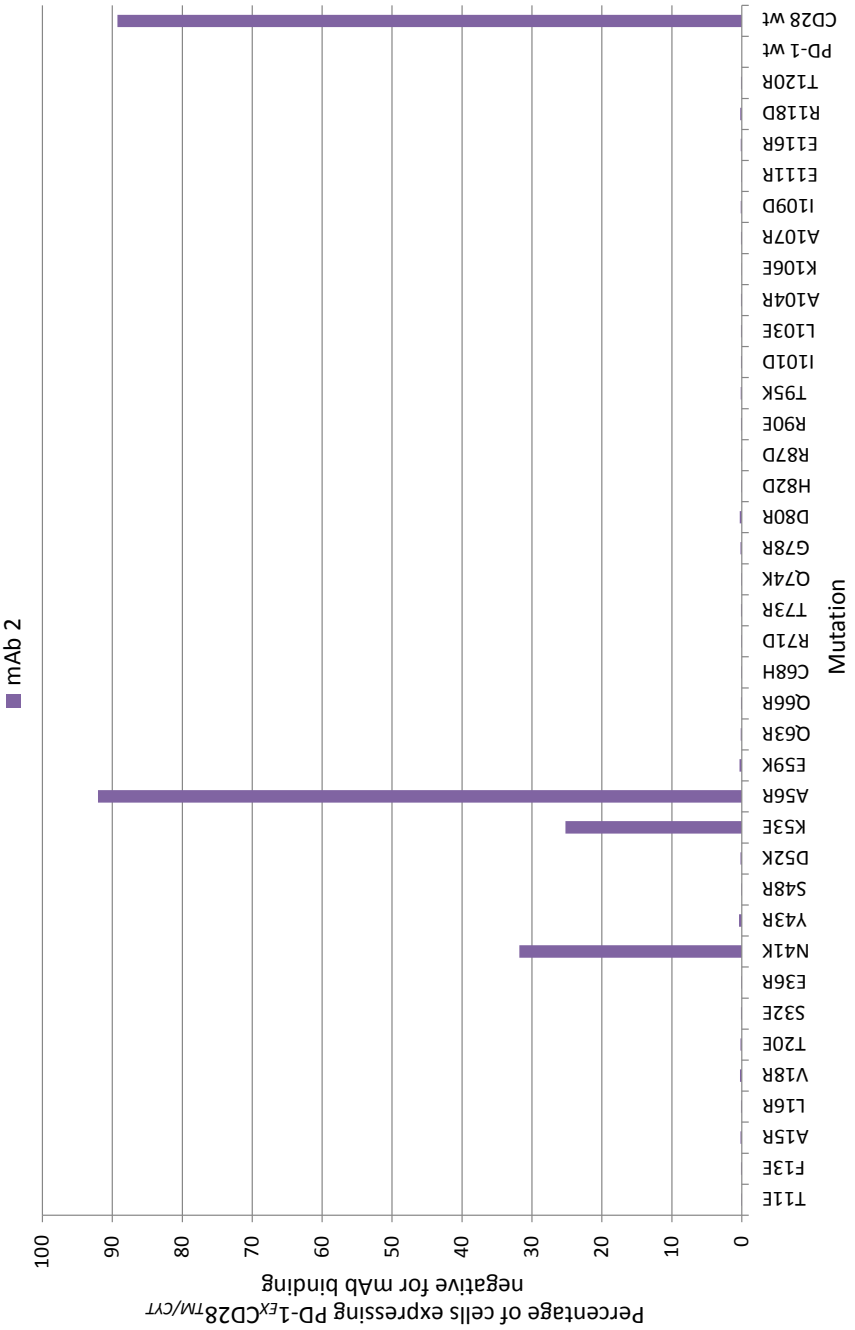


Figure 3.16: Human PD-1 mAb 2 epitope mapping. Thirty seven PD-1_{EX}CD$28_{TM/CYT}$ mutants, wild type PD-1_{EX}CD$28_{TM/CYT}$ and hmCD in pGFP^2-N3 were transiently expressed in HEK-293T cells for 24 hours. Cells were then harvested and assayed by flow cytometry for PD-1 mAb 2 binding. Cells were stained with 5μg/ml PD-1 antibody 2 secondary staining with Donkey anti-mouse AlexaFluor®647 conjugate at 5μg/ml. Successfully transfected cells were identified by gating for GFP^2 expression. Transfected cells positive for PD-1 antibody binding were recorded by gating for AlexaFluor®647 positive cells. To identify residues of which mutations affected mAb binding data is expressed as the percentage of PD-1_{EX}CD$28_{TM/CYT}$ positive cells that are negative for mAb binding.

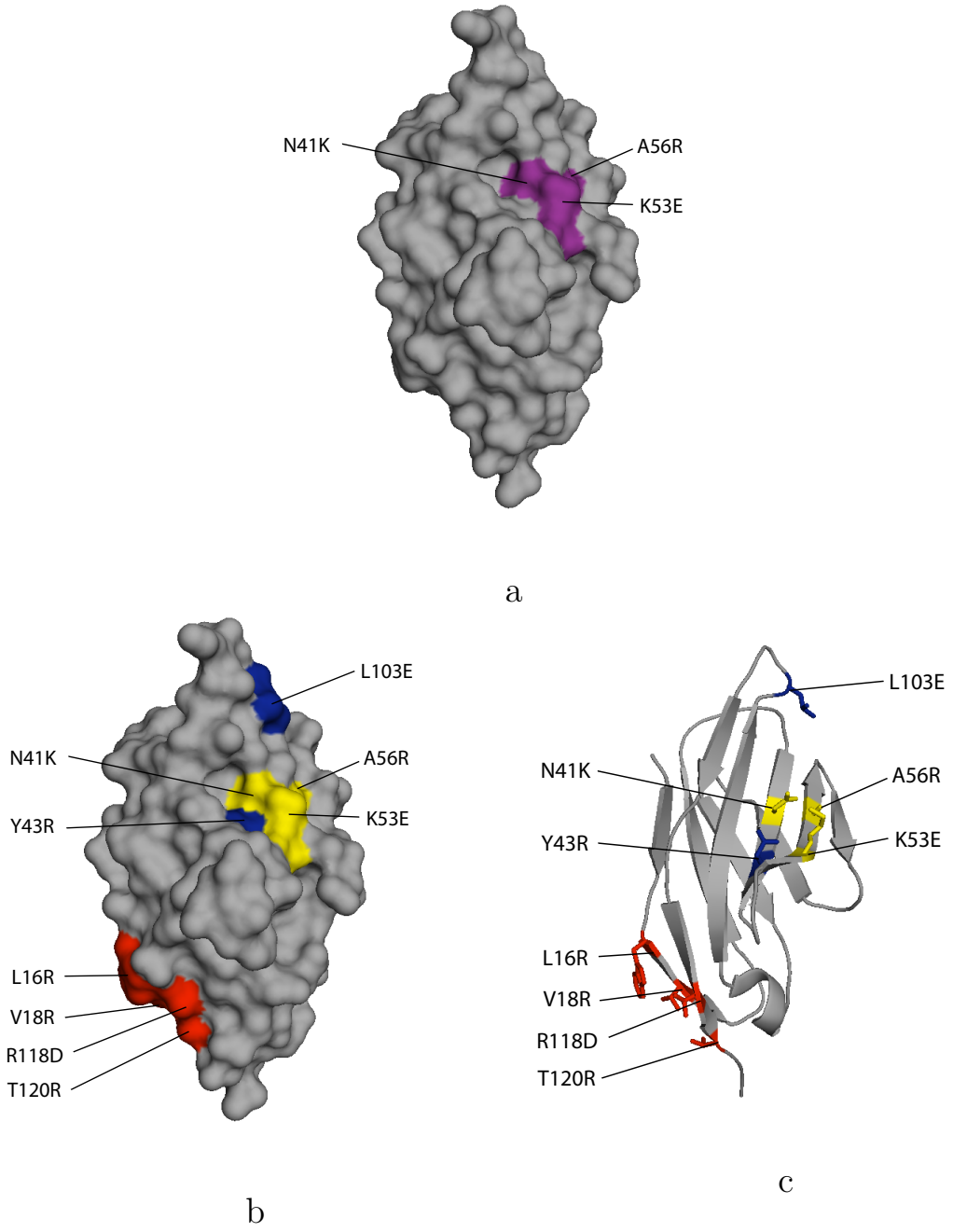


Figure 3.17: Epitopes of human PD-1 mAbs 2, 10 and 19. (a) The epitope of PD-1 mAb 2 on a representation of the molecular surface of PD-1. Mutations which resulted in reduced or abolished PD-1 mAb 2 binding are coloured purple. (b) The molecular surface of PD-1 showing the epitopes of PD-1 mAbs 2, 10 and 19. Residues involved in the epitope of mAb 10 are labelled in blue, residues involved in the mAb 19 epitope are labelled red. Residues which are involved in the mAb 2 epitope that overlap with the residues involved in the mAb 10 epitope are labelled yellow. (c) A ribbon diagram of PD-1 showing the epitopes of PD-1 mAbs 2, 10 and 19.

This places the epitope in a membrane distal region of PD-1. Significantly, these amino acids also make up part of the mAb 10 epitope. Residues A56, K53 and N41 all significantly reduced the binding of mAb 10, but unlike mAb 2, the mutation K53E not A56R had the biggest effect on mAb binding. This shows that although the epitopes of mAbs 10 and 2 overlap, the core epitope residues that are crucial for antibody binding differ.

PD-1 mAb 2 binding kinetics

Through the epitope mapping of mAb 2 a second PD-1 mAb has been identified with a membrane distal epitope. To investigate if mAb 2 has binding kinetics similar to mAb 19, SPR kinetic analysis was performed. Figure 3.18 shows the sensorgram obtained from the injection of PD-1 over directly immobilised PD-1 mAb 2.

Initial observation of the mAb 2 sensorgram shows that it has similar binding properties to mAb 19 (Figure 3.12), with PD-1 observed binding to the mAb relatively rapidly and at 15 minutes post injection PD-1 still associates with mAb 2. Direct comparison of the dissociation phase data of all the characterised PD-1 mAbs (Figure 3.19) shows that PD-1 mAb 2 has an off rate which is comparable with mAb 19, but it is more similar to that of mAb 29.

Unlike mAbs 10, 19 and 29 it was not possible to calculate kinetic data from the sensorgram data collected for mAb 2 using the 1:1 Langmuir binding model simultaneously. This was shown to be due to the fast k_{on} calculated for mAb when the k_{on} and k_{off} were calculated separately. While the low number of data points used to calculate the mAb 2 k_{on} of 2.43×10^5 $M^{-1}s^{-1}$, mean that the final value derived may not be

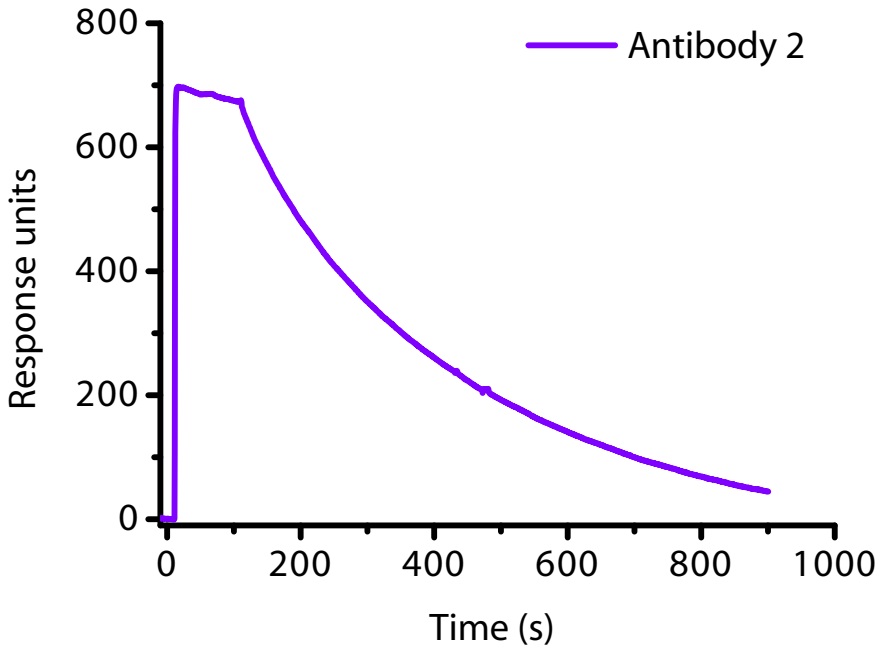
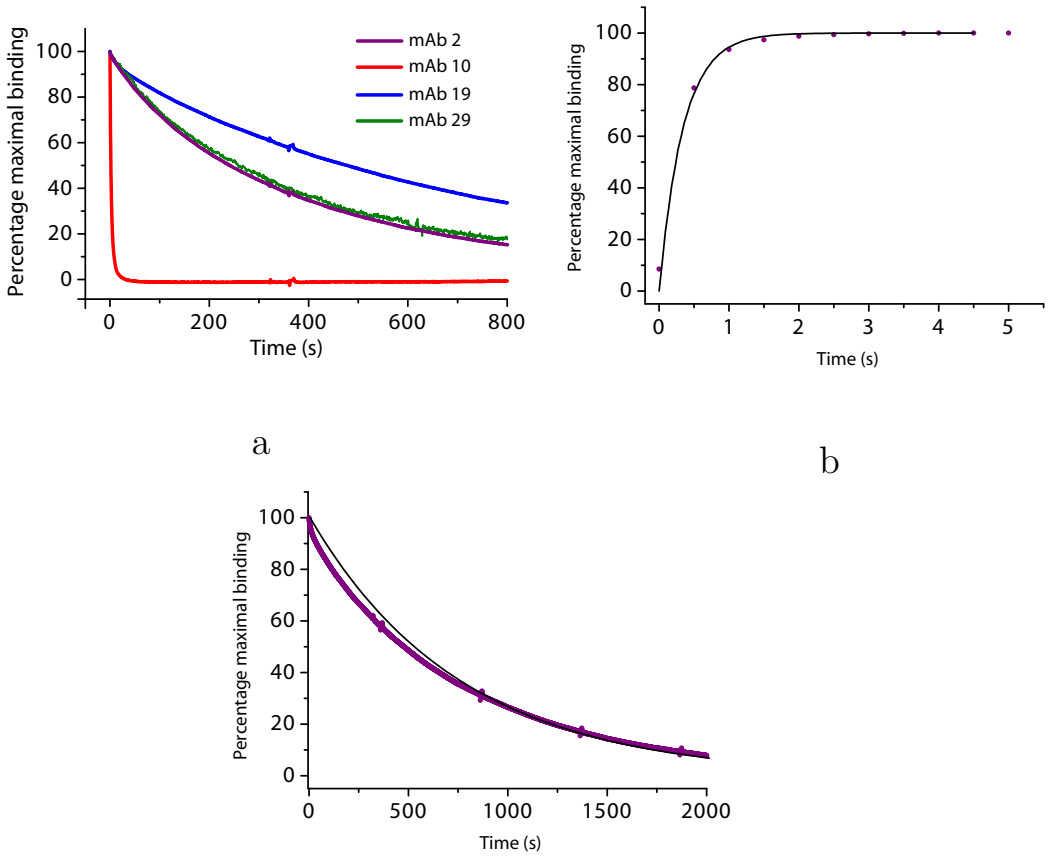


Figure 3.18: Sensorgram of human PD-1 binding to PD-1 mAb 2. 23.6μM monomeric PD-1 was kinetically injected directly over directly immobilised PD-1 mAb 2 (2953 RU) and control mouse IgG1 OX-7 (2983 RU) at 30μl/min at 25°C. mAb 2 and OX7 were directly immobilised via amine coupling. Data was recorded for 15 minutes. Sensorgram data recorded for the control mouse IgG1 was subtracted from PD-1 mAb data to account for background non-specific protein interactions and buffer effects.



PD-1 antibody	K_{off} (s^{-1})	K_{on} (m^{-1} s^{-1})	K_d (M)
2	$2.70x10^{-3}$	$2.43x10^{5}$	$1.11x10^{-8}$
10	$2.16x10^{-1}$	$2.69x10^{4}$	$8.03x10^{-6}$
19	$1.17x10^{-3}$	$3.22x10^{4}$	$5.32x10^{-8}$
29	$2.31x10^{-3}$	$2.01x10^{3}$	$1.15x10^{-6}$

d

Figure 3.19: Kinetic data of PD-1 mAb 2. (a) A comparison of the off rates of PD-1 mAbs 2, 10, 19 and 29. Percentage maximal binding was calculated from the dissociation phase data collected in Figure 3.12 and Figure 3.18. Antibody dissociation data was divided by the maximal PD-1 binding value for that antibody and expressed as a percentage. Collected data used to generate (b) an association rate (k_{on}) and (c) dissociation rate (k_{off}) using a 1:1 Langmuir binding model. (d) The binding affinities of human PD-1 mAb 2 as calculated from the binding data collected in (b) and (c) alongside the binding affinities of human PD-1 mAbs 10, 19 and 29 as shown in Figure 3.13.

completely accurate, it does give an overall indication of the very fast k_{on} of mAb 2. In comparison with the other PD-1 mAbs this association rate is approximately eight times greater than that of mAb 19 (3.22×10^4 $M^{-1}s^{-1}$) which is the largest association rate of all the other characterised PD-1 mAbs. As the dissociation phase data suggests, the k_{off} for mAb 2 (2.7×10^{-3} s^{-1}) is very similar to that of mAb 29 (2.31×10^{-3} s^{-1}) and only approximately two times larger than mAb 19 (1.17×10^{-3} s^{-1}). It is the combination of the differences in k_{on} and k_{off} which account for four fold difference in K_d between mAb 2 and 19.

3.4 Discussion

3.4.1 Summary of findings

The work in this chapter resulted in the characterisation of four previously undescribed human PD-1 mAbs. The epitopes of three of the mAbs (mAbs 2, 10 and 19) were identified through the use of drastic mutation epitope mapping. The epitopes of mAb 2 and 10 have similarly positioned epitopes, which are centred around the C and C′ strands of PD-1. The epitope of mAb 19 is located across the A′ and G′ strands of PD-1. However, this method failed to identify the epitope of mAb 29. Further investigations suggested that PD-1 glycan groups may be involved in the epitope of this mAb. Analysis of the mAbs using SPR analysis revealed that two of the mAbs had a K_d in the μM range mAb 10 and 29, whereas the dissociation constants of mAb 2 and 19 were significantly lower, in the nM range, indicating stronger binding to PD-1.

3.4.2 Predictions of superagonism by epitope mapping

Through the characterisation of mitogenic CD28 mAbs a clear correlation between antibody epitope position and superagonistic activity has been established [217,218,285]. CD28 mAbs with epitopes in a proximal position to the cell membrane elicit superagonistic stimulatory effects on T cells, whereas antibodies which have membrane distal epitopes require a second stimulus to achieve T cell activation. Although the signalling outcomes of CD28 and PD-1 are different, both molecules are activated through phosphorylation of tyrosine motifs and both modify antigen receptor signalling [262, 286]. Because of this, PD-1 is a molecule which can be used to investigate whether the principles observed in CD28 superagonism, *i.e.* that the strength of an activating signal induced by a mAb is dependent on its epitope location, can be applied to molecules other than CD28. Through the investigation of antibody signalling in PD-1 more information may be gathered about these agonistic mAbs and potentially therapeutic mAbs may be generated.

Through epitope mapping, one PD-1 mAb (mAb 19) was identified with an epitope located in a membrane proximal region. If predictions about the activating potential of a mAb can be made from epitope location alone, mAb 19 is predicted to have "agonistic" activities. *In vivo* this agonistic effect is predicted to be a strong signalling ability which should exceed the native ligand binding signal. It therefore follows that the two PD-1 mAbs which were identified with membrane distal epitopes (mAbs 2 and 10), would then be predicted to have "conventional" properties, inducing weaker signal from PD-1. Only further investigation into the effects of these mAb on PD-1

signalling *in vivo* and *in vitro* will be able to ascertain if these predictions based on superagonism can be applied to antibodies of T cell signalling molecules other than CD28.

3.4.3 PD-1 mAb 29

Although much effort has been put into identifying the epitope of PD-1 mAb 29, where this mAbs binds to PD-1 is still unknown. Manipulation of PD-1 glycosylation showed that mAb 29 was able to bind to PD-1 when it was expressed without complex sugars. But when glycans were completely removed from PD-1, a reduction of binding of PD-1 by mAb 29 was observed. The direct immobilisation of PD-1 for SPR analysis was the only other condition under which mAb 29 binding was affected. The low pH conditions in which the amine coupling reaction takes place (acetate buffer, pH 4.5), or the covalent binding of amine groups to the activated chip during the amine coupling process could alter the epitope of mAb 29 on PD-1/Fc, reducing the amount of PD-1 to which mAb 29 can bind. From this evidence collected, it is probable that the sugars present on PD-1, stabilise or partially form the epitope of mAb 29. By removing the glycan groups from PD-1 or placing PD-1 under conditions which may destabilise its sugar or protein structures, mAb binding is reduced, due to a decrease in the form of PD-1 to which mAb 29 can bind.

3.4.4 Superagonism and antibody binding affinities

In principle, effects of immune modulating antibodies could be attributed to their binding affinity as well as their epitope [262]. The binding kinetics of CD28 superagonist mAbs are not well characterised. Tacke *et al.* (1997) found that the binding of superagonistic mAbs to CD28 on purified resting lymph node T cells was slower than co-stimulatory mAbs, whereas when the same experiment was conducted on CD28 transfected cells the amount of superagonistic mAb bound to the cells was consistently higher than the co-stimulatory CD28 mAb. Of the four PD-1 mAbs described here, the mAbs can be separated into two groups based on their dissociation constants. The first group has a lower affinity for PD-1. mAb 10 has a very fast off rate whereas mAb 29 has a very slow on rate but despite their differences, they have dissociation constants in the μM range. The second group of PD-1 mAbs have a stronger affinity for PD-1. mAb 2 and mAb 19 share similar binding kinetics and as a result have dissociation constants in the nM range. Like the first group, they have similar dissociation constants, but unlike the first group, mAbs 2 and 19 both have well defined epitopes. It is the opposing nature of these epitopes which makes them good candidates for investigation into PD-1 "agonism". Because of the membrane distal epitope of mAb 2 and the membrane proximal epitope of mAb 19, any observed differences in stimulatory activity during PD-1 activation testing will be attributable to epitope position alone.

Chapter 4

Superagonistic signalling by PD-1 monoclonal antibodies

4.1 Introduction

4.1.1 PD-1 superagonistic monoclonal antibodies

Since their initial identification [216,217], the characterisation of mitogenic CD28 monoclonal antibodies (mAbs) has established a link between CD28 mAb epitope location and their 'superagonistic' abilities [218]. A mechanism for how these mAbs induce superagonism, proposed by Evans *et al.* (2005) [184], suggests that that superagonistic activity in CD28 can be predicted from epitope position alone. Currently, superagonism has only been observed in CD28, but it is possible mAbs can be generated to other T cell surface molecules and agonists identified based on epitope location. PD-1 is a T cell surface molecule that has been identified as an attractive target for agonist mAbs. As an inhibitory molecule that has a key role in immune tolerance, agonist mAbs generated against PD-1 would have potential therapeutic value in the treatment of a variety of auto-immune diseases. The monomeric nature of PD-1 would also allow these mAbs to be used in the investigation of the role mAb-induced aggregation plays in the mechanism of superagonism. But most importantly, the identification

and characterisation of agonist mAbs to PD-1 would broaden the hypothesis of epitope location-dependent mAb signalling to other T cell surface molecules. For these reasons a group of PD-1 mAbs were generated and characterised, and based on epitope location, one of the mAbs, PD-1 mAb 19, is predicted to be agonistic (See Chapter 3).

4.1.2 Assays for superagonism

PD-1 is an inhibitory T cell molecule [287] and whilst this makes it an interesting target for agonist mAbs, the inhibitory effects produced upon PD-1 ligation make it difficult to assay for agonistic activities. These effects also make the comparison of assays involving PD-1 and CD28 difficult, as the stimulation outcomes of each molecule is different. Our chosen solution to this problem is the creation of chimeric PD-1 molecules which allow binding of mAbs to PD-1 but create a signalling outcome which is directly comparable between PD-1 and CD28.

This chapter outlines work to recreate a robust *in vitro* assay for CD28 superagonism, using T cell hybridoma cell lines expressing human or rat CD28. This assay was then developed to include the use of cell lines expressing chimeric human PD-1 that could be used to identify agonistic PD-1 mAbs.

4.2 Materials and methods

4.2.1 Generation of chimeric cell lines

Lentiviral expression vectors were used to express chimeric proteins in DO11.10, a mouse T cell hybridoma. The chimeras were created using multi-step chimeric PCR and were designed to contain a 5′ rat CD4 ribosomal binding sequence and 5′ and 3′ restriction endonuclease sites to allow sub-cloning into a variety of expression vectors. More detailed molecular cloning methods can be found in Section 2.1. All oligonucleotides used in the creation of chimeric cell lines can be found in Tables 4.1, 4.2 and 4.3.

Construct	Oligo Name	Number	Primer Sequence	Restriction
$hCD28_{EX}mCD28_{TM/CYT}$	hCD28 5′	985	TAGTAGGAATTCCTCAAGCAGGCCACCATGCTCA	*Eco*RI
	mouse CD28 3′	986	CTACTAGGATCCGGGGCGGTACGCTGCAAAGTC	*Bam*HI
	hCD28/mCD28 int 5′	987	CTATTTCCCGGACCTTCTAAGCCCTTTTGGGCACTG GTCGTGGTTGCT	–
	hCD28/mCD28 int 3′	988	AGCAACCACGACCAGTGCCCAAAAGGGCTTAGAAGG TCCGGGAAATAG	–
$rCD28_{EX}mCD28_{TM/CYT}$	rCD28 BamHI	1597	TAGTAGGAATTCCTCAAGCAGGCCACCATGACACTC AGACTGCTA	*Bam*HI
	rCD28mCD28 int5′	1595	TGCTCAGACGTCTCCTAAGCCACTGGTCGTGGTTGC T	–
	rCD28mCD28 int3′	1596	AGCAACCACGACCAGTGGCTTAGGAGACGTCTGAGC A	–
$PD\text{-}1_{EX}CD28_{TM/CYT}$	5′hPD-1BglII	1737	TAGTAGAGATCTCTCAAGCAGGCCACCATGCAAATC CCACAGGCGCCCTGG	*Bgl*II
	hPD-1/mCD28 int 5′	990	GCCAGCCGGCCAGTTCCAAACCTTTTGGGCACTGGT CGTGGTTGCT	—
	hPD-1/mCD28 int 3′	991	AGCAACCACGACCAGTGCCCAAAAGGTTTGGAACTG GCCGGCTGGC	—
$PD\text{-}1_{EX}CD28_{ST/TM/CYT}$	5′hPD-1/mCD28	1738	GACCTCAGGGTGACAGAGAAGCTTAAACATCTTTGC CATACTCAG	–
	3′hPD-1/mCD28	1739	CTGAGTATGGCAAAGATGTTTAAGCTTCTCTGTCAC CCTGAGGTC	–
$PD\text{-}1_{EX}CD28_{TM/CYT}CJun_{ZIP}$	mouse c-jun 3′BglII	1750	TAGTAGAGATCTCTGGAGCGGATCGCTCGGCTA	*Bgl*II
	mouse c-jun 5′BamHI	1751	CTACTAGGATCCGACTTTCTGCTTAAGCTGTGCCAC	*Bam*HI
	C3 c-jun BamHI/XhoI 3′	1759	CTCGAGCTAGGATCCGACTTTCTGCTTAAGCTGTGC CAC	*Bam*HI/*Xho*I

Table 4.1: Oligonucleotide primers used to produce the constructs detailed in this chapter

Construct	Oligo Name	Number	Primer Sequence	Restriction
PD-1_{EX}CD28$_{TM}$CJun$_{ZIP}$CD28$_{CYT}$	3′CD28 BamHI/XhoI	1753	CTACTACTCGAGCTAGGATCCGGGGC GGTACGCTGCAAAGTC	*Bam*HI/*Xho*I
	PD-1 chim2 rev	1754	CTAGCCGAGCGATCCGCTCCAGTGTC CAGATAACACAAAGAGCCAC	–
	PD-1 chim2 for	1755	GTGGCTCTTTGTGTTATCTGGACACT GGAGCGGATCGCTCGGCTAG	–
	PD-1 5′BglII	1758	TAGTAGAGATCTCTCAAGCAGGCCAC CATGCAG	*Bgl*II
PD1$_{EX}$CTLA4$_{ST}$CD28$_{TM}$CJun$_{ZIP}$CD28$_{CYT}$	C3-CTLA4 5′	1756	TAGTAGAAGCTTATTGATCCAGAACC GTGCCCAGATTCTGACTTCCTCCTCT TTTGGGCACTGGTCGTGGTTGCT	–
	3 oligo PD-1 chim1 rev3	1793	GAGTCTGTTCCTTCTACTATTGACTT TCTGCTTAAGCTGTGCCACCTGTTCC CTG	*Bam*HI
	3 oligo PD-1 chim1 rev4	1794	TGGTAGTCACTTGTTGAAGGAGTCTG TTCCTTCTACTATTGACTTTCTGCT	*Bam*HI
PD-1_{EX}CD28$_{TM}$CD3ζ_{CYT}	mCD28/CD3ζ -5′	1356	GACAGTGGCTCTTTGTGTTATCTGGA GAGCAAAATTCAGCAGGAGTGCA	–
	mCD28/CD3ζ -3′	1357	TGCACTCCTGCTGAATTTTGCTCTCC AGATAACACAAAGAGCCACTGTC	–
	3′CD3ζ MluStpXho1	1944	CTCGAGCTACTAACGCGTGCGAGGGG CCAGGGTCTGCAT	*Mlu*I/*Xho*I
PD-1_{EX}CD3$\zeta_{ST/TM/CYT}$	5′hPD-1/mCD3ζWTBamHI	1740	TCAGCCGGATCCTTCCAAACCCTGGT GCTCTGCTACTTGCTAGATGG	*Bam*HI
	3′hPD-1/mCD3ζWTBamHI	1741	CCATCTAGCAAGTAGCAGAGCACCAG GGTTTGGAAGGATCCGGCTGA	*Bam*HI

Table 4.2: Oligonucleotide primers used to produce the constructs detailed in this chapter

Construct	Oligo Name	Number	Primer Sequence	Restriction
PD-1$_{EX}$CD3$\zeta_{ST/TM\text{-}D9E/CYT}$	5′hPD-1/mCD3ζD9EBamHI	1813	TCAGCCGGATCCTTCCAAACCCTGGTGCTCTGCTAC TTGCTAGAGGGAATC	*Bam*HI
	3′hPD-1/mCD3ζD9EBamHI	1814	GATTCCCTCTAGCAAGTAGCAGAGCACCAGGGTTTG GAAGGATCCGGCTGA	*Bam*HI
PD-1$_{EX}$CD3$\zeta_{ST/TM\text{-}D9K/CYT}$	5′hPD-1/mCD3ζMTBamHI	1742	TCAGCCGGATCCTTCCAAACCCTGGTGCTCTGCTAC TTGCTAAGGGAATC	*Bam*HI
	3′hPD-1/mCD3ζMTBamHI	1743	GATTCCCTTTAGCAAGTAGCAGAGCACCAGGGTTTG GAAGGATCCGGCTGA	*Bam*HI
PD-1$_{EX}$CD3$\zeta_{ST/TM}$CD28$_{CYT}$	5′mCD3ζ/mCD28	1746	ATCACAGCCCTGTACCTGAATAGTAGAAGGAACAGA	–
	3′mCD3ζ/mCD28	1747	TCTGTTCCTTCTACTATTCAGGTACAGGGCTGTGAT	–

Table 4.3: Oligonucleotide primers used to produce the constructs detailed in this chapter

hCD28$_{EX}$mCD28$_{TM/CYT}$

To create hCD28$_{EX}$mCD28$_{TM/CYT}$, the oligonucleotides 985 and 988 were used to amplify a 5′ *Eco*RI restriction endonuclease site and the signal peptide and extracellular domain of human CD28 (residues 1 to 152 of the mature peptide). This oligonucleotide fused human CD28 with the first 9 residues of the transmembrane domain and intracellular domain of mouse CD28. A second PCR reaction was performed using oligonucleotides 987 (the complementary sequence to 988) and 986. This amplified the last 8 residues of the human CD28 extracellular domain and the mouse transmembrane and intracelluar domain (residues 151 to 218 of the mature peptide) with a 3′ *Bam*HI restriction endonuclease site. These two products were purified and used as template in a chimeric PCR reaction using oligonucleotides 985 and 986 to create the full chimeric protein.

rCD28$_{EX}$mCD28$_{TM/CYT}$

rCD28$_{EX}$mCD28$_{TM/CYT}$ was made using the same principles. The first PCR was performed with oligonucleotide 1597 and 1596. This amplifying a 5′ *Eco*RI restriction endonuclease site prior to the rat CD28 signal peptide and transmembrane domain (residues 1 to 150 of the mature peptide). This fused to the first 8 residues of the mouse CD28 transmembrane domain. The second PCR amplified the last 8 residues of the rat extracellular domain and the mouse CD28 transmembrane and intracellular domain (residues 1 to 150 of the mature peptide) and a 3′ *Bam*HI restriction endonuclease site using oligonucleotide 1595 and 986. Mouse CD28 was amplified from

hCD28$_{EX}$mCD28$_{TM/CYT}$, and the rat CD28 section of the chimera was amplified from rat thymus cDNA (OriGene). The products were used as templates in the chimeric PCR using oligonucleotides 1597 and 986 which created the final rCD28$_{EX}$mCD28$_{TM/CYT}$ construct. A product with the correct sequence was then sub-cloned into pHR-SIN-BX-IRES-EM, pGFP^2-N3 and pRluc-N3 using *Bgl*II.

PD-1$_{EX}$CD28$_{TM/CYT}$

The PD-1$_{EX}$CD28$_{TM/CYT}$ construct consists of the human PD-1 signal peptide and extracellular domain (residues 1 to 148) fused to the mouse transmembrane and intracellular domain of CD28 (residues 132 to 198). It was created by amplifying the construct from the existing pGFP^2-N3-hPD-1/mCD28 vector (Section 3.2.4). The oligonucleotides 1737 and 986 were used to insert a 3′ *Bgl*II and 5′ *Mlu*I/*Xho*I restriction endonuclease sites. These restriction sites were used to ligate the construct into pHR-SIN-BX-IRES-EM (using *Bgl*II and *Xho*I) and pRluc-N3 (using *Bgl*II and *Mlu*I).

PD-1$_{EX}$CD28$_{ST/TM/CYT}$

A PD-1 chimeric molecule similar to PD-1$_{EX}$CD28$_{TM/CYT}$ was created which contained the stalk region of mCD28. Using a chimeric PCR protocol, residues 1 to 144 of human PD-1 were amplified from the pGFP^2-N3-PD-1$_{EX}$CD28$_{TM/CYT}$ vector using oligonucleotides 1737 and 1739. The 3′ end of this PCR product contained a *Hind*III restriction endonuclease site and residues 137 to 144 of mouse CD28. The complementary oligonucleotide 1738 was used along with 1944 to amplify residues 137 to 218 of

mouse CD28 from mouse DO11.10 cDNA. The products of these reactions were used as templates in a chimeric PCR reaction using oligonucleotides 1737 and 1944 to create the full length PD-1_{EX}CD$28_{ST/TM/CYT}$ molecule. PD-1_{EX}CD$28_{ST/TM/CYT}$ was ligated into pHR-SIN-BX-IRES-EM (using *Bgl*II and *Xho*I) and pRluc-N3 (using *Bgl*II and *Mlu*I).

PD-1_{EX}CD$28_{TM/CYT}$CJun$_{ZIP}$

The PD-1_{EX}CD$28_{TM/CYT}$CJun$_{ZIP}$ construct consists of the PD-1_{EX}CD$28_{TM/CYT}$ construct fused to a 3′ mouse c-jun leucine zipper domain (residues 277 to 315). Mouse c-jun was amplified from mouse DO11.10 cDNA using the oligonucleotides 1750 and 1751 and digested with *Bgl*II and *Bam*HI. The pGFP^2-N3-PD-1_{EX}CD$28_{TM/CYT}$ vector was cut with *Bam*HI and ligated to the digested c-jun fragment. Clones were screened for correct orientation of c-jun using oligonucleotides 1751 and 990 and sequenced. Correct constructs were sub-cloned into pRluc-N3 using *Bam*HI. For use in pHR-SIN-BX-IRES-EM, full length PD-1_{EX}CD$28_{TM/CYT}$CJun$_{ZIP}$ was amplified with a 3′ stop codon using oligonucleotides 1737 and 1759 and ligating into the vector using *Bgl*II and *Xho*I.

PD-1_{EX}CD28_{TM}CJun$_{ZIP}$CD28_{CYT}

To create PD-1_{EX}CD28_{TM}CJun$_{ZIP}$CD28_{CYT}, the leucine zipper domain of c-jun was amplified from PD-1_{EX}CD$28_{TM/CYT}$CJun$_{ZIP}$ with oligonucleotides 1750 and 1755. These amplified c-jun with a 5′ *Bgl*II site and the 3′ end of c-jun fused to the first 9 amino acids of the mouse CD28 intracellular domain. PD-1_{EX}CD$28_{TM/CYT}$CJun$_{ZIP}$ was also used in the next PCR reaction as a template to amplify the mouse CD28 intracellular domain

with oligonucleotides 1755 and 1753. 1755 is the complementary sequence of 1754 and 1753 adds the 3′ restriction endonuclease sites *Bam*HI and *Xho*I and are separated by a stop codon. The products of these two PCR reactions were used in a chimeric PCR as templates with oligonucleotides 1750 and 1753 to create the mouse c-jun leucine zipper domain fused to the mouse CD28 intracellular domain. The human PD-1 extracellular domain fused to the mouse CD28 transmembrane domain was amplified from PD-1_{EX}CD$28_{TM/CYT}$CJun$_{ZIP}$ with the oligonucleotides 1758 which contains a *Bgl*II restriction endonuclease site, rat CD4 ribosome binding sequence and the first two residues of human PD-1 and 1754 which is the complementary sequence of 1755. The hPD-1/mCD28 product of this reaction was used along with the c-jun/mCD28 product of the previous chimeric PCR as a template in the final chimeric PCR using the oligonucleotides 1758 and 1753. PD-1_{EX}CD28_{TM}CJun$_{ZIP}$CD28_{CYT} was ligated into pHR-SIN-BX-IRES-EM using *Bgl*II and *Xho*I and the BRET vectors pGFP^2-N3 and pRluc-N3 using *Bgl*II and *Bam*HI.

PD1$_{EX}$CTLA4$_{ST}$CD28$_{TM/CYT}$CJun$_{ZIP}$

PD1$_{EX}$CTLA4$_{ST}$CD28$_{TM/CYT}$CJun$_{ZIP}$ was created by first digesting pRluc-N3-PD-1$_{EX}$ CD$28_{ST/TM/CYT}$ with the restriction endonucleases *Bam*HI and *Hind*III to excise a mouse CD28 fragment (residues 137 to 144) leaving the human PD-1 Ig V-set domain (residues 1 to 144) remaining. The digested vector was treated with alkaline phosphatase. A *Hind*III restriction endonuclease site was inserted in front of the stalk region of extracellular CTLA-4 (residues 152-164) and fused to the transmembrane and intracellular region

of PD-1_{EX}CD$28_{TM/CYT}$CJun$_{ZIP}$, in a PCR reaction using the oligonucleotides 1756 and 1759 and using PD-1_{EX}CD$28_{TM/CYT}$CJun$_{ZIP}$ as a template. The product from this PCR was digested with *Bam*HI and *Hind*III and ligated into the digested pRluc-N3- PD-1_{EX}CD$28_{ST/TM/CYT}$ vector. The resultant PD1_{EX}CTLA4_{ST}CD$28_{TM/CYT}$CJun$_{ZIP}$ product was sub-cloned into pGFP^2-N3 using *Bgl*II and *Bam*HI. For insertion into pHR-SIN-BX-IRES-EM, PD1_{EX}CTLA4_{ST}CD$28_{TM/CYT}$CJun$_{ZIP}$ was amplified from pRluc-N3- PD1_{EX}CTLA4_{ST}CD$28_{TM/CYT}$ template using oligonucleotides 1737 and 1759 and digested with *Bgl*II and *Xho*I before ligation into pHR-SIN-BX-IRES-EM .

PD1_{EX}CTLA4_{ST}CD28_{TM}CJun$_{ZIP}$CD28_{CYT}

The fourth human PD-1/mouse CD28 chimera (PD1_{EX}CTLA4_{ST}CD28_{TM}CJun$_{ZIP}$CD28_{CYT}) was created to contain the transmembrane and intracellular domain of PD-1_{EX}CD28_{TM} CJun$_{ZIP}$CD28_{CYT} (a mouse CD28 transmembrane domain and an intracellular domain consisting of the mouse c-jun leucine zipper domain followed by intracellular mouse CD28) and the extracellular domain of PD1_{EX}CTLA4_{ST}CD$28_{TM/CYT}$CJun$_{ZIP}$ (the human PD-1 Ig V-set domain followed by 12 residues of the extracellular stalk region of human CTLA-4). Oligonucleotides 1756 and 1756 were used to amplify the transmembrane and intracellular domain from PD-1_{EX}CD28_{TM}CJun$_{ZIP}$CD28_{CYT} with a 5′ *Hind*III site, human CTLA-4 stalk and 3′ *Xho*I restriction endonuclease site. The amplified product of this PCR reaction was digested with both *Hind*III and *Xho*I. The vector pHR-SIN-BX-IRES-EM -PD-1_{EX}CD$28_{TM/CYT}$ was digested with *Hind*III and *Xho*I. This removed the human PD-1 stalk and the transmembrane and intracellu-

lar mouse CD28 domains. The digested PCR product was ligated into the digested pHR-SIN-BX-IRES-EM -PD-1_{EX}CD$28_{TM/CYT}$. The sequence of the resultant pHR-SIN-BX-IRES-EM -PD1_{EX}CTLA4_{ST}CD28_{TM}CJun$_{ZIP}$CD28_{CYT} vector was verified and then used as as a template in a PCR reaction with the oligos 1737 and 1753 to amplify the full length PD1_{EX}CTLA4_{ST}CD28_{TM}CJun$_{ZIP}$CD28_{CYT} vector for ligation into the pGFP^2-N3 and pRluc-N3 using *Bgl*II and *Mlu*I.

PD-1_{EX}CD28_{TM}CD3ζ_{CYT}

Oligonucleotides 1737 and 1357 were used to amplify the extracellular domain and transmembrane domain of the construct pHR-SIN-BX-IRES-EM -PD-1_{EX}CD$28_{TM/CYT}$ fused to the first 8 amino acids of mouse CD3ζ using oligonucleotides 1737 and 1356. A second PCR reaction then amplified the last 8 amino acids of the mouse CD28 transmembrane domain fused to the intracellular domain of mouse CD3ζ (residues 52 to 164) using oligonucleotides 1356 and 1944. Mouse CD3ζ was amplified from DO11.10 T cell hybridoma cDNA template. The products of these two PCR reactions were purified and used as templates in the chimeric PCR reaction using oligonucleotides 1737 and 1944 to produce a full chimeric PD-1_{EX}CD28_{TM}CD3ζ_{CYT} construct. All chimeric PD-1 constructs containing CD3ζ sequence were TOPO® cloned into pCR®4-TOPO® for sequence analysis. Chimeras with the correct sequence were then sub-cloned into pHR-SIN-BX-IRES-EM using *Bgl*II and *Xho*I and the BRET vectors pGFP^2-N3 and pRluc-N3 using *Bgl*II and *Mlu*I.

PD-1$_{EX}$CD3$\zeta_{ST/TM}$CD28$_{CYT}$ and mutants

The human PD-1$_{EX}$CD3$\zeta_{ST/TM}$CD28$_{CYT}$ chimeras were designed to contain the extracellular domain of PD-1 (residues 1 to 148) fused to the transmembrane domain of CD3ζ (residues 8 to 29) followed by the mouse intracellular domain (residues 159 to 199). In a multi-step chimeric PCR reaction the pGFP^2-N3-PD-1$_{EX}$CD28$_{TM/CYT}$ vector was used as a template to amplify the human PD-1 extracellular domain using the oligonucleotides 1737 and 1741, and the mouse CD28 intracellular domain using 1746 and 986. The PD-1 extracellular domain was amplified to contain the first seven amino acids of the CD3ζ transmembrane domain at the 3$'$ end. The 5$'$ end of the CD28 intracellular domain was amplified containing the last six amino acid residues of the CD3ζ transmembrane domain. The full length CD3ζ transmembrane domain was amplified from DO11.10 cDNA using the oligonucleotides 1740 and 1747. To created the full length chimera, first the PD-1 PCR fragment and the CD3ζ transmembrane domain PCR product were used as template in a chimeric PCR reaction using the oligonucleotides 1737 and 1747. The resultant PD-1$_{EX}$CD3$\zeta_{ST/TM}$CD28$_{CYT}$ fusion product was then used as a template with the CD28 intracellular domain PCR product in a final chimeric PCR using the oligonucleotides 1737 and 986. To create the D9E and D9K CD3ζ mutant variants of this construct, the oligonucleotides 1740 and 1741 were substituted with either 1813 and 1814 (D9E) or 1742 and 1743 (D9K). The sequence of all constructs were verified then sub-cloned into pHR-SIN-BX-IRES-EM using *Bgl*II and *Xho*I and the BRET vectors pGFP^2-N3 and pRluc-N3 using *Bgl*II and *Mlu*I.

PD-1_{EX}CD3$\zeta_{ST/TM/CYT}$ and mutants

The PD-1_{EX}CD3$\zeta_{ST/TM}$CD28$_{CYT}$ constructs contain the extracellular domain of human PD-1 (residues 1 to 148) fused to the transmembrane and intracellular domain of mouse CD3ζ (residues 1 to 142). The human PD-1 extracellular domain of PD-1 was amplified from using the oligonucleotides 1737 and 1741. In a second PCR reaction the intracellular domain of mouse CD3ζ was amplified from DO11.10 cDNA using the oligonucleotides 1740 and 1944. The products of these two reactions were used as template for the final chimeric PCR reaction using 1737 and 1741, which produced the fused PD-1_{EX}CD3$\zeta_{ST/TM}$CD28$_{CYT}$ chimera. PD-1_{EX}CD3$\zeta_{ST/TM\text{-}D9E}$CD28$_{CYT}$ and PD-1_{EX}CD3$\zeta_{ST/TM\text{-}D9K}$CD28$_{CYT}$ mutant chimeras were created by substituting the oligonucleotides 1740 and 1741 for either 1813 and 1814 (D9E) or 1742 and 1743 (D9K). Once a construct sequence was checked to be correct by sequence analysis, it was sub-cloned into the vectors pHR-SIN-BX-IRES-EM (using *Bgl*II and *Xho*I), pGFP^2-N3 and pRluc-N3 (using *Bgl*II and *Mlu*I).

4.2.2 Construction of hybridoma cell lines

DO11.10 T cell hybridoma cell lines were created expressing one of a variety of CD28 or PD-1 chimeras. Cells were transduced with chimera-encoding lentivirus to allow constitutive and stable expression of the encoded gene. To produce lentivirus containing chimeric genes, first a 6 well plate was seeded with 6×10^5 HEK 293T cells and were grown to 60-80% confluency. Then to create the virus, the pHR-SIN-BX-IRES-EM vector encoding the chimeric molecule was transfected into the cells along with

the lentiviral vectors p8.91 and pMDG [275]. The transfection media was prepared by adding of 3μl GeneJuice® transfection reagent (Novagen, Merck) was added dropwise to 100μl DMEM (Sigma), gently mixed and left at room temperature for 10 minutes. Then 1μg of the pHR-SIN-BX-IRES-EM vector, p8.91 and pMDG were combined together and made up to 20μl using sterile water. This DNA mix was added dropwise to the transfection media, flicked gently to mix and left at room temperature for 30 minutes for the transfection complex to form. The transfection complex was then added directly to the HEK 293T cells and incubated at 37°C5% CO_2. After 72 hours, the tissue culture medium containing lentivirus was harvested from the transfected cells. It was microfuged at 13,000rpm for 5 minutes to remove cell debris and the supernatant collected. Approximately 1×10^5 of the target mouse DO11.10 cells were pelleted at 1,300rpm and resuspended in the lentivirus containing tissue culture supernatant. The DO11.10 cells were left to be transduced by the virus for 24 hours at 37°C5% CO_2, before the cells were transfered into a 25cm^2 tissue culture flask with 5ml JMEM (Section 2.2.3). The cells were cultured until they reached a density of 1×10^6 at which point they were assayed for emGFP expression using flow cytometry analysis. The CD28 specific mAbs 5.11A1 [218] and JJ319 [217], and PD-1 mAb 10 were used to stain for chimeric protein surface expression. Donkey anti-mouse AlexaFluor®647 (Molecular Probes, Invitrogen) was used as a secondary conjugate. To obtain a population of DO11.10 cells with homologous expression of the transduced proteins, cells were fluorescence-activated cell sorted (FACS sorted) for both chimeric protein and emGFP expression.

4.2.3 BRET analysis

For use in BRET assays the genes were cut from the chimeric genes and sub-cloned into the pRluc-N3 and pGFP^2-N3 BRET vectors. The vectors were transfected into HEK-293T cells and assayed for cell surface oligomerisation using the method outlined in Section 2.5.

4.2.4 Confocal microscopy

To visualise protein expression at the cell surface the chimeric proteins in the pGFP^2-N3 vector were transiently expressed in HEK-293T cells grown on coverslips. This vector fuses GFP^2 to the C-terminus of the expressed protein allowing visualisation of fusion proteins when excited at 488nm. The cells were mounted on slides and visualised through an oil immersed 60x objective. Fluorescence emission was detected in the 515$\pm$15nm channel. For more information of the method used see section 2.4.2.

4.2.5 Antibody stimulation assay

DO11.10 cell lines expressing chimeric proteins were used in an antibody stimulation assay as follows. 96-well flat-bottomed plates (Costar EIA/RIA plates) were coated overnight at 4°C with 500μg/ml donkey anti-mouse IgG (H+L) (Jackson Immunoresearch) in coating buffer (15mM Na_2CO_3, 35mM $NaHCO_3$, pH 9.6). For anti-mouse CD3 stimulations assays, the donkey anti-mouse coated plates were washed 3 times with 200μl chilled PBS, and coated overnight at 4°C with 3μg/ml KT-3 [288] in coating buffer. For all assays, prior to cell loading, the plates were washed 3 times with 200μl

chilled PBS. 5×10^5 chimeric DO11.10 cells/well were centrifuged and resuspended with the mAb being tested in complete JMEM media pre-warmed to 37°C for 30 minutes at room temperature. Cells were then plated out in triplicate onto the coated plates. For PD-1 mAb cross-linking experiments with the PD-1_{EX}CD$28_{TM/CYT}$ cell line, the cells were centrifuged and washed with 1ml PBS after a 30 minute incubation with mAb 19. The cells then underwent a 30 minute incubation with mAb 10, before the cells were plated out on in triplicate on to pre-coated 96 well plates. Cells were incubated at 37°C, 5% CO_2 for 48 hours before the cell culture supernatant was removed and assayed for mouse interleukin-2 (IL-2) by ELISA.

4.2.6 IL-2 ELISA

IL-2 produced during the antibody stimulation assay was quantified using the DuoSet mouse IL-2 ELISA (DY402 - R&D Systems). The capture antibody (rat anti-mouse IL-2) was diluted to a working concentration of 1μg/ml with PBS. Costar flat-bottomed 96-well EIA/RIA plates were coated with capture antibody at 100μl per well, sealed and incubated overnight at room temperature. Each well was aspirated and washed three times with 400μl wash buffer (0.05% Tween® 20 in PBS with 0.05% NaN_3). 300μl block buffer 1% Bovine serum albumin in PBS with 0.05% NaN_3) was added to each well and incubated at room temperature for 1 hour. The wells were washed for another three times with 400μl wash buffer before adding 100μl of sample or standard. Samples and standard were covered and incubated for 2 hours at room temperature. The recombinant mouse IL-2 standard was plated using seven 2-fold serial dilutions in reagent

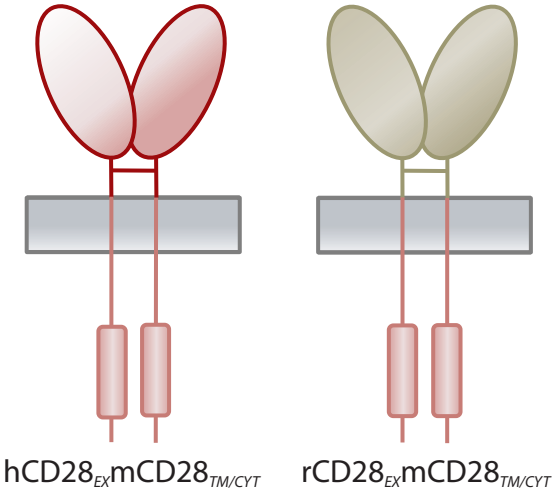
diluent (0.1% Bovine serum albumin, 0.05% Tween® 20 in Tris-buffered Saline (20mM Trizma base, 150mM NaCl), pH7.2-7.4, 0.2μm filtered), using a 1000pg/ml high standard. The wells were aspirated and washed with 400μl wash buffer three times. The detection antibody (biotinylated goat anti-mouse IL-2) was diluted to 400ng/ml in reagent diluent. 100μl was added to each well, before covering and incubation at room temperature for 2 hours. The wash step was repeated with 400μl wash buffer. Streptavidin conjugated to horseradish-peroxidase was diluted 1 in 200 with reagent diluent and 100μl was added to each well. Plates were covered and incubated for 20 minutes at room temperature in the dark. After an aspiration and wash step, 100μl substrate solution (3,3′,5,5′-Tetramethylbenzidine (TMB) liquid substrate system for ELISA - Sigma) was added to each well and incubated at room temperature in the dark for 20 minutes. The reaction was stopped by adding 50μl 2N H_2SO_4. The optical density of each well was read immediately using a Fusion microplate analyser (PerkinElmer) at 515nm. The triplicate readings for each sample were averaged and the mean zero standard optical density subtracted from each sample result from this data the standard error calculated. To calculate IL-2 in pg/ml a seven point standard curve was created by plotting corrected average standard IL-2 concentrations against the optical density.

4.3 Results

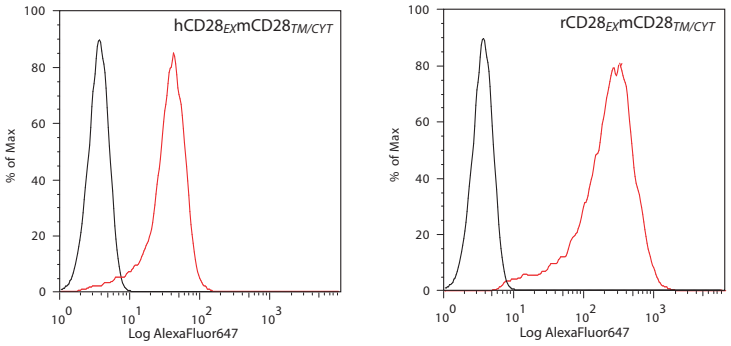
4.3.1 CD28 superagonism assay

Species chimeric CD28 molecules have previously been used to successfully assay for TCR signalling independent superagonistic activity of rat and human CD28 mAbs in T cell hybridomas [285]. This assay was recreated to produce a positive read-out for superagonistic activation prior to the development of an assay that would enable the testing of PD-1 mAbs for agonistic activity. A mouse T cell hybridoma cell line was transduced with a lentivirus that encoded one of two CD28 chimeras. This used the lentiviral vector pHR-SIN-BX-IRES-EM that contains an IRES sequence and emGFP (Emerald GFP) downstream of the chimeras. The expression of emGFP allows confirmation that the vector has been inserted into the DO11.10 genome. The chimeras encoded the extracellular domain of either human or rat CD28 fused to the transmembrane domain and intracellular domain of mouse CD28 ($hCD28_{EX}mCD28_{TM/CYT}$ and $rCD28_{EX}mCD28_{TM/CYT}$ respectively) (Figure 4.1). Hybridomas successfully transduced were sorted to create stable cell lines expressing either ($hCD28_{EX}mCD28_{TM/CYT}$ or $rCD28_{EX}mCD28_{TM/CYT}$ (Figure 4.1).

To investigate the expression of the chimeras, each construct was transiently expressed in HEK 293T cells using the pGFP^2-N3 vector. This vector, also used in BRET analysis, fuses a GFP^2 to the C-terminus of the chimera. The resultant fusion protein can be visualised using confocal microscopy allowing information about the cellular localisation of the chimeras to be collected. Both chimeric CD28 constructs, and the



a



b

Figure 4.1: Construction and expression of $hCD28_{EX}mCD28_{TM/CYT}$ and $rCD28_{EX}mCD28_{TM/CYT}$ in DO11.10 T cell hybridomas. (a) Schematic representations of the chimeric $hCD28_{EX}mCD28_{TM/CYT}$ and $rCD28_{EX}mCD28_{TM/CYT}$ constructs. (b) Expression levels of chimeric constructs in DO11.10 cell lines. DO11.10 cells transduced with lentivirus encoding either $hCD28_{EX}mCD28_{TM/CYT}$ or $rCD28_{EX}mCD28_{TM/CYT}$ were FACS sorted to created stable cell lines. Positive cells were gated for both emGFP and CD28 expression. The resultant cell lines (red) along with control untransduced DO11.10 cells (black) were analysed by flow cytometry, staining with $5\mu g/ml$ CD28 mAb (either 5.11A1 or JJ319 for $hCD28_{EX}mCD28_{TM/CYT}$ or $rCD28_{EX}mCD28_{TM/CYT}$ respectively) and $5\mu g/ml$ donkey anti mouse AlexaFluor®647 (Molecular Probes, Invitrogen) secondary conjugate. All cells were gated for emGFP and CD28 expression.

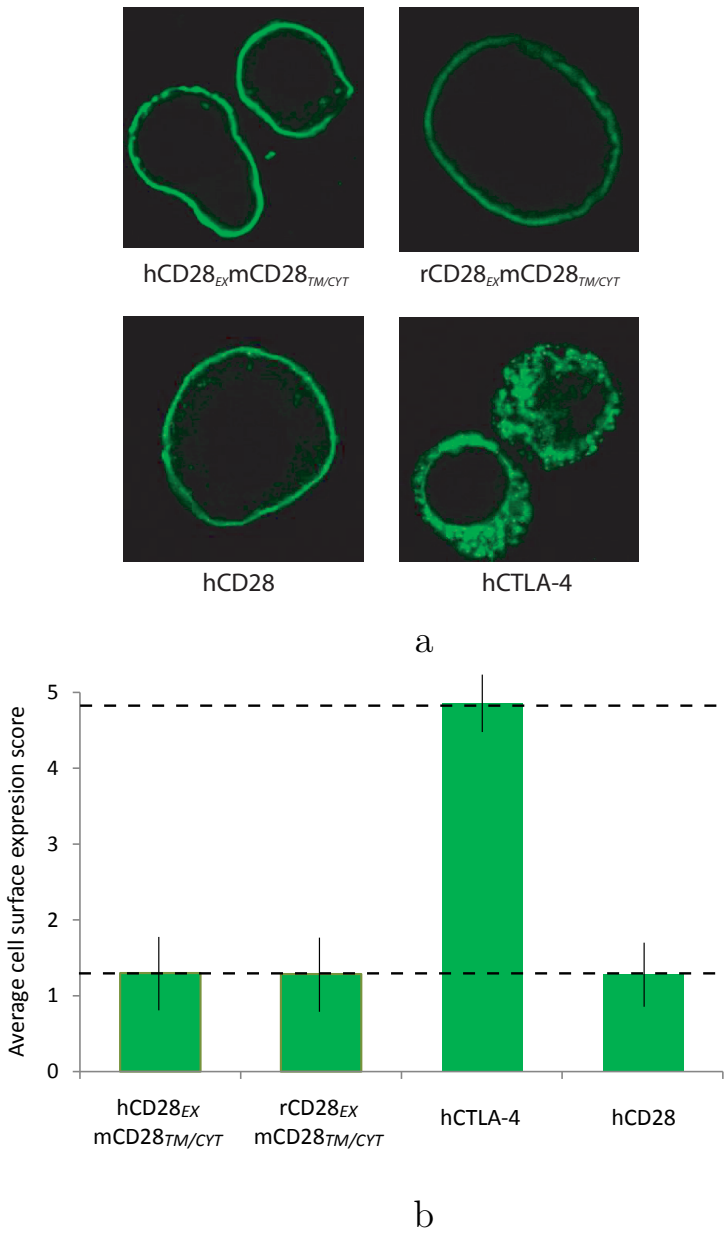
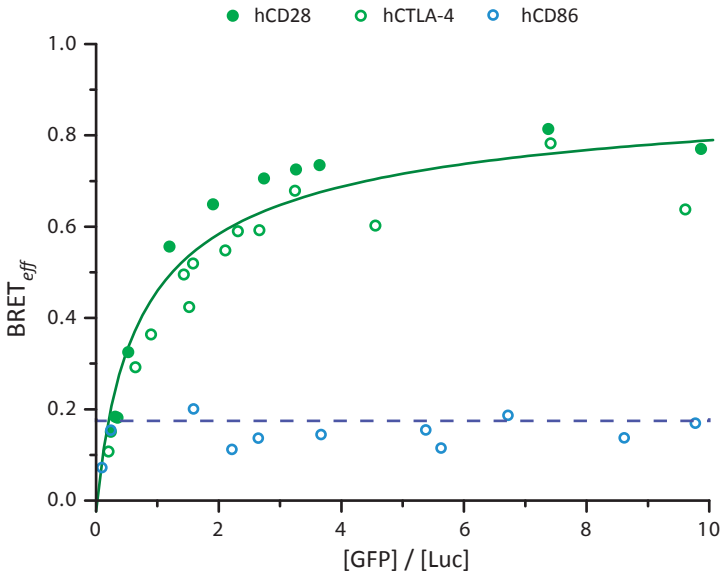


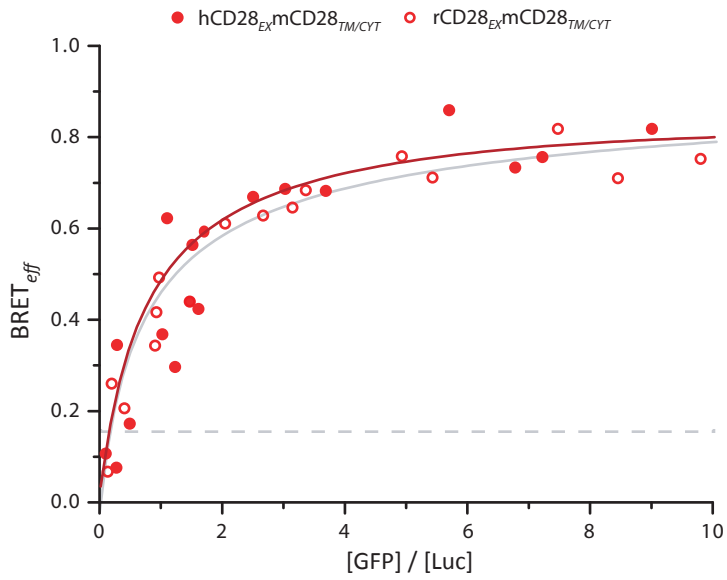
Figure 4.2: Confocal microscopy analysis of the expression of $hCD28_{EX}mCD28_{TM/CYT}$, $rCD28_{EX}mCD28_{TM/CYT}$, hCD28 and hCTLA-4. (a) The chimeric or control constructs in the vector $pGFP^2$-N3 vector were transiently expressed in HEK 293T cells on cover-slides for 24 hours. Cells were excited at 488nm and observed through a 60x objective lens. (b) Average cell surface expression scores for control and chimeric construct expression in HEK 293T cells. Transfected cells were observed and scored on a scale for cell surface expression, where a score of 1 indicates cell surface expression only and 5 indicates complete intracellular localisation. A minimum 20 cells were scored for each construct expressed. The average cell surface expression score for the each construct is displayed. The dotted lines represent levels of cell surface expression representative for hCD28 (expressed solely on the cell surface) and hCTLA-4 (largely complete intracellular localisation).

controls human CD28 and human CTLA-4, were visualised at the cell surface using confocal microscopy analysis (Figure 4.2). Expression levels and cellular localisation of the chimeras were equivalent to that of a full length wild type hCD28 control, and unlike the internal localisation observed in cells expressing hCTLA-4 which is predominately localised to the intracellular compartment [114, 289]. This suggests that all the chimeras were correctly processed and trafficked through the cellular compartment to the cell surface. To confirm correct oligomeric presentation at the cell surface, the CD28 chimeras were analysed using BRET (Figure 4.3). When compared to the covalent dimers hCTLA-4 and wild type hCD28 [280] used as controls, both chimeric forms of CD28 show almost identical $BRET_{eff}$ values. This indicates that the substitution of the extracellular domain of CD28 with another CD28 of a different species has no direct effect on its expression and oligomerisation at the cell surface.

Once correct expression of the CD28 chimeras was establised, human and rat mAbs were used in the assay to test for superagonistic activity in the hybridoma cell lines. Human mAb 7.3B6 and rat mAb JJ319 are non-mitogenic antibodies that bind in a membrane distal region of CD28. Human mAb 5.11A and rat mAb JJ316 are mitogenic, and are able to activate T cells in the absence of an additional stimulus and have membrane proximal epitopes [218]. *In vitro*, the mitogenic effects of superagonists are only observed when the CD28 mAb is immobilised [184, 217, 290]. Based on superagonistic assays used by Luhder *et al.* (2003) [218], chimeric cell lines were first incubated with CD28 mAb before transfer to assay plates that were pre-coated with immobilised anti-mouse IgG.

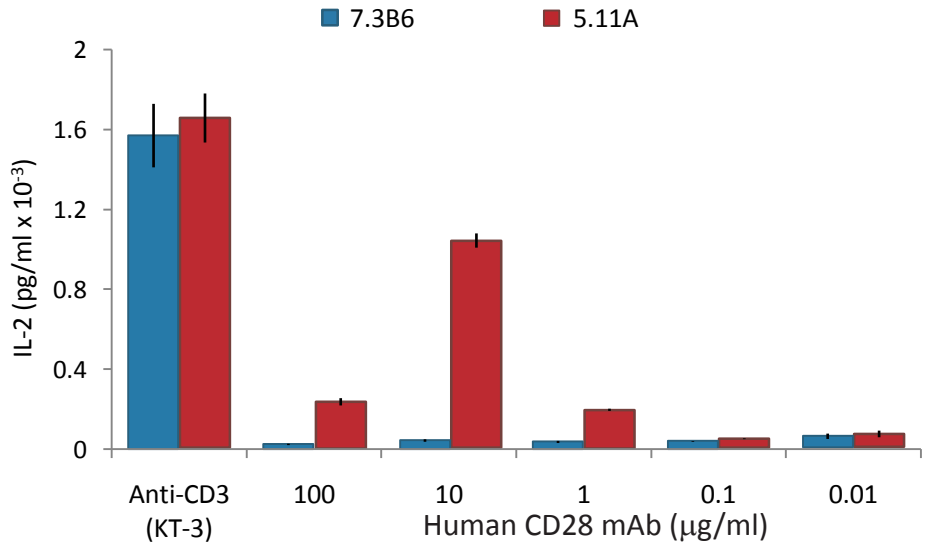


a

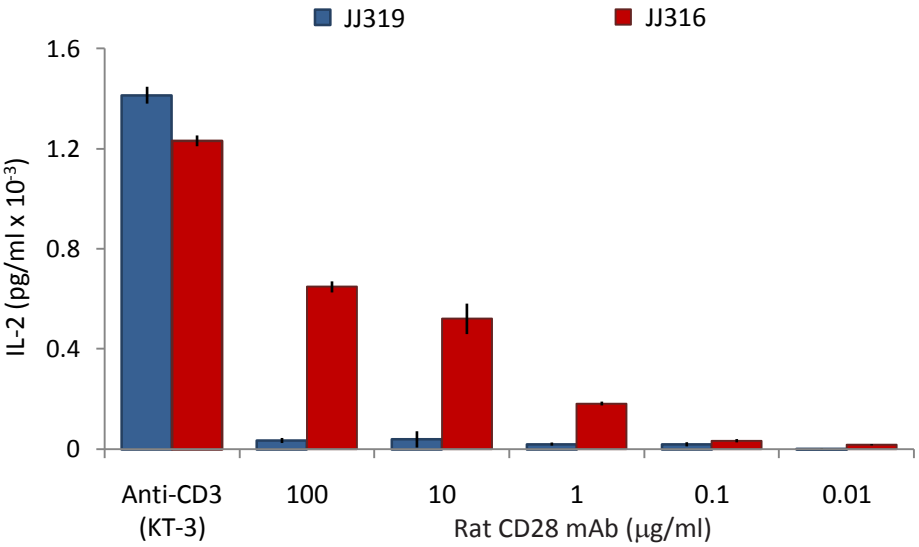


b

Figure 4.3: BRET signals arising from oligomeric and random T-cell surface molecule interactions. (a) BRET$_{eff}$ values recorded from varying acceptor:donor ratios of dimeric (green) and monomeric (blue) control T cell surface molecules. Solid lines show fits of data obtained for the indicated BRET pairs to an equation as predicted for dimers, and the dotted line shows the fit to an equation as predicted for random interactions (See section 2.5) (b) The observed BRET signals for rCD28$_{EX}$mCD28$_{TM/CYT}$ and hCD28$_{EX}$mCD28$_{TM/CYT}$. The grey solid line indicates the fit of the dimeric control data, and the grey dotted line represents the fit of monomeric control data as observed in (a).

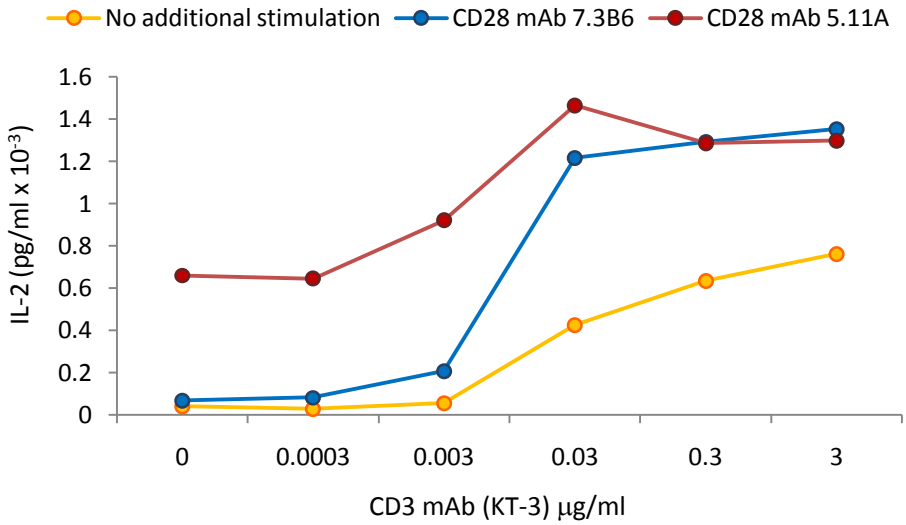


a

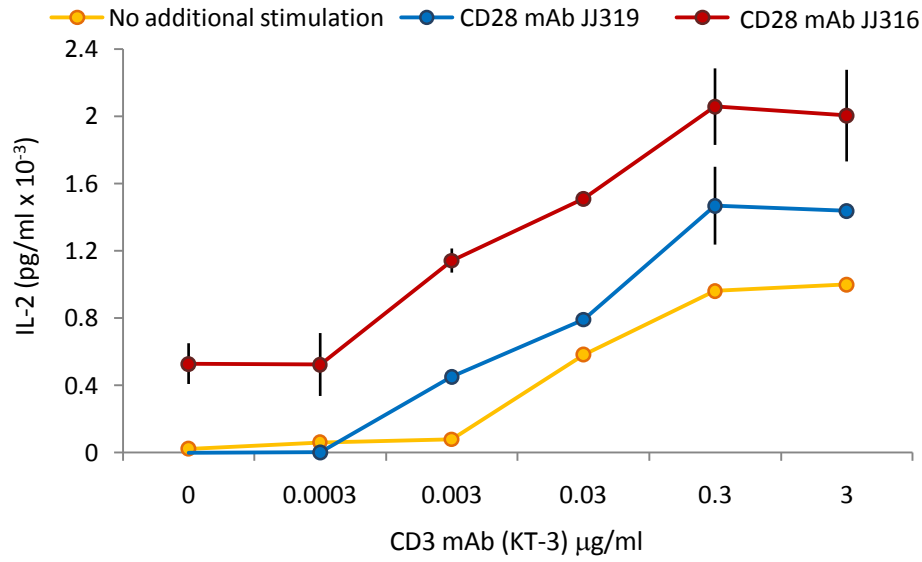


b

Figure 4.4: Antibody stimulation of chimeric CD28 expressing T cell hybridomas. DO11.10 cells expressing either (a) $hCD28_{EX}mCD28_{TM/CYT}$ or (b) $rCD28_{EX}mCD28_{TM/CYT}$ were stimulated with a titration of CD28 mitogenic (5.11A or JJ316) or non-mitogenic (7.3B6 or JJ319) mAbs before incubation in donkey anti-mouse IgG (500μg/ml) coated 96 well plates for 48 hours. The cell lines were also stimulated by plate immobilised mitogenic CD3 specific mAb (KT-3 at 3 μg/ml). The resultant tissue culture supernatant was assayed for IL-2 by ELISA.



a



b

Figure 4.5: Co-stimulation of chimeric CD28 expressing T cell hybridomas. DO11.10 cells expressing either (a) $hCD28_{EX}mCD28_{TM/CYT}$ or (b) $rCD28_{EX}mCD28_{TM/CYT}$ were stimulated with CD28 mitogenic (5.11A or JJ316) or non-mitogenic (7.3B6 or JJ319) mAbs at 10μg/ml, before incubation on 96 well plates pre-coated with a titration of CD3 mitogenic mAb (KT-3 from 3μg/ml to 0.0003μg/ml) and donkey anti-mouse IgG (at 500μg/ml). The resultant supernatant was assayed for IL-2 by ELISA.

When stimulated with the mitogenic mAbs 5.11A and JJ316, a strong induction of IL-2 was observed in each respective CD28 chimeric hybridoma cell line (Figure 4.4). In both $hCD28_{EX}mCD28_{TM/CYT}$ and $rCD28_{EX}mCD28_{TM/CYT}$ cell lines, optimal stimulation with mitogenic antibodies led to IL-2 induction at approximately half that observed for stimulation with a CD3 mAb. The mitogenic CD28 mAbs activated the hybridomas in a concentration dependent manner. This mirrors the observation of Tacke *et al.* (1997) [217], who observed the same effect in rat CD28 mitogenic mAbs. Interestingly, although both rat and human mAbs both appear to be concentration dependent, their optimal concentrations differ by an order of magnitude. As expected, the non-mitogenic CD28 mAbs 7.3B6 and JJ319 failed to elicit an IL-2 response in the CD28 cell lines. The CD28 cell lines were next tested for co-stimulation to confirm that the mAbs 7.3B6 and JJ319 were also active within the chimeric hybridoma system (Figure 4.5). Both mAbs 7.3B6 and JJ319 co-stimulated the cell lines at sub-optimal concentrations of plate immobilised CD3 mAb. As reported previously [217,218], both mitogenic and non-mitogenic mAbs showed co-stimulatory activity in the nanogram range of CD3 mAb activation, but at sub-optimal CD3 stimulation concentrations, the co-stimulatory activity observed with the mitogenic mAbs was stronger than with the non-mitogenic mAbs.

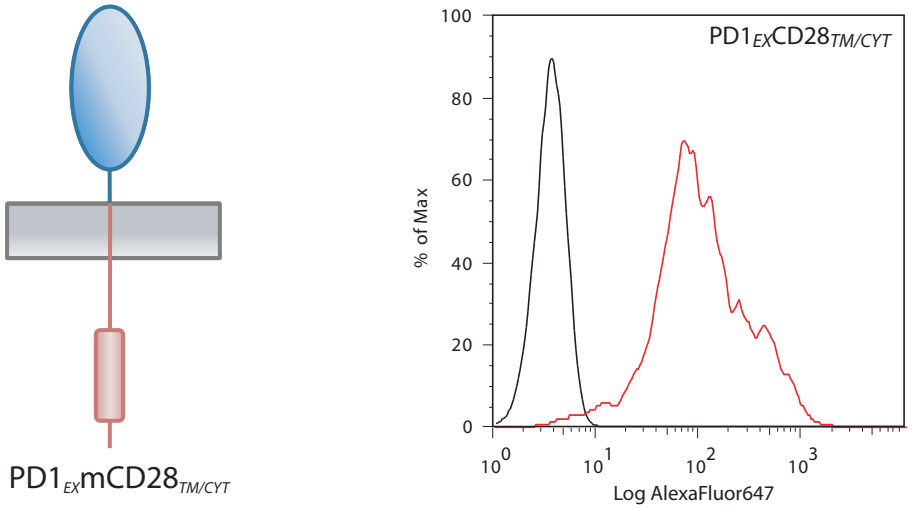
4.3.2 $PD\text{-}1_{EX}CD28_{TM/CYT}$ cell line is not triggered by PD-1 mAbs

The observation of superagonism in the *in vitro* CD28 chimeric cell line system leads to this system being used as a basis for the development of an agonist PD-1 mAb assay.

Using the same mouse CD28 intracellular domain signalling components, PD-1 extracellular domain chimeras were constructed to trigger the CD28 signalling pathway by stimulating it with PD-1 mAbs.

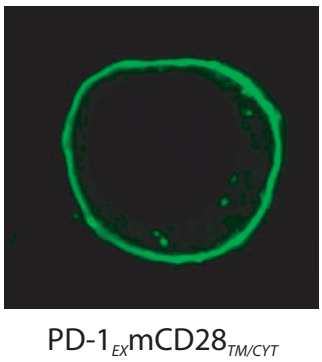
The first PD-1 chimera constructed contained the extracellular domain of PD-1 and the transmembrane domain and intracellular domains of CD28 (PD-1_{EX}CD$28_{TM/CYT}$) (Figure 4.6). Confocal microscopy of transient PD-1_{EX}CD$28_{TM/CYT}$ expression in HEK 293T cells shows that the PD-1 chimera shows no intracellular localisation and successfully expressed at the cell surface (Figure 4.7). The chimera was expressed in DO11.10 cells, and a cell line produced by FACS sorting for PD-1_{EX}CD$28_{TM/CYT}$ expression (Figure 4.6). Using this chimeric cell line, the PD-1 mAbs 2, 10 and 19 were assessed for agonistic activity. As previously described (See section 3), based on the epitope location, mAb 19 is predicted to be a PD-1 agonist. When stimulated with all the PD-1 mAbs over a range of concentrations, no significant stimulation was observed (Figure 4.8); the IL-2 levels recorded for stimulated PD-1_{EX}CD$28_{TM/CYT}$ hybridomas were ~ 50 fold lower than those observed for CD28 chimeric hybridomas. However, the PD-1_{EX}CD$28_{TM/CYT}$ cell line responded well to stimulation with CD3 mAb. As a result of this, the cell line was assayed for activation under co-stimulatory conditions (Figure 4.8), but at sub-optimal KT-3 concentrations none of the PD-1 mAbs elicited an IL-2 response that was substantially above that observed for CD3 mAbs alone.

One structural difference between PD-1 and CD28 is that CD28 is a homodimer at the cell surface due to an extracellular interchain disulphide bond [184]. But PD-1 is believed to be monomeric, unlike other CD28 family members (e.g.CD28, CTLA-

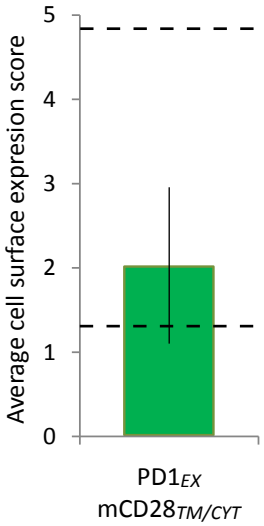


a b

Figure 4.6: Construction and expression of PD-1_{EX}CD$28_{TM/CYT}$ in DO11.10 hybridoma cells. (a) Schematic representation of the PD-1_{EX}CD$28_{TM/CYT}$ construct. (b) Expression levels of PD-1_{EX}CD$28_{TM/CYT}$ in the DO11.10 cell line. DO11.10 cells were transduced with lentivirus encoding PD-1_{EX}CD$28_{TM/CYT}$ and FACS sorted by gating for both emGFP and PD-1 expression. The resultant cell line (red) and control untransduced DO11.10 cells (black) were analysed by flow cytometry, staining with a 5μg/ml PD-1 mAb 10 and 5μg/ml donkey anti-mouse AlexaFluor®647 (Molecular Probes, Invitrogen) secondary conjugate.

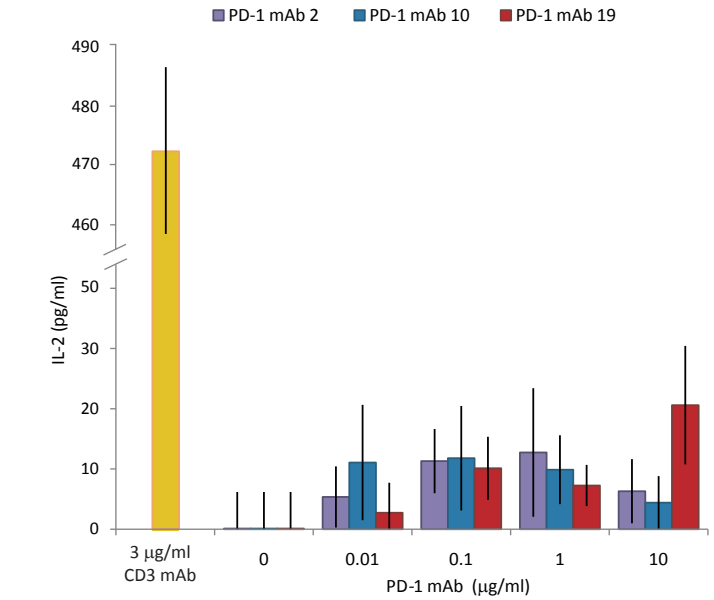


a

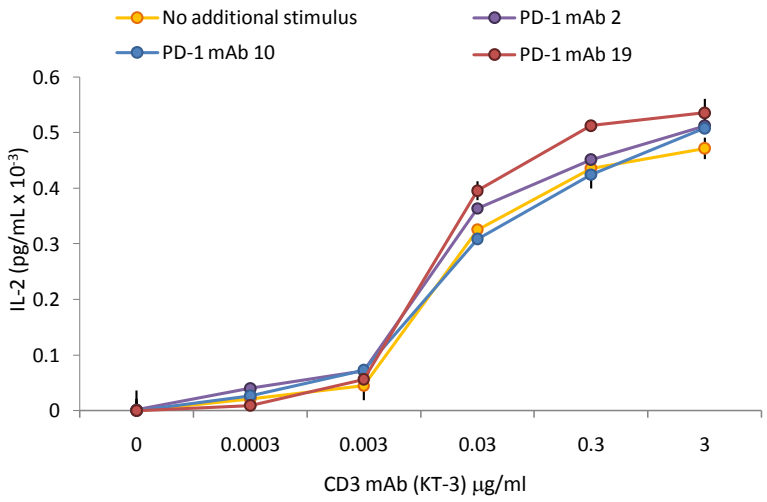


b

Figure 4.7: (a) Confocal microscopy analysis of the expression of $hCD28_{EX}mCD28_{TM/CYT}$. $hCD28_{EX}mCD28_{TM/CYT}$ in the $pGFP^2$-N3 vector was transiently expressed in HEK 293T cells on cover-slides for 24 hours. Cells were excited at 488nm and observed through a 60x objective lens. (b) Average cell surface expression scores for $hCD28_{EX}mCD28_{TM/CYT}$ in HEK 293T cells. Transfected cells were observed and scored on a scale for cell surface expression, where a score of 1 indicates cell surface expression only and 5 indicates complete intracellular localisation. A minimum 20 cells were scored for each construct expressed. The average cell surface expression score for the each construct is displayed. The dotted lines represent levels of cell surface expression representative for hCD28 (expressed solely on the cell surface) and hCTLA-4 (largely complete intracellular localisation).



a



b

Figure 4.8: PD-1_{EX}CD$28_{TM/CYT}$ cells are unresponsive when directly stimulated and co-stimulated. (a) Stimulation of PD-1_{EX}CD$28_{TM/CYT}$ hybridomas with either PD-1 mAb 2, 10 or 19. DO11.10 hybridomas expressing the PD-1_{EX}CD$28_{TM/CYT}$ chimera were incubated with PD-1 mAbs 2, 10 and 19 in a titration from 100 μg/ml to 0.01 μg/ml. Cell lines were also stimulated with plate immobilised CD3 mitogenic mAb (KT-3 at 3μg/ml). Cells were incubated in 96 well plates coated with donkey anti-mouse IgG (500 μg/ml) for 48 hours. The resulting tissue culture supernatant was assayed for IL-2. (b) Stimulation of PD-1_{EX}CD$28_{TM/CYT}$ hybridomas with PD-1 mAbs in co-stimulatory conditions. DO11.10 hybridomas expressing the PD-1_{EX}CD$28_{TM/CYT}$ chimera were incubated with either PD-1 mAb 2, 10 or 19 (5 μg/ml) before incubation for 48 hours on CD3 mAb (titration of KT-3, from 3 μg/ml to 0.0003 μg/ml) and donkey anti-mouse IgG antibody (500 μg/ml) on 96 well plates. Cells were incubated for 48 hours and the resulting tissue culture supernatant was assayed for IL-2. Il-2 levels were assayed by ELISA.

4 and ICOS) [269] due to the absence of an extracellular cysteine [287]. This was confirmed using BRET (Figure 4.9). When expressed in the pGFP^2 and pRLuc vectors, PD-1_{EX}CD$28_{TM/CYT}$ showed monomeric activity with an average $BRET_{eff}$ ratio of ~ 0.2. This is equivalent to those observed for another non-interacting monomeric T cell membrane protein, CD86 [280]), and for full length wild type PD-1. This indicates that the PD-1_{EX}CD$28_{TM/CYT}$ chimera is a monomer at the cell surface.

4.3.3 The generation of hPD-1 dimeric constructs

An explanation for the absence of activation in the PD-1_{EX}CD$28_{TM/CYT}$ cell line is that two adjacent cytoplasmic domains are required for optimal CD28 signalling. With this in mind, a further five chimeric PD-1 molecules were designed and created with the aim of expressing a dimeric PD-1/CD28 chimera.

The construct PD-1_{EX}CD$28_{ST/TM/CYT}$ (Figure 4.10) was designed to contain the stalk region of mouse CD28. This sequence of seven amino acids stretches from the beginning of the CD28 extracellular domain to just before the CD28 Ig V-set domain, and contains the cysteine that forms the interchain disulphide bond, creating the homodimer [291]. To encourage the chimera to dimerise at the cell surface, this sequence was fused between the Ig V-set domain of human PD-1 and the mouse CD28 cytoplasmic domain.

Ctwo, both contain a mouse C-Jun leucine zipper domain (Figure 4.10). C-Jun is a proto-oncogene that, together with C-Fos, forms the AP-1 transcription factor which controls a variety of cellular processes [292, 293]. C-Jun is able to heterodimerise

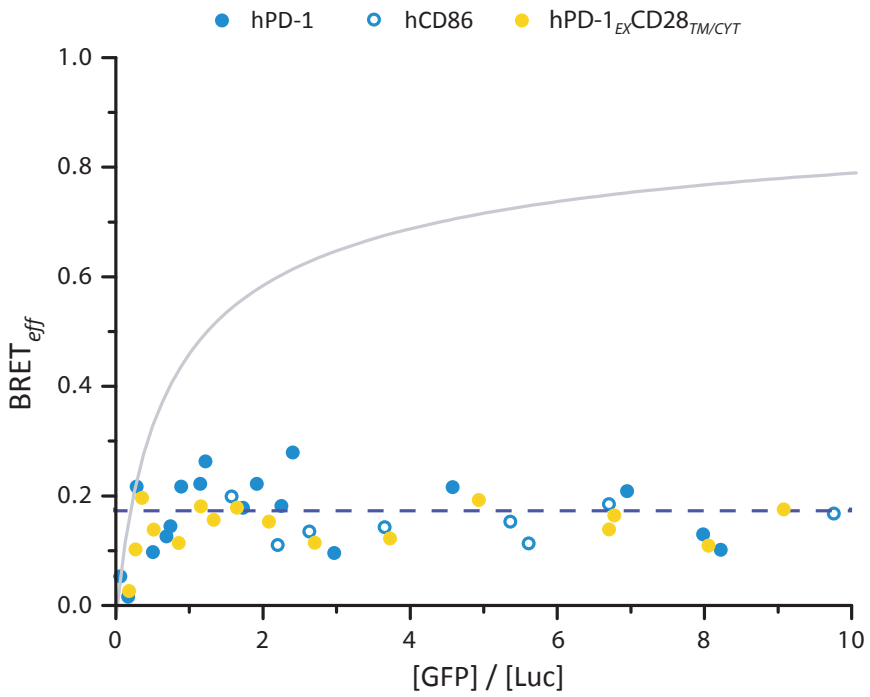


Figure 4.9: BRET signals arising from PD-1_{EX}CD$28_{TM/CYT}$, hPD-1 and hCD86 cell surface interactions. The observed BRET $BRET_{eff}$ values for PD-1_{EX}CD$28_{TM/CYT}$, hPD-1 and hCD86 recorded from varying acceptor:donor ratios of each molecule at the cell surface. The blue dotted line represents the fit of monomeric hPD-1 and hCD86 data. The grey solid line indicates the fit of the dimeric control data as observed in Figure 4.3.

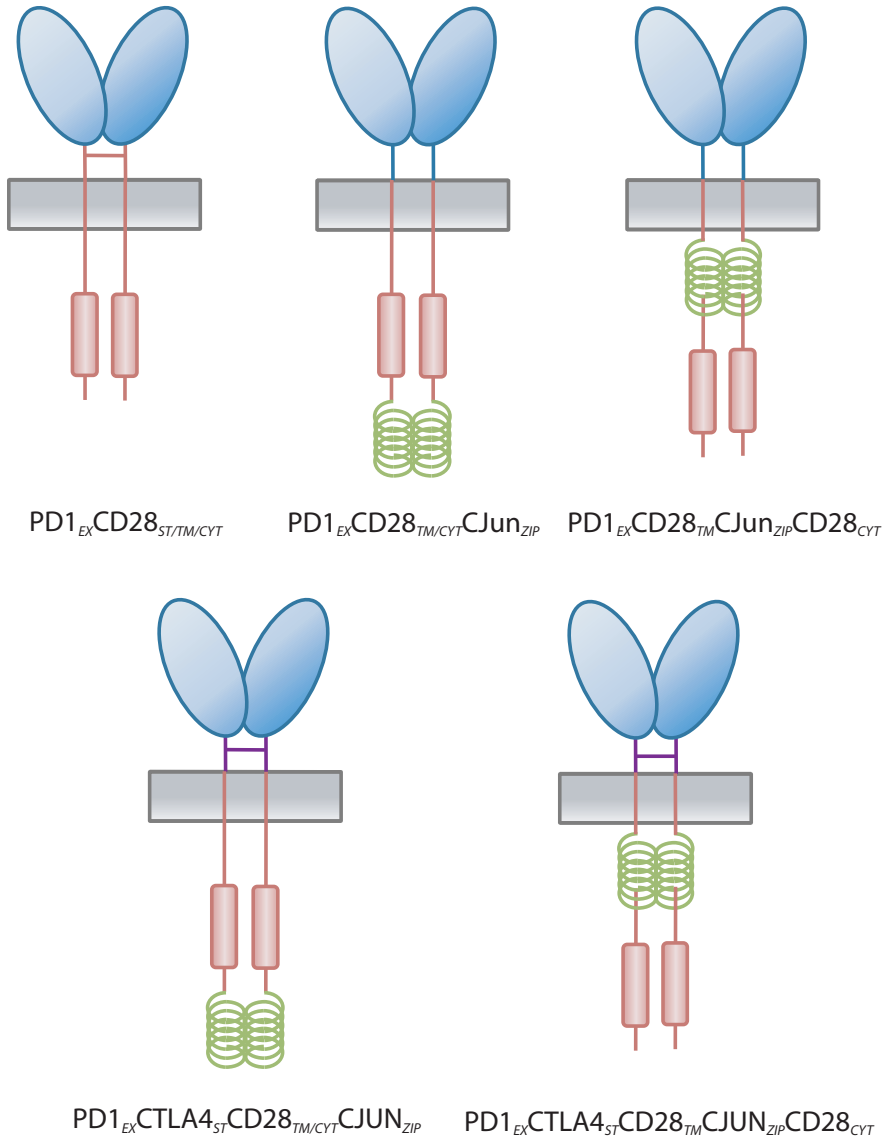


Figure 4.10: Schematic representations of the dimeric PD-1 constructs PD-$1_{EX}CD28_{ST/TM/CYT}$, PD-$1_{EX}CD28_{TM/CYT}CJun_{ZIP}$, PD-$1_{EX}CD28_{TM}CJun_{ZIP}CD28_{CYT}$, $PD1_{EX}CTLA4_{ST}CD28_{TM/CYT}CJun_{ZIP}$ and $PD1_{EX}CTLA4_{ST}CD28_{TM}CJun_{ZIP}CD28_{CYT}$.

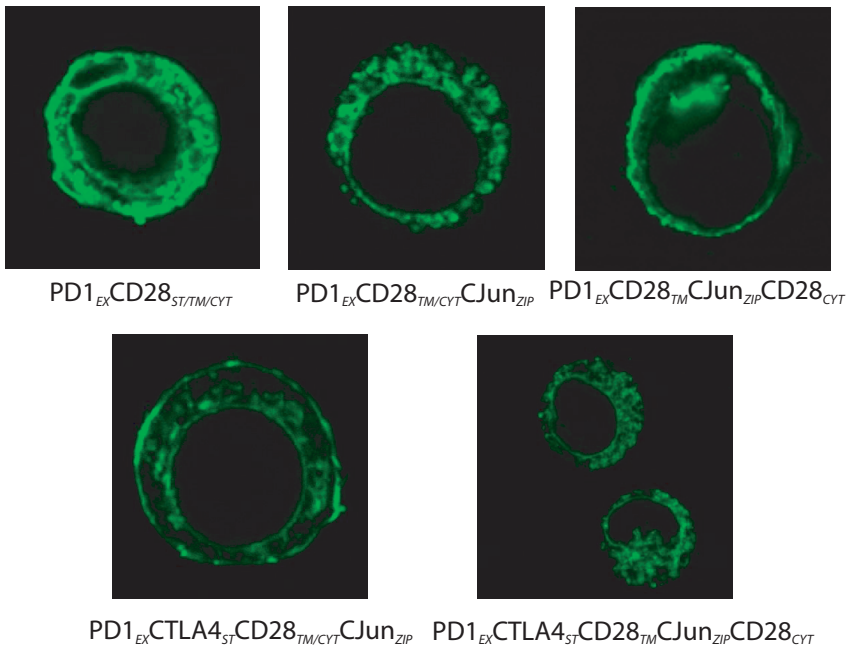
to C-Fos, and homodimerise via a hydrophobic leucine ridge forming a 28 amino acid α helix, creating a "leucine zipper" [294]. Because the signalling potential of mouse CD28 might be disrupted by its fusion with a c-jun leucine zipper, two constructs were designed. The first construct placed the zipper at the C-terminus of the CD28 cytoplasmic domain, while the second placed it at the N-terminal end (PD-1_{EX}CD28$_{TM/CYT}$CJun$_{ZIP}$ and PD-1_{EX}CD28$_{TM}$CJun$_{ZIP}$CD28$_{CYT}$ respectively).

As with the PD-1_{EX}CD28$_{ST/TM/CYT}$ chimera, the short stalk region between the PD-1 transmembrane and V-set domain in PD1_{EX}CTLA4$_{ST}$CD28$_{TM/CYT}$CJun$_{ZIP}$ and PD1_{EX} CTLA4$_{ST}$CD28$_{TM}$CJun$_{ZIP}$CD28$_{CYT}$ was replaced, although in these chimeras it was replaced with the equivalent stalk region from human CTLA-4 (Figure 4.10). CTLA-4 is an ortholog of CD28 [194] and its stalk also contains an interchain disulphide bond, enabling it to form a homodimer. The presence of the CTLA-4 stalk in a chimera may encourage dimer formation. In addition to the CTLA-4 stalk, the chimeras contain the C-Jun leucine zipper either at the N or C-terminus of the the CD28 cytoplasmic domain (PD1_{EX}CTLA4$_{ST}$CD28$_{TM}$CJun$_{ZIP}$CD28$_{CYT}$ and PD1_{EX}CTLA4$_{ST}$CD28$_{TM/CYT}$CJun$_{ZIP}$ respectively).

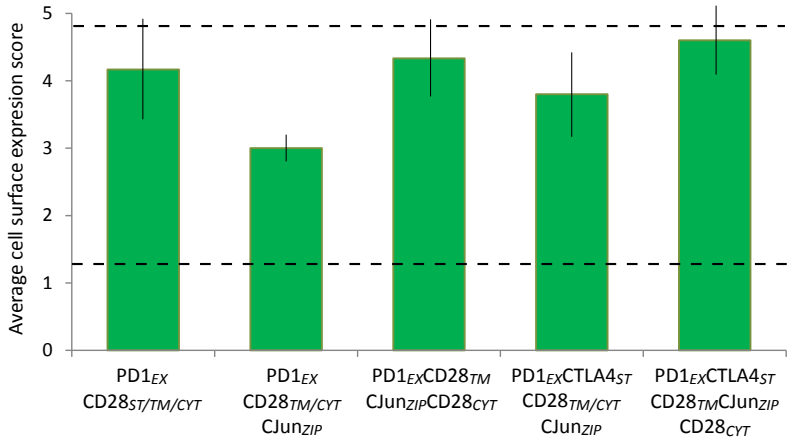
Visualisation of the chimeras at the cell surface by confocal microscopy, through transient expression in HEK 293T cells using the pGFP^2-N3 vector, showed that all five constructs displayed varying levels of intracellular localisation (Figure 4.11). A large amount of PD-1_{EX}CD28$_{TM/CYT}$CJun$_{ZIP}$ localised to the cell surface, and showed the best surface expression but a significant amount of aggregation of the construct was also observed within the transfected cells. Chimeras PD-1_{EX}CD28$_{ST/TM/CYT}$ and

$PD1_{EX}CTLA4_{ST}CD28_{TM/CYT}CJun_{ZIP}$ both show surface expression, but accompanied with a large amount of aggregation within the cell. Visual evidence of the expression of $PD\text{-}1_{EX}CD28_{TM}CJun_{ZIP}CD28_{CYT}$ and $PD1_{EX}CTLA4_{ST}CD28_{TM}CJun_{ZIP}CD28_{CYT}$ was limited to the cellular compartment with very little of the construct seen to express at the cell surface. The transient expression of the constructs was also analysed by flow cytometry. When probed with PD-1 mAb, all but $PD1_{EX}CTLA4_{ST}CD28_{TM}CJun_{ZIP}CD28_{CYT}$ were found to express at the cell surface (data not shown).

The aggregation of the constructs, as observed by confocal microscopy, suggest that the chimeric constructs are not processed correctly within the cellular compartment and therefore may not be expressed as typical dimers at the cell surface. To investigate this and identify which constructs were suitable to use in the creation of stable cell lines, the chimeras were examined using BRET analysis (Figure 4.12). Of the four constructs to be successfully expressed at the cell surface, it was not possible to fit data recorded for $PD\text{-}1_{EX}CD28_{TM}CJun_{ZIP}CD28_{CYT}$ or $PD1_{EX}CTLA4_{ST}CD28_{TM/CYT}CJun_{ZIP}$ to the BRET dimer model. This further indicates aggregation for these constructs. However, $BRET_{eff}$ values for $PD\text{-}1_{EX}CD28_{TM/CYT}CJun_{ZIP}$ fitted to a dimer model successfully and the curve reaches BRET levels recorded for wild type CD28. This evidence suggests that although aggregation is observed, the $PD\text{-}1_{EX}CD28_{TM/CYT}CJun_{ZIP}$ presented to the cell surface is dimeric. The $BRET_{eff}$ values recorded for the $PD\text{-}1_{EX}CD28_{ST/TM/CYT}$ construct also can be fitted by the dimer model, but have lower average $BRET_{eff}$ values than the covalent dimer wild type CD28. These lower $BRET_{eff}$ values suggest that the hPD-1/mCD28dimer forms a weaker dimer at the cell surface.



a



b

Figure 4.11: Construction and expression of the PD-1 dimer constructs in HEK293T cells. (a) Confocal microscopy analysis of the expression of PD-$1_{EX}CD28_{ST/TM/CYT}$, PD-$1_{EX}CD28_{TM/CYT}CJun_{ZIP}$, PD-$1_{EX}CD28_{TM}CJun_{ZIP}CD28_{CYT}$, $PD1_{EX}CTLA4_{ST}CD28_{TM/CYT}CJun_{ZIP}$ and $PD1_{EX}CTLA4_{ST}CD28_{TM}CJun_{ZIP}CD28_{CYT}$. Constructs in the $pGFP^2$-N3 vector were transiently expressed in HEK 293T cells on cover-slides for 24 hours. Cells were excited at 488nm and observed through a 60x objective lens. (b) Average cell surface expression scores for PD-1 dimer construct expression in HEK 293T cells. Transfected cells were observed and scored on a scale for cell surface expression, where a score of 1 indicates cell surface expression only and 5 indicates complete intracellular localisation. A minimum 20 cells were scored for each construct expressed. The average cell surface expression score for the each construct is displayed. The dotted lines represent levels of cell surface expression representative for hCD28 (expressed solely on the cell surface) and hCTLA-4 (largely complete intracellular localisation).

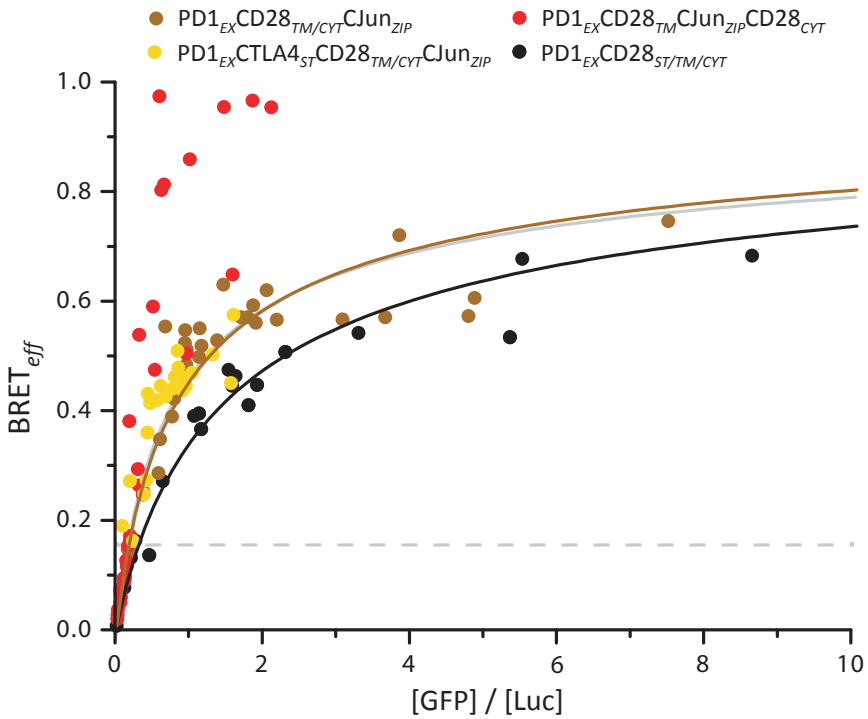
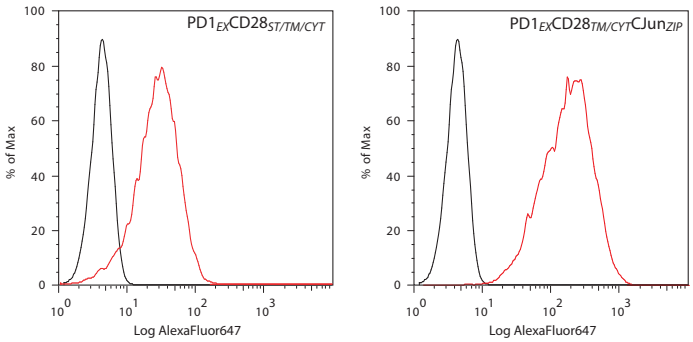
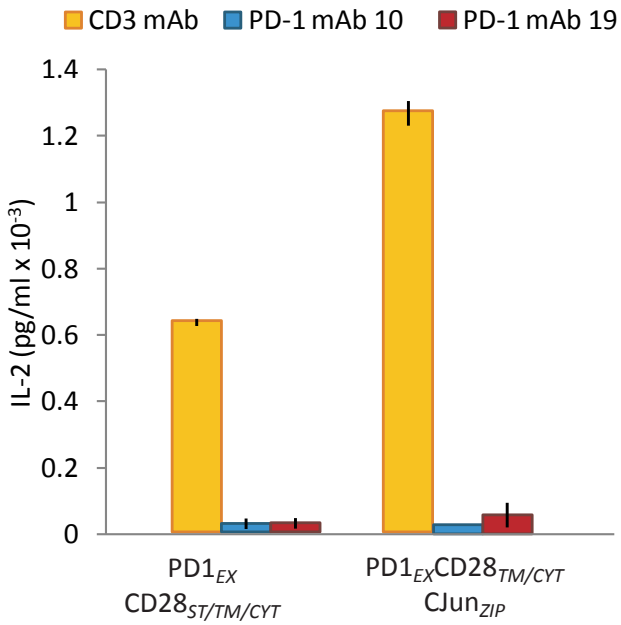


Figure 4.12: BRET signals arising from cell surface interactions of PD-$1_{EX}CD28_{TM/CYT}CJun_{ZIP}$, PD-$1_{EX}CD28_{TM}CJun_{ZIP}CD28_{CYT}$, $PD1_{EX}CTLA4_{ST}CD28_{TM/CYT}CJun_{ZIP}$ and PD-$1_{EX}CD28_{ST/TM/CYT}$. Solid lines show fits of data obtained for the indicated BRET pairs to an equation as predicted for dimers. The grey solid line indicates the fit for constitutive dimer controls CTLA-4 and CD28, and the grey dotted line represents the fit of monomeric CD86 and PD-1 control data.



a



b

Figure 4.13: Expression levels of PD-1_{EX}CD$28_{ST/TM/CYT}$ and PD-1_{EX}CD$28_{TM/CYT}$CJun$_{ZIP}$ are high in the DO11.10 cell line, but stimulation of the cell lines with PD-1 mAbs does not result in activation. (a) DO11.10 cells were transduced with lentivirus encoding either construct and FACS sorted by gating for both emGFP and PD-1 expression. The resultant cell lines (red) and untransduced DO11.10 cells (black) were analysed by flow cytometry, staining with a 5μg/ml PD-1 mAb 10 and 5μg/ml donkey anti mouse AlexaFluor®647 (Molecular Probes, Invitrogen) secondary conjugate. Cells were gated for emGFP and PD-1 expression. (b) The PD-1 dimeric cell lines are unresponsive when directly stimulated with PD-1 mAbs. DO11.10 hybridomas expressing PD-1_{EX}CD$28_{ST/TM/CYT}$ and PD-1_{EX}CD$28_{TM/CYT}$CJun$_{ZIP}$ were stimulated with PD-1 mAbs (mAb 10 or 19 at 10μg/ml) or plate bound CD3 mAb (KT-3 at 3μg/ml). Cells were then incubated in 96 well plates coated with donkey anti-mouse IgG antibody (500μg/ml) for 48 hours, before the resultant tissue culture supernatant was assayed for IL-2. Il-2 levels were assayed using ELISA.

Both PD-1_{EX}CD$28_{ST/TM/CYT}$ and PD-1_{EX}CD$28_{TM/CYT}$CJun$_{ZIP}$ were transduced using lentivirus into a T cell hybridoma cell line. When probed with PD-1 mAb by flow cytometry analysis, both were successfully expressed on the T cell hybridomas (Figure 4.13) and from these transductions stable cell lines were created. The cell lines expressing PD-1_{EX}CD$28_{ST/TM/CYT}$ and PD-1_{EX}CD$28_{TM/CYT}$CJun$_{ZIP}$ were both stimulated successfully with CD3 mAb to produce high levels of IL-2 (Figure 4.13) but when stimulated with PD-1 mAbs 10 and 19, IL-2 secretion was low. The small variations in IL-2 levels recorded in response to PD-1 mAb stimulation were not found to be consistent in repeats of the assay. Despite the levels of intracellular aggregation shown by the chimeras, PD-1_{EX}CD$28_{ST/TM/CYT}$ and PD-1_{EX}CD$28_{TM/CYT}$CJun$_{ZIP}$ both expressed at the cell surface as dimers. The inactivity in these cell lines when stimulated with PD-1 mAbs is surprising given the levels of dimerisation observed for the expressed protein. The possibility that the structural factors that lead to the dimerisation and associated cellular aggregation of these proteins might also have a deleterious effect on their signalling potential is discussed later.

4.3.4 PD-1_{EX}CD28_{TM}CD$3\zeta_{CYT}$ chimeras are unresponsive to all mAb stimulation

The addition of leucine zippers and CD28 or CTLA-4 stalk regions to encourage PD-1 dimer formation resulted in intracellular aggregation of the constructs containing them. This led to a different approach which had been used successfully in the past to create chimeric signaling T cell molecules involving the use of CD3ζ domains. The

ζ subunit of the TCR/CD3 complex is a disulpide linked homodimer [295] which contains cytoplasmic immunoreceptor tyrosine based activation motifs (ITAMs) [296]. The ITAMs found on CD3ζ are phosphorylated upon TCR/CD3 triggering, a step that leads to a signalling cascade, ultimately resulting in the activation of the IL-2 gene and T cell activation. The signalling potential of the CD3ζ cytoplasmic domain has been used in chimeric molecules to investigate the initial triggering [161] and signalling steps [297] of T cell activation. Because of the previous use of CD3ζ in such investigations and its dimeric nature, a series of human PD-1/mouse CD3ζ chimeras was created to investigate the stimulatory nature of the PD-1 mAbs.

The first chimera to be created comprised the human PD-1 extracellular domain, the mouse CD28 transmembrane domain and the mouse CD3ζ cytoplasmic domain (PD-1_{EX}CD28_{TM}CD$3\zeta_{CYT}$) (Figure 4.14). This construct was created to harness the signalling potential of the CD3ζ intracellular domain, as used in the 2B4-CD3ζ or CD8-CD3ζ chimeras created by Choudhuri *et al.* (2005) and Irving & Weiss (1991) respectively [161, 297]. The chimera successfully expressed at the cell surface after lentiviral transfection and the cells positive for PD-1 expression were FACS sorted to create a PD-1_{EX}CD28_{TM}CD$3\zeta_{CYT}$ T cell hybridoma cell line (Figure 4.15). When stimulated with both CD3 mAb and the PD-1 mAbs (as above), the cell line was non-responsive (not shown). No IL-2 induction was observed even at high stimulatory concentrations of CD3 mAb. The lack of IL-2 induction, despite stimulation with potentially superagonistic PD-1 mAbs, could be explained by the lack of the CD3ζ transmembrane and short extracellular domain, which are essential for dimer formation [298]. The

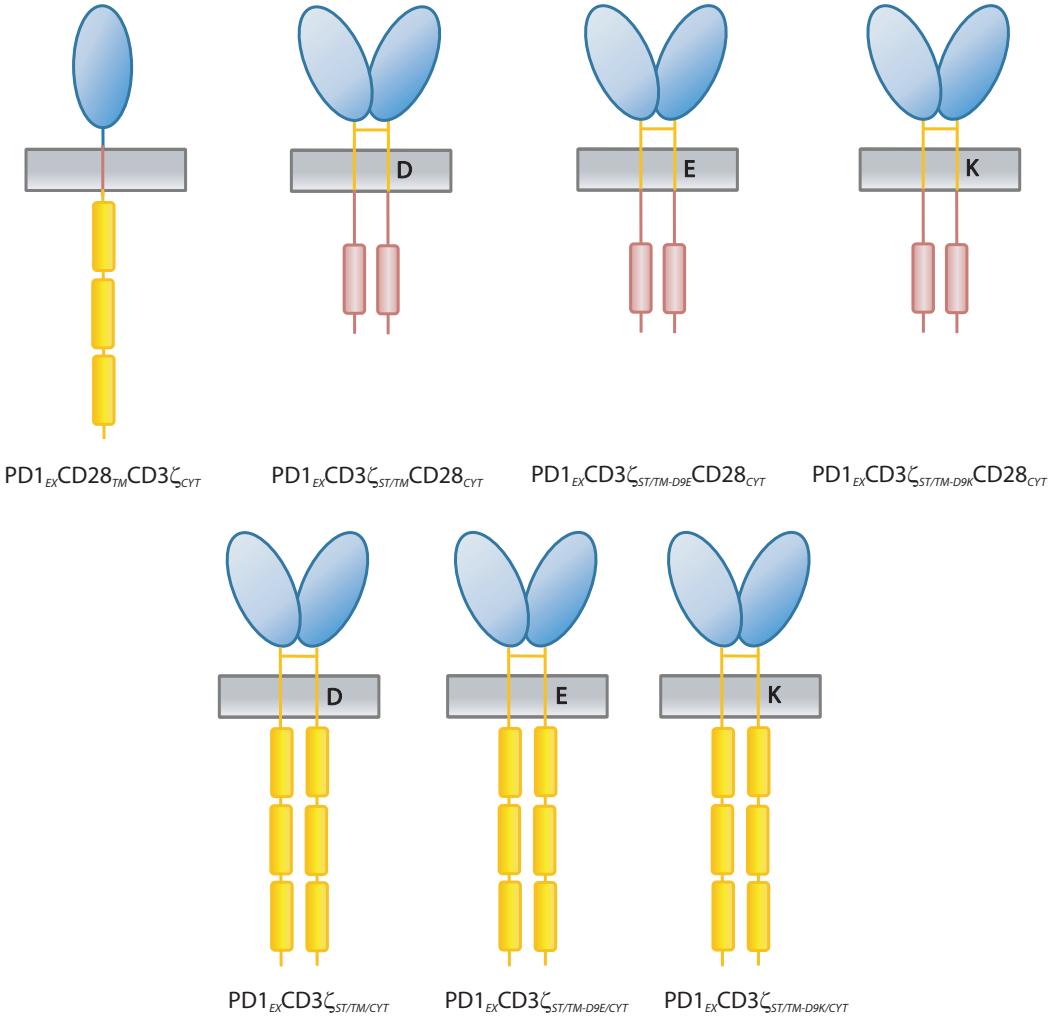


Figure 4.14: Schematic representations of the PD-1 constructs PD-1_{EX}CD28_{TM}CD$3\zeta_{CYT}$, PD-1_{EX}CD$3\zeta_{ST/TM}$CD28_{CYT}, PD-1_{EX}CD$3\zeta_{ST/TM\text{-}D9E}CD28_{CYT}$, PD-$1_{EX}CD3\zeta_{ST/TM\text{-}D9K}CD28_{CYT}$, PD-$1_{EX}CD3\zeta_{ST/TM/CYT}$, PD-$1_{EX}CD3\zeta_{ST/TM\text{-}D9E/CYT}$ and PD-1_{EX}CD$3\zeta_{ST/TM\text{-}D9K/CYT}$.

transmembrane domain was included in the 2B4-CD3ζ chimeric signalling molecule created by Choudhuri *et al.*(2005), and both the CD3ζ transmembrane and extracellular region were included in the CD8-CD3ζ chimera created by Irving & Weiss (1991). Both these chimeras were successful signalling molecules, which supports the observation that the dimerisation of CD3ζ is essential for its signalling function [299]. The reason for the lack of stimulation observed with CD3 mAb is less clear. The DO11.10 T cell hybridomas contain endogenous TCR/CD3 complexes that have been successfully activated in the other PD-1 cell lines created, so it is the expression of the PD-1_{EX}CD28_{TM}CD$3\zeta_{CYT}$ construct that prevents signalling through the TCR/CD3 complex.

4.3.5 Activation of the PD-1_{EX}CD$3\zeta_{ST/TM}$CD28_{CYT} cell line by PD-1 mAbs

The second group of CD3ζ chimeras to be created used the extracellular and transmembrane domain of CD3ζ in an attempt to induce dimerisation in a hPD-1/mCD28 chimera. Rutledge *et al.* (1992) [298] showed that the α chain of the IL-2 receptor can be expressed as a disulphide linked dimer through the replacement of the wild type transmembrane domain with that of CD3ζ. The first construct, PD-1_{EX}CD$3\zeta_{ST/TM}$CD28_{CYT} (Figure 4.14), was successfully expressed at the cell surface (Figure 4.16). A cell line expressing PD-1_{EX}CD$3\zeta_{ST/TM}$CD28_{CYT} was created (Figure 4.15) and stimulated with CD3 mAb and PD-1 mAb 2, 10, 19 and 29 (Figure 4.17). A high level of activation was observed in response to CD3 mAb stimulation, as seen in other PD-1 chimeras. In response to PD-1 mAb stimulation the PD-1_{EX}CD$3\zeta_{ST/TM}$CD28_{CYT} cell line responded in

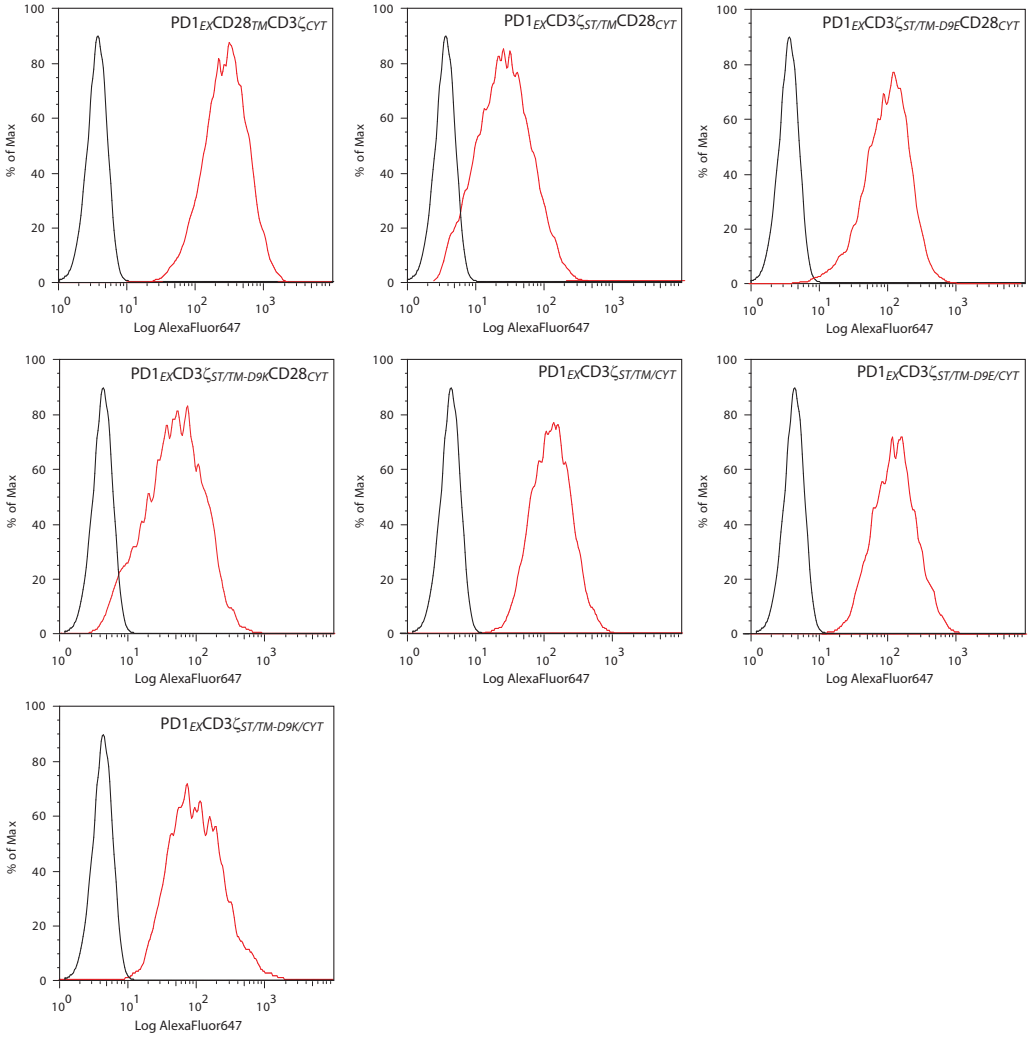
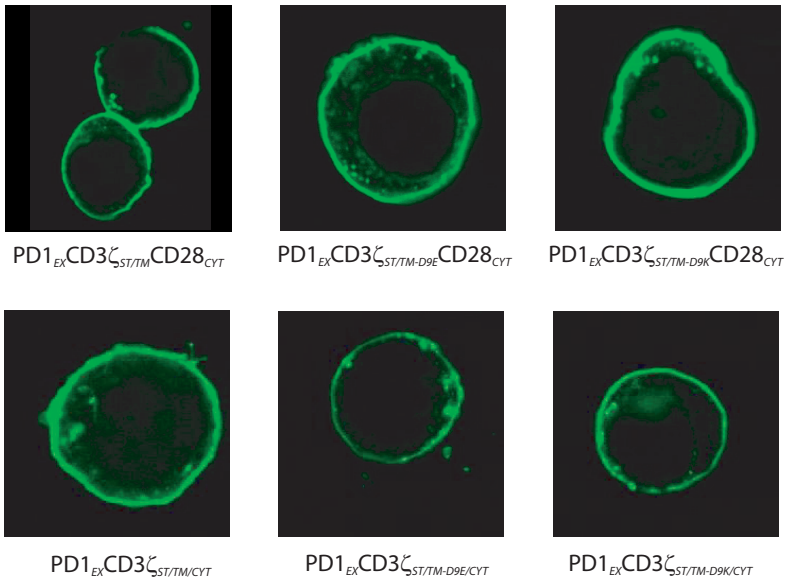


Figure 4.15: Expression levels of PD-1 chimeric constructs containing CD3ζ domains are high in DO11.10 cell lines. DO11.10 cells were transduced with lentivirus encoding each construct and FACS sorted by gating for both emGFP and PD-1 expression. The resultant cell lines (red) and untransduced control DO110.10 cells (black) were analysed by flow cytometry, staining with a 5μg/ml PD-1 mAb 10 and 5μg/ml donkey anti mouse AlexaFluor®647 (Molecular Probes, Invitrogen) secondary conjugate. Cells were gated for emGFP and PD-1 expression.

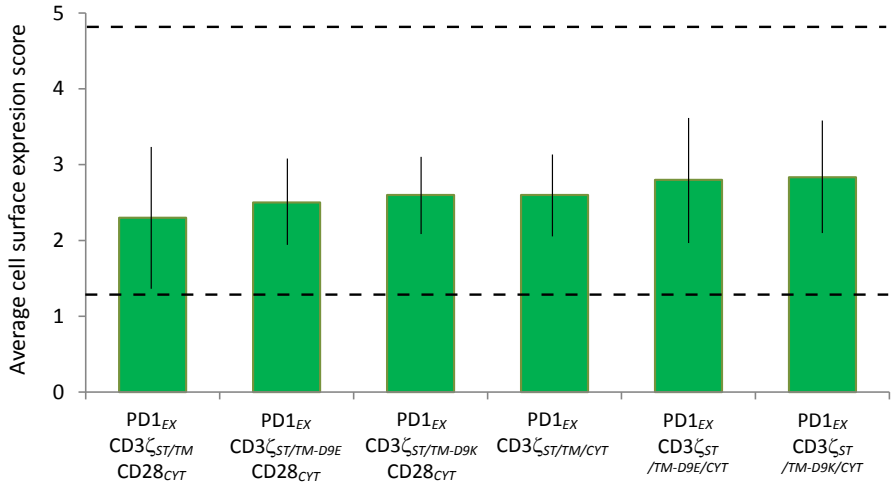
varying degrees.

PD-1 mAb 19, predicted to be agonistic due to its membrane proximal epitope, triggered the highest levels of IL-2 secretion, with an activation level close to that of CD3 mAb. Both PD-1 mAb 2 and 10 were predicted to be non-agonistic, based on their membrane distal epitope location, but both were able to stimulate the PD-1_{EX}CD3$\zeta_{ST/TM}$CD28$_{CYT}$ cell line to significant levels of activation. In repeated experiments, mAb 2 consistently activated the PD-1_{EX}CD3$\zeta_{ST/TM}$CD28$_{CYT}$ expressing cells to IL-2 levels around half of that observed for mAb 19, and PD-1 mAb 10 activated PD-1_{EX}CD3$\zeta_{ST/TM}$CD28$_{CYT}$ expressing cells to levels between half and one third those observed for mAb 19. Of the two predicted non-agonistic antibodies, mAb 2 was reproducibly a stronger activator than mAb 10. Because of the unexpected stimulation observed with mAb 2 and 10 PD-1, mAb 29, which has an undefined epitope, was also included in the stimulation assays. However, no significant stimulation was observed when the PD-1_{EX}CD3$\zeta_{ST/TM}$CD28$_{CYT}$ cell lines were stimulated with mAb 29.

As well as being essential for its oligomerisation, the transmembrane and extracellular domains of CD3ζ are important for the assembly and function of the TCR/CD3 complex [299, 300]. The charged residues found within the transmembrane domain have been shown to be crucial for the incorporation of CD3ζ into the TCR/CD3 complex [299]. The PD-1_{EX}CD3$\zeta_{ST/TM}$CD28$_{CYT}$ chimera contains these charged residues in its transmembrane domain and therefore also associate with the TCR. To investigate if the stimulation observed with all three PD-1 mAbs was influenced by an association with the TCR/CD3 complex, an aspartic acid residue in the CD3ζ transmembrane



a



b

Figure 4.16: Expression of the PD-1 constructs containing CD3ζ elements in HEK 293T cells. (a) Confocal microscopy of the expression of PD-1_{EX}CD28$_{TM}$CD3ζ$_{CYT}$, PD-1_{EX}CD3ζ$_{ST/TM}$CD28$_{CYT}$, PD-1_{EX}CD3ζ$_{ST/TM-D9E}$CD28$_{CYT}$, PD-1_{EX}CD3ζ$_{ST/TM-D9K}$CD28$_{CYT}$, PD-1_{EX}CD3ζ$_{ST/TM/CYT}$, PD-1_{EX}CD3ζ$_{ST/TM-D9E/CYT}$ and PD-1_{EX}CD3ζ$_{ST/TM-D9K/CYT}$. Constructs in the pGFP^2-N3 vector was transiently expressed in HEK 293T cells on cover-slides for 24 hours. Cells were excited at 488nm and observed through a 60x objective lens. (b) Average cell surface expression scores for the constructs expressed in HEK 293T cells. Transfected cells were observed and scored on a scale for cell surface expression, where a score of 1 indicates cell surface expression only and 5 indicates complete intracellular localisation. A minimum 20 cells were scored for each construct expressed. The average cell surface expression score for the each construct is displayed. The dotted lines represent levels of cell surface expression representative for hCD28 (expressed solely on the cell surface) and hCTLA-4 (largely complete intracellular localisation).

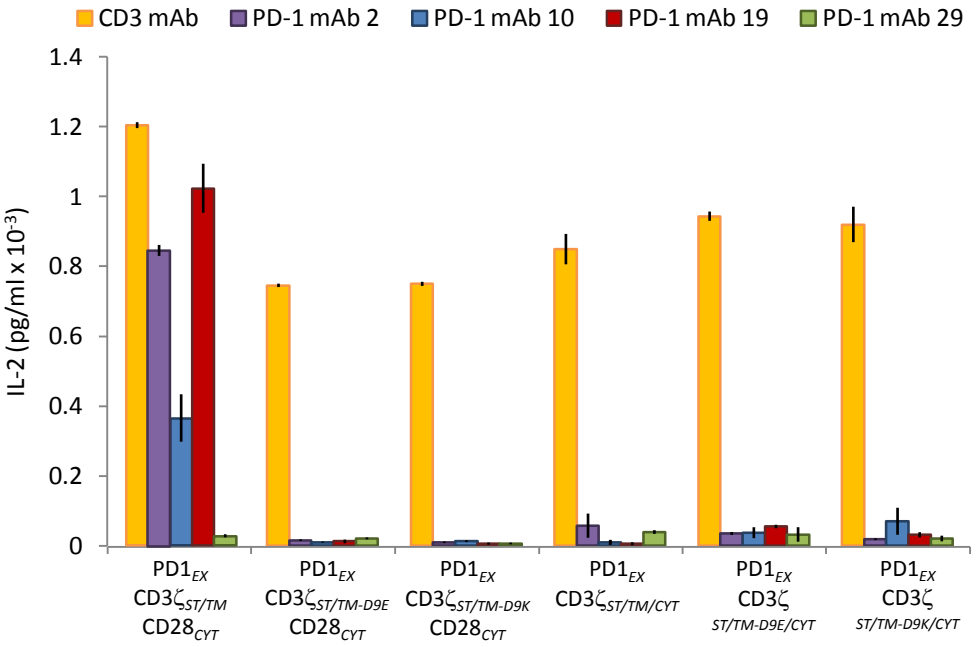


Figure 4.17: The PD-1_{EX}CD3$\zeta_{ST/TM}$CD28$_{CYT}$ cell line is the only cell line containing a CD3ζ domain that when directly stimulated with PD-1 mAbs produces significant levels of IL-2. DO11.10 hybridomas expressing the PD-1_{EX}CD28$_{TM}$CD3ζ_{CYT}, PD-1_{EX}CD3$\zeta_{ST/TM}$CD28$_{CYT}$, PD-1_{EX}CD3$\zeta_{ST/TM\text{-}D9E}$CD28$_{CYT}$, PD-1_{EX}CD3$\zeta_{ST/TM\text{-}D9K}$CD28$_{CYT}$, PD-1_{EX}CD3$\zeta_{ST/TM/CYT}$, PD-1_{EX}CD3$\zeta_{ST/TM\text{-}D9E/CYT}$ and PD-1_{EX}CD3$\zeta_{ST/TM\text{-}D9K/CYT}$ chimeras were incubated with PD-1 mAbs (mAb 2, 10, 19 or 29 at 10μg/ml) or plate bound CD3 mAb (KT-3 at 3μg/ml). Cells were incubated in 96 well plates coated with donkey anti-mouse IgG antibody (500μg/ml) for 48 hours, before the resultant tissue culture supernatant was assayed for IL-2 by ELISA.

domain was mutated, which has been sown to reduce TCR/CD3 complex association. An alanine mutation of the transmembrane domain aspartic acid results in reduced dimer formation [299], but if substituted with some other charged residue (glutamic acid or lysine), dimerisation is restored to wild type levels whilst preventing the incorporation of CD3ζ into the TCR/CD3 complex [298, 299]. Based on this evidence the mutants PD-1_{EX}CD3$\zeta_{ST/TM\text{-}D9E}$CD28$_{CYT}$and PD-1_{EX}CD3$\zeta_{ST/TM\text{-}D9K}$CD28$_{CYT}$ were created.

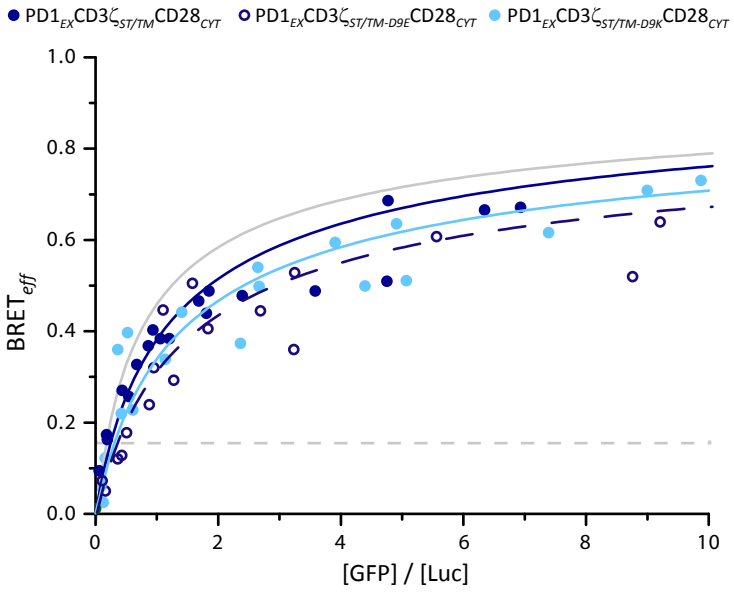
When transiently expressed and observed using confocal microscopy, the mutants PD-1_{EX}CD3$\zeta_{ST/TM\text{-}D9E}$CD28$_{CYT}$and PD-1_{EX}CD3$\zeta_{ST/TM\text{-}D9K}$CD28$_{CYT}$ both expressed successfully at the cell surface (Figure 4.16). Cell lines expressing PD-1_{EX}CD3$\zeta_{ST\text{-}D9E/TM}$ CD28$_{CYT}$ and PD-1_{EX}CD3$\zeta_{ST/TM\text{-}D9K}$CD28$_{CYT}$ (Figure 4.15) were stimulated with CD3 mAb and PD-1 mAbs 2, 10, 19 and 29 (Figure 4.17). Although the cell lines produced high levels of IL-2 when stimulated with CD3 mAb, no significant activation was observed through PD-1 mAb stimulation. The absence of PD-1 mAb-induced signalling in the cell lines containing a mutated CD3ζ transmembrane domain suggests that the activation observed in PD-1_{EX}CD3$\zeta_{ST/TM}$CD28$_{CYT}$, when stimulated with PD-1 mAb, is due to an association with the TCR/CD3 complex.

As described, certain mutations of the aspartic acid found in the transmembrane can severely affect CD3ζ dimerisation. Although the amino acid substitutions used in these experiments have been shown not to affect dimerisation [298, 299], as they are used as part of a chimeric construct it is possible that the mutations made have may have an adverse effect on oligomerisation. Any differences in dimerisation between the PD-1_{EX}CD3$\zeta_{ST/TM\text{-}D9E}$CD28$_{CYT}$ and PD-1_{EX} CD3$\zeta_{ST/TM\text{-}D9K}$ CD28$_{CYT}$ cell lines and PD-

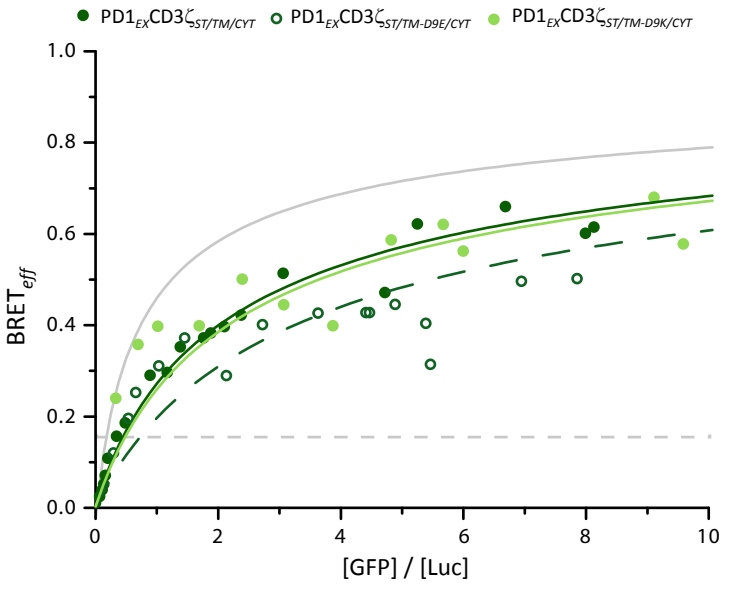
$1_{EX}CD3\zeta_{ST/TM}CD28_{CYT}$ would prevent direct comparisons of any signalling observed. To investigate the oligomeric state of these chimeras at the cell surface, all three constructs were analysed using BRET (Figure 4.18). All of the constructs show a high level of dimerisation, with the $BRET_{eff}$ values of PD-$1_{EX}CD3\zeta_{ST/TM}CD28_{CYT}$ showing dimerisation closest to that of the CD28 and CTLA-4 dimer controls. It is clear that the aspartic acid substitution in the transmembrane domain causes the slightly lower dimerisation levels observed in the PD-$1_{EX}CD3\zeta_{ST/TM\text{-}D9E}CD28_{CYT}$ and PD-$1_{EX}CD3\zeta_{ST/TM\text{-}D9K}CD28_{CYT}$ constructs. However, it is unclear if this decrease in dimerisation is significant enough to cause the differences observed in PD-1 mAb signalling between the constructs.

4.3.6 PD-$1_{EX}CD3\zeta_{ST/TM/CYT}$ cell lines are not activated by PD-1 mAbs

The construct PD-$1_{EX}CD3\zeta_{ST/TM}CD28_{CYT}$ contains a CD28 signalling domain, however the absence of activation observed in the cell lines expressing mutated CD3ζ transmembrane domains suggests an important role for the TCR/CD3 complex in the signalling of PD-$1_{EX}CD3\zeta_{ST/TM}CD28_{CYT}$. To further investigate the association with the TCR/CD3 complex, PD-$1_{EX}CD3\zeta_{ST/TM}CD28_{CYT}$ chimeras were adapted by replacing the CD28 signalling domain with that of CD3ζ (Figure 4.14). If PD-1 mAb stimulation is observed in a PD-$1_{EX}CD3\zeta_{ST/TM/CYT}$ cell line, but not in PD-$1_{EX}CD3\zeta_{ST/TM\text{-}D9E/CYT}$ and PD-$1_{EX}CD3\zeta_{ST/TM\text{-}D9K/CYT}$ cell lines, the signalling involvement of the TCR/CD3 complex would be confirmed. The chimeras PD-$1_{EX}CD3\zeta_{ST/TM/CYT}$, PD-$1_{EX}CD3\zeta_{ST/TM\text{-}D9E/CYT}$ and PD-$1_{EX}CD3\zeta_{ST/TM\text{-}D9K/CYT}$ all successfully expressed at the cell surface as shown by confocal microscopy (Figure 4.16), so each construct was transduced into D011.10 cells to



a



b

Figure 4.18: BRET signals arising from cell surface interactions of hPD-1 chimeras containing CD3ζ domains. (a) $BRET_{eff}$ values recorded for PD-$1_{EX}CD3\zeta_{ST/TM}CD28_{CYT}$, PD-$1_{EX}CD3\zeta_{ST/TM\text{-}D9E}CD28_{CYT}$ and PD-$1_{EX}CD3\zeta_{ST/TM\text{-}D9K}CD28_{CYT}$. (b) $BRET_{eff}$ values recorded for PD-$1_{EX}CD3\zeta_{ST/TM/CYT}$, PD-$1_{EX}CD3\zeta_{ST/TM\text{-}D9E/CYT}$ and PD-$1_{EX}CD3\zeta_{ST/TM\text{-}D9K/CYT}$. Solid and dotted coloured lines show fits of data obtained for the indicated BRET pairs to an equation as predicted for dimers. The grey solid line indicates the fit for constitutive dimer controls CTLA-4 and CD28, and the grey dotted line represents the fit of monomeric CD86 and PD-1 control data.

create stable cell lines (Figure 4.15). When stimulated with CD3 mAb, all three cell lines produced high levels of IL-2 (Figure 4.17). This is in contrast to the unresponsiveness observed in the PD-1_{EX}CD28_{TM}CD$3\zeta_{CYT}$ cell line which also contains a CD3ζ cytoplasmic domain. Surprisingly, no activation was observed in either the wild type or mutant cell lines when stimulated with any of the PD-1 mAbs. To investigate if this absence of signalling is related to some change in the oligomeric status of the chimeras as suggested by PD-1_{EX}CD$3\zeta_{ST/TM}$CD28_{CYT} BRET results, all three constructs were investigated by BRET analysis (Figure 4.18). PD-1_{EX}CD$3\zeta_{ST/TM/CYT}$, PD-1_{EX}CD$3\zeta_{ST/TM\text{-}D9E/CYT}$ and PD-1_{EX}CD$3\zeta_{ST/TM\text{-}D9K/CYT}$ all form weak dimers at the cell surface. PD-1_{EX}CD$3\zeta_{ST/TM\text{-}D9E/CYT}$is the weakest dimer, with PD-1_{EX}CD$3\zeta_{ST/TM/CYT}$ and PD-1_{EX}CD$3\zeta_{ST/TM\text{-}D9K/CYT}$ dimerising to a higher, almost identical level. The level of dimerisation of PD-1_{EX}CD$3\zeta_{ST/TM/CYT}$, PD-1_{EX}CD$3\zeta_{ST/TM\text{-}D9E/CYT}$ and PD-1_{EX}CD3- $\zeta_{ST\text{-}D9K/TM/CYT}$ is equal or lower than that seen for the PD-1_{EX}CD$3\zeta_{ST/TM\text{-}D9E}CD28_{CYT}$ and PD-1_{EX}CD$3\zeta_{ST/TM\text{-}D9K}CD28_{CYT}$ constructs which also were not stimulated by PD-1 mAbs indicating that reduced dimerisation could be a factor in the weak stimulatory potential of the constructs.

4.3.7 Stimulation of the PD-1_{EX}CD$28_{TM/CYT}$ cell line by cross-linking

While T cell activation was observed in a dimeric PD-1 chimera, evidence suggests that the stimulation seen in the PD-1_{EX}CD$3\zeta_{ST/TM}$CD28_{CYT} cell line is due to association with the TCR complex. The reason for the absence of mAb induced signalling through monomeric PD-1_{EX}CD$28_{TM/CYT}$ may be due the function of the CD28 cytoplasmic tail, but it also may be due to the absence of mAb cross-linking. The concentra-

tion dependent activation observed in CD28 chimeric cell lines when stimulated with superagonists suggests a role for antibody cross-linking in CD28 superagonism. A propensity for cross-linking and lattice formation by CD28 superagonists have been proposed as mechanisms for superagonism by Hunig *et al.* (2005) and Dennehy *et al.* (2006) [219, 285]. If cross-linking is an important component of CD28 signalling or CD28 superagonism, the monomeric PD-1_{EX}CD$28_{TM/CYT}$ would be expected to be inactive because it is unable to form a cross-linked lattice at any mAb concentration due to its monomeric nature. To investigate if PD-1_{EX}CD$28_{TM/CYT}$ hybridoma activation could be observed by cross-linking the chimera with PD-1 mAbs, two PD-1 mAbs with distinct non-overlapping epitopes (mAbs 10 and 19) were cross titrated together in the same stimulation (Figure 4.19). At a nanogram range of PD-1 mAb concentration, the level of IL-2 induced was low and equivalent to that observed in unstimulated cells.

However, when the concentration of PD-1 mAb 10 was increased to the microgram range, IL-2 levels increased significantly. When stimulated with 10μg/ml mAb 10 and any concentration of mAb 19, the IL-2 induction increased 5-fold, but at all concentrations of mAb 19 the IL-2 level reduced at 100μg/ml mAb 10. Cross-linking of PD-1_{EX}CD$28_{TM/CYT}$ with PD-1 mAbs therefore clearly has a stimulatory effect on the T cell hybridoma system, but the levels of activation are significantly lower than those observed for CD28 superagonist antibodies. The dependence of activation on the concentration of mAb 10 indicates that the concentration of this antibody is the critical factor in any cross-linking or other mechanism causing the observed activation. This suggests that the absence of activation using single PD-1 mAb stimulation is in part

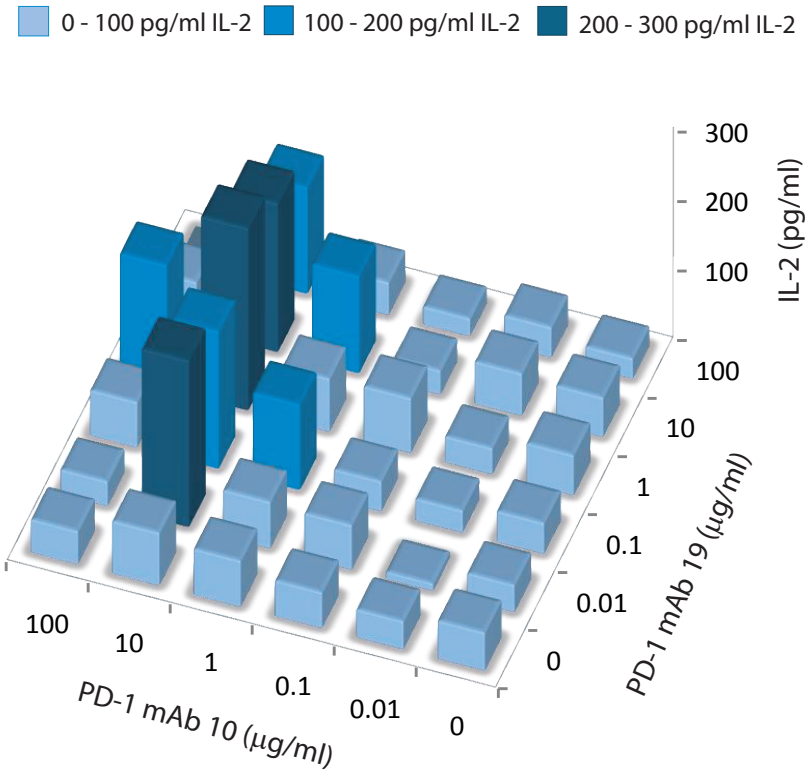


Figure 4.19: Stimulation of the PD-1_{EX}CD$28_{TM/CYT}$ cell line with titrations of PD-1 mAbs 10 and 19. DO11.10 hybridomas expressing PD-1_{EX}CD$28_{TM/CYT}$ were incubated with titrations of PD-1 mAb 19 (from 100μg/ml to 0μg/ml) and PD-1 mAb 10 (from 100μg/ml to 0μg/ml). Cells were incubated in donkey anti-mouse IgG antibody coated (500μg/ml) 96 well plates for 48 hours before tissue culture supernatant was assayed for IL-2 by ELISA.

due to the inability of PD-1 monomers to form mAb cross-linked complexes.

4.4 Discussion

4.4.1 Summary of findings

This chapter describes work performed to successfully recreate an assay for CD28 superagonism which, using a chimeric CD28 hybridoma cell line, was able to show the mitogenic effects of CD28 superagonistic mAbs *in vitro*. To enable the investigation of potentially agonistic PD-1 mAb the chimeric hybridoma cell line strategy used in the CD28 superagonist assay was then adapted to create an assay which could use a stimulatory outcome to identify and investigate PD-1 agonist mAbs. Using a cell line expressing the monomeric PD-1_{EX}CD$28_{TM/CYT}$ chimera, low levels of activation were observed, but only in the presence of two PD-1 mAbs and in the correct concentration that encouraged cross-linking of the chimeric protein. Efforts to produce a dimeric PD-1 resulted in the generation of a number of chimeric cell lines, of which one, expressing the weakly associating dimer PD-1_{EX}CD$3\zeta_{ST/TM}$CD28_{CYT}, was successfully stimulated by PD-1 mAbs. Investigation into the signalling of the PD-1_{EX}CD$3\zeta_{ST/TM}$CD28_{CYT} cell line showed that, although it contained a CD28 signalling domain, the presence of a CD3ζ transmembrane domain caused an association with the TCR/CD3 complex, an association that influenced its ability to trigger an IL-2 response.

4.4.2 Applications of the CD28 superagonism assay

To investigate if the principles of CD28 superagonistic mAbs can be applied to other T cell signalling molecules, an assay must be available to identify agonists. The work in

this chapter re-establishes an *in vitro* assay that has been used elsewhere to illustrate the mitogenic action of superagonistic CD28 antibodies [184]. This assay was then used to study PD-1 mAb agonism by a group of PD-1 mAbs. The use of a common signalling domain (mouse CD28) in both the successful CD28 and PD-1 assays allows for a common assay result for two molecules which, when stimulated in their native environment, would otherwise effect very different outcomes. The use of chimeric signalling molecules may lead to the development of further assays which can identify mAbs with agonistic characteristics to other T cell signalling molecules.

4.4.3 The identification of correctly processed and presented cell surface proteins

Confocal microscopy, BRET and flow cytometry analysis were all used to ascertain if the chimeric proteins designed and expressed in this chapter were correctly presented at the cell surface. Confidence in correct cell surface presentation can then be transferred to the signalling ability of a given chimera. Through the use of these methods it was hoped that confidence could be gained in their ability to act as functional signalling molecules and understanding of the mechanisms of activation could be gleaned. Each method alone can give insightful results as to the expression of a chimeric protein, but it is only by using all methods that the expression can be fully understood. This is illustrated in the case of CTLA-4, which was used as both a control for intracellular localisation and dimerisation. If evidence collected from confocal microscopy analysis alone was used to assess the presentation of CTLA-4, a conclusion of intracellular aggregation could be made due to the intracellular localisation.

But BRET analysis shows that it forms efficient dimers on the intracellular membranes where it is stored, suggesting correct expression. Without the further knowledge that the majority of CTLA-4 is stored in the intracellular compartment until T cell activation [114,289], each result alone could have led to erroneous conclusions, but together they allow a better understanding of the expression of the protein.

4.4.4 Strategies for the formation of dimeric chimeras

Through the expression of monomeric and then dimeric chimeras the roles of dimerisation and mAb cross-linking in CD28 superagonistic and PD-1 agonistic signalling were investigated. A number of methods were chosen to create dimeric chimeras that would enable the assaying of the PD-1 mAbs. Some of the approaches used, such as the inclusion of the CD3ζ transmembrane domain, were successful in creating dimeric molecules capable of signalling when stimulated with PD-1 mAbs. However, a number of domains that were fused to the PD-1 extracellular or CD28 cytoplasmic domains destabilised the resulting proteins, preventing either correct signalling or processing in the intracellular compartment. In the case of $PD1_{EX}CTLA4_{ST}CD28_{TM}CJun_{ZIP}CD28_{CYT}$, the combination of the CTLA-4 stalk and the placement of a leucine zipper at the C-terminus of the CD28 cytoplasmic domain seemed to be particularly disastrous for expression.

In some chimeras, the insertion of domains to induce dimerisation not only affected protein stability but may also have affected a chimera's signalling potential. The results suggest that the placement of a leucine zipper at the N- terminus of the CD28 cytoplasmic domain is a destabilising factor for a chimeric protein (as observed in both

PD-1_{EX}CD28_{TM}CJun$_{ZIP}$CD28_{CYT} and PD1_{EX}CTLA4_{ST}CD28_{TM}CJun$_{ZIP}$CD28_{CYT}) but, when placed at the C-terminus of the cytoplasmic domain, as seen in PD-1_{EX}CD$28_{TM/CYT}$ CJun$_{ZIP}$, it induces the formation of a strong chimeric dimer. Despite the strong dimerisation observed, this chimera did not signal when stimulated with PD-1 mAbs. A likely reason for this is that the position of the leucine zipper in PD-1_{EX}CD$28_{TM/CYT}$ CJun$_{ZIP}$ could bring together the two CD28 signalling domains in a way not seen in wildtype CD28. This may reduce or prevent access of cytoplasmic elements to the CD28 signalling domains needed for the initiation of signalling. This example shows that in the design of chimeric molecules, the effect of each structural element should be considered, to achieve the expression of a well folded and functional chimera.

Chapter 5

Structural correlates of CD28 superagonism

5.1 Introduction

5.1.1 The mechanism of CD28 superagonism

Despite recent research investigating the signalling and wider immune effects of superagonistic CD28 mAbs [228, 231, 301, 302], the mechanism by which they initiate T cell activation through CD28 is not fully understood. To fully explain their action, a mechanism has to account for two major characteristics of CD28 superagonists as observed in human, mouse and rat CD28 mAbs. Firstly, a superagonist mAb can be differentiated from non-mitogenic mAbs by its membrane proximal epitope, and secondly, superagonist mAbs are not active in solution and require immobilisation to show mitogenic activity [218, 219]. A variety of mechanisms have been proposed to explain the mitogenic actions of CD28 superagonists, which include the preferential engagement of signalling competent CD28 [218], differential cross-linking [219], mAb induced CD28 conformational changes [303] and epitope dependent size exclusion of phosphatases [153]. All of the suggested mechanisms give the epitope topology of CD28 superagonists a key role in the mechanism, but only the epitope dependent size exclusion of phosphatases by CD28 superagonist mAbs, as explained using the kinetic

segregation model, also explains the requirement of immobilisation.

5.1.2 Methods for the investigation of the mechanism of CD28 superagonism

Through the generation and characterisation of mAbs with membrane proximal epitopes to another T cell signalling molecule (PD-1), it was hoped to show that epitope location alone could be used to predict mAb agonism using a chimeric PD-1/CD28 signalling system established in Chapter 4. While agonism was observed within a chimeric PD-1/CD3ζ system, we were unable to create a PD-1/CD28 dimer which could signal "natively" through the CD28 pathway. A signalling effect was observed in a cell line expressing a monomeric PD-1/CD28 chimera (PD-1_{EX}CD$28_{TM/CYT}$), but only when cross-linked with two PD-1 mAbs with discrete epitopes. The signalling observed suggests that mAb cross-linking plays a role in mAb initiated CD28 signalling.

This chapter details a study of superagonism that asks whether epitope location is the most important factor in the mechanism of CD28 superagonism. Recombinant CD28 molecules with increased dimensions were created to investigate the effects of moving a CD28 superagonistic epitope further away from the cell membrane. Using the hybridoma stimulation assay, developed and described previously (see Section 4), the effect of this size change on the activity of CD28 superagonist mAbs was tested.

5.2 Materials and methods

5.2.1 Generation of constructs

All recombinant constructs were created using multi-step chimeric PCR and molecular cloning methods as described in Section 2 and all oligonucleotides used to produce the constructs in this chapter are listed in Table 5.1. Each construct was designed to contain a 5′ rat CD4 ribosomal binding sequence and also contain unique 5′ and 3′ restriction endonuclease sites that allowed the sub-cloning of completed constructs into a variety of expression vectors.

rCD28$_{EX}$mCD28$_{TM/CYT}$L#X

To create a form of CD28 with an extended stalk the existing pCR®4-TOPO®-rCD28$_{EX}$ mCD28$_{TM/CYT}$ vector was used as a template. In the first construct created (rCD28$_{EX}$ mCD28$_{TM/CYT}$L#0), the stalk region of CD28 (amino acids 120-132 of the mature rCD28 peptide) was removed and a *Sal*I restriction site inserted in its place. The oligonucleotides 985 and 988 were used to amplify the extracellular domain of rat CD28. This created a PCR product encoding a *Bgl*II restriction site, rat CD4 ribosome binding domain, amino acids 1-120 of rat CD28, and a *Sal*I site fused to the first six amino acids of the mouse CD28 transmembrane domain.

Construct	Oligo Name	Number	Primer Sequence	Restriction
rCD28$_{EX}$mCD28$_{TM/CYT}$L#X	rCD28-BglII-5′	985	TAGTAGAGATCTCTCAAGCAGGCCACCATGACGCTCA GGCTGCTATTCTTGGCT	*Bgl*II
	mCD28-Mlu-stp-Xho1-stp-3′	986	TTTGCAGCGTACCGCCCCACGCGTTAGTAGCTCGAGT AGTAG	*Mlu*I + *Xho*I
	rCD28-SalI-mCD28-5′	987	ATTATTCACATCAAGGAGGTCGACTTTTGGGCGCTGG TCGTG	*Sal*I
	rCD28-SalI-mCD28-3′	988	CACGACCAGCGCCCAAAAGTCGACCTCCTTGATGTGA ATAAT	*Sal*I
	rCD28-C123-5′	—	TCGAGAAACATCTTTGTCATGCTCAGACGTCTCCTAA GCTGG	*Xho*I + *Sal*I
	rCD28-C123-3′	—	TCGACCAGCTTAGGAGACGTCTGAGCATGACAAAGAT GTTTC	*Sal*I + *Xho*I
rCD28hFc$_{EX}$mCD28$_{TM/CYT}$	rCD28-BglI-5′	—	TAGTAGAGATCTCTCAAGCAGGCCACCATGACGCTCA GGCTGCTATTCTTGGCT	*Bgl*II
	rCD28-hIgG-5′	2103	GCTCAGACGTCTCCTAAGCTGGAGCCCAAATCTAGTG ACAAAACTCACACATCGCCACCGTCGCCAGCACCTGA ATTCG	—
	rCD28-hIgG-3′	2104	CGAATTCAGGTGCTGGCGACGGTGGCGATGTGTGAGT TTTGTCACTAGATTTGGGCTCCAGCTTAGGAGACGTC TGAGC	—
	hIgG-mCD28-5′	2101	CCCTGTCTCCGGGTAAACTGTTTTGGGCACTGGTCGT GG	—
	hIgG-mCD28-3′	2102	CCACGACCAGTGCCCAAAACAGTTTACCCGGAGACAG GG	—
	mCD28-Mlu-stp-Xho1-stp-3′	986	TTTGCAGCGTACCGCCCCACGCGTTAGTAGCTCGAGT AGTAG	*Mlu*I + *Xho*I

Table 5.1: Oligonucleotide primers used to produce the constructs detailed in this chapter

The mouse transmembrane and cytoplasmic domains of mouse CD28 were amplified with the oligonucleotides 987, which is the complementary sequence of 988, and 986. This amplified amino acids 114-120 of the rat CD28 extracellular domain, a *Sal*I site, the mouse transmembrane and cytoplasmic domain of mouse CD28 fused to a *Mlu*I and a *Xho*I restriction site separated by a stop codon. The overlapping PCR products created in these reactions were used as template in the subsequent chimeric PCR that created the full length construct. Freshly made $rCD28_{EX}mCD28_{TM/CYT}$L#0 was TOPO® cloned into the pCR®4-TOPO® vector and the sequence verified.

To re-insert the stalk region back into rmCD28L#0 the oligonucleotides rCD28-C123-5′ and rCD28-C123-3′ were designed. They are complementary oligonucleotides that encode the twelve amino acid stalk region of rat CD28 and have *Xho*I and *Sal*I compatible ends at their 5′ and 3′ ends respectively. rCD28-C123-5′ and rCD28-C123-3′ were first treated with T4 polynucleotide kinase in the following reaction.

	Company	Conc^{n}.	Volume
Ligase buffer	New England Biolabs	10 ×	1.0μl
T4 polynucleotide kinase	New England Biolabs	10 U/μl	1.0μl
ddH_2O	Sigma	—	4.5μl
Oligonucleotide	Sigma-Genosys	100 μM	2.5μl

This reaction was run using a DNA Engine Tetrad (RJ Research) on the following programme.

Step	Temp.(°C)	Time
1	37	1 hr
2	95	2 min
3	25	10 min

T4 polynucleotide kinase adds a phosphate group to the 5′ end of the oligonucleotides allowing them to be ligated after the following annealing step. The oligonu-

cleotides were annealed by mixing equal amounts of each complementary oligonucleotide and incubating them at the following temperatures and the annealed rCD28-C123 fragment was stored on ice prior to ligation.

Step	Temp.(°C)	Time
1	95	2 min
2	65	10 min
3	37	10 min
4	25	5 min

The vector pCR®4-TOPO®-rCD28$_{EX}$mCD28$_{TM/CYT}$L#0 was digested with *Sal*I and ligated to the annealed and kinased rCD28-C123. The ligation reactions were transformed and, to estimate the number of stalk units inserted into the pCR®4-TOPO®-rCD28$_{EX}$mCD28$_{TM/CYT}$L#0 vector, resultant clones were PCR screened using the oligonucleotides 985 and 986. To confirm the number stalks inserted into the vector, the constructs were sequenced. Constructs containing single and multiple inserts were sub-cloned into the lentiviral vector pHR-SIN-BX-IRES-EM using *Bgl*II and *Xho*I.

rCD28hFc$_{EX}$mCD28$_{TM/CYT}$

The rCD28hFc$_{EX}$mCD28$_{TM/CYT}$ construct was created in a series of five steps. In the first step, the oligonucleotide 985 was used in a PCR with oligonucleotide 2104. 2104 encodes the last seven residues of the rat CD28 extracellular domain (up to residue 150 of the mature polypeptide), followed by 58 bases encoding the human IgG1 Fc hinge, CH_2 and CH_3 domains. Residues 102, 108 and 111 of the mature human IgG Fc region were mutated from cysteines to serines. In the second step, the complementary oligonucleotide to 2104, 2103, was used in a PCR reaction with 2102 which encodes the COOH-terminal end of the transmembrane region of human IgG Fc, followed by

the first 19 bases encoding the NH2-termincal end of the mouse CD28 cytoplasmic domain. In the third step, the purified reaction products of steps one and two were used as templates in a chimeric PCR reaction using oligonucleotides 985 and 2102 to create a sequence encoding the extracellular region of CD28 fused with the human IgG Fc hinge, CH_2 and CH_3 domains. In step four, the oligonucleotide 2101, the complementary oligonucleotide to 2102, was used in a PCR reaction with 986 to amplify the mouse CD28 cytoplasmic domain. The purified product of this reaction was fused to the rCD28/hFc sequence in a chimeric PCR reaction using oligonucleotides 985 and 986. The product of this reaction was gel purified and cloned into pCR®4-TOPO®. The rat and mouse CD28 were amplified using pCR®4-TOPO®-rmCD28 as a template. The human IgG Fc was amplified from HuCD44FLFc, a gift from Dr Neale Banerji of the MRC Human Immunology Unit, The Weatherall Institute of Molecular Medicine, Oxford University.

The completed and sequenced rCD28hFc$_{EX}$mCD28$_{TM/CYT}$ construct was sub-cloned from the pCR®4-TOPO®-rCD28$_{EX}$mCD28$_{TM/CYT}$ sequencing vector into pHR-SIN-BX-IRES-EM using the restriction endonucleases BglII and *Xho*I and the BRET vectors pGFP^2-N3 and pRluc-N3 using *Bgl*II and *Bam*HI.

5.2.2 Generation of hybridoma cell lines

HEK-293T cells were transfected with a pHR-SIN-BX-IRES-EM vector either encoding rCD28$_{EX}$mCD28$_{TM/CYT}$L#X or rCD28hFc$_{EX}$mCD28$_{TM/CYT}$, along with the vectors p8.91 and pMDG. Each transfection mix was created by adding 3μl GeneJuice® transfection

reagent (Novagen, Merck) drop wise to 100μl DMEM (Sigma). After gentle mixing and incubation at room temperature for 5 minutes, 1μg of each appropriate vector was added. The reactions were gently mixed again and left for 30 minutes for the transfection complexes to form. The transfection reactions were added directly to 6×10^5 HEK-293T cells at 60-80% confluency. After 72 hours, the cell culture supernatant containing the lentivirus was harvested, microfuged at 13,000rpm for 5 minutes to remove cell debris and added to 1×10^5 DO11.10 T cell hybridomas. DO11.10 cells were maintained and propagated in JMEM until they reached a density of 1×10^6, at which point they were assayed for surface construct and emGFP expression using flow cytometry. Hybridomas were probed for construct surface expression using the rat CD28 monoclonal antibody JJ319 (eBioscience Ltd). Donkey anti-mouse AlexaFluor®647 (Molecular Probes, Invitrogen) was used as a secondary conjugate. To obtain a homogenus population of cells expressing transduced proteins, cells were fluorescence-activated cell sorted (FACS sorted) for both emGFP expression and JJ319 staining.

5.2.3 BRET

For use in the BRET assay both rmCD28L#*X* and rCD28/hFc/mCD28 were subcloned into pGFP²-N3 and pRluc-N3 using the restriction endonucleases BglII and *Mlu*I. These vectors were transfected into HEK-293T cells and the oligomerisation of the constructs assayed using in the BRET assay as outlined in Section 2.5.

5.2.4 Confocal microscopy

To visualise protein expression at the cell surface the chimeric proteins in the pGFP^2-N3 vector were transiently expressed in HEK-293T cells grown on coverslips. This vector fuses GFP^2 to the C-terminus of the expressed protein allowing visualisation of fusion proteins when excited at 488nm. 1μg/ml of vector 24 hours post transfection the cells were mounted on slides and illuminated through an oil immersed 60x objective by light filtered in a channel of 515$\pm$15nm. For more information of the method used see Section 2.4.2. To obtain the average cell surface expression score, transfected cells were observed and the level of cell surface expression of the GFP fusion chimeras was scored. A minimum of twenty cells were scored between one and five for each transfected construct. A score of one was given to cells in which the construct was visualised at the cell surface only, whereas a score of five was given to cells which showed the highest levels of chimeric intracellular localisation. The average score for the cells was then calculated as the average cell surface expression score.

5.2.5 Surface plasmon resonance

All surface plasmon resonance (SPR) experiments were performed using a BIACORE 3000® machine, BIAcore software and reagents (GE Healthcare UK Ltd.).

Experiments were performed using CM5 sensor chips (research grade) at 25°C in the running buffer HBS (10mM HEPES ph4.7, 150mM NaCl, 2mM EDTA, 0.005% surficant P-20), buffer premixed from BIAcore (GE Healthcare UK Ltd.). BAFF-R/human IgG1 Fc fusion protein (BAFFR/Fc) and CD40/human IgG1 Fc fusion protein (CD40/Fc)

were kind gifts from Dr. Neale Banarji (Human Immunology Unit, The Weatherall Institute of Molecular Medicine, Oxford University). CTLA-4-FcHis was produced by Heather Walsh (Human Immunology Unit, The Weatherall Institute of Molecular Medicine, Oxford University). For further details of SPR methods used see Section 3.2.5.

5.2.6 Antibody stimulation assay

DO11.10 cell lines expressing chimeric proteins were used in an antibody stimulation assay as follows. 96-well flat bottomed plates (Costar EIA/RIA plates) were coated overnight with 500μg/ml donkey anti-mouse IgG (H+L) (Jackson Immunoresearch) in coating buffer (15mM Na_2CO_3, 35mM $NaHCO_3$, pH 9.6) at 4°C. In CD3 stimulation assays, plates coated with donkey anti-mouse were washed three times with 200μl chilled PBS, and then additionally coated with 3μg/ml KT-3 in coating buffer. Prior to cell loading the plates were washed three times with 200μl chilled PBS. Stimulating antibodies were added to 5×10^5 DO11.10 cell line cells per well in JMEM media for 20 minutes. Cells were plated out in triplicate on coated plates. Cell culture supernatants were removed after 48 hours at 37°C, 5% CO_2 and assayed for mouse IL-2. Antibodies used for the stimulation of cell lines were anti-rat CD28 JJ319 and JJ316 mAb (eBioscience Ltd), and anti-mouse IgG1 mAbs HP6091 (AdB Serotec) and A57H (AdB Serotec) and F890 (A kind gift from Dr John Young, Institute of Animal Health, Compton, Berkshire, UK). The rCD28hFc$_{EX}$mCD28$_{TM/CYT}$ hybridoma cell line was also stimulated with the isotype contols MOPC-21 (Mr.Alistair Waugh, Human

Immunolgy Unit, Weatherall Institute of Molecular Medicine, University of Oxford), MM-30 (Abcam), MG2a-53 (Abcam).

5.2.7 ELISAs

The levels of mouse IL-2 were measured in supernatants obtained in the antibody stimulation assay, using DuoSet mouse IL-2 ELISA (R&D Systems). The method used is outlined in Chapter 4. The binding of donkey anti-mouse IgG to mouse anti-human IgG1 Fc mAbs was assayed by sandwich ELISA. First 96-well flat bottomed plates (Costar EIA/RIA plates) were coated with 500μg/ml donkey anti-mouse IgG (H+L) (Jackson Immunoresearch) in coating buffer (15mM Na_2CO_3, 35mM $NaHCO_3$), pH 9.6), sealed and incubated overnight at 4°C. Each well was aspirated and washed three times with 400μl wash buffer (0.05% Tween®20 in PBS with 0.05% NaN_3) before 200μl block buffer (1% casein (VWR BDH Prolabo) in PBS with 0.05% NaN_3) was added and the plates sealed. After a 30 minute incubation with block buffer, at 4°C, the wells were again aspirated and washed three times with 400μl wash buffer. 50μl of 10-fold dilutions (from 10μg/ml to 0.01μg/ml) of mAbs JJ319, A57H, HP6091, F890 and a mouse IgM control (MM-30, Abcam, Cambridge, UK) in DMEM were added to the plates in duplicate, sealed and incubated at 4°C for 2 hours. Wells were aspirated and washed three times with 400μl wash buffer. The secondary antibody, anti-mFAB peroxidise conjugate (Sigma), was added at 50μl per well pre-diluted 1/3000 with DMEM without FCS. Plates were sealed and incubated at 4°C for 1 hour. Wells were aspirated and washed three times with 400μl wash buffer before the addition of 100μl fresh

substrate (2,2′-Azino-bis(3-Ehtylbenzthiazoline-6-sulfonic acid) (ABTS) tablet (Sigma) dissolved in 0.05M phosphate-citrate buffer (27.7ml 0.2M anhydrous HNa_2PO_4 and 24.3ml 0.1M citric acid made up to 100ml with deionised water) with 25μl 30% H_2O_2 added immediately prior to use. Plates were stored in the dark for 20 minutes before the optical density of each well was recorded using a Fusion microplate analyser (PerkinElmer) at 515nm. The duplicate readings for each sample were averaged and standard deviation calculated.

5.3 Results

5.3.1 Manipulation of the CD28 stalk region in a rat/mouseCD28 chimera prevents expression

Two approaches were used to attempt to increase the dimensions of CD28. The first was to create a construct that contained multiple repeats of the rat CD28 extracellular stalk region (Figure 5.1). This strategy, of incrementally increasing the distance between the cell membrane and CD28, could allow the role of epitope location on CD28 superagonism to be investigated without altering the V-set domain of CD28. The initial construct, $rCD28_{EX}mCD28_{TM/CYT}$L#0, was designed so that the twelve amino acid stalk region of extracellular rat CD28 was removed and replaced with a *Sal*I restriction endonuclease site. To restore and increase the dimensions of CD28, multiple copies of the stalk were inserted into this restriction site using the oligonucleotide rCD28-C123 (Figure 5.1). rCD28-C123 contains a 5′ *Xho*I and 3′ *Sal*I restriction site that means that

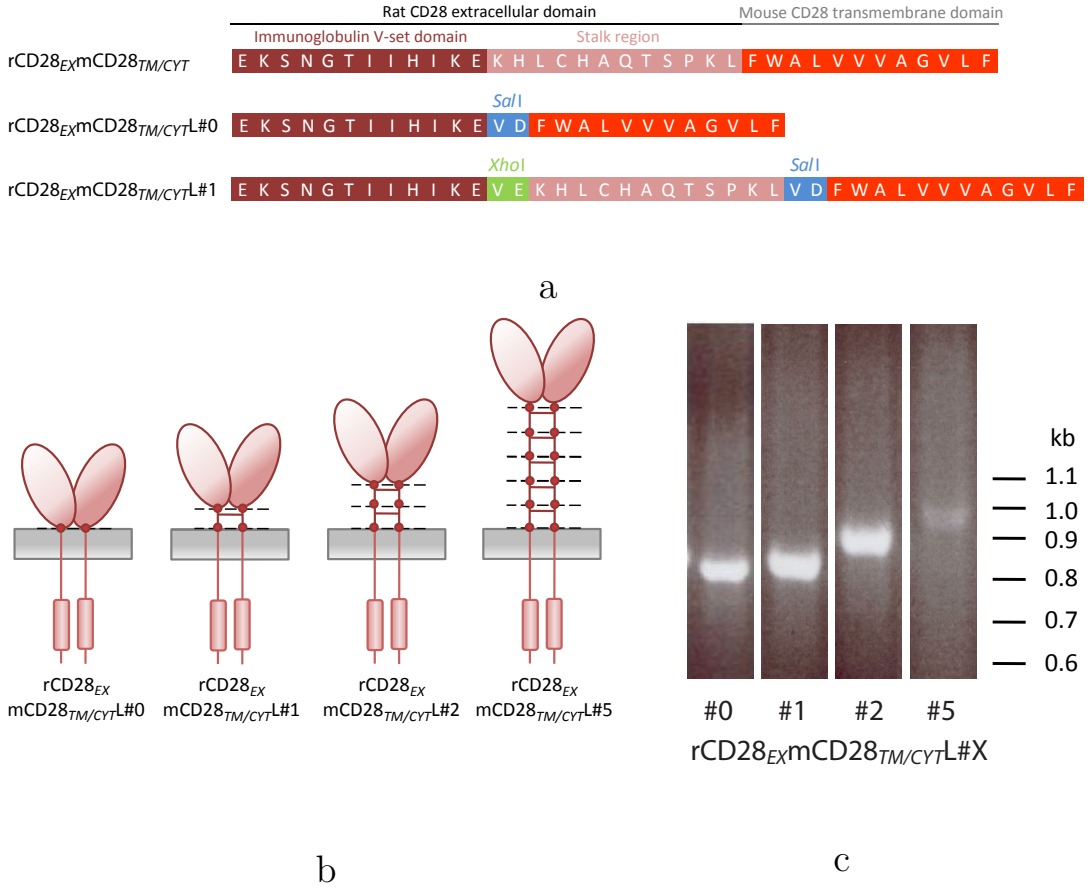


Figure 5.1: The construction of the rCD28$_{EX}$mCD28$_{TM/CYT}$L#X constructs. (a) A representation of the rCD28$_{EX}$mCD28$_{TM/CYT}$, rCD28$_{EX}$mCD28$_{TM/CYT}$L#0 and rCD28$_{EX}$mCD28$_{TM/CYT}$L#1 protein sequence at the fusion junction of the CD28 extracellular and transmembrane domain to illustrate the position of restriction endonuclease site insertions. The extracelluar domain is represented by last twelve residues of the rat CD28 immunoglobulin V-set domain of the CD28 and the twelve residues which comprise the rat CD28 stalk region (maroon and pink respectively). The first twelve residues of the mouse CD28 cytoplasmic domain is represented in red. The insertion of restriction sites in the rCD28$_{EX}$mCD28$_{TM/CYT}$L#X constructs are coloured blue (*SalI*) and green (*XhoI*). (b) Schematic representations of the constructs rCD28$_{EX}$mCD28$_{TM/CYT}$L#0, rCD28$_{EX}$mCD28$_{TM/CYT}$L#1, rCD28$_{EX}$mCD28$_{TM/CYT}$L#2 and rCD28$_{EX}$mCD28$_{TM/CYT}$L#5 which contain 0, 1, 2 and 5 repeats of the twelve residue stalk extracellular region of rat CD28 respectively. (c) PCR products of 811bp, 847bp, 883bp and 991bp produced from the amplification of the constructs rCD28$_{EX}$mCD28$_{TM/CYT}$L#0, rCD28$_{EX}$mCD28$_{TM/CYT}$L#1, rCD28$_{EX}$mCD28$_{TM/CYT}$L#2 and rCD28$_{EX}$mCD28$_{TM/CYT}$L#5 respectively. The rCD28$_{EX}$mCD28$_{TM/CYT}$L#X constructs in pCR®4-TOPO®were PCR screened for the addition of stalk units using the oligonucleotides M13F and M13R. The resultant products were run on a 1% agarose gel.

once annealed, the 3′ end of the oligonucleotide can be re-digested whereas the 5′ sequence cannot. This design allows the addition of extra stalk regions into a construct sequentially if required. The initial ligation of the oligonucleotide rCD28-C123 into *Sal*I digested rCD28$_{EX}$mCD28$_{TM/CYT}$L#0 resulted in the insertion of one, two and five stalk units into *Sal*I, which were amplified and visualized on an agarose gel (Figure 5.1). Confirmation of the number of inserts and the correct orientation of the inserted units was performed by sequence analysis.

The rCD28$_{EX}$mCD28$_{TM/CYT}$L#X constructs were first expressed in HEK-293T cells using the pGFP^2-N3 vector to check for successful expression at the cell surface. When probed for rat CD28 expression, none of the rCD28$_{EX}$mCD28$_{TM/CYT}$L#X constructs were found to be expressed at the cell surface (Figure 5.2). To assess if the fusion of GFP^2 to the C-terminus of the constructs, which occurs in the pGFP^2-N3 vector, affected the expression of the different forms of CD28, the constructs were also transiently expressed in the vector pHR-SIN-BX-IRES-EM which expresses the native construct alone. When expressed in this vector, all four constructs also failed to be detected at the cell surface by flow cytometry when probed with rat CD28 mAb (results not shown). The absence of expression found for the restored rCD28$_{EX}$mCD28$_{TM/CYT}$L#1 as well as rCD28$_{EX}$mCD28$_{TM/CYT}$L#0 suggests that the insertion of restriction sites around the stalk sequence is responsible for the lack of expression of these forms of CD28.

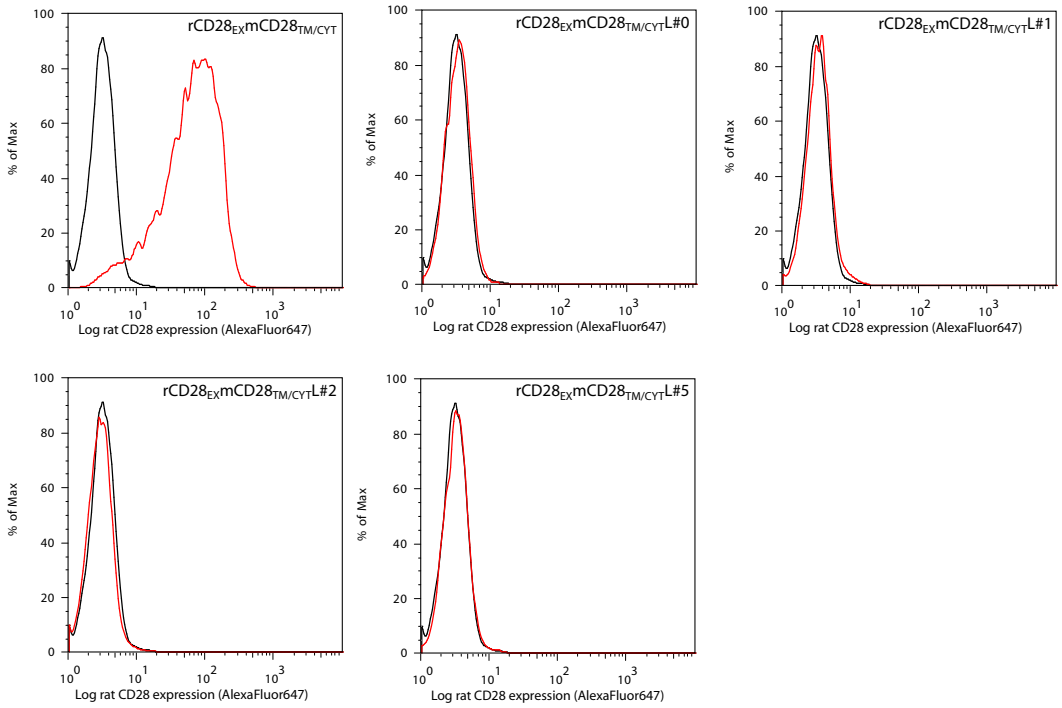
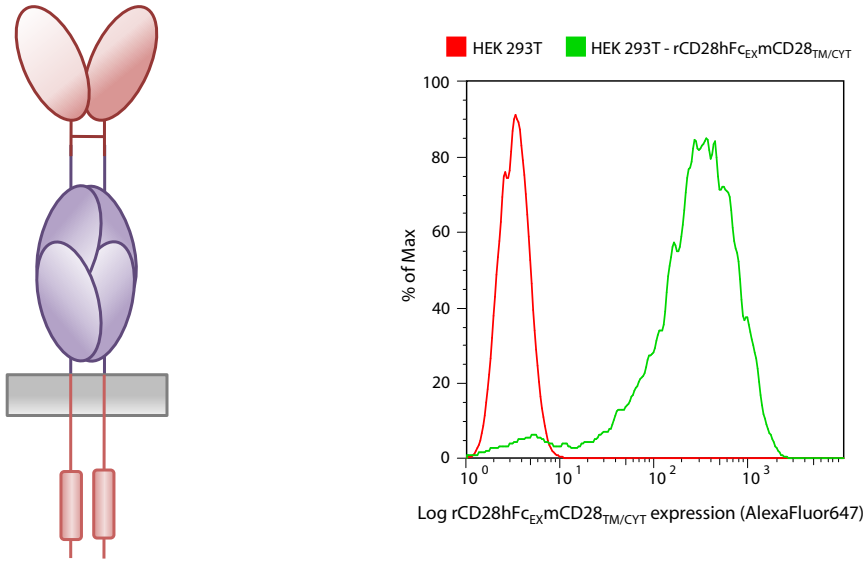


Figure 5.2: CD28 constructs rCD28$_{EX}$mCD28$_{TM/CYT}$L#0, rCD28$_{EX}$mCD28$_{TM/CYT}$L#1, rCD28$_{EX}$mCD28$_{TM/CYT}$L#2 and rCD28$_{EX}$mCD28$_{TM/CYT}$L#5 do not express at the cell surface. HEK-293T cells were transfected with the pGFP^2-N3-rCD28$_{EX}$mCD28$_{TM/CYT}$L#X constructs and rCD28$_{EX}$mCD28$_{TM/CYT}$. After 24 hours, transfected (red) and untransfected (black) control HEK-293T cells were assayed for CD28 expression using flow cytometry. Cells were probed with rat CD28 antibody JJ319 at and the secondary antibody donkey anti-mouse AlexaFluor®647. Cells were gated for GFP expression and AlexaFluor®647 to identify transfected cells and CD28 surface expression

5.3.2 Expression of CD28 lengthened by the insertion of a IgG Fc

The failure of rCD28$_{EX}$mCD28$_{TM/CYT}$L#X to express at the cell surface indicates that manipulation of the stalk region of CD28 can lead to protein instability, therefore a second approach to increase the dimensions of CD28 was used. Previously, soluble forms of CD28 have been successfully expressed as a CD28/IgG Fc fusion protein [184, 304, 305]. The human Fc/CD28 fusion constructs used by Greene *et al.* (1996) [304] and Brodie *et al.* (2000) [305] were shown to successfully ligate to the natural ligands of CD28, CD80 and CD86, by SPR analysis. Also the structure of human CD28 in complex with a superagonist mAb was successfully solved using a form of CD28 initally expressed as a Fc fusion protein [184]. The successful ligand binding shown by these fusions suggests that the fusion of an Fc domain to has no adverse effect on the Ig V-set domain of CD28. With this in mind, the chimeric construct rCD28hFc$_{EX}$mCD28$_{TM/CYT}$ was created (Figure 5.3). Like the soluble CD28/Fc proteins described above, rCD28hFc$_{EX}$mCD28$_{TM/CYT}$ fused the extracellular domain of rat CD28 to the hinge, CH_2 and CH_3 domains of human IgG1. But, unlike the soluble CD28/Fc fusions, in rCD28hFc$_{EX}$mCD28$_{TM/CYT}$ the C-terminus of the IgG1 CH_3 domain is fused to the transmembrane and cytoplasmic domain of mouse CD28. This creates a chimeric CD28 protein in which the CD28 V-set Ig domain is not only separated from the membrane by its own stalk but also a human Fc domain.

As used to investigate the expression of chimeric PD-1 cell surface proteins (Chapter 4), a combination of three methods (flow cytometry, confocal microscopy and BRET) were used to examine the cell surface expression of rCD28hFc$_{EX}$mCD28$_{TM/CYT}$.



a b

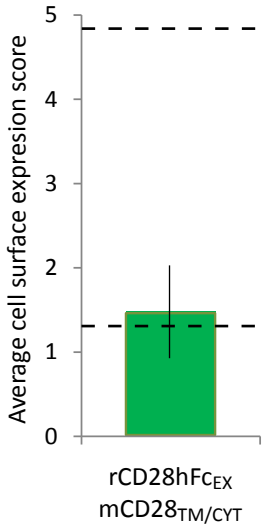
Figure 5.3: Construction and transient expression of rCD28hFc$_{EX}$mCD28$_{TM/CYT}$. (a) Schematic representation of the construct rCD28hFc$_{EX}$mCD28$_{TM/CYT}$. (b) Flow cytometry analysis of transient expression of rCD28hFc$_{EX}$mCD28$_{TM/CYT}$. rCD28hFc$_{EX}$mCD28$_{TM/CYT}$ was transiently expressed in HEK-293T cells in the pGFP^2-N3 vector. Cells were probed for rat CD28 using anti-rat CD28 mAb JJ319 and an anti-mouse AlexaFluor®647 secondary conjugate. Transfected cells were identified by first gating for GFP followed by gating for CD28 expression.

When probed for CD28 expression, HEK-293T cells transiently transfected with rCD28 $hFc_{EX}mCD28_{TM/CYT}$ in the vector $pGFP^2$-N3, showed high levels of expression at the cell surface (Figure 5.3). This was confirmed using confocal microscopy analysis. Transient $pGFP^2$-N3-$rCD28hFc_{EX}mCD28_{TM/CYT}$ expression in HEK-293T cells showed that $rCD28hFc_{EX}$ $mCD28_{TM/CYT}$ was expressed at the cell surface at levels close to those recorded for wild type human CD28 (Figure 5.4). The clear expression at the cell surface and absence of cytoplasmic localisation suggests that $rCD28hFc_{EX}mCD28_{TM/CYT}$ is processed efficiently within the cellular compartment and is readily presented at the cell surface.

Based on the protein sequence used by Greene *et al.* (1996) to successfully express soluble CD28/Fc, three cysteine residues were removed from human IgG1 hinge domain in $rCD28hFc_{EX}mCD28_{TM/CYT}$. These cysteines are essential for the dimerisation of immunoglobulin heavy chain [306] and their removal may influence the formation of $rCD28hFc_{EX}mCD28_{TM/CYT}$ as a dimer at the cell surface. To effectively compare any activation initiated through $rCD28hFc_{EX}mCD28_{TM/CYT}$ with activation through $rCD28_{EX}mCD28_{TM/CYT}$ the oligomeric state of both molecules must be identical. Therefore BRET analysis was used to investigate whether $rCD28hFc_{EX}mCD28_{TM/CYT}$ was expressed as a dimer at the cell surface. Results from BRET analysis showed that even in the absence of these cysteine residues the construct was expressed as a stable dimer at the cell surface, with calculated $rCD28hFc_{EX}mCD28_{TM/CYT}$ $BRET_{eff}$ values very close to those observed for the dimeric controls human CD28 and human CTLA-4 (Figure 5.5).



a



b

Figure 5.4: Confocal microscopy analysis of the expression of rCD28hFc$_{EX}$mCD28$_{TM/CYT}$. (a) Visualisation of rCD28hFc$_{EX}$mCD28$_{TM/CYT}$ expressed by the vector pGFP^2-N3 at the cell surface. rCD28hFc$_{EX}$mCD28$_{TM/CYT}$ was transiently expressed in HEK-293T cells which were then grown on cover-slides for 24 hours. Cells were excited at 488nm and observed through a 60x objective lens. (b) Average cell surface expression scores for rCD28hFc$_{EX}$mCD28$_{TM/CYT}$ in HEK-293T cells. Transfected cells were observed and scored on a scale for cell surface expression, where a score of 1 indicates cell surface expression only and 5 indicates complete cytoplasmic localisation. The average cell surface expression score for rCD28hFc$_{EX}$mCD28$_{TM/CYT}$ is shown. The dotted lines represent levels of cell surface expression representative for hCD28 (expressed solely on the cell surface) and hCTLA-4 (largely complete cytoplasmic localisation).

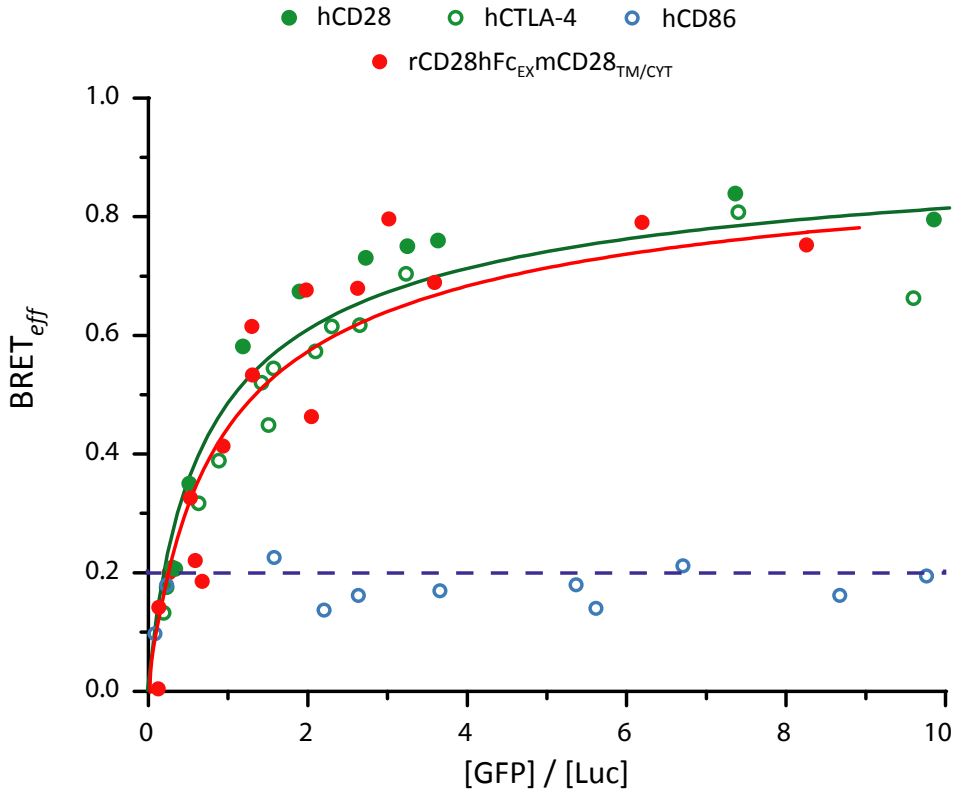


Figure 5.5: BRET signals arising from rCD28hFc$_{EX}$mCD28$_{TM/CYT}$ and control monomeric and dimeric molecule cell surface interactions. BRET$_{eff}$ values recorded from varying acceptor:donor ratios of rCD28hFc$_{EX}$mCD28$_{TM/CYT}$ (red), control dimeric T cell surface molecules (green - hCD28 and hCTLA-4) and control monomeric T cell surface molecules (blue - hCD86). Solid lines show fits of data obtained for the indicated BRET pairs to an equation as predicted for dimers, and the dotted line shows the fit to an equation as predicted for random interactions (Section 2.5).

When combined, the evidence collected by flow cytometry, confocal microscopy and BRET analysis, suggests that rCD28hFc$_{EX}$mCD28$_{TM/CYT}$ is correctly processed in the cytoplasmic compartment, and presented at the cell surface as a dimer in the same manner as wild type CD28 and the chimeric rCD28$_{EX}$mCD28$_{TM/CYT}$. These results allowed this extended form of CD28 produced by rCD28hFc$_{EX}$mCD28$_{TM/CYT}$ to be used alongside rCD28$_{EX}$mCD28$_{TM/CYT}$ to investigate the role of epitope location in CD28 mAb superagonism.

5.3.3 Supergonistic activity of JJ316 is not observed in the rCD28hFc$_{EX}$m CD28$_{TM/CYT}$ cell line

To investigate how increasing the dimensions of CD28 affected the stimulatory activity of superagonistic CD28 mAbs, a T cell hybridoma cell line expressing rCD28hFc$_{EX}$ mCD28$_{TM/CYT}$ was generated. DO11.10 hybridomas were infected with a lentivirus encoding rCD28hFc$_{EX}$mCD28$_{TM/CYT}$ and FACS sorted for CD28 expression to create a stable rCD28hFc$_{EX}$mCD28$_{TM/CYT}$ cell line. This cell line was then stimulated with the mAb JJ316 (Figure 5.6), a CD28 mAb that has been shown to be superagonistic both *in vitro* (Chapter 4) and *in vivo* [217, 218]. Using the superagonistic assay established in Chapter 4, where hybridomas expressing chimeric cell surface molecules are incubated with stimulatory mAbs immobilised by a plate bound secondary antibody, the rCD28hFc$_{EX}$mCD28$_{TM/CYT}$ cell line was stimulated with a titration of superagonistic CD28 mAb JJ316. In this assay, the rCD28$_{EX}$mCD28$_{TM/CYT}$ cell line was also stimulated with mAb JJ316, which acted as a positive control for CD28 superagonism.

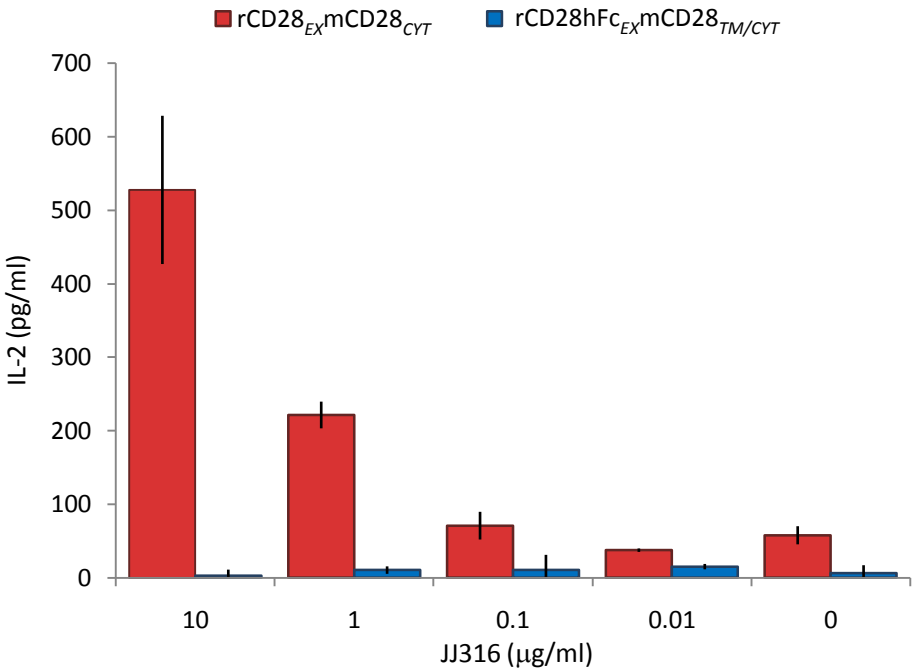


Figure 5.6: Superagonism is observed in the rCD28$_{EX}$mCD28$_{TM/CYT}$ cell line when stimulated with JJ316, but is not seen in a cell line expressing rCD28hFc$_{EX}$mCD28$_{TM/CYT}$ when stimulated under the same conditions. DO11.10 cells expressing either rCD28$_{EX}$mCD28$_{TM/CYT}$ or rCD28hFc$_{EX}$mCD28$_{TM/CYT}$ were stimulated with a titration of CD28 mAb JJ316 from 100μg/ml to 0.01μg/ml, before incubation for 48 hours on 96 well plates coated with donkey anti-mouse IgG antibody at (500μg/ml). The resulting tissue culture supernatant was assayed for IL-2 by ELISA.

When the rCD28hFc$_{EX}$mCD28$_{TM/CYT}$ and rCD28$_{EX}$mCD28$_{TM/CYT}$ cell lines were stimulated with JJ316, the rCD28$_{EX}$mCD28$_{TM/CYT}$ cell line produced IL-2 at high levels of JJ316, as described previously (Section 4). However, no stimulation was observed in the rCD28hFc$_{EX}$mCD28$_{TM/CYT}$ cell line when stimulated with the same levels of JJ316. To confirm the signalling competence of the rCD28hFc$_{EX}$mCD28$_{TM/CYT}$ cell line it was tested for co-stimulation (Figure 5.7). Stimulation with CD3 mAb at 0.3μg/ml or above, successfully induced a high level of IL-2 production in the rCD28hFc$_{EX}$ mCD28$_{TM/CYT}$ cell line and when co-stimulated with mAbs JJ316 and JJ319, high IL-2 levels were observed at sub optimal CD3 mAb concentrations. In repeated experiments comparable levels of co-stimulation were observed for both CD28 mAbs, with no one mAb displaying significantly stronger activating effects. This result is in contrast with co-stimulatory results recorded in the rCD28$_{EX}$mCD28$_{TM/CYT}$ cell line (Chapter 4). In the cell line expressing CD28 with conventional dimensions, both the mitogenic mAb, JJ316, and the co-mitogenic mAb, JJ319, displayed costimulatory activity in the nanogram range of CD3 mAb activation, but the mitogenic JJ316 showed significantly stronger overall co-stimulatory activity. The observed differences between the two cell lines when stimulated with CD28 mAb JJ316, indicate that by increasing the distance between mAb epitope and the cell membrane the stimulatory potential of JJ316 is altered. In the rCD28hFc$_{EX}$mCD28$_{TM/CYT}$ cell line, JJ316 is no longer superagonistic and instead acts to co-stimulate the cell line to the same level as the mAb JJ319. The co-stimulatory activity of JJ319 is observed in both cell lines suggesting that the increased dimensions of the rCD28hFc$_{EX}$mCD28$_{TM/CYT}$ construct does not af-

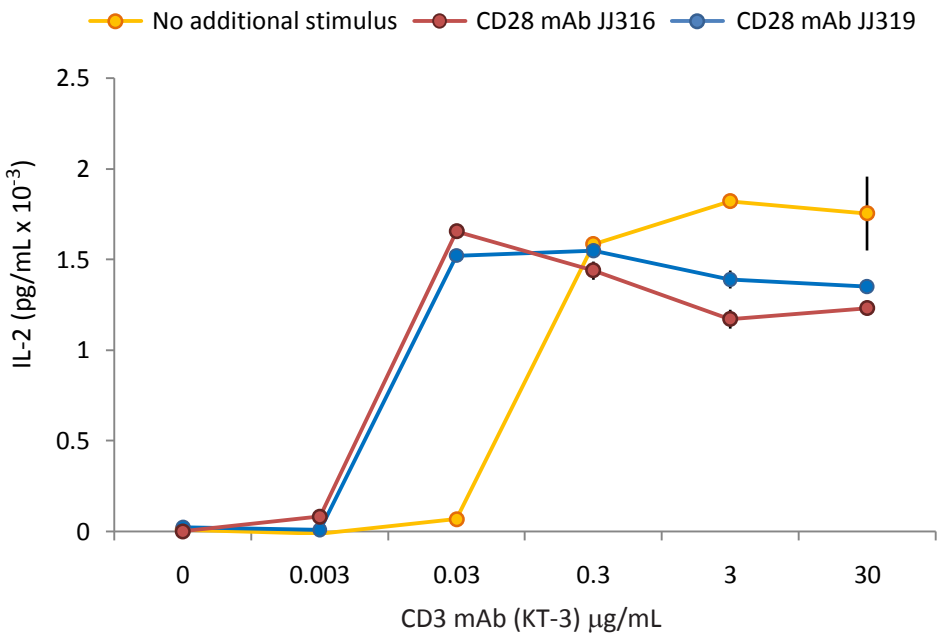


Figure 5.7: The CD28 mAbs JJ316 and JJ319 are equally co-stimulatory for the rCD28hFc$_{EX}$mCD28$_{TM/CYT}$ DO11.10 cell line. DO11.10 cells expressing rCD28hFc$_{EX}$mCD28$_{TM/CYT}$ were stimulated with or without CD28 mAbs JJ316 or JJ319 at 10μg/ml before incubation on 96 well plates pre-coated with a titration of CD3 mitogenic mAb (KT-3 from 3μg/ml to 0.0003μg/ml) and donkey anti-mouse IgG (at 500μg/ml. After 48 hours, the resultant supernatants were assayed for IL-2 by ELISA.

fect its co-stimulatory ability. In rCD28$_{EX}$mCD28$_{TM/CYT}$ JJ316 has a membrane proximal epitope whereas JJ319 has an epitope located to towards the top of CD28 (Figure 5.8).

By increasing the distance between CD28 and the cell membrane, which occurs in rCD28hFc$_{EX}$mCD28$_{TM/CYT}$, the epitopes of both mAbs are moved to a membrane distal position abolishing the superagonistic potential of JJ316 and causing both CD28 mAbs to be co-stimulatory. These results indicate a clear link between epitope position and the stimulatory strength of CD28 mAbs.

5.3.4 Antibodies to the human IgG1 Fc domain are superagonistic in the rCD28hFc$_{EX}$mCD28$_{TM/CYT}$ cell line

If, as observed in the rCD28hFc$_{EX}$mCD28$_{TM/CYT}$ cell line, by moving the epitope of a CD28 superagonist away from the membrane proximal region, it is possible to abrogate the mitogenic effect of a CD28 superagonist mAb, then the following prediction can be made: that any other mAb that binds rCD28hFc$_{EX}$mCD28$_{TM/CYT}$ close to the membrane will be superagonistic. To test this hypothesis, three mAbs with human IgG1 Fc specific epitopes were selected. mAb HP6091, is an IgG2 mAb and was first described by Jefferis *et al.* (1985) [308]. Using domain switched chimeric IgG, it was found to bind to the CH_2 domain of IgG1 [309, 310] and the epitope was further defined through the use of point mutation analysis, which identified asparagine 276 to be a contributing residue in the HP6091 epitope. The second mAb used, A57H, is an IgM mAb specific to an eight amino acid sequence of the IgG1 Fc CH_3 domain (residues 383-390 SNGQPENN, Eu numbering) [311]. The third mAb used is mAb

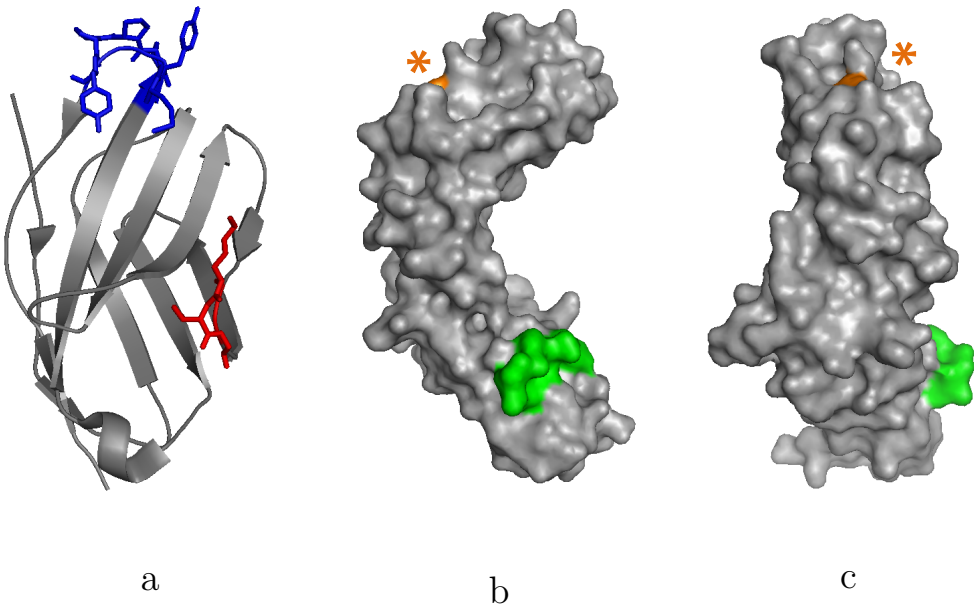


Figure 5.8: Epitopes of the mAbs JJ316, JJ319, A57H and HP6091. (a) Ribbon diagram of the structure of the human CD28 V-set domain [184]. Equivalent residues identified that contribute to the epitopes of the rat CD28 mAbs JJ316 and JJ319 are coloured red and blue respectively. (b) Surface representation of the structure of the CH_2 and CH_3 domains of human IgG1 [307]. (c) A 90° rotation of the surface representation. Residues identified to make up the epitope of human IgG1 CH_3 mAb A57H are represented in green. An asparagine residue believed to contribute to the epitope of the human IgG1 CH_2 mAb HP6091 is represented in orange and highlighted with an asterisk of the same colour.

F890. A human IgG1 Fc specific mAb, this antibody was identified from a panel of mAbs raised against a CD80/human IgGFc fusion protein (Unpublished data, Dr John Young, Institute of Animal Health, Compton, Berkshire, UK.), but the epitope and the isotype of this mAb are not known.

Two of the three IgG1 Fc mAbs have clearly defined epitopes. When mapped on IgG1 Fc (Figure 5.8), the epitope of HP6091 is located in the upper face of the CH_2 domain. This is in contrast to the epitope of A57H, which is positioned on the CH_3 domain, close to the membrane. If used to stimulate the rCD28hFc$_{EX}$mCD28$_{TM/CYT}$ cell line, the proximity of the epitope of A57H to the membrane is similar to that of the superagonist JJ316 on rCD28$_{EX}$mCD28$_{TM/CYT}$. This suggests that it could have mitogenic properties in a rCD28hFc$_{EX}$mCD28$_{TM/CYT}$ hybridoma system. As the epitope of HP6091 on rCD28hFc$_{EX}$mCD28$_{TM/CYT}$ is positioned at a greater distance from the membrane than the co-stimulatory JJ319 on rCD28$_{EX}$mCD28$_{TM/CYT}$, it is predicted to have a weaker stimulatory effect or to only be co-stimulatory.

Each of the Fc mAbs were raised against soluble wild type forms of IgG1, but if used to stimulate the rCD28hFc$_{EX}$mCD28$_{TM/CYT}$ cell line, they will be required to bind to a chimeric membrane bound form of IgG1 Fc. The fusion of the CD28 extracellular domain and the proximity of the CH_3 domain to the cell membrane may affect the accessibility of the mAbs A57H and HP6091 to their epitopes. Therefore prior to the testing of the mAbs for stimulatory activity, the efficiency of the binding of each mAb to the rCD28hFc$_{EX}$mCD28$_{TM/CYT}$ cell line was investigated. Using flow cytometry analysis, the binding of each anti-IgG1 Fc mAb, along with IgG1, IgG2a and IgM

isotype controls and positive controls, CD28 mAb JJ316 and JJ319, was assayed (Figure 5.9). F890 and HP6091 were both found to bind rCD28hFc$_{EX}$mCD28$_{TM/CYT}$ at 10μg/ml, however F890 binds at a significantly higher level than HP6091. When probed with A57H at 10μg/ml, no A57H was observed binding to rCD28hFc$_{EX}$mCD28$_{TM/CYT}$ (not shown). Only at 100μg/ml A57H was a small amount of binding recorded (Figure 5.9). The low level of binding to rCD28hFc$_{EX}$mCD28$_{TM/CYT}$ observed by A57H at high concentrations may indicate that A57H has a low affinity for its epitope or that access to the epitope of A57H is restricted by the cell membrane.

To confirm that A57H could bind to an Fc fusion protein and to gain additional information on the epitope of F890, competition SPR analysis was carried out using a soluble human IgG1 fusion protein (BAFFR-Fc) and the three IgG1 Fc mAbs. A57H, HP6091 and F890 were passed sequentially over directly immobilised BAFF-R/human IgG1 Fc fusion protein (BAFFR/Fc) using an SPR based binding assay as described in Section 3.2.5. Both A57H and F890 were observed to bind to BAFFR/Fc, however the binding curves for both mAbs were significantly different (Figure 5.10). The high level of binding of F890 to BAFFR/Fc saturated with A57H indicates that the two mAbs have discrete epitopes which do not overlap. Surprisingly, no binding of BAFFR/Fc was observed by HP6091. If no information was available on the epitope of HP6091, the data would suggest that the prior binding of A57H to BAFFR/Fc obscures the HP6091 epitope and prevents binding. However, the Fc domain residue asparagine 276 has been identified to contribute to the HP6091 epitope [310], so this cannot be the case. In repeated SPR experiments, involving injections of HP6091 over directly im-

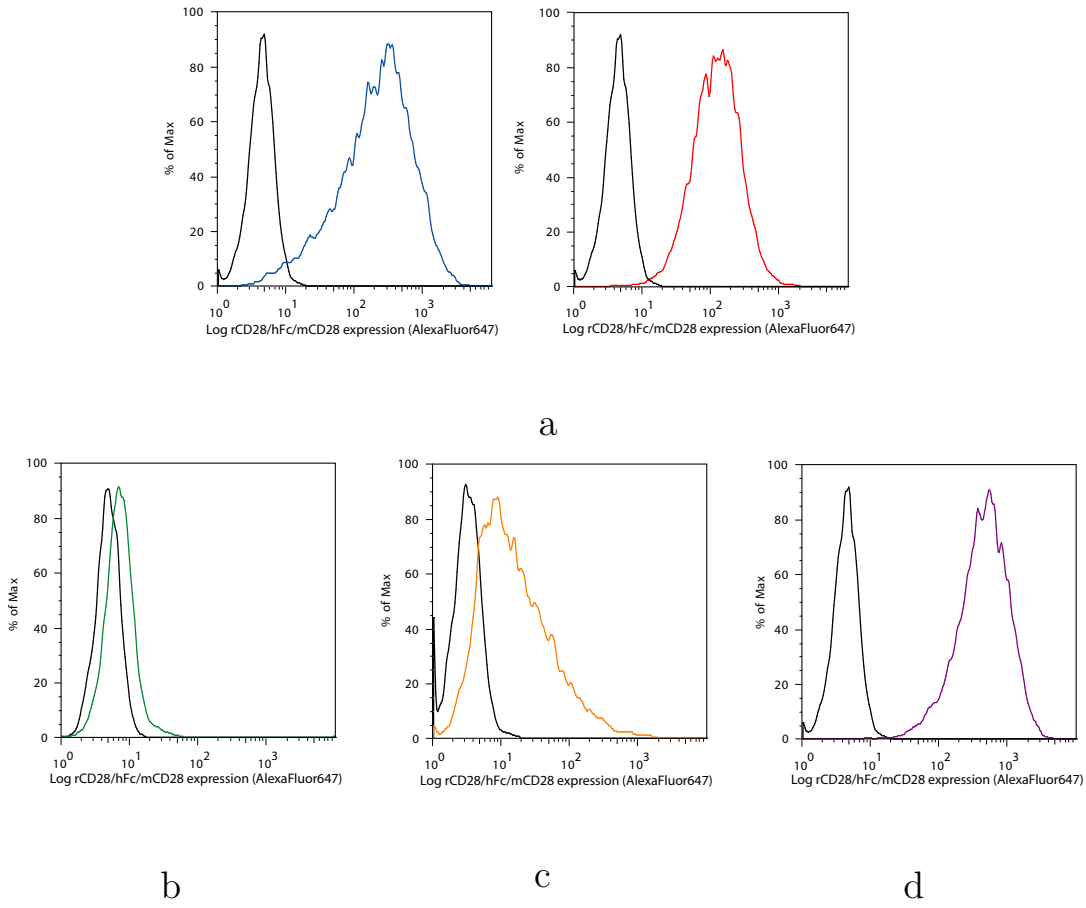


Figure 5.9: Binding of various rat CD28 and human IgG-Fc specific mAbs to the rCD28hFc$_{EX}$mCD28$_{TM/CYT}$ D011.10 cell line. The rCD28hFc$_{EX}$mCD28$_{TM/CYT}$ DO11.10 cell line was created by sorting DO11.10 cells transduced with lentivirus (encoding rCD28hFc$_{EX}$mCD28$_{TM/CYT}$) for high expression of rat CD28, using the CD28 mAb JJ319. The flow cytometry data shown represents mAb specificity for the rCD28hFc$_{EX}$mCD28$_{TM/CYT}$ cell line when probed with (a) mAbs JJ319 (blue) and JJ316 (red) and an IgG1 isotype control (MOPC-21) (black), (b) mAb A57H (green) and an IgM isotype control (MM-30) (black), (c) mAb HP6091 (orange) and an IgG2 isotype control (MG2a-53) (black) and (d) mAb F890 (purple) and an IgG1 isotype control MOPC-21 (black). Cells were probed with primary mAb at a concentration of 10μg/ml apart from mAb A57H and its IgM isotype control where a concentration of 100μg/ml was used. 5μg/ml donkey anti-mouse AlexaFluor®647 was used as a secondary conjugate for IgG1 and IgG2a probed cells. IgM probed cells were, further stained with a secondary IgM specific mAb (LO-MM-9 - AdB Serotec) at 5μg/ml then with 5μg/ml donkey anti-mouse AlexaFluor®647.

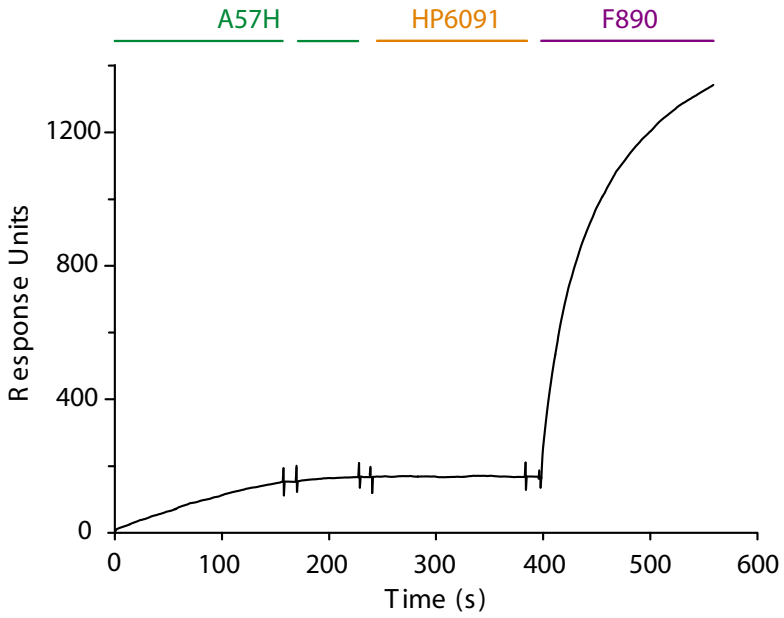


Figure 5.10: Competition binding of anti-human IgG1 mAbs to directly immobilised BAFFR-Fc. ∼1150 RU of BAFFR-Fc and ∼1400 RU of control protein CTLA-4-mouseFcHis (both at 100 μg/ml) were directly immobilised by amine coupling in pH 4.5 acetate to a CM5 BIAcore sensor chip. Two successive injections of 55μl and 20μl IgG1 mAb A57H at 100μg/ml were made over the immobilised BAFFR-Fc and CTLA-4-FcHis at 30μl/min at 25°C. This injection was followed by two 55μl injections of IgG1 mAbs HP6091 (100μg/ml) and F890 (100μg/ml). Sensorgram data recorded for the control protein CTLA-4-FcHis was subtracted from BAFFR-Fc data to account for background non-specific protein interactions and buffer effects.

mobilised BAFFR/Fc or a second Fc fusion protein, CD44/Fc (not shown), no HP6091 was observed binding to soluble human IgG1 Fc fusion protein. Despite the absence of binding observed to soluble IgG Fc fusion protein, both A57H and HP6091 when analysed by flow cytometry, bind to rCD28hFc$_{EX}$mCD28$_{TM/CYT}$ expressed on DO11.10 hybridomas, the environment in which the stimulation assay takes place. Therefore all three mAbs were used in the hybridoma stimulation assay. Each mAb was tested for stimulatory activity in the rCD28hFc$_{EX}$mCD28$_{TM/CYT}$ cell line by titration using the mAb stimulation assay established in Chapter 4 (Figure 5.11). When used in the absence of any other stimulus, the IgG1 Fc mAbs A57H and F890 were mitogenic at a mAb concentration in the microgram range. The superagonistic activity of both A57H and F890 is concentration dependent, although the optimal concentration of F890 at which superagonism is observed is 10x lower than A57H. At all concentrations of HP6091, no significant IL-2 stimulation was observed. Having seen no superagonism with the membrane distal-binding mAb (HP6091), we determined whether the mAb was capable of co-stimulatory activity. The rCD28hFc$_{EX}$ mCD28$_{TM/CYT}$ cell line was stimulated with each IgG1 Fc mAb in the presence of stimulatory CD3 mAb in titration (Figure 5.12). In the rCD28hFc$_{EX}$mCD28$_{TM/CYT}$ cell line HP6091 is not superagonistic, but under co-stimulatory conditions it is able to stimulate IL-2 production at sub-optimal CD3 mAb concentrations. In a pattern observed previously in the rCD28$_{EX}$mCD28$_{TM/CYT}$ cell line (Section 4.3.1), A57H and F890 stimulation also results in increased stimulation at sub-optimal CD3 mAb concentrations, however, the levels of activation observed at high CD3 mAb concentrations are only equivalent to those seen for CD3 stimulation

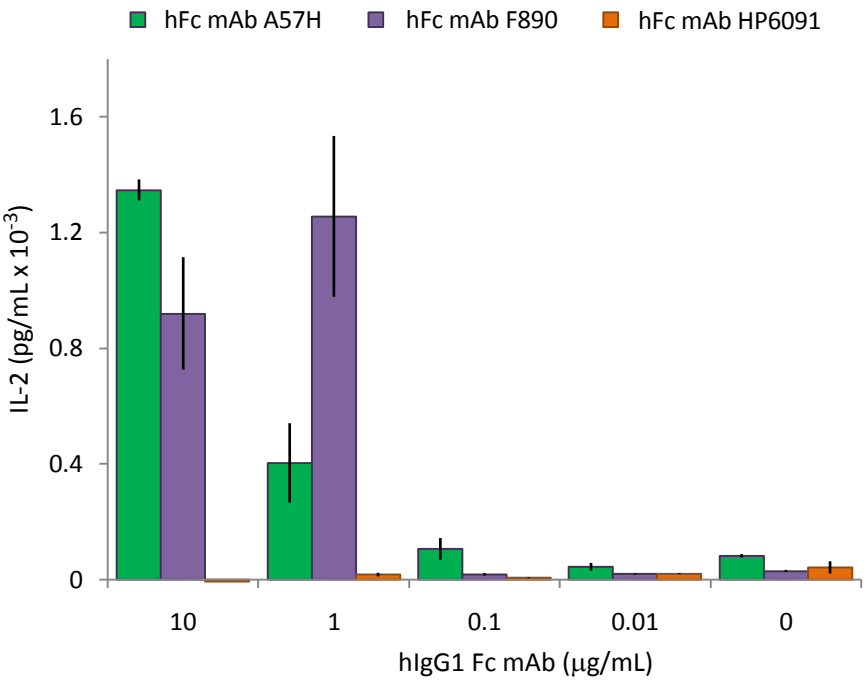


Figure 5.11: The human Fc specific mAbs A57H and F890 are superagonistic for the rCD28hFc$_{EX}$mCD28$_{TM/CYT}$ DO11.10 cell line. DO11.10 cells expressing rCD28hFc$_{EX}$mCD28$_{TM/CYT}$ were stimulated with a titration of human IgG Fc mAbs A57H, HP6091 or F890 from 100μg/ml to 0.01μg/ml, before incubation for 48 hours on 96 well plates coated with donkey anti-mouse IgG antibody at (500μg/ml). The resulting tissue culture supernatant was assayed for IL-2 by ELISA.

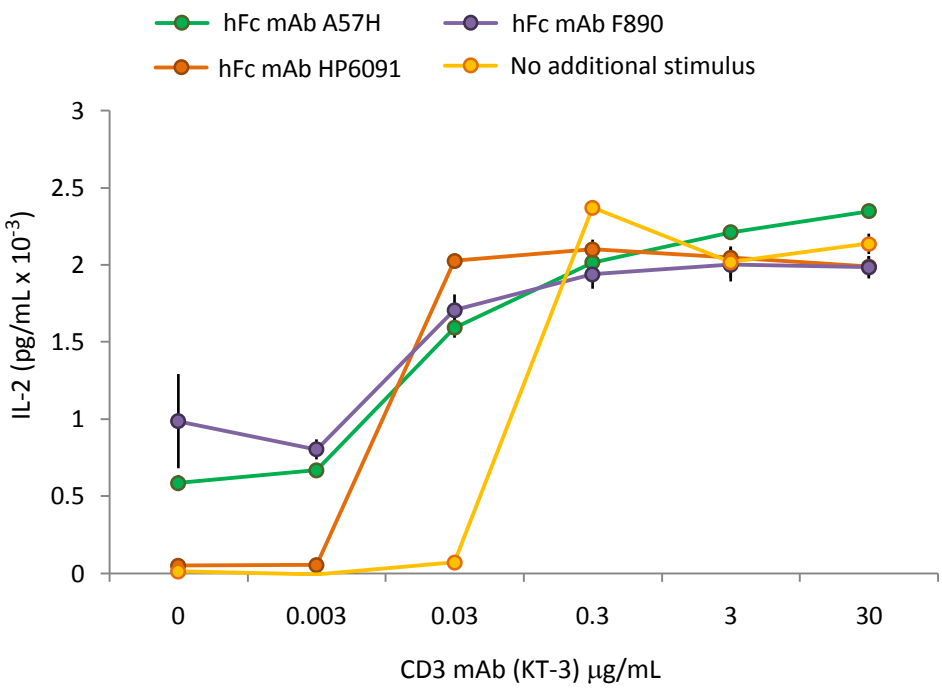


Figure 5.12: The human Fc specific mAbs A57H, HP6091 and F890 are all co-stimulatory for the rCD28hFc$_{EX}$mCD28$_{TM/CYT}$ DO11.10 cell line. DO11.10 cells expressing rCD28hFc$_{EX}$mCD28$_{TM/CYT}$ were stimulated with a titration of plate immobilised CD3 mitogenic mAb (KT-3) either with or without human IgG1 Fc mAbs A57H, HP6091 or F890 at 10μg/ml immobilised with donkey anti-mouse IgG. After incubation for 48 hours, the resultant tissue culture supernatant was assayed for IL-2 by ELISA.

and not higher, as observed with CD28 superagonists.

5.3.5 Cross-linking of the A57H mAb does not significantly contribute to its superagonistic properties

The superagonism observed in rCD28hFc$_{EX}$mCD28$_{TM/CYT}$ when stimulated with A57H, is strong evidence for the link between the mitogenic nature of superagonists and their membrane proximal epitopes. However, direct comparisons between the CD28 mitogenic mAb JJ316 and A57H could not initially be made without further investigation. A57H is of an IgM isotype whereas all other superagonists used in this study are IgG. IgM antibodies are pentameric and as such can potentially cause cross-linking alone. As previously shown (Section 4.3.7), cross-linking alone can induce low level activation in a monomeric PD-1/CD28 expressing hybridoma cell line. This evidence along with the dimeric nature of CD28 and the concentration dependent nature of CD28 superagonism suggests that cross-linking may play a role in initiation of CD28 mAb induced activation. The cross-linking potential of an IgM mAb to CD28 is greatly increased due to its ten possible antigen binding sites, compared to the two of an IgG. Dennehy *et al.* (2006) [219] propose a mechanism of superagonism where mitogenic mAb cross-linking and lattice formation can initiate activation alone. If this mechanism is correct, A57H could, through its increased valency, cross-link more efficiently and this alone could cause the activation observed.

An essential aspect in the observation of CD28 superagonism *in vitro* is the immobilisation of superagonist mAbs through a plate bound secondary antibody. If

the epitope of A57H plays no role in the superagonism observed and the increased cross-linking by A57H alone can initiate activation, this immobilisation will not be required.

The immobilising antibody (donkey anti-mouse IgG) used in the stimulatory assays is polyclonal and specific to IgG, therefore it may not effectively immobilise the IgM A57H. To investigate this, the relative specificity of donkey anti-mouse IgG for the mAbs A57H, F890, HP6091, JJ319 and a mouse IgM control was assayed by sandwich ELISA (Figure 5.13). As expected the IgG antibodies F890, HP60917 and JJ319 were all bound by donkey anti-mouse IgG at sub-microgram levels. While donkey anti-mouse IgG binds both IgM mAbs, they are bound weakly and at high concentrations they are bound at different levels. At 10μg/ml, A57H binding is at a level just short of that observed for IgG JJ316, whereas the binding of the IgM control is only half of that of A57H. Despite the weaker binding, the sandwich ELISA clearly shows that the immobilising donkey anti-mouse IgG used in the stimulation assays has an affinity for A57H despite its described specificity for IgG.

With the confirmation that the A57H used in the superagonism stimulation assay is immobilised by donkey anti-mouse IgG, the effect of removing this immobilising antibody from the A57H superagonism assay was investigated. The rCD28hFc$_{EX}$ mCD28$_{TM/CYT}$ cell line was stimulated with A57H and incubated on either uncoated plates or plates coated with donkey anti-mouse IgG (Figure 5.14). At the optimum A57H stimulatory concentration, cells incubated on plates coated with immobilising antibody produce IL-2 at levels three times that of those incubated on uncoated plates.

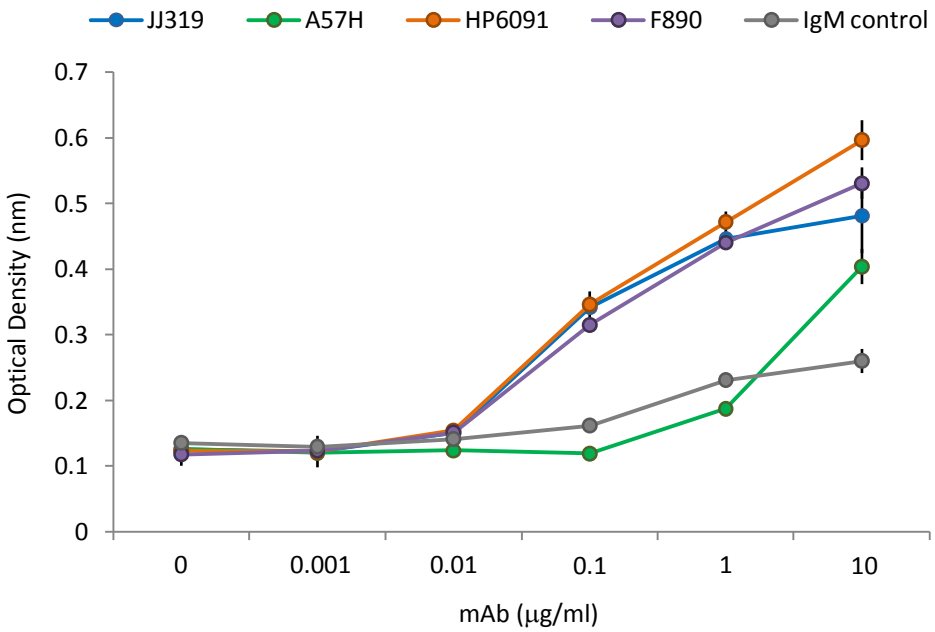


Figure 5.13: The mouse IgG specific immobilising antibody used in the cell line stimulation assays, donkey anti-mouse IgG, also binds mouse IgM. Binding was assayed by sandwich ELISA, first coating a 96 well plate overnight with 500μg/ml donkey anti-mouse IgG, before the addition the stimulation mAbs, A57H, F890, HP6091, JJ319 and mouse IgM control, which were titrated from 10μg/ml to 0.001μg/ml. A secondary anti-mouse Ig (Fab specific) peroxidase conjugate was added at 1/3000 dilution before the addition of the ABTS substrate. The resultant optical density of each well was recorded after 20 minutes at 515nm.

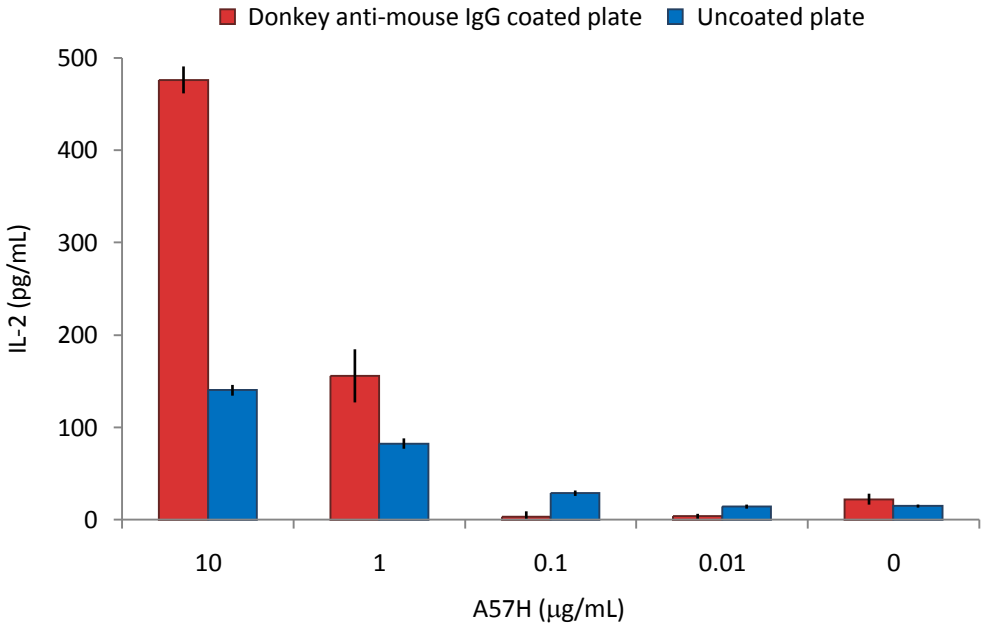


Figure 5.14: A57H is most superagonistic for the rCD28hFc$_{EX}$mCD28$_{TM/CYT}$ cell line when immoblised with donkey anti-mouse IgG. The rCD28hFc$_{EX}$mCD28$_{TM/CYT}$ cell line was stimulated with a titration of A57H from 10μg/ml to 0.01μg/ml, before incubation for 48 hours on either uncoated 96 well plates or 96 well plates pre-coated with donkey anti-mouse IgG at 500μg/ml.

An increase in stimulation is observed in rCD28hFc$_{EX}$mCD28$_{TM/CYT}$ cells incubated in the absence of immobilising antibody at 10μg/ml A57H. This suggests that at high concentrations of multivalent A57H a low level of activation in the rCD28hFc$_{EX}$mCD28$_{TM/CYT}$ cell line can be induced. However, the significant decrease of stimulation recorded in the rCD28hFc$_{EX}$mCD28$_{TM/CYT}$ cell line upon the removal of immobilising antibody shows that the major factor in A57H superagonism is probably not cross-linking but epitope location.

5.4 Discussion

5.4.1 Summary of findings

The work described in this chapter, outlines two strategies in which chimeric rat CD28 molecules were designed and constructed that increased the dimensions of CD28 in order to investigate the role of epitope location on superagonism. An initial strategy to use repeated units of the CD28 stalk region to create such a chimera was unsuccessful. However, a second approach which inserted an Fc domain between CD28 and the cell membrane resulted in a chimeric protein (rCD28hFc$_{EX}$mCD28$_{TM/CYT}$) that was successfully expressed at the cell surface. A characterised superagonist with a membrane proximal CD28 epitope, was unable to activate a cell line expressing this chimera alone, whereas the same mAb activated the cell line in a co-stimulatory environment. The requirement for a membrane proximal epitope as the defining characteristic in the mechanism of CD28 superagonism was confirmed when these cells were stimu-

lated with a mAb not specific to CD28 (A57H) but specific to a membrane proximal Fc portion of the rCD28hFc$_{EX}$mCD28$_{TM/CYT}$ chimera. The mitogenic mechanism of A57H was further investigated to show that epitope location and not cross-linking was the dominant cause of its stimulatory effects.

5.4.2 IgG1 Fc mAbs

When selecting IgG1 Fc mAbs which could be used to further investigate CD28 superagonism, the choice of mAbs was limited due the low number for which the epitopes had been mapped. This limited choice led to the use of two mAbs (HP6091 and A57H), which through investigation, were shown not to have characteristics comparable to the CD28 mAbs used. When first described and characterised as part of a WHO study to evaluate mAbs specific for human IgG sub-classes [308], HP6091 was noted for showing a very low avidity for IgG1 by ELISA, a lack of specificity by immunofixation and was also inactive in particle counting immunoassays (a latex agglutination method). However in contrast, it did show good specificity for IgG1 in haemagglutination inhibition and immunofluorimetric assays. These contrasting results are similar to the contrasting results obtained here using flow cytometry and SPR analysis. The evidence indicates that HP6091 does bind to the CH_2 domain of rCD28hFc$_{EX}$mCD28$_{TM/CYT}$, but the factors which affect the extent of its binding are still unclear.

With a clearly defined epitope in a membrane proximal position, A57H was an ideal choice of IgG1 Fc mAb to investigate superagonism in the rCD28hFc$_{EX}$mCD28$_{TM/CYT}$ cell line. However, the IgM isotype of A57H meant that its stimulatory characteris-

tics could in principle be attributed to this isotype alone due to its ability to induce cross-linking. This was shown not to be the case, but another characteristic of the antibody could also have influenced the results. IgM antibodies are produced early in the humoral immune response and are produced before B cells have undergone somatic hypermutation and affinity maturation [312]. Because of this they tend to be of low affinity, which was suggested by flow cytometry and SPR analysis to be the case for A57H. This weak affinity may have lessened the observed effect of cross-linking observed for A57H.

Although previously the epitope of F890 was defined only by its specificity to IgG1 Fc, the results from this chapter allow some new predictions on the location of its epitope to be made. If, as shown in this chapter, a membrane proximal epitope is enough to predict the superagonistic characteristic of a mAb within a CD28 system, then the mitogenic properties in the rCD28hFc$_{EX}$mCD28$_{TM/CYT}$ cell line suggests that the epitope of F890 is localised to a membrane proximal region. In addition to this the epitope will be distinct from that of A57H based on SPR competition analysis.

5.4.3 Strategies for the construction of large forms of CD28

The form of CD28 that successfully expressed at the cell surface was created through the insertion of complete foreign domains (human Fc) between CD28 and the cell surface. The insertion of this domain was chosen due to the previous successful expression of soluble CD28/Fc fusions [184, 304, 305]. It was based on the construction of these successful fusions that three cysteine residues found in the hinge region

were mutated to serines. This removal may have had an effect on the dimerisation of the resultant chimera at the cell surface, as these residues are responsible for the formation of the heavy chain inter chain disulphide bond. However, BRET analysis showed that rCD28hFc$_{EX}$mCD28$_{TM/CYT}$ is presented as a stable dimer at the cell membrane. The presence of the cysteines responsible for the interchain disulphide bond in CD28 maybe enough to replace those removed from the Fc hinge. This, along with the non-covalent interactions between the CH_2 and CH_3 domains [313,314] is likely to have ensured dimerisation throughout the entire chimera.

Evidence collected from the expression of the rCD28$_{EX}$mCD28$_{TM/CYT}$L#X constructs indicates that the mutations made to insert restriction endonuclease sites around the CD28 stalk region are not tolerated by the resultant protein and cause misfolding. The lysine residues mutated to insert the restriction sites are conserved in human, rat, mouse and bovine CD28 [315–318] which is indicative of structural importance. The change in charge resulting from the mutation, from a positively charged lysine to a non-polar leucine or valine, is therefore the probable cause of this instability. Whether the residue substitutions at the CD28 V-set domain end, cell membrane end or both ends of the CD28 stalk are detrimental to the structure of CD28 is unclear.

Although the strategy to increase the stalk size of CD28 was unsuccessful in this instance, the introduction of small repeated units beneath CD28, would be an excellent method to investigate the distance from the cell membrane at which a superagonist mAb epitope has to be to abrogate its mitogenic activity.

Chapter 6

General Discussion

6.1 Current understanding of T cell activation

The capacity of the adaptive immune response to protect the body is dependent on its ability to identify and respond to invading pathogens. For T cells, the recognition of intracellular pathogens or extrinsically-derived antigens presented on MHC molecules by the TCR is well characterised and the role this process plays as the initiating factor in T cell activation is well established. The intracellular signalling cascades and the subsequent cellular responses resulting from TCR ligation are also becoming elucidated and understood. However, the weak point in our knowledge of this chain of events is how a signal initiated by TCR ligation crosses the cell membrane and affects the phosphorylation of the TCR, initiating intracellular signalling. While many models have been proposed for this process, the mechanism of signal transfer is still widely debated [162].

Any theory of TCR triggering, while addressing the key characteristics and evidence for triggering through the TCR, must also consider the broader context of T cell activation. The stimulatory signal initiated by p:MHC/TCR ligation is modulated by co-stimulatory molecules, whose own triggering systems are, likewise, unclear. When ligated, many of these signal modulating T cell surface proteins are triggered under

the same local conditions as the p:MHC/TCR. Many of these proteins, like the TCR, also have similar ligand/receptor complex sizes and require extrinsic kinases to phosphorylate tyrosines in their cytoplasmic signalling motifs. Any proposed mechanism for TCR triggering has to consider the numerous molecules that affect the result of T cell activation, and, in addition, consider how this mechanism fits within the broader framework of triggering for similar T cell surface receptors.

6.2 Results from this thesis

Based on the hypothesis that epitope location alone causes, and can be used to predict, the stimulatory characteristics of CD28 superagonistic mAbs, this thesis examines whether the hypothesis can be extended to other molecules and considers the mechanistic basis of CD28 superagonism. The effect of epitope dependent agonist mAbs on other T cell surface signalling molecules was investigated by the generation and characterisation of human PD-1 mAbs. In addition, through the refinement and development of existing methods used to investigate CD28 superagonism, the link between epitope location and CD28 superagonistic activity was further explored. The results from these experiments are discussed here.

6.2.1 The triggering of chimeric receptors in cell lines using human PD-1 mAbs

The observation that the epitope location of CD28 mAbs is linked to their stimulatory activity led us to hypothesise that mAbs could be generated to other T cell surface

signalling molecules that, dependent on epitope location, could also have stimulatory properties. Based upon the results of epitope mapping of PD-1 mAbs 2, 10, 19 and 29, as described in Chapter 3, we predicted the potential stimulatory activity of the PD-1 mAbs. The initial strategy of generating a monomeric PD-1/CD28 chimera for testing mAbs for *in vitro* PD-1 triggering activity, which aimed to stimulate IL-2 production through CD28 stimulatory pathways, was unsuccessful. This suggested that in a monomeric molecule the CD28 cytoplasmic domain is not able to initiate activating signalling pathways and therefore in the context of CD28, superagonism may be linked to its dimeric form. mAb induced signalling was observed only in a cell line expressing a chimera that associated with the TCR. Surprisingly, three of the four PD-1 mAbs showed strong stimulatory activity in a cell line expressing PD-1 linked to the wild type CD3ζ transmembrane domain. The levels of stimulation observed correlated with their epitope position, as predicted. However the differences in stimulation observed between the two mAbs with very similar epitopes at the "top" of the molecule, i.e. mAbs 2 and 10, suggested that mAb stimulatory activity in this system involves factors other than epitope location.

A comparison of the stimulatory properties of each mAb in the cell line expressing the PD-1/CD28 chimera with the CD3ζ transmembrane domain and the K_d of each mAb suggests a possible link between mAb binding affinity and agonistic potential. mAb 19 has the lowest K_d of the mAbs tested, and induced the highest level of stimulation, whereas mAb 29 has the highest K_d of all the PD-1 mAbs tested and showed no stimulatory activity. The very low affinities of mAb 10 and 29 correlates with their

lower signalling abilities as there will overall less PD-1 binding. However, the stimulatory responses of the mAbs do not appear to be simply proportional to their binding affinities. The signalling strength of mAb 2 is approximately 33-50% stronger than that of mAb 10, but there is an approximate 40-fold difference in K_d between the two. The comparison of triggering by mAb 2 and 19, which share a similar K_d, in this system shows that mAb 19, which has a membrane proximal epitope, elicits 20% more IL-2 production on triggering than mAb 2 that has a membrane distal epitope. When considered together, there is evidence that, within this cell line, both binding affinity and epitope location affect the strength of PD-1 mAb agonist triggering.

Despite the identification of a role for the TCR/CD3 complex in the signalling mechanism of the cell line expressing the PD-1/CD28 chimera with the CD3ζ transmembrane domain, the exact nature of how signalling occurs in these cells is unclear. Mutations of the CD3ζ transmembrane domain initially showed that the TCR/CD3 complex was involved in the signalling pathway induced by the PD-1 mAbs. The absence of PD-1 mAb induced activation in the mutant chimeras was consistent with the hypothesis that charged residues in the CD3ζ transmembrane domain caused association with the TCR, leading to signals passing through the ITAMs of the TCR/CD3 complex as well as or instead of the CD28 tyrosine signalling domains. However, when attempts to confirm this theory were performed, PD-1 mAb induced signalling was not observed in a cell line expressing the chimera containing the transmembrane and cytoplasmic domains of CD3ζ, which would be expected to associate with the TCR complex in an identical manner. In addition to this, there was no clear observed link

between protein dimerisation levels and signalling efficacy in either chimera containing the CD3ζ chain transmembrane domain. Therefore a clear conclusion on signalling pathways triggered by constructs containing the CD3ζ transmembrane domain by the PD-1 mAbs cannot be reached, however it is likely that the TCR/CD3 complex plays some role in the stimulation observed.

6.2.2 The native PD-1 triggering properties of human PD-1 mAbs

While stimulation of hybridomas expressing a PD-1 chimera showed that the signalling initiated by mAb 19 is the strongest, investigations into the effects of mAb 10 and 19 stimulation on native PD-1 have yielded contrasting results (unpublished data; Dr. C. Jessup, Weatherall Institute of Molecular Medicine). When *ex vivo* cultured peripheral blood lymphocytes were stimulated with bead-bound PD-1 mAbs, mAb 10 triggered the strongest inhibitory signal. Cell proliferation dropped by 5% when stimulated with mAb 19 compared to the 15% observed after stimulation with mAb 10. The PD-1 triggering effect of mAb 10 has also been investigated by Petrovas *et al.* (2007) [319]. Rhesus Macaque SIV specific $CD8^+$ T cells cultured in the presence of mAb 10 for 6 days showed reduced T cell cellular proliferation and an increased sensitivity to apoptotic death. This inhibitory effect was observed most in those SIV specific $CD8^+$ T cells that showed the highest levels of PD-1 expression.

This evidence highlights a conflict in the strength of mAb 10 and 19 induced PD-1 signalling. In a cell line expressing a chimeric PD-1 molecule containing the transmembrane region of CD3ζ and the intracellular domain of CD28, mAb 19 induces

higher levels of IL-2 production. However, when use to trigger native PD-1 in cultured peripheral blood lymphocytes the strength of the inhibitory signals, mAb 10 triggers the stronger inhibitory response. This difference may be explained by the nature of the PD-1 signalling domains. The ITSM domain of PD-1 has been shown to be key in the suppressive function of PD-1 in both B cells and T cells, but the role of the ITIM domain, also present in the cytoplasmic tail of PD-1, remains unclear [271,320,321]. In native PD-1, the level of signalling induced by a mAb may dictate the type or strength of the inhibitory signal generated. From the inhibitory effects of mAb 10 ligation observed by Dr. C. Jessup (unpublished data), the strength of signalling induced by mAb 10 may cause the phosphorylation of the PD-1 ITSM and subsequent SHP2 recruitment. However, the increase in the strength of signal initiated by mAb 19 ligation may result in the phosphorylation of the ITIM as well as the ITSM. This may cause the recruitment of as yet unknown signalling factors that may dampen the overall PD-1 inhibitory signal and account for the reduced inhibitory effect of mAb 19 as seen in cultured peripheral blood lymphocytes.

6.2.3 The application of PD-1 mAbs as immune modulating therapeutics

Despite the gaps in our knowledge concerning the mechanism underlying T cell activation, several novel mAbs that modulate T cell signalling have been developed into human therapeutics. The potential of both triggering and blocking mAbs targeted to T cell surface receptors is significant. The number of novel therapeutic mAbs that are able to inhibit or trigger T cells by targeting cell surface signalling molecules may

eventually be limited only by the number of such receptors. Such mAbs could be used to treat a variety of auto-immune diseases, influence the immune response to infectious diseases, modulate tumour immunity or prevent organ transplant rejection.

A phase I clinical trial of PD-1 mAb CT-011 and a phase II clinical trial of PD-1 mAb MDX-1106 have recently been completed [322, 323]. Both mAbs, which have PD-1 blocking abilities, were developed for the treatment of malignant cancers, and the results of the trials indicated some therapeutic effect [322–324]. The therapeutic benefit of targeting T cell inhibitory molecules has also been seen with the CTLA-4 blocking mAB ipilimumab, which has shown to decrease tumor size and slow tumor progression in cases of metastatic melanoma [325, 326]. However, it is unclear how ipilimumab enhances the immume responses against cancer [327]. The mAbs generated and characterised in this thesis have been shown to have potential PD-1 agonistic properties. While these could be used to treat autoimmune diseases, the epitopes of mAbs 2 and 10 are located in the PD-1 ligand binding region and suggest an additional therapeutic PD-1 blocking role. But what distinguishes a blocking antagonist from a receptor signalling agonist mAb? Using the kinetic segregation (KS) model-based mechanism of triggering, we would argue that it is the presence of FcγR binding regions in the hinge and CH_2 domains of the mAb Fc. The binding of a cell bound FcγR to receptor bound mAb with a blocking epitope would mimic native receptor/ligand binding by bringing the membranes of the receptor and FcγR expressing cells into close proximity, thereby initiating signalling. A blocking mAb without the capacity to recruit an FcγR would therefore not have a signalling effect,

but through its association with the ligand binding region might prevent ligation of the receptor's native ligand. Mutations are often introduced into the Fc domain of therapeutic mAbs to prevent antibody dependent cellular toxicity that is mediated by FcγR binding [328,329]. PD-1 mAb MDX-1106 contains these mutations, and so is not expected to induce signalling but will retain its blocking abilities. Although the binding affinity of Macaque FcγR to mouse IgG Fc is not known, the Fc region of the mAb 10 used to stimulate a macaque *ex vivo* lymphocyte culture was unmodified [319]. Therefore the agonistic characteristics of mAb 10 observed could have been caused by the ligation of T cell expressed FcγRIIA [10] to mAb 10 Fc. If the therapeutic action of a mAb can be modulated by regulating its interaction with FcγR expressing cells, the scope of therapeutic treatments of any blocking mAb to molecules triggered according to the KS model would be increased by varying Fc receptor binding.

The clinical trials of TGN1412 provide a very important and general caveat for the development of immune modulating mAbs before the mechanisms of immune triggering are fully understood. TGN1412 is a humanised CD28 superagonist mAb that was developed to treat autoimmune disease [285]. Pre-clinical data suggested that it activated only a certain subset of T cells and showed no major side effects [222,330]. But, during the first phase I clinical trial in humans, recipients of TGN1412 suffered an immune-mediated cytokine storm leading to multiorgan failure within 24 hours [223]. More research, therefore, must go into the molecular mechanisms and systemic immune effects which underlie the therapeutic effects of drugs targeting T cell surface receptors. This will enable the development of better and much safer drugs, and

provide clear insights into the workings of the immune system

6.2.4 The mechanism of CD28 superagonism

Using an experimental strategy that increased the distance between the epitope of a CD28 superagonist and the cell membrane without disrupting the epitope or its location on the CD28 V-set domain, it was possible to show that an epitope's proximity to the cell surface is the major determinant of CD28 mAb superagonism. This suggests that the above interpretation of the mechanism of CD28 superagonism within the context of the KS model of T cell activation is possibly correct. The superagonistic signalling observed in this system when stimulated by a non-CD28 mAb with a membrane proximal epitope not only acts as additional evidence for a KS based mechanism for CD28 superagonism, but also shows that the mAb induced differential CD28 conformational model, as proposed by Margulies (2003) [303], for superagonism cannot be the cause of the triggering observed in this system, as the mAbs involved do not bind CD28. However, while the evidence presented here conclusively disproves a conformational change model of CD28 mAb superagonism, other mechanisms that have been proposed as models of CD28 superagonism may have an influencing role in a KS based size exclusion model of CD28 superagonism.

Evidence from the triggering of hybridoma cells expressing a monomeric PD-1/CD28 chimera by a combination of two PD-1 mAbs experiments points to a role for cross-linking within the mechanism of superagonism. Stimulation of a cell line expressing CD28 fused to a membrane proximal Fc domain clearly shows that the

membrane proximal epitope of mAb A57H is the determining factor in the superagonism observed. However, a low level of signalling is observed in the absence of immobilisation, and this can be attributed to cross linking. Also, despite a lack of stimulation observed when the monomeric PD-1/CD28 chimera expressing cell line was stimulated with a single PD-1 mAb, when cross-linked by two PD-1 mAbs, the cell line is triggered and produces of IL-2. Aggregation of CD28 through mAb cross-linking is the basis of two other theories of CD28 superagonism. Dennehy *et al.* (2006) [219] suggest that CD28 superagonists have a preference for bivalent CD28 binding, compared to monovalent ligand binding, thus encouraging the formation of mAb/CD28 lattices that induce signalling. Hunig *et al.* (2005) [285] and Beyersdorf *et al.* (2006) [331], both predict that superagonistic mAbs assume a "flat" position on the membrane due to their epitope location, which encourages cross-linking. In both theories it is suggested that superagonist mAbs form a more stable lattice at the cell surface, which in turn initiates signalling. The concentration dependent activity observed with the CD28 superagonistic mAbs is similar to the "prozone" effect observed in agglutination and precipitation immunoreactions [332]. At an optimum concentration, cross-linked CD28/mAb complexes form that enhance CD28 signalling domain aggregation induced by superagonist mAbs. At higher concentrations, an excess of mAb leads to the saturation of CD28 and so prevents bivalent mAb binding. While the need for an optimum concentration of mAb indicates a role for cross-linking, the theories proposed by Dennehy *et al.* (2006) and Hunig *et al.* (2005) [219, 285], ignore the requirement for superagonist mAb immobilisation. The role that distinct bivalent

binding plays in the triggering of CD28 by superagonist mAb suggested by Dennehy *et al.* (2006) [219] is at direct odds with evidence presented in the same paper, where non-mitogenic mAbs also bind CD28 bivalently, although at high concentrations [219]. Also, experiments involving cell lines expressing CD28 fused to a membrane proximal Fc domain show that bivalent CD28 binding cannot be the cause of superagonistic signalling. This is because all the evidence suggested that the CD28 domain is expressed as wildtype in this chimera, yet stimulation with superagonist CD28 mAbs did not result in signalling. It is hard to see how the valency of CD28 changes in this chimera compared to wild type extracellular CD28 as would have to occur in the theory proposed by Dennehy *et al.*. Also, it is very unlikely that ligand valency is the distinguishing factor between superagonist and co-stimulatory anti Fc mAbs in the same cell line. Therefore, rather than being the initiating mechanism of CD28 mAb superagonistic signalling, it is possible that mAb cross-linking plays a secondary role in the mechanism, allowing for the stabilisation and expansion of close contact zones initially formed by the membrane proximal binding of superagonistic mAbs.

There is no evidence in the context of CD28 superagonism that a correlation exists between activation and mAb affinity [217]. However, triggering observed with PD-1 mAbs suggests that the affinity of agonist mAbs may have an influence on the signalling mechanism of molecules other than CD28. As previously described in this chapter, there is a correlation between mAb affinity and signalling strength in cells expressing a PD-1 chimera containing the transmembrane domain of CD3ζ. Moreover, the limiting factor observed in the activation of cells expressing a monomeric form of

PD-1 through the cross linking of mAbs 10 and 19, was the concentration of mAb 10, an mAb with a much weaker affinity for PD-1.

The evidence presented in Chapter 5 clearly shows that epitope location is the key determinant in CD28 mAbs superagonistic signalling. However, some results suggests that other factors may influence this mechanism in CD28 and also need to be considered in the study of epitope dependent agonistic mAbs that bind to other T cell signalling molecules.

With the evidence presented in this thesis implicating a KS-based mechanism in the superagonist activation of T cells, what are the implications of this on the known membrane proximal signalling events of superagonist triggering? Based on the KS model, it would be expected that phosphorylation of CD28 in these close contact zones would initiate the signalling pathways specific to CD28, which have been identified via co-stimulation signalling studies. However, research so far has shown no role for the CD28 specific PI3K or PKB pathways in CD28 superagonist signalling [227–229]. Instead CD28 superagonist signalling feeds into TCR signalling pathways at the SLP-76 signalosome stage [227,228,230]. How this occurs is unclear. There is some dispute as to whether the TCR specific kinase ZAP-70 is phosphorylated on superagonistic stimulation [227,228,231], but it is clear that functional ZAP-70 and TCR complexes must be present for superagonism to be observed. There is some evidence that SLP-76 can associate with CD28 independently of TCR signalling via the Vav adaptor [193], which could account for the absence of proximal TCR signalling in superagonism. However, this is unlikely as the signalling resulting from SLP-76/Vav complex association with

CD28 results in actin filament reorganisation, which has been shown to be deficient in cells activated by superagonist mAbs [193, 228, 229]. The KS model predicts that TCR not engaged with cognate p:MHC in close contact zones diffuses out of the area and that these are not triggered [153], therefore the role of TCR signalling pathways in CD28 superagonist signalling is puzzling. Through the employment of total internal reflection microscopy techniques, it may be possible to visualise the interactions of both membrane bound and membrane proximal cytoplasmic signalling proteins at the initiation of CD28 superagonism to understand the signalling pathways initiated by superagonists in the context of the KS model.

6.3 Implications for T cell function

6.3.1 TCR complex signalling

The incorporation of CD3ζ structural and signalling sequences into PD-1 chimeras allowed the observation of PD-1 mAb-induced signalling. However, results obtained from one of the constructs, which failed to signal, may yield information on the signalling of the CD3 complex. When a PD-1 chimera expressing the cytoplasmic domain of CD3ζ was expressed at high levels in a T cell hybridoma cell line, triggering with PD-1 mAbs did not result in any activation above background. This was perhaps not unexpected. The transmembrane residues which cause CD3ζ dimerisation are evolutionarily conserved [299], suggesting that dimerisation plays a key role in the function of CD3ζ. These residues were absent from this chimera, resulting in its

likely monomeric expression at the cell surface. However, the surprising lack of endogenous CD3 triggering by anti-CD3 mAb in the cell line indicates that whilst this form of PD-1 may not be a functional signalling molecule, its high expression in the cell induces a dominant negative CD3 signalling phenotype. How this is achieved is unclear, but it could be hypothesised that whilst the ITAMs of this construct may not be functional in their monomeric form, they can still be phosphorylated and bind kinases (Lck and ZAP70) or downstream adaptors (LAT). Its high level of expression compared to endogenous CD3 may mean that the kinases or adaptors are sequestered by the monomeric PD-1/CD3ζ chimera thus preventing endogenous CD3 signalling.

6.3.2 CD28 superagonism - Further support for KS-based signalling?

The evidence that the positioning of the epitope of a CD28 superagonist away from the membrane prevents superagonist signalling is further evidence for the KS model. In a similar experiment that illustrates the role size plays in T cell receptor triggering, Choudhuri *et al.* (2005) [161] showed, that by increasing the dimensions of the TCR:pMHC interaction via the elongation of the pMHC extracellular domain, TCR triggering was reduced without affecting TCR/p:MHC interactions. Both results support the KS model, showing that increasing the distance between the cell surface and the position of ligand/receptor or mAb/epitope ligation has a negative effect on T cell surface receptor triggering. Both actions, it would seem, ultimately increase the inter-membrane or membrane/immobilisation surface distance, allowing CD45 and other phosphatases greater access to the engaged receptors, reducing or preventing

receptor signalling.

The correlation observed between the strength of PD-1 mAb signalling and epitope location is also evidence for the KS model, and shows that this mechanism of triggering probably also applies to other small T cell signalling molecules dependent on extrinsic tyrosine kinases. The evidence for the KS model shown through the triggering of the TCR and CD28 allows these molecules to be used as models for this mechanism. However, the work in this thesis shows that the individual structural and signalling characteristics of a given signalling molecule may necessitate the inclusion of other factors in the overall mechanism of receptor triggering.

Bibliography

[1] Padlan, E.A. (1994) *Anatomy of the antibody molecule*. Mol Immunol, **31**:169–217

[2] Early, P., Huang, H., Davis, M., Calame, K. & Hood, L. (1980) *An immunoglobulin heavy chain variable region gene is generated from three segments of DNA: VH, D and JH*. Cell, **19**:981–92

[3] Stavnezer, J. (1996) *Immunoglobulin class switching*. Curr Opin Immunol, **8**:199–205

[4] Campbell, K.S. & Cambier, J.C. (1990) *B lymphocyte antigen receptors (mIg) are non-covalently associated with a disulfide linked, inducibly phosphorylated glycoprotein complex*. EMBO J, **9**:441–8

[5] Nemazee, D.A. & Burki, K. (1989) *Clonal deletion of B lymphocytes in a transgenic mouse bearing anti-MHC class I antibody genes*. Nature, **337**:562–6

[6] Gay, D., Saunders, T., Camper, S. & Weigert, M. (1993) *Receptor editing: an approach by autoreactive B cells to escape tolerance*. J Exp Med, **177**:999–1008

[7] Lederman, S., Yellin, M.J., Covey, L.R., Cleary, A.M., Callard, R. & Chess, L. (1993) *Non-antigen signals for B-cell growth and differentiation to antibody secretion*. Curr Opin Immunol, **5**:439–44

[8] Pecanha, L.M., Snapper, C.M., Finkelman, F.D. & Mond, J.J. (1991) *Dextran-conjugated anti-Ig antibodies as a model for T cell-independent type 2 antigen-mediated stimulation of Ig secretion in vitro. I. Lymphokine dependence*. J Immunol, **146**:833–9

[9] Jacob, J., Kelsoe, G., Rajewsky, K. & Weiss, U. (1991) *Intraclonal generation of antibody mutants in germinal centres*. Nature, **354**:389–92

[10] Daeron, M. (1997) *Fc receptor biology*. Annu Rev Immunol, **15**:203–34

[11] Biron, C.A., Nguyen, K.B., Pien, G.C., Cousens, L.P. & Salazar-Mather, T.P. (1999) *Natural killer cells in antiviral defense: function and regulation by innate cytokines*. Annu Rev Immunol, **17**:189–220

[12] Tomlinson, S. (1993) *Complement defense mechanisms*. Curr Opin Immunol, **5**:83–9

[13] Bjorkman, P.J., Saper, M.A., Samraoui, B., Bennett, W.S., Strominger, J.L. & Wiley, D.C. (1987) *Structure of the human class I histocompatibility antigen, HLA-A2*. Nature, **329**:506–12

[14] Purcell, A.W. & Elliott, T. (2008) *Molecular machinations of the MHC-I peptide loading complex*. Curr Opin Immunol, **20**:75–81

[15] Brown, J.H., Jardetzky, T.S., Gorga, J.C., Stern, L.J., Urban, R.G., Strominger, J.L. & Wiley, D.C. (1993) *Three-dimensional structure of the human class II histocompatibility antigen HLA-DR1*. Nature, **364**:33–9

[16] Rocha, N. & Neefjes, J. (2008) *MHC class II molecules on the move for successful antigen presentation*. EMBO J, **27**:1–5

[17] Shortman, K., Egerton, M., Spangrude, G.J. & Scollay, R. (1990) *The generation and fate of thymocytes*. Semin Immunol, **2**:3–12

[18] Dudley, E.C., Petrie, H.T., Shah, L.M., Owen, M.J. & Hayday, A.C. (1994) *T cell receptor beta chain gene rearrangement and selection during thymocyte development in adult mice*. Immunity, **1**:83–93

[19] von Boehmer, H. & Fehling, H.J. (1997) *Structure and function of the pre-T cell receptor*. Annu Rev Immunol, **15**:433–52

[20] Marrack, P. & Kappler, J. (1997) *Positive selection of thymocytes bearing alpha beta T cell receptors*. Curr Opin Immunol, **9**:250–5

[21] Strasser, A., Puthalakath, H., O'Reilly, L.A. & Bouillet, P. (2008) *What do we know about the mechanisms of elimination of autoreactive T and B cells and what challenges remain*. Immunol Cell Biol, **86**:57–66

[22] Ashton-Rickardt, P.G., Bandeira, A., Delaney, J.R., Van Kaer, L., Pircher, H.P., Zinkernagel, R.M. & Tonegawa, S. (1994) *Evidence for a differential avidity model of T cell selection in the thymus*. Cell, **76**:651–63

[23] Alberola-Ila, J., Hogquist, K.A., Swan, K.A., Bevan, M.J. & Perlmutter, R.M. (1996) *Positive and negative selection invoke distinct signaling pathways*. J Exp Med, **184**:9–18

[24] Lafferty, K.J., Andrus, L. & Prowse, S.J. (1980) *Role of lymphokine and antigen in the control of specific T cell responses*. Immunol Rev, **51**:279–314

[25] Steinbrink, K., Mahnke, K., Grabbe, S., Enk, A.H. & Jonuleit, H. (2009) *Myeloid dendritic cell: From sentinel of immunity to key player of peripheral tolerance?* Hum Immunol, **70**:289–93

[26] Celli, S., Garcia, Z., Beuneu, H. & Bousso, P. (2008) *Decoding the dynamics of T cell-dendritic cell interactions in vivo*. Immunol Rev, **221**:182–7

[27] Banchereau, J. & Steinman, R.M. (1998) *Dendritic cells and the control of immunity*. Nature, **392**:245–52

[28] Chen, X. & Jensen, P.E. (2008) *The role of B lymphocytes as antigen-presenting cells*. Arch Immunol Ther Exp (Warsz), **56**:77–83

[29] Miyasaka, M. & Tanaka, T. (2004) *Lymphocyte trafficking across high endothelial venules: dogmas and enigmas*. Nat Rev Immunol, **4**:360–70

[30] Jenkins, M.K., Chen, C.A., Jung, G., Mueller, D.L. & Schwartz, R.H. (1990) *Inhibition of antigen-specific proliferation of type 1 murine T cell clones after stimulation with immobilized anti-CD3 monoclonal antibody*. J Immunol, **144**:16–22

[31] Minami, Y., Kono, T., Miyazaki, T. & Taniguchi, T. (1993) *The IL-2 receptor complex: its structure, function, and target genes*. Annu Rev Immunol, **11**:245–68

[32] Griffiths, G.M. (1995) *The cell biology of CTL killing*. Curr Opin Immunol, **7**:343–8

[33] Medana, I.M., Gallimore, A., Oxenius, A., Martinic, M.M., Wekerle, H. & Neumann, H. (2000) *MHC class I-restricted killing of neurons by virus-specific CD8+ T lymphocytes is effected through the Fas/FasL, but not the perforin pathway*. Eur J Immunol, **30**:3623–33

[34] Romagnani, S. (1997) *The Th1/Th2 paradigm*. Immunol Today, **18**:263–6

[35] Mosmann, T.R. & Coffman, R.L. (1989) *TH1 and TH2 cells: different patterns of lymphokine secretion lead to different functional properties*. Annu Rev Immunol, **7**:145–73

[36] Lee, B.O., Haynes, L., Eaton, S.M., Swain, S.L. & Randall, T.D. (2002) *The biological outcome of CD40 signaling is dependent on the duration of CD40 ligand expression: reciprocal regulation by interleukin (IL)-4 and IL-12*. J Exp Med, **196**:693–704

[37] Harrington, L.E., Hatton, R.D., Mangan, P.R., Turner, H., Murphy, T.L., Murphy, K.M. & Weaver, C.T. (2005) *Interleukin 17-producing CD4+ effector T cells develop via a lineage distinct from the T helper type 1 and 2 lineages*. Nat Immunol, **6**:1123–32

[38] Liang, S.C., Tan, X.Y., Luxenberg, D.P., Karim, R., Dunussi-Joannopoulos, K., Collins, M. & Fouser, L.A. (2006) *Interleukin (IL)-22 and IL-17 are coexpressed by Th17 cells and cooperatively enhance expression of antimicrobial peptides*. J Exp Med, **203**:2271–9

[39] Acosta-Rodriguez, E.V., Rivino, L., Geginat, J., Jarrossay, D., Gattorno, M., Lanzavecchia, A., Sallusto, F. & Napolitani, G. (2007) *Surface phenotype and antigenic specificity of human interleukin 17-producing T helper memory cells*. Nat Immunol, **8**:639–46

[40] Milner, J.D., Brenchley, J.M., Laurence, A., Freeman, A.F., Hill, B.J., Elias, K.M., Kanno, Y., Spalding, C., Elloumi, H.Z., Paulson, M.L., Davis, J., Hsu, A., Asher, A.I., O'Shea, J., Holland, S.M., Paul, W.E. & Douek, D.C. (2008) *Impaired T(H)17 cell differentiation in subjects with autosomal dominant hyper-IgE syndrome*. Nature, **452**:773–6

[41] Fujino, S., Andoh, A., Bamba, S., Ogawa, A., Hata, K., Araki, Y., Bamba, T. & Fujiyama, Y. (2003) *Increased expression of interleukin 17 in inflammatory bowel disease*. Gut, **52**:65–70

[42] Koenders, M.I., Joosten, L.A. & van den Berg, W.B. (2006) *Potential new targets in arthritis therapy: interleukin (IL)-17 and its relation to tumour necrosis factor and IL-1 in experimental arthritis*. Ann Rheum Dis, **65 Suppl 3**:iii29–33

[43] Vignali, D.A., Collison, L.W. & Workman, C.J. (2008) *How regulatory T cells work*. Nat Rev Immunol, **8**:523–32

[44] Piccirillo, C.A. (2008) *Regulatory T cells in health and disease*. Cytokine, **43**:395–401

[45] Lighvani, A.A., Frucht, D.M., Jankovic, D., Yamane, H., Aliberti, J., Hissong, B.D., Nguyen, B.V., Gadina, M., Sher, A., Paul, W.E. & O'Shea, J.J. (2001) *T-bet is rapidly induced by interferon-gamma in lymphoid and myeloid cells*. Proc Natl Acad Sci U S A, **98**:15,137–42

[46] Le Gros, G., Ben-Sasson, S.Z., Seder, R., Finkelman, F.D. & Paul, W.E. (1990) *Generation of interleukin 4 (IL-4)-producing cells in vivo and in vitro: IL-2 and IL-4 are required for in vitro generation of IL-4-producing cells*. J Exp Med, **172**:921–9

[47] Curotto de Lafaille, M.A. & Lafaille, J.J. (2009) *Natural and adaptive foxp3+ regulatory T cells: more of the same or a division of labor?* Immunity, **30**:626–35

[48] Bannard, O., Kraman, M. & Fearon, D. (2009) *Pathways of memory CD8+ T-cell development*. Eur J Immunol, **39**:2083–7

[49] Taghon, T. & Rothenberg, E.V. (2008) *Molecular mechanisms that control mouse and human TCR-alphabeta and TCR-gammadelta T cell development*. Semin Immunopathol, **30**:383–98

[50] Chien, Y.H., Jores, R. & Crowley, M.P. (1996) *Recognition by gamma/delta T cells*. Annu Rev Immunol, **14**:511–32

[51] Hayes, S.M. & Love, P.E. (2002) *Distinct structure and signaling potential of the gamma delta TCR complex*. Immunity, **16**:827–38

[52] Bendelac, A., Lantz, O., Quimby, M.E., Yewdell, J.W., Bennink, J.R. & Brutkiewicz, R.R. (1995) *CD1 recognition by mouse NK1+ T lymphocytes*. Science, **268**:863–5

[53] Balato, A., Unutmaz, D. & Gaspari, A.A. (2009) *Natural killer T cells: an unconventional T-cell subset with diverse effector and regulatory functions*. J Invest Dermatol, **129**:1628–42

[54] Zlotnik, A., Godfrey, D.I., Fischer, M. & Suda, T. (1992) *Cytokine production by mature and immature CD4-CD8- T cells. Alpha beta-T cell receptor+ CD4-CD8- T cells produce IL-4*. J Immunol, **149**:1211–5

[55] Godfrey, D.I., MacDonald, H.R., Kronenberg, M., Smyth, M.J. & Van Kaer, L. (2004) *NKT cells: what's in a name?* Nat Rev Immunol, **4**:231–7

[56] Benlagha, K., Weiss, A., Beavis, A., Teyton, L. & Bendelac, A. (2000) *In vivo identification of glycolipid antigen-specific T cells using fluorescent CD1d tetramers*. J Exp Med, **191**:1895–903

[57] Mercer, J.C., Ragin, M.J. & August, A. (2005) *Natural killer T cells: rapid responders controlling immunity and disease*. Int J Biochem Cell Biol, **37**:1337–43

[58] Kakimi, K., Guidotti, L.G., Koezuka, Y. & Chisari, F.V. (2000) *Natural killer T cell activation inhibits hepatitis B virus replication in vivo*. J Exp Med, **192**:921–30

[59] Garcia, K.C., Tallquist, M.D., Pease, L.R., Brunmark, A., Scott, C.A., Degano, M., Stura, E.A., Peterson, P.A., Wilson, I.A. & Teyton, L. (1997) *Alphabeta T cell receptor interactions with syngeneic and allogeneic ligands: affinity measurements and crystallization*. Proc Natl Acad Sci U S A, **94**:13,838–43

[60] Samelson, L.E., Harford, J.B. & Klausner, R.D. (1985) *Identification of the components of the murine T cell antigen receptor complex*. Cell, **43**:223–31

[61] Brenner, M.B., Trowbridge, I.S. & Strominger, J.L. (1985) *Cross-linking of human T cell receptor proteins: association between the T cell idiotype beta subunit and the T3 glycoprotein heavy subunit*. Cell, **40**:183–90

[62] Wegener, A.M., Hou, X., Dietrich, J. & Geisler, C. (1995) *Distinct domains of the CD3-gamma chain are involved in surface expression and function of the T cell antigen receptor*. J Biol Chem, **270**:4675–80

[63] Sussman, J.J., Bonifacino, J.S., Lippincott-Schwartz, J., Weissman, A.M., Saito, T., Klausner, R.D. & Ashwell, J.D. (1988) *Failure to synthesize the T cell CD3-zeta chain: structure and function of a partial T cell receptor complex*. Cell, **52**:85–95

[64] Call, M.E. & Wucherpfennig, K.W. (2004) *Molecular mechanisms for the assembly of the T cell receptor-CD3 complex*. Mol Immunol, **40**:1295–305

[65] Kjer-Nielsen, L., Dunstone, M.A., Kostenko, L., Ely, L.K., Beddoe, T., Mifsud, N.A., Purcell, A.W., Brooks, A.G., McCluskey, J. & Rossjohn, J. (2004) *Crystal*

structure of the human T cell receptor CD3 epsilon gamma heterodimer complexed to the therapeutic mAb OKT3. Proc Natl Acad Sci U S A, **101**:7675–80

[66] Arnett, K.L., Harrison, S.C. & Wiley, D.C. (2004) *Crystal structure of a human CD3-epsilon/delta dimer in complex with a UCHT1 single-chain antibody fragment*. Proc Natl Acad Sci U S A, **101**:16,268–73

[67] Kuhns, M.S. & Davis, M.M. (2007) *Disruption of extracellular interactions impairs T cell receptor-CD3 complex stability and signaling*. Immunity, **26**:357–69

[68] Smith-Garvin, J.E., Koretzky, G.A. & Jordan, M.S. (2009) *T cell activation*. Annu Rev Immunol, **27**:591–619

[69] van Oers, N.S., Killeen, N. & Weiss, A. (1996) *Lck regulates the tyrosine phosphorylation of the T cell receptor subunits and ZAP-70 in murine thymocytes*. J Exp Med, **183**:1053–62

[70] van Oers, N.S., Killeen, N. & Weiss, A. (1994) *ZAP-70 is constitutively associated with tyrosine-phosphorylated TCR zeta in murine thymocytes and lymph node T cells*. Immunity, **1**:675–85

[71] Veillette, A. & Fournel, M. (1990) *The CD4 associated tyrosine protein kinase p56lck is positively regulated through its site of autophosphorylation*. Oncogene, **5**:1455–62

[72] Xu, W., Doshi, A., Lei, M., Eck, M.J. & Harrison, S.C. (1999) *Crystal structures of c-Src reveal features of its autoinhibitory mechanism*. Mol Cell, **3**:629–38

[73] Shiroo, M., Goff, L., Biffen, M., Shivnan, E. & Alexander, D. (1992) *CD45 tyrosine phosphatase-activated p59fyn couples the T cell antigen receptor to pathways of diacylglycerol production, protein kinase C activation and calcium influx*. EMBO J, **11**:4887–97

[74] Ostergaard, H.L., Shackelford, D.A., Hurley, T.R., Johnson, P., Hyman, R., Sefton, B.M. & Trowbridge, I.S. (1989) *Expression of CD45 alters phosphorylation of the lck-encoded tyrosine protein kinase in murine lymphoma T-cell lines*. Proc Natl Acad Sci U S A, **86**:8959–63

[75] Furukawa, T., Itoh, M., Krueger, N.X., Streuli, M. & Saito, H. (1994) *Specific interaction of the CD45 protein-tyrosine phosphatase with tyrosine-phosphorylated CD3 zeta chain*. Proc Natl Acad Sci U S A, **91**:10,928–32

[76] Mustelin, T., Williams, S., Tailor, P., Couture, C., Zenner, G., Burn, P., Ashwell, J.D. & Altman, A. (1995) *Regulation of the p70zap tyrosine protein kinase in T cells by the CD45 phosphotyrosine phosphatase*. Eur J Immunol, **25**:942–6

[77] Zhang, W., Sloan-Lancaster, J., Kitchen, J., Trible, R.P. & Samelson, L.E. (1998) *LAT: the ZAP-70 tyrosine kinase substrate that links T cell receptor to cellular activation*. Cell, **92**:83–92

[78] Zhang, W., Trible, R.P., Zhu, M., Liu, S.K., McGlade, C.J. & Samelson, L.E. (2000) *Association of Grb2, Gads, and phospholipase C-gamma 1 with phosphorylated LAT tyrosine residues. Effect of LAT tyrosine mutations on T cell angigen receptor-mediated signaling*. J Biol Chem, **275**:23,355–61

[79] Bubeck Wardenburg, J., Fu, C., Jackman, J.K., Flotow, H., Wilkinson, S.E., Williams, D.H., Johnson, R., Kong, G., Chan, A.C. & Findell, P.R. (1996) *Phosphorylation of SLP-76 by the ZAP-70 protein-tyrosine kinase is required for T-cell receptor function*. J Biol Chem, **271**:19,641–4

[80] Liu, S.K., Fang, N., Koretzky, G.A. & McGlade, C.J. (1999) *The hematopoietic-specific adaptor protein gads functions in T-cell signaling via interactions with the SLP-76 and LAT adaptors*. Curr Biol, **9**:67–75

[81] Koretzky, G.A., Abtahian, F. & Silverman, M.A. (2006) *SLP76 and SLP65: complex regulation of signalling in lymphocytes and beyond*. Nat Rev Immunol, **6**:67–78

[82] Oh-hora, M. & Rao, A. (2008) *Calcium signaling in lymphocytes*. Curr Opin Immunol, **20**:250–8

[83] Vallabhapurapu, S. & Karin, M. (2009) *Regulation and function of NF-kappaB transcription factors in the immune system*. Annu Rev Immunol, **27**:693–733

[84] Ebinu, J.O., Bottorff, D.A., Chan, E.Y., Stang, S.L., Dunn, R.J. & Stone, J.C. (1998) *RasGRP, a Ras guanyl nucleotide- releasing protein with calcium- and diacylglycerol-binding motifs*. Science, **280**:1082–6

[85] Roose, J.P., Mollenauer, M., Gupta, V.A., Stone, J. & Weiss, A. (2005) *A diacylglycerol-protein kinase C-RasGRP1 pathway directs Ras activation upon antigen receptor stimulation of T cells*. Mol Cell Biol, **25**:4426–41

[86] Olson, M.F. & Marais, R. (2000) *Ras protein signalling*. Semin Immunol, **12**:63–73

[87] Dong, C., Davis, R.J. & Flavell, R.A. (2002) *MAP kinases in the immune response*. Annu Rev Immunol, **20**:55–72

[88] Finco, T.S., Kadlecek, T., Zhang, W., Samelson, L.E. & Weiss, A. (1998) *LAT is required for TCR-mediated activation of PLCgamma1 and the Ras pathway*. Immunity, **9**:617–26

[89] Roose, J.P., Mollenauer, M., Ho, M., Kurosaki, T. & Weiss, A. (2007) *Unusual interplay of two types of Ras activators, RasGRP and SOS, establishes sensitive and robust Ras activation in lymphocytes*. Mol Cell Biol, **27**:2732–45

[90] Zeng, R., Cannon, J.L., Abraham, R.T., Way, M., Billadeau, D.D., Bubeck-Wardenberg, J. & Burkhardt, J.K. (2003) *SLP-76 coordinates Nck-dependent Wiskott-Aldrich syndrome protein recruitment with Vav-1/Cdc42-dependent Wiskott-Aldrich syndrome protein activation at the T cell-APC contact site*. J Immunol, **171**:1360–8

[91] Lewis, C.M., Broussard, C., Czar, M.J. & Schwartzberg, P.L. (2001) *Tec kinases: modulators of lymphocyte signaling and development*. Curr Opin Immunol, **13**:317–25

[92] Norcross, M.A. (1984) *A synaptic basis for T-lymphocyte activation*. Ann Immunol (Paris), **135D**:113–34

[93] Kupfer, A., Swain, S.L., Janeway, C. A., J. & Singer, S.J. (1986) *The specific direct interaction of helper T cells and antigen-presenting B cells*. Proc Natl Acad Sci U S A, **83**:6080–3

[94] Geiger, B., Rosen, D. & Berke, G. (1982) *Spatial relationships of microtubule-organizing centers and the contact area of cytotoxic T lymphocytes and target cells*. J Cell Biol, **95**:137–43

[95] Dustin, M.L., Olszowy, M.W., Holdorf, A.D., Li, J., Bromley, S., Desai, N., Widder, P., Rosenberger, F., van der Merwe, P.A., Allen, P.M. & Shaw, A.S. (1998) *A novel adaptor protein orchestrates receptor patterning and cytoskeletal polarity in T-cell contacts*. Cell, **94**:667–77

[96] Grakoui, A., Bromley, S.K., Sumen, C., Davis, M.M., Shaw, A.S., Allen, P.M. & Dustin, M.L. (1999) *The immunological synapse: a molecular machine controlling T cell activation*. Science, **285**:221–7

[97] Monks, C.R., Freiberg, B.A., Kupfer, H., Sciaky, N. & Kupfer, A. (1998) *Three-dimensional segregation of supramolecular activation clusters in T cells*. Nature, **395**:82–6

[98] Dustin, M.L. & Chan, A.C. (2000) *Signaling takes shape in the immune system*. Cell, **103**:283–94

[99] Lee, K.H., Holdorf, A.D., Dustin, M.L., Chan, A.C., Allen, P.M. & Shaw, A.S. (2002) *T cell receptor signaling precedes immunological synapse formation*. Science, **295**:1539–42

[100] Bunnell, S.C., Hong, D.I., Kardon, J.R., Yamazaki, T., McGlade, C.J., Barr, V.A. & Samelson, L.E. (2002) *T cell receptor ligation induces the formation of dynamically regulated signaling assemblies*. J Cell Biol, **158**:1263–75

[101] Yokosuka, T., Sakata-Sogawa, K., Kobayashi, W., Hiroshima, M., Hashimoto-Tane, A., Tokunaga, M., Dustin, M.L. & Saito, T. (2005) *Newly generated T cell receptor microclusters initiate and sustain T cell activation by recruitment of Zap70 and SLP-76*. Nat Immunol, **6**:1253–62

[102] Varma, R., Campi, G., Yokosuka, T., Saito, T. & Dustin, M.L. (2006) *T cell receptor-proximal signals are sustained in peripheral microclusters and terminated in the central supramolecular activation cluster*. Immunity, **25**:117–27

[103] Krummel, M.F., Sjaastad, M.D., Wulfing, C. & Davis, M.M. (2000) *Differential clustering of CD4 and CD3zeta during T cell recognition*. Science, **289**:1349–52

[104] Dustin, M.L. (2009) *The cellular context of T cell signaling*. Immunity, **30**:482–92

[105] Bunnell, S.C., Kapoor, V., Trible, R.P., Zhang, W. & Samelson, L.E. (2001) *Dynamic actin polymerization drives T cell receptor-induced spreading: a role for the signal transduction adaptor LAT*. Immunity, **14**:315–29

[106] Yokosuka, T., Kobayashi, W., Sakata-Sogawa, K., Takamatsu, M., Hashimoto-Tane, A., Dustin, M.L., Tokunaga, M. & Saito, T. (2008) *Spatiotemporal regulation of T cell costimulation by TCR-CD28 microclusters and protein kinase C theta translocation*. Immunity, **29**:589–601

[107] Tseng, S.Y., Waite, J.C., Liu, M., Vardhana, S. & Dustin, M.L. (2008) *T cell-dendritic cell immunological synapses contain TCR-dependent CD28-CD80 clusters that recruit protein kinase C theta*. J Immunol, **181**:4852–63

[108] Freiberg, B.A., Kupfer, H., Maslanik, W., Delli, J., Kappler, J., Zaller, D.M. & Kupfer, A. (2002) *Staging and resetting T cell activation in SMACs*. Nat Immunol, **3**:911–7

[109] Stinchcombe, J.C., Majorovits, E., Bossi, G., Fuller, S. & Griffiths, G.M. (2006) *Centrosome polarization delivers secretory granules to the immunological synapse*. Nature, **443**:462–5

[110] Beal, A.M., Anikeeva, N., Varma, R., Cameron, T.O., Norris, P.J., Dustin, M.L. & Sykulev, Y. (2008) *Protein kinase C theta regulates stability of the peripheral adhesion ring junction and contributes to the sensitivity of target cell lysis by CTL*. J Immunol, **181**:4815–24

[111] Sabatos, C.A., Doh, J., Chakravarti, S., Friedman, R.S., Pandurangi, P.G., Tooley, A.J. & Krummel, M.F. (2008) *A synaptic basis for paracrine interleukin-2 signaling during homotypic T cell interaction*. Immunity, **29**:238–48

[112] Cemerski, S., Das, J., Giurisato, E., Markiewicz, M.A., Allen, P.M., Chakraborty, A.K. & Shaw, A.S. (2008) *The balance between T cell receptor signaling and degradation at the center of the immunological synapse is determined by antigen quality*. Immunity, **29**:414–22

[113] Valitutti, S. & Lanzavecchia, A. (1997) *Serial triggering of TCRs: a basis for the sensitivity and specificity of antigen recognition*. Immunol Today, **18**:299–304

[114] Linsley, P.S., Bradshaw, J., Greene, J., Peach, R., Bennett, K.L. & Mittler, R.S. (1996) *Intracellular trafficking of CTLA-4 and focal localization towards sites of TCR engagement*. Immunity, **4**:535–43

[115] Maldonado, R.A., Irvine, D.J., Schreiber, R. & Glimcher, L.H. (2004) *A role for the immunological synapse in lineage commitment of CD4 lymphocytes*. Nature, **431**:527–32

[116] Davis, M.M., Boniface, J.J., Reich, Z., Lyons, D., Hampl, J., Arden, B. & Chien, Y. (1998) *Ligand recognition by alpha beta T cell receptors*. Annu Rev Immunol, **16**:523–44

[117] Bockaert, J. & Pin, J.P. (1999) *Molecular tinkering of G protein-coupled receptors: an evolutionary success*. EMBO J, **18**:1723–9

[118] Unwin, N., Miyazawa, A., Li, J. & Fujiyoshi, Y. (2002) *Activation of the nicotinic acetylcholine receptor involves a switch in conformation of the alpha subunits*. J Mol Biol, **319**:1165–76

[119] Garcia, K.C., Teyton, L. & Wilson, I.A. (1999) *Structural basis of T cell recognition*. Annu Rev Immunol, **17**:369–97

[120] Beddoe, T., Chen, Z., Clements, C.S., Ely, L.K., Bushell, S.R., Vivian, J.P., Kjer-Nielsen, L., Pang, S.S., Dunstone, M.A., Liu, Y.C., Macdonald, W.A., Perugini, M.A., Wilce, M.C., Burrows, S.R., Purcell, A.W., Tiganis, T., Bottomley, S.P., McCluskey, J. & Rossjohn, J. (2009) *Antigen ligation triggers a conformational change within the constant domain of the alphabeta T cell receptor*. Immunity, **30**:777–88

[121] Kuhns, M.S., Davis, M.M. & Garcia, K.C. (2006) *Deconstructing the form and function of the TCR/CD3 complex*. Immunity, **24**:133–9

[122] Ma, Z., Janmey, P.A. & Finkel, T.H. (2008) *The receptor deformation model of TCR triggering*. FASEB J, **22**:1002–8

[123] Gil, D., Schamel, W.W., Montoya, M., Sanchez-Madrid, F. & Alarcon, B. (2002) *Recruitment of Nck by CD3 epsilon reveals a ligand-induced conformational change essential for T cell receptor signaling and synapse formation*. Cell, **109**:901–12

[124] Xu, C., Gagnon, E., Call, M.E., Schnell, J.R., Schwieters, C.D., Carman, C.V., Chou, J.J. & Wucherpfennig, K.W. (2008) *Regulation of T cell receptor activation by dynamic membrane binding of the CD3epsilon cytoplasmic tyrosine-based motif*. Cell, **135**:702–13

[125] Sun, Z.J., Kim, K.S., Wagner, G. & Reinherz, E.L. (2001) *Mechanisms contributing to T cell receptor signaling and assembly revealed by the solution structure of an ectodomain fragment of the CD3 epsilon gamma heterodimer*. Cell, **105**:913–23

[126] Ottemann, K.M., Xiao, W., Shin, Y.K. & Koshland, D. E., J. (1999) *A piston model for transmembrane signaling of the aspartate receptor*. Science, **285**:1751–4

[127] Aivazian, D. & Stern, L.J. (2000) *Phosphorylation of T cell receptor zeta is regulated by a lipid dependent folding transition*. Nat Struct Biol, **7**:1023–6

[128] Gil, D., Schrum, A.G., Alarcon, B. & Palmer, E. (2005) *T cell receptor engagement by peptide-MHC ligands induces a conformational change in the CD3 complex of thymocytes*. J Exp Med, **201**:517–22

[129] Davis, M.M. (2002) *A new trigger for T cells*. Cell, **110**:285–7

[130] Szymczak, A.L., Workman, C.J., Gil, D., Dilioglou, S., Vignali, K.M., Palmer, E. & Vignali, D.A. (2005) *The CD3epsilon proline-rich sequence, and its interaction with Nck, is not required for T cell development and function*. J Immunol, **175**:270–5

[131] Walter, M.R., Windsor, W.T., Nagabhushan, T.L., Lundell, D.J., Lunn, C.A., Zauodny, P.J. & Narula, S.K. (1995) *Crystal structure of a complex between interferon-gamma and its soluble high-affinity receptor*. Nature, **376**:230–5

[132] Cunningham, B.C., Ultsch, M., De Vos, A.M., Mulkerrin, M.G., Clauser, K.R. & Wells, J.A. (1991) *Dimerization of the extracellular domain of the human growth hormone receptor by a single hormone molecule*. Science, **254**:821–5

[133] Jura, N., Endres, N.F., Engel, K., Deindl, S., Das, R., Lamers, M.H., Wemmer, D.E., Zhang, X. & Kuriyan, J. (2009) *Mechanism for activation of the EGF receptor catalytic domain by the juxtamembrane segment*. Cell, **137**:1293–307

[134] Mohammadi, M., Olsen, S.K. & Ibrahimi, O.A. (2005) *Structural basis for fibroblast growth factor receptor activation*. Cytokine Growth Factor Rev, **16**:107–37

[135] Irvine, D.J., Purbhoo, M.A., Krogsgaard, M. & Davis, M.M. (2002) *Direct observation of ligand recognition by T cells*. Nature, **419**:845–9

[136] Purbhoo, M.A., Irvine, D.J., Huppa, J.B. & Davis, M.M. (2004) *T cell killing does not require the formation of a stable mature immunological synapse*. Nat Immunol, **5**:524–30

[137] Harding, C.V. & Unanue, E.R. (1990) *Quantitation of antigen-presenting cell MHC class II/peptide complexes necessary for T-cell stimulation*. Nature, **346**:574–6

[138] Christinck, E.R., Luscher, M.A., Barber, B.H. & Williams, D.B. (1991) *Peptide binding to class I MHC on living cells and quantitation of complexes required for CTL lysis*. Nature, **352**:67–70

[139] Trautmann, A. & Randriamampita, C. (2003) *Initiation of TCR signalling revisited*. Trends Immunol, **24**:425–8

[140] Delon, J., Gregoire, C., Malissen, B., Darche, S., Lemaitre, F., Kourilsky, P., Abastado, J.P. & Trautmann, A. (1998) *CD8 expression allows T cell signaling by monomeric peptide-MHC complexes*. Immunity, **9**:467–73

[141] Locksley, R.M., Reiner, S.L., Hatam, F., Littman, D.R. & Killeen, N. (1993) *Helper T cells without CD4: control of leishmaniasis in CD4-deficient mice*. Science, **261**:1448–51

[142] Schilham, M.W., Fung-Leung, W.P., Rahemtulla, A., Kuendig, T., Zhang, L., Potter, J., Miller, R.G., Hengartner, H. & Mak, T.W. (1993) *Alloreactive cytotoxic T cells can develop and function in mice lacking both CD4 and CD8*. Eur J Immunol, **23**:1299–304

[143] Krogsgaard, M., Li, Q.J., Sumen, C., Huppa, J.B., Huse, M. & Davis, M.M. (2005) *Agonist/endogenous peptide-MHC heterodimers drive T cell activation and sensitivity*. Nature, **434**:238–43

[144] Minguet, S. & Schamel, W.W. (2008) *Permissive geometry model*. Adv Exp Med Biol, **640**:113–20

[145] Minguet, S. & Schamel, W.W. (2008) *A permissive geometry model for TCR-CD3 activation*. Trends Biochem Sci, **33**:51–7

[146] Rudolph, M.G., Stanfield, R.L. & Wilson, I.A. (2006) *How TCRs bind MHCs, peptides, and coreceptors*. Annu Rev Immunol, **24**:419–66

[147] Sundberg, E.J., Deng, L. & Mariuzza, R.A. (2007) *TCR recognition of peptide/MHC class II complexes and superantigens*. Semin Immunol, **19**:262–71

[148] Krishna, S., Benaroch, P. & Pillai, S. (1992) *Tetrameric cell-surface MHC class I molecules*. Nature, **357**:164–7

[149] Matko, J., Bushkin, Y., Wei, T. & Edidin, M. (1994) *Clustering of class I HLA molecules on the surfaces of activated and transformed human cells*. J Immunol, **152**:3353–60

[150] Manger, B., Weiss, A., Imboden, J., Laing, T. & Stobo, J.D. (1987) *The role of protein kinase C in transmembrane signaling by the T cell antigen receptor complex. Effects of stimulation with soluble or immobilized CD3 antibodies*. J Immunol, **139**:2755–60

[151] Geppert, T.D. & Lipsky, P.E. (1988) *Activation of T lymphocytes by immobilized monoclonal antibodies to CD3. Regulatory influences of monoclonal antibodies to additional T cell surface determinants*. J Clin Invest, **81**:1497–505

[152] Geppert, T.D., Wacholtz, M.C., Davis, L.S. & Lipsky, P.E. (1988) *Activation of human T4 cells by cross-linking class I MHC molecules*. J Immunol, **140**:2155–64

[153] Davis, S.J. & van der Merwe, P.A. (2006) *The kinetic-segregation model: TCR triggering and beyond*. Nat Immunol, **7**:803–9

[154] Davis, S.J. & van der Merwe, P.A. (1996) *The structure and ligand interactions of CD2: implications for T-cell function*. Immunol Today, **17**:177–87

[155] Springer, T.A. (1990) *Adhesion receptors of the immune system*. Nature, **346**:425–34

[156] Secrist, J.P., Burns, L.A., Karnitz, L., Koretzky, G.A. & Abraham, R.T. (1993) *Stimulatory effects of the protein tyrosine phosphatase inhibitor, pervanadate, on T-cell activation events*. J Biol Chem, **268**:5886–93

[157] Mustelin, T., Coggeshall, K.M. & Altman, A. (1989) *Rapid activation of the T-cell tyrosine protein kinase pp56lck by the CD45 phosphotyrosine phosphatase*. Proc Natl Acad Sci U S A, **86**:6302–6

[158] Trowbridge, I.S. & Thomas, M.L. (1994) *CD45: an emerging role as a protein tyrosine phosphatase required for lymphocyte activation and development*. Annu Rev Immunol, **12**:85–116

[159] Irles, C., Symons, A., Michel, F., Bakker, T.R., van der Merwe, P.A. & Acuto, O. (2003) *CD45 ectodomain controls interaction with GEMs and Lck activity for optimal TCR signaling*. Nat Immunol, **4**:189–97

[160] Lin, C.H. & Hunig, T. (2003) *Efficient expansion of regulatory T cells in vitro and in vivo with a CD28 superagonist*. Eur J Immunol, **33**:626–38

[161] Choudhuri, K., Wiseman, D., Brown, M.H., Gould, K. & van der Merwe, P.A. (2005) *T-cell receptor triggering is critically dependent on the dimensions of its peptide-MHC ligand*. Nature, **436**:578–82

[162] Choudhuri, K. & van der Merwe, P.A. (2007) *Molecular mechanisms involved in T cell receptor triggering*. Semin Immunol, **19**:255–61

[163] Varma, R. (2008) *TCR triggering by the pMHC complex: valency, affinity, and dynamics*. Sci Signal, **1**:pe21

[164] Horejsi, V. (2005) *Lipid rafts and their roles in T-cell activation*. Microbes Infect, **7**:310–6

[165] Zech, T., Ejsing, C.S., Gaus, K., de Wet, B., Shevchenko, A., Simons, K. & Harder, T. (2009) *Accumulation of raft lipids in T-cell plasma membrane domains engaged in TCR signalling*. EMBO J, **28**:466–76

[166] Sadra, A., Cinek, T. & Imboden, J.B. (2004) *Translocation of CD28 to lipid rafts and costimulation of IL-2*. Proc Natl Acad Sci U S A, **101**:11,422–7

[167] Patel, V.P., Moran, M., Low, T.A. & Miceli, M.C. (2001) *A molecular framework for two-step T cell signaling: Lck Src homology 3 mutations discriminate distinctly regulated lipid raft reorganization events*. J Immunol, **166**:754–64

[168] Shaw, A.S. (2006) *Lipid rafts: now you see them, now you don't*. Nat Immunol, **7**:1139–42

[169] Munro, S. (2003) *Lipid rafts: elusive or illusive?* Cell, **115**:377–88

[170] Schwartz, R.H., Mueller, D.L., Jenkins, M.K. & Quill, H. (1989) *T-cell clonal anergy*. Cold Spring Harb Symp Quant Biol, **54 Pt 2**:605–10

[171] June, C.H., Ledbetter, J.A., Linsley, P.S. & Thompson, C.B. (1990) *Role of the CD28 receptor in T-cell activation*. Immunol Today, **11**:211–6

[172] Brunet, J.F., Denizot, F., Luciani, M.F., Roux-Dosseto, M., Suzan, M., Mattei, M.G. & Golstein, P. (1987) *A new member of the immunoglobulin superfamily–CTLA-4*. Nature, **328**:267–70

[173] Rudd, C.E., Taylor, A. & Schneider, H. (2009) *CD28 and CTLA-4 coreceptor expression and signal transduction*. Immunol Rev, **229**:12–26

[174] Azuma, M., Ito, D., Yagita, H., Okumura, K., Phillips, J.H., Lanier, L.L. & Somoza, C. (1993) *B70 antigen is a second ligand for CTLA-4 and CD28*. Nature, **366**:76–9

[175] Freeman, G.J., Borriello, F., Hodes, R.J., Reiser, H., Gribben, J.G., Ng, J.W., Kim, J., Goldberg, J.M., Hathcock, K., Laszlo, G. & et al. (1993) *Murine B7-2, an alternative CTLA4 counter-receptor that costimulates T cell proliferation and interleukin 2 production*. J Exp Med, **178**:2185–92

[176] Waterhouse, P., Penninger, J.M., Timms, E., Wakeham, A., Shahinian, A., Lee, K.P., Thompson, C.B., Griesser, H. & Mak, T.W. (1995) *Lymphoproliferative disorders with early lethality in mice deficient in Ctla-4*. Science, **270**:985–8

[177] Tivol, E.A., Borriello, F., Schweitzer, A.N., Lynch, W.P., Bluestone, J.A. & Sharpe, A.H. (1995) *Loss of CTLA-4 leads to massive lymphoproliferation and fatal multiorgan tissue destruction, revealing a critical negative regulatory role of CTLA-4*. Immunity, **3**:541–7

[178] Sharpe, A.H. (2009) *Mechanisms of costimulation*. Immunol Rev, **229**:5–11

[179] Hara, T., Fu, S.M. & Hansen, J.A. (1985) *Human T cell activation. II. A new activation pathway used by a major T cell population via a disulfide-bonded dimer of a 44 kilodalton polypeptide (9.3 antigen)*. J Exp Med, **161**:1513–24

[180] Naluai, A.T., Nilsson, S., Samuelsson, L., Gudjonsdottir, A.H., Ascher, H., Ek, J., Hallberg, B., Kristiansson, B., Martinsson, T., Nerman, O., Sollid, L.M. & Wahlstrom, J. (2000) *The CTLA4/CD28 gene region on chromosome 2q33 confers susceptibility to celiac disease in a way possibly distinct from that of type 1 diabetes and other chronic inflammatory disorders*. Tissue Antigens, **56**:350–5

[181] Lenschow, D.J., Walunas, T.L. & Bluestone, J.A. (1996) *CD28/B7 system of T cell costimulation*. Annu Rev Immunol, **14**:233–58

[182] Green, J.M., Noel, P.J., Sperling, A.I., Walunas, T.L., Gray, G.S., Bluestone, J.A. & Thompson, C.B. (1994) *Absence of B7-dependent responses in CD28-deficient mice*. Immunity, **1**:501–8

[183] Lucas, P.J., Negishi, I., Nakayama, K., Fields, L.E. & Loh, D.Y. (1995) *Naive CD28-deficient T cells can initiate but not sustain an in vitro antigen-specific immune response*. J Immunol, **154**:5757–68

[184] Evans, E.J., Esnouf, R.M., Manso-Sancho, R., Gilbert, R.J., James, J.R., Yu, C., Fennelly, J.A., Vowles, C., Hanke, T., Walse, B., Hunig, T., Sorensen, P., Stuart, D.I. & Davis, S.J. (2005) *Crystal structure of a soluble CD28-Fab complex*. Nat Immunol, **6**:271–9

[185] Thompson, C.B., Lindsten, T., Ledbetter, J.A., Kunkel, S.L., Young, H.A., Emerson, S.G., Leiden, J.M. & June, C.H. (1989) *CD28 activation pathway regulates the production of multiple T-cell-derived lymphokines/cytokines*. Proc Natl Acad Sci U S A, **86**:1333–7

[186] Sperling, A.I., Auger, J.A., Ehst, B.D., Rulifson, I.C., Thompson, C.B. & Bluestone, J.A. (1996) *CD28/B7 interactions deliver a unique signal to naive T cells that regulates cell survival but not early proliferation*. J Immunol, **157**:3909–17

[187] Boise, L.H., Minn, A.J., Noel, P.J., June, C.H., Accavitti, M.A., Lindsten, T. & Thompson, C.B. (1995) *CD28 costimulation can promote T cell survival by enhancing the expression of Bcl-XL*. Immunity, **3**:87–98

[188] Shahinian, A., Pfeffer, K., Lee, K.P., Kundig, T.M., Kishihara, K., Wakeham, A., Kawai, K., Ohashi, P.S., Thompson, C.B. & Mak, T.W. (1993) *Differential T cell costimulatory requirements in CD28-deficient mice*. Science, **261**:609–12

[189] Seder, R.A., Germain, R.N., Linsley, P.S. & Paul, W.E. (1994) *CD28-mediated costimulation of interleukin 2 (IL-2) production plays a critical role in T cell priming for IL-4 and interferon gamma production*. J Exp Med, **179**:299–304

[190] Andres, P.G., Howland, K.C., Dresnek, D., Edmondson, S., Abbas, A.K. & Krummel, M.F. (2004) *CD28 signals in the immature immunological synapse*. J Immunol, **172**:5880–6

[191] Ikemizu, S., Gilbert, R.J., Fennelly, J.A., Collins, A.V., Harlos, K., Jones, E.Y., Stuart, D.I. & Davis, S.J. (2000) *Structure and dimerization of a soluble form of B7-1*. Immunity, **12**:51–60

[192] Gross, J.A., Callas, E. & Allison, J.P. (1992) *Identification and distribution of the costimulatory receptor CD28 in the mouse*. J Immunol, **149**:380–8

[193] Rudd, C.E. & Schneider, H. (2003) *Unifying concepts in CD28, ICOS and CTLA4 co-receptor signalling*. Nat Rev Immunol, **3**:544–56

[194] Greenwald, R.J., Freeman, G.J. & Sharpe, A.H. (2005) *The B7 family revisited*. Annu Rev Immunol, **23**:515–48

[195] Chikuma, S. & Bluestone, J.A. (2003) *CTLA-4 and tolerance: the biochemical point of view*. Immunol Res, **28**:241–53

[196] Metzler, W.J., Bajorath, J., Fenderson, W., Shaw, S.Y., Constantine, K.L., Naemura, J., Leytze, G., Peach, R.J., Lavoie, T.B., Mueller, L. & Linsley, P.S. (1997) *Solution structure of human CTLA-4 and delineation of a CD80/CD86 binding site conserved in CD28*. Nat Struct Biol, **4**:527–31

[197] Collins, A.V., Brodie, D.W., Gilbert, R.J., Iaboni, A., Manso-Sancho, R., Walse, B., Stuart, D.I., van der Merwe, P.A. & Davis, S.J. (2002) *The interaction properties of costimulatory molecules revisited*. Immunity, **17**:201–10

[198] Linsley, P.S., Brady, W., Urnes, M., Grosmaire, L.S., Damle, N.K. & Ledbetter, J.A. (1991) *CTLA-4 is a second receptor for the B cell activation antigen B7*. J Exp Med, **174**:561–9

[199] Diehn, M., Alizadeh, A.A., Rando, O.J., Liu, C.L., Stankunas, K., Botstein, D., Crabtree, G.R. & Brown, P.O. (2002) *Genomic expression programs and the integration of the CD28 costimulatory signal in T cell activation*. Proc Natl Acad Sci U S A, **99**:11,796–801

[200] Riley, J.L., Mao, M., Kobayashi, S., Biery, M., Burchard, J., Cavet, G., Gregson, B.P., June, C.H. & Linsley, P.S. (2002) *Modulation of TCR-induced transcriptional profiles by ligation of CD28, ICOS, and CTLA-4 receptors*. Proc Natl Acad Sci U S A, **99**:11,790–5

[201] Prasad, K.V., Cai, Y.C., Raab, M., Duckworth, B., Cantley, L., Shoelson, S.E. & Rudd, C.E. (1994) *T-cell antigen CD28 interacts with the lipid kinase phosphatidylinositol 3-kinase by a cytoplasmic Tyr(P)-Met-Xaa-Met motif*. Proc Natl Acad Sci U S A, **91**:2834–8

[202] Truitt, K.E., Hicks, C.M. & Imboden, J.B. (1994) *Stimulation of CD28 triggers an association between CD28 and phosphatidylinositol 3-kinase in Jurkat T cells*. J Exp Med, **179**:1071–6

[203] Raab, M., Cai, Y.C., Bunnell, S.C., Heyeck, S.D., Berg, L.J. & Rudd, C.E. (1995) *p56Lck and p59Fyn regulate CD28 binding to phosphatidylinositol 3-kinase, growth factor receptor-bound protein GRB-2, and T cell-specific protein-tyrosine kinase ITK: implications for T-cell costimulation*. Proc Natl Acad Sci U S A, **92**:8891–5

[204] Sasaki, T., Irie-Sasaki, J., Jones, R.G., Oliveira-dos Santos, A.J., Stanford, W.L., Bolon, B., Wakeham, A., Itie, A., Bouchard, D., Kozieradzki, I., Joza, N., Mak, T.W., Ohashi, P.S., Suzuki, A. & Penninger, J.M. (2000) *Function of PI3Kgamma in thymocyte development, T cell activation, and neutrophil migration*. Science, **287**:1040–6

[205] Alessi, D.R., Deak, M., Casamayor, A., Caudwell, F.B., Morrice, N., Norman, D.G., Gaffney, P., Reese, C.B., MacDougall, C.N., Harbison, D., Ashworth, A. & Bownes, M. (1997) *3-Phosphoinositide-dependent protein kinase-1 (PDK1): structural and functional homology with the Drosophila DSTPK61 kinase*. Curr Biol, **7**:776–89

[206] Kim, H.H., Tharayil, M. & Rudd, C.E. (1998) *Growth factor receptor-bound protein 2 SH2/SH3 domain binding to CD28 and its role in co-signaling*. J Biol Chem, **273**:296–301

[207] Raab, M., Pfister, S. & Rudd, C.E. (2001) *CD28 signaling via VAV/SLP-76 adaptors: regulation of cytokine transcription independent of TCR ligation*. Immunity, **15**:921–33

[208] Bustelo, X.R. (2000) *Regulatory and signaling properties of the Vav family*. Mol Cell Biol, **20**:1461–77

[209] Harada, Y., Ohgai, D., Watanabe, R., Okano, K., Koiwai, O., Tanabe, K., Toma, H., Altman, A. & Abe, R. (2003) *A single amino acid alteration in cytoplasmic domain determines IL-2 promoter activation by ligation of CD28 but not inducible costimulator (ICOS)*. J Exp Med, **197**:257–62

[210] Sanchez-Lockhart, M., Graf, B. & Miller, J. (2008) *Signals and sequences that control CD28 localization to the central region of the immunological synapse*. J Immunol, **181**:7639–48

[211] Takeda, K., Harada, Y., Watanabe, R., Inutake, Y., Ogawa, S., Onuki, K., Kagaya, S., Tanabe, K., Kishimoto, H. & Abe, R. (2008) *CD28 stimulation triggers NF-kappaB activation through the CARMA1-PKCtheta-Grb2/Gads axis*. Int Immunol, **20**:1507–15

[212] Annibaldi, A., Sajeva, A., Muscolini, M., Ciccosanti, F., Corazzari, M., Piacentini, M. & Tuosto, L. (2008) *CD28 ligation in the absence of TCR promotes RelA/NF-kappaB recruitment and trans-activation of the HIV-1 LTR*. Eur J Immunol, **38**:1446–51

[213] Tavano, R., Contento, R.L., Baranda, S.J., Soligo, M., Tuosto, L., Manes, S. & Viola, A. (2006) *CD28 interaction with filamin-A controls lipid raft accumulation at the T-cell immunological synapse*. Nat Cell Biol, **8**:1270–6

[214] Hayashi, K. & Altman, A. (2006) *Filamin A is required for T cell activation mediated by protein kinase C-theta*. J Immunol, **177**:1721–8

[215] Bromley, S.K., Iaboni, A., Davis, S.J., Whitty, A., Green, J.M., Shaw, A.S., Weiss, A. & Dustin, M.L. (2001) *The immunological synapse and CD28-CD80 interactions*. Nat Immunol, **2**:1159–66

[216] Siefken, R., Kurrle, R. & Schwinzer, R. (1997) *CD28-mediated activation of resting human T cells without costimulation of the CD3/TCR complex*. Cell Immunol, **176**:59–65

[217] Tacke, M., Hanke, G., Hanke, T. & Hunig, T. (1997) *CD28-mediated induction of proliferation in resting T cells in vitro and in vivo without engagement of the T cell receptor: evidence for functionally distinct forms of CD28*. Eur J Immunol, **27**:239–47

[218] Luhder, F., Huang, Y., Dennehy, K.M., Guntermann, C., Muller, I., Winkler, E., Kerkau, T., Ikemizu, S., Davis, S.J., Hanke, T. & Hunig, T. (2003) *Topological requirements and signaling properties of T cell-activating, anti-CD28 antibody superagonists*. J Exp Med, **197**:955–66

[219] Dennehy, K.M., Elias, F., Zeder-Lutz, G., Ding, X., Altschuh, D., Luhder, F. & Hunig, T. (2006) *Cutting edge: monovalency of CD28 maintains the antigen dependence of T cell costimulatory responses*. J Immunol, **176**:5725–9

[220] Kitazawa, Y., Fujino, M., Sakai, T., Azuma, H., Kimura, H., Isaka, Y., Takahara, S., Hunig, T., Abe, R. & Li, X.K. (2008) *Foxp3-expressing regulatory T cells expanded with CD28 superagonist antibody can prevent rat cardiac allograft rejection*. J Heart Lung Transplant, **27**:362–71

[221] Schmidt, J., Elflein, K., Stienekemeier, M., Rodriguez-Palmero, M., Schneider, C., Toyka, K.V., Gold, R. & Hunig, T. (2003) *Treatment and prevention of experimental autoimmune neuritis with superagonistic CD28-specific monoclonal antibodies*. J Neuroimmunol, **140**:143–52

[222] Beyersdorf, N., Gaupp, S., Balbach, K., Schmidt, J., Toyka, K.V., Lin, C.H., Hanke, T., Hunig, T., Kerkau, T. & Gold, R. (2005) *Selective targeting of regulatory T cells with CD28 superagonists allows effective therapy of experimental autoimmune encephalomyelitis*. J Exp Med, **202**:445–55

[223] Suntharalingam, G., Perry, M.R., Ward, S., Brett, S.J., Castello-Cortes, A., Brunner, M.D. & Panoskaltsis, N. (2006) *Cytokine storm in a phase 1 trial of the anti-CD28 monoclonal antibody TGN1412*. N Engl J Med, **355**:1018–28

[224] Health, D.o. (2006) *Expert Scientific Group on phase one clinical trials: A consultation*

[225] St Clair, E.W. (2008) *The calm after the cytokine storm: lessons from the TGN1412 trial*. J Clin Invest, **118**:1344–7

[226] Stebbings, R., Findlay, L., Edwards, C., Eastwood, D., Bird, C., North, D., Mistry, Y., Dilger, P., Liefooghe, E., Cludts, I., Fox, B., Tarrant, G., Robinson, J., Meager, T., Dolman, C., Thorpe, S.J., Bristow, A., Wadhwa, M., Thorpe, R. & Poole, S. (2007) *"Cytokine storm" in the phase I trial of monoclonal antibody TGN1412: better understanding the causes to improve preclinical testing of immunotherapeutics*. J Immunol, **179**:3325–31

[227] Dennehy, K.M., Elias, F., Na, S.Y., Fischer, K.D., Hunig, T. & Luhder, F. (2007) *Mitogenic CD28 signals require the exchange factor Vav1 to enhance TCR signaling at the SLP-76-Vav-Itk signalosome*. J Immunol, **178**:1363–71

[228] Waibler, Z., Sender, L.Y., Merten, C., Hartig, R., Kliche, S., Gunzer, M., Reichardt, P., Kalinke, U. & Schraven, B. (2008) *Signaling signatures and functional properties of anti-human CD28 superagonistic antibodies*. PLoS ONE, **3**:e1708

[229] Sester, U., Wabnitz, G.H., Kirchgessner, H. & Samstag, Y. (2007) *Ras/PI3kinase/cofilin-independent activation of human CD45RA+ and CD45RO+ T cells by superagonistic CD28 stimulation*. Eur J Immunol, **37**:2881–91

[230] Dennehy, K.M., Kerstan, A., Bischof, A., Park, J.H., Na, S.Y. & Hunig, T. (2003) *Mitogenic signals through CD28 activate the protein kinase Ctheta-NF-kappaB pathway in primary peripheral T cells*. Int Immunol, **15**:655–63

[231] Levin, S.E., Zhang, C., Kadlecek, T.A., Shokat, K.M. & Weiss, A. (2008) *Inhibition of ZAP-70 kinase activity via an analog-sensitive allele blocks T cell receptor and CD28 superagonist signaling*. J Biol Chem, **283**:15,419–30

[232] Ishida, Y., Agata, Y., Shibahara, K. & Honjo, T. (1992) *Induced expression of PD-1, a novel member of the immunoglobulin gene superfamily, upon programmed cell death*. EMBO J, **11**:3887–95

[233] Nishimura, H., Nose, M., Hiai, H., Minato, N. & Honjo, T. (1999) *Development of lupus-like autoimmune diseases by disruption of the PD-1 gene encoding an ITIM motif-carrying immunoreceptor*. Immunity, **11**:141–51

[234] Nishimura, H., Okazaki, T., Tanaka, Y., Nakatani, K., Hara, M., Matsumori, A., Sasayama, S., Mizoguchi, A., Hiai, H., Minato, N. & Honjo, T. (2001) *Autoimmune dilated cardiomyopathy in PD-1 receptor-deficient mice*. Science, **291**:319–22

[235] Keir, M.E., Francisco, L.M. & Sharpe, A.H. (2007) *PD-1 and its ligands in T-cell immunity*. Curr Opin Immunol, **19**:309–14

[236] Sharpe, A.H., Wherry, E.J., Ahmed, R. & Freeman, G.J. (2007) *The function of programmed cell death 1 and its ligands in regulating autoimmunity and infection*. Nat Immunol, **8**:239–45

[237] Liang, S.C., Latchman, Y.E., Buhlmann, J.E., Tomczak, M.F., Horwitz, B.H., Freeman, G.J. & Sharpe, A.H. (2003) *Regulation of PD-1, PD-L1, and PD-L2 expression during normal and autoimmune responses*. Eur J Immunol, **33**:2706–16

[238] Nishimura, H., Agata, Y., Kawasaki, A., Sato, M., Imamura, S., Minato, N., Yagita, H., Nakano, T. & Honjo, T. (1996) *Developmentally regulated expression of the PD-1 protein on the surface of double-negative (CD4-CD8-) thymocytes*. Int Immunol, **8**:773–80

[239] Agata, Y., Kawasaki, A., Nishimura, H., Ishida, Y., Tsubata, T., Yagita, H. & Honjo, T. (1996) *Expression of the PD-1 antigen on the surface of stimulated mouse T and B lymphocytes*. Int Immunol, **8**:765–72

[240] Raimondi, G., Shufesky, W.J., Tokita, D., Morelli, A.E. & Thomson, A.W. (2006) *Regulated compartmentalization of programmed cell death-1 discriminates CD4+CD25+ resting regulatory T cells from activated T cells*. J Immunol, **176**:2808–16

[241] Dong, H., Zhu, G., Tamada, K. & Chen, L. (1999) *B7-H1, a third member of the B7 family, co-stimulates T-cell proliferation and interleukin-10 secretion*. Nat Med, **5**:1365–9

[242] Freeman, G.J., Long, A.J., Iwai, Y., Bourque, K., Chernova, T., Nishimura, H., Fitz, L.J., Malenkovich, N., Okazaki, T., Byrne, M.C., Horton, H.F., Fouser, L., Carter, L., Ling, V., Bowman, M.R., Carreno, B.M., Collins, M., Wood, C.R. & Honjo, T. (2000) *Engagement of the PD-1 immunoinhibitory receptor by a novel B7 family member leads to negative regulation of lymphocyte activation*. J Exp Med, **192**:1027–34

[243] Latchman, Y., Wood, C.R., Chernova, T., Chaudhary, D., Borde, M., Chernova, I., Iwai, Y., Long, A.J., Brown, J.A., Nunes, R., Greenfield, E.A., Bourque, K., Boussiotis, V.A., Carter, L.L., Carreno, B.M., Malenkovich, N., Nishimura, H., Okazaki, T., Honjo, T., Sharpe, A.H. & Freeman, G.J. (2001) *PD-L2 is a second ligand for PD-1 and inhibits T cell activation*. Nat Immunol, **2**:261–8

[244] Tseng, S.Y., Otsuji, M., Gorski, K., Huang, X., Slansky, J.E., Pai, S.I., Shalabi, A., Shin, T., Pardoll, D.M. & Tsuchiya, H. (2001) *B7-DC, a new dendritic cell molecule with potent costimulatory properties for T cells*. J Exp Med, **193**:839–46

[245] Yamazaki, T., Akiba, H., Iwai, H., Matsuda, H., Aoki, M., Tanno, Y., Shin, T., Tsuchiya, H., Pardoll, D.M., Okumura, K., Azuma, M. & Yagita, H. (2002) *Expression of programmed death 1 ligands by murine T cells and APC*. J Immunol, **169**:5538–45

[246] Nakae, S., Suto, H., Iikura, M., Kakurai, M., Sedgwick, J.D., Tsai, M. & Galli, S.J. (2006) *Mast cells enhance T cell activation: importance of mast cell costimulatory molecules and secreted TNF*. J Immunol, **176**:2238–48

[247] Barber, D.L., Wherry, E.J., Masopust, D., Zhu, B., Allison, J.P., Sharpe, A.H., Freeman, G.J. & Ahmed, R. (2006) *Restoring function in exhausted CD8 T cells during chronic viral infection*. Nature, **439**:682–7

[248] Nishimura, H., Honjo, T. & Minato, N. (2000) *Facilitation of beta selection and modification of positive selection in the thymus of PD-1-deficient mice*. J Exp Med, **191**:891–8

[249] Keir, M.E., Latchman, Y.E., Freeman, G.J. & Sharpe, A.H. (2005) *Programmed death-1 (PD-1):PD-ligand 1 interactions inhibit TCR-mediated positive selection of thymocytes*. J Immunol, **175**:7372–9

[250] Blank, C., Brown, I., Marks, R., Nishimura, H., Honjo, T. & Gajewski, T.F. (2003) *Absence of programmed death receptor 1 alters thymic development and enhances generation of CD4/CD8 double-negative TCR-transgenic T cells*. J Immunol, **171**:4574–81

[251] Brown, J.A., Dorfman, D.M., Ma, F.R., Sullivan, E.L., Munoz, O., Wood, C.R., Greenfield, E.A. & Freeman, G.J. (2003) *Blockade of programmed death-1 ligands on dendritic cells enhances T cell activation and cytokine production*. J Immunol, **170**:1257–66

[252] Guleria, I., Khosroshahi, A., Ansari, M.J., Habicht, A., Azuma, M., Yagita, H., Noelle, R.J., Coyle, A., Mellor, A.L., Khoury, S.J. & Sayegh, M.H. (2005) *A critical role for the programmed death ligand 1 in fetomaternal tolerance*. J Exp Med, **202**:231–7

[253] Sabapatha, A., Gercel-Taylor, C. & Taylor, D.D. (2006) *Specific isolation of placenta-derived exosomes from the circulation of pregnant women and their immunoregulatory consequences*. Am J Reprod Immunol, **56**:345–55

[254] Hori, J., Wang, M., Miyashita, M., Tanemoto, K., Takahashi, H., Takemori, T., Okumura, K., Yagita, H. & Azuma, M. (2006) *B7-H1-induced apoptosis as a mechanism of immune privilege of corneal allografts*. J Immunol, **177**:5928–35

[255] Ansari, M.J., Salama, A.D., Chitnis, T., Smith, R.N., Yagita, H., Akiba, H., Yamazaki, T., Azuma, M., Iwai, H., Khoury, S.J., Auchincloss, H., J. & Sayegh, M.H. (2003) *The programmed death-1 (PD-1) pathway regulates autoimmune diabetes in nonobese diabetic (NOD) mice*. J Exp Med, **198**:63–9

[256] Fife, B.T., Guleria, I., Gubbels Bupp, M., Eagar, T.N., Tang, Q., Bour-Jordan, H., Yagita, H., Azuma, M., Sayegh, M.H. & Bluestone, J.A. (2006) *Insulin-induced remission in new-onset NOD mice is maintained by the PD-1-PD-L1 pathway*. J Exp Med, **203**:2737–47

[257] Wolf, A., Kabat, E. & Bezer, A. (1947) *The patholgy of acute disseminated encephalomyelitis produced experimentally in the rhesus monkey and its resemblance to*

human demyelinating disease. Journal of Neuropathology and Experimental Neurology, **6**:333–357

[258] Olitsky, P.K. & Yager, R.H. (1949) *Experimental disseminated encephalomyelitis in white mice*. J Exp Med, **90**:213–24

[259] Salama, A.D., Chitnis, T., Imitola, J., Ansari, M.J., Akiba, H., Tushima, F., Azuma, M., Yagita, H., Sayegh, M.H. & Khoury, S.J. (2003) *Critical role of the programmed death-1 (PD-1) pathway in regulation of experimental autoimmune encephalomyelitis*. J Exp Med, **198**:71–8

[260] Carter, L.L., Leach, M.W., Azoitei, M.L., Cui, J., Pelker, J.W., Jussif, J., Benoit, S., Ireland, G., Luxenberg, D., Askew, G.R., Milarski, K.L., Groves, C., Brown, T., Carito, B.A., Percival, K., Carreno, B.M., Collins, M. & Marusic, S. (2007) *PD-1/PD-L1, but not PD-1/PD-L2, interactions regulate the severity of experimental autoimmune encephalomyelitis*. J Neuroimmunol, **182**:124–34

[261] Okazaki, T. & Honjo, T. (2007) *PD-1 and PD-1 ligands: from discovery to clinical application*. Int Immunol, **19**:813–24

[262] Keir, M.E., Butte, M.J., Freeman, G.J. & Sharpe, A.H. (2008) *PD-1 and its ligands in tolerance and immunity*. Annu Rev Immunol, **26**:677–704

[263] Sandner, S.E., Clarkson, M.R., Salama, A.D., Sanchez-Fueyo, A., Domenig, C., Habicht, A., Najafian, N., Yagita, H., Azuma, M., Turka, L.A. & Sayegh, M.H. (2005) *Role of the programmed death-1 pathway in regulation of alloimmune responses in vivo*. J Immunol, **174**:3408–15

[264] Ozkaynak, E., Wang, L., Goodearl, A., McDonald, K., Qin, S., O'Keefe, T., Duong, T., Smith, T., Gutierrez-Ramos, J.C., Rottman, J.B., Coyle, A.J. & Hancock, W.W. (2002) *Programmed death-1 targeting can promote allograft survival*. J Immunol, **169**:6546–53

[265] Freeman, G.J., Wherry, E.J., Ahmed, R. & Sharpe, A.H. (2006) *Reinvigorating exhausted HIV-specific T cells via PD-1-PD-1 ligand blockade*. J Exp Med, **203**:2223–7

[266] Urbani, S., Amadei, B., Tola, D., Massari, M., Schivazappa, S., Missale, G. & Ferrari, C. (2006) *PD-1 expression in acute hepatitis C virus (HCV) infection is associated with HCV-specific CD8 exhaustion*. J Virol, **80**:11,398–403

[267] Maier, H., Isogawa, M., Freeman, G.J. & Chisari, F.V. (2007) *PD-1:PD-L1 interactions contribute to the functional suppression of virus-specific CD8+ T lymphocytes in the liver*. J Immunol, **178**:2714–20

[268] Shinohara, T., Taniwaki, M., Ishida, Y., Kawaichi, M. & Honjo, T. (1994) *Structure and chromosomal localization of the human PD-1 gene (PDCD1)*. Genomics, **23**:704–6

[269] Zhang, X., Schwartz, J.C., Guo, X., Bhatia, S., Cao, E., Lorenz, M., Cammer, M., Chen, L., Zhang, Z.Y., Edidin, M.A., Nathenson, S.G. & Almo, S.C. (2004) *Structural and functional analysis of the costimulatory receptor programmed death-1*. Immunity, **20**:337–47

[270] Carter, L., Fouser, L.A., Jussif, J., Fitz, L., Deng, B., Wood, C.R., Collins, M., Honjo, T., Freeman, G.J. & Carreno, B.M. (2002) *PD-1:PD-L inhibitory pathway affects both CD4(+) and CD8(+) T cells and is overcome by IL-2*. Eur J Immunol, **32**:634–43

[271] Chemnitz, J.M., Parry, R.V., Nichols, K.E., June, C.H. & Riley, J.L. (2004) *SHP-1 and SHP-2 associate with immunoreceptor tyrosine-based switch motif of programmed death 1 upon primary human T cell stimulation, but only receptor ligation prevents T cell activation*. J Immunol, **173**:945–54

[272] Sheppard, K.A., Fitz, L.J., Lee, J.M., Benander, C., George, J.A., Wooters, J., Qiu, Y., Jussif, J.M., Carter, L.L., Wood, C.R. & Chaudhary, D. (2004) *PD-1 inhibits T-cell receptor induced phosphorylation of the ZAP70/CD3zeta signalosome and downstream signaling to PKCtheta*. FEBS Lett, **574**:37–41

[273] Parry, R.V., Chemnitz, J.M., Frauwirth, K.A., Lanfranco, A.R., Braunstein, I., Kobayashi, S.V., Linsley, P.S., Thompson, C.B. & Riley, J.L. (2005) *CTLA-4 and PD-1 receptors inhibit T-cell activation by distinct mechanisms*. Mol Cell Biol, **25**:9543–53

[274] Sambrook, J Russel, D. (2001). *Molecular cloning: a laboratory manual.*

[275] Demaison, C., Parsley, K., Brouns, G., Scherr, M., Battmer, K., Kinnon, C., Grez, M. & Thrasher, A.J. (2002) *High-level transduction and gene expression in hematopoietic repopulating cells using a human immunodeficiency [correction of imunodeficiency] virus type 1-based lentiviral vector containing an internal spleen focus forming virus promoter*. Hum Gene Ther, **13**:803–13

[276] DuBridge, R.B., Tang, P., Hsia, H.C., Leong, P.M., Miller, J.H. & Calos, M.P. (1987) *Analysis of mutation in human cells by using an Epstein-Barr virus shuttle system*. Mol Cell Biol, **7**:379–87

[277] Haskins, K., Kubo, R., White, J., Pigeon, M., Kappler, J. & Marrack, P. (1983) *The major histocompatibility complex-restricted antigen receptor on T cells. I. Isolation with a monoclonal antibody*. J Exp Med, **157**:1149–69

[278] White, J., Haskins, K.M., Marrack, P. & Kappler, J. (1983) *Use of I region-restricted, antigen-specific T cell hybridomas to produce idiotypically specific anti-receptor antibodies*. J Immunol, **130**:1033–7

[279] Marrack, P., Shimonkevitz, R., Hannum, C., Haskins, K. & Kappler, J. (1983) *The major histocompatibility complex-restricted antigen receptor on T cells. IV. An antiidiotypic antibody predicts both antigen and I-specificity*. J Exp Med, **158**:1635–46

[280] James, J.R., Oliveira, M.I., Carmo, A.M., Iaboni, A. & Davis, S.J. (2006) *A rigorous experimental framework for detecting protein oligomerization using bioluminescence resonance energy transfer*. Nat Methods, **3**:1001–6

[281] Karlsson, R., Michaelsson, A. & Mattsson, L. (1991) *Kinetic analysis of monoclonal antibody-antigen interactions with a new biosensor based analytical system*. J Immunol Methods, **145**:229–40

[282] Shental-Bechor, D. & Levy, Y. (2008) *Effect of glycosylation on protein folding: a close look at thermodynamic stabilization*. Proc Natl Acad Sci U S A, **105**:8256–61

[283] Chang, V.T., Crispin, M., Aricescu, A.R., Harvey, D.J., Nettleship, J.E., Fennelly, J.A., Yu, C., Boles, K.S., Evans, E.J., Stuart, D.I., Dwek, R.A., Jones, E.Y., Owens, R.J. & Davis, S.J. (2007) *Glycoprotein structural genomics: solving the glycosylation problem*. Structure, **15**:267–73

[284] Maley, F., Trimble, R.B., Tarentino, A.L. & Plummer, T. H., J. (1989) *Characterization of glycoproteins and their associated oligosaccharides through the use of endoglycosidases*. Anal Biochem, **180**:195–204

[285] Hunig, T. & Dennehy, K. (2005) *CD28 superagonists: mode of action and therapeutic potential*. Immunol Lett, **100**:21–8

[286] Acuto, O. & Michel, F. (2003) *CD28-mediated co-stimulation: a quantitative support for TCR signalling*. Nat Rev Immunol, **3**:939–51

[287] Riley, J.L. & June, C.H. (2005) *The CD28 family: a T-cell rheostat for therapeutic control of T-cell activation*. Blood, **105**:13–21

[288] Tomonari, K. (1988) *A rat antibody against a structure functionally related to the mouse T-cell receptor/T3 complex*. Immunogenetics, **28**:455–8

[289] Alegre, M.L., Noel, P.J., Eisfelder, B.J., Chuang, E., Clark, M.R., Reiner, S.L. & Thompson, C.B. (1996) *Regulation of surface and intracellular expression of CTLA4 on mouse T cells*. J Immunol, **157**:4762–70

[290] Hanke, T. (2006) *Lessons from TGN1412*. Lancet, **368**:1569–70; author reply 1570

[291] Lazar-Molnar, E., Almo, S.C. & Nathenson, S.G. (2006) *The interchain disulfide linkage is not a prerequisite but enhances CD28 costimulatory function*. Cell Immunol, **244**:125–9

[292] Angel, P. & Karin, M. (1991) *The role of Jun, Fos and the AP-1 complex in cell-proliferation and transformation*. Biochim Biophys Acta, **1072**:129–57

[293] Bohmann, D., Bos, T.J., Admon, A., Nishimura, T., Vogt, P.K. & Tjian, R. (1987) *Human proto-oncogene c-jun encodes a DNA binding protein with structural and functional properties of transcription factor AP-1*. Science, **238**:1386–92

[294] Landschulz, W.H., Johnson, P.F. & McKnight, S.L. (1988) *The leucine zipper: a hypothetical structure common to a new class of DNA binding proteins*. Science, **240**:1759–64

[295] Ashwell, J.D. & Klusner, R.D. (1990) *Genetic and mutational analysis of the T-cell antigen receptor*. Annu Rev Immunol, **8**:139–67

[296] Reth, M. (1989) *Antigen receptor tail clue*. Nature, **338**:383–4

[297] Irving, B.A. & Weiss, A. (1991) *The cytoplasmic domain of the T cell receptor zeta chain is sufficient to couple to receptor-associated signal transduction pathways*. Cell, **64**:891–901

[298] Rutledge, T., Cosson, P., Manolios, N., Bonifacino, J.S. & Klausner, R.D. (1992) *Transmembrane helical interactions: zeta chain dimerization and functional association with the T cell antigen receptor*. EMBO J, **11**:3245–54

[299] Call, M.E., Schnell, J.R., Xu, C., Lutz, R.A., Chou, J.J. & Wucherpfennig, K.W. (2006) *The structure of the zetazeta transmembrane dimer reveals features essential for its assembly with the T cell receptor*. Cell, **127**:355–68

[300] Minguet, S., Swamy, M. & Schamel, W.W. (2008) *The short length of the extracellular domain of zeta is crucial for T cell antigen receptor function*. Immunol Lett, **116**:195–202

[301] Muller, N., van den Brandt, J., Odoardi, F., Tischner, D., Herath, J., Flugel, A. & Reichardt, H.M. (2008) *A CD28 superagonistic antibody elicits 2 functionally distinct waves of T cell activation in rats*. J Clin Invest, **118**:1405–16

[302] Gogishvili, T., Langenhorst, D., Luhder, F., Elias, F., Elflein, K., Dennehy, K.M., Gold, R. & Hunig, T. (2009) *Rapid regulatory T-cell response prevents cytokine storm in CD28 superagonist treated mice*. PLoS ONE, **4**:e4643

[303] Margulies, D.H. (2003) *CD28, costimulator or agonist receptor?* J Exp Med, **197**:949–53

[304] Greene, J.L., Leytze, G.M., Emswiler, J., Peach, R., Bajorath, J., Cosand, W. & Linsley, P.S. (1996) *Covalent dimerization of CD28/CTLA-4 and oligomerization of CD80/CD86 regulate T cell costimulatory interactions*. J Biol Chem, **271**:26,762–71

[305] Brodie, D., Collins, A.V., Iaboni, A., Fennelly, J.A., Sparks, L.M., Xu, X.N., van der Merwe, P.A. & Davis, S.J. (2000) *LICOS, a primordial costimulatory ligand?* Curr Biol, **10**:333–6

[306] Frangione, B., Milstein, C. & Franklin, E.C. (1968) *Intrachain disulphide bridges in immunoglobulin G heavy chains. The Fc fragment*. Biochem J, **106**:15–21

[307] Krapp, S., Mimura, Y., Jefferis, R., Huber, R. & Sondermann, P. (2003) *Structural analysis of human IgG-Fc glycoforms reveals a correlation between glycosylation and structural integrity*. J Mol Biol, **325**:979–89

[308] Jefferis, R., Reimer, C.B., Skvaril, F., de Lange, G., Ling, N.R., Lowe, J., Walker, M.R., Phillips, D.J., Aloisio, C.H., Wells, T.W. & et al. (1985) *Evaluation of monoclonal antibodies having specificity for human IgG sub-classes: results of an IUIS/WHO collaborative study*. Immunol Lett, **10**:223–52

[309] Phillips, D.J., Wells, T.W. & Reimer, C.B. (1987) *Estimation of association constants of 42 monoclonal antibodies to human IgG epitopes using a fluorescent sequential-saturation assay*. Immunology Letters, **17**:159–168

[310] Hamilton, R.G. & Morrison, S.L. (1993) *Epitope mapping of human immunoglobulin-specific murine monoclonal antibodies with domain-switched, deleted and point-mutated chimeric antibodies*. J Immunol Methods, **158**:107–22

[311] Feinstein, A. & Beale, D. (1981) *Structure and Function of Antibodies (Chapter 8)*. Wiley, Chichester

[312] Janeway, C.J., Travers, P., Walport, M. & Shlomchik, Mark, J. (2001). *Immunobiology: the immune system in health and disease*

[313] Guddat, L.W., Herron, J.N. & Edmundson, A.B. (1993) *Three-dimensional structure of a human immunoglobulin with a hinge deletion*. Proc Natl Acad Sci U S A, **90**:4271–5

[314] Dorrington, K.J. (1978) *The structural basis for the functional versatility of immunoglobulin G1*. Can J Biochem, **56**:1087–101

[315] Aruffo, A. & Seed, B. (1987) *Molecular cloning of a CD28 cDNA by a high-efficiency COS cell expression system*. Proc Natl Acad Sci U S A, **84**:8573–7

[316] Clark, G.J. & Dallman, M.J. (1992) *Identification of a cDNA encoding the rat CD28 homologue*. Immunogenetics, **35**:54–7

[317] Gross, J.A., St John, T. & Allison, J.P. (1990) *The murine homologue of the T lymphocyte antigen CD28. Molecular cloning and cell surface expression*. J Immunol, **144**:3201–10

[318] Parsons, K.R., Young, J.R., Collins, B.A. & Howard, C.J. (1996) *Cattle CTLA-4, CD28 and chicken CD28 bind CD86: MYPPPY is not conserved in cattle CD28*. Immunogenetics, **43**:388–91

[319] Petrovas, C., Price, D.A., Mattapallil, J., Ambrozak, D.R., Geldmacher, C., Cecchinato, V., Vaccari, M., Tryniszewska, E., Gostick, E., Roederer, M., Douek, D.C., Morgan, S.H., Davis, S.J., Franchini, G. & Koup, R.A. (2007) *SIV-specific CD8+ T cells express high levels of PD1 and cytokines but have impaired proliferative capacity in acute and chronic SIVmac251 infection*. Blood, **110**:928–36

[320] Riley, J.L. (2009) *PD-1 signaling in primary T cells*. Immunol Rev, **229**:114–25

[321] Okazaki, T., Maeda, A., Nishimura, H., Kurosaki, T. & Honjo, T. (2001) *PD-1 immunoreceptor inhibits B cell receptor-mediated signaling by recruiting src homology 2-domain-containing tyrosine phosphatase 2 to phosphotyrosine*. Proc Natl Acad Sci U S A, **98**:13,866–71

[322] Berger, R., Rotem-Yehudar, R., Slama, G., Landes, S., Kneller, A., Leiba, M., Koren-Michowitz, M., Shimoni, A. & Nagler, A. (2008) *Phase I safety and pharmacokinetic study of CT-011, a humanized antibody interacting with PD-1, in patients with advanced hematologic malignancies*. Clin Cancer Res, **14**:3044–51

[323] Brahmer, J.R., Topalian, S.L., Powderly, J., Wollner, I., Picus, J., Drake, C.G., Stankevich, E., Korman, A., Pardoll, D. & Lowy, I. (2009) *Phase II experience with MDX-1106 (Ono-4538), an anti-PD-1 monoclonal antibody, in patients with selected refractory or relapsed malignancies*. J Clin Oncol (Meeting Abstracts), **27**:3018–

[324] Brahmer, J.R., Topalian, S., Wollner, I., Powderly, J.D., Picus, J., Drake, C., Covino, J., Korman, A., Pardoll, D. & Lowy, I. (2008) *Safety and activity of MDX-1106 (ONO-4538), an anti-PD-1 monoclonal antibody, in patients with selected refractory or relapsed malignancies*. J Clin Oncol (Meeting Abstracts), **26**:3006–

[325] Weber, J. (2007) *Review: anti-CTLA-4 antibody ipilimumab: case studies of clinical response and immune-related adverse events*. Oncologist, **12**:864–72

[326] Di Giacomo, A.M., Danielli, R., Guidoboni, M., Calabro, L., Carlucci, D., Miracco, C., Volterrani, L., Mazzei, M.A., Biagioli, M., Altomonte, M. & Maio,

M. (2009) *Therapeutic efficacy of ipilimumab, an anti-CTLA-4 monoclonal antibody, in patients with metastatic melanoma unresponsive to prior systemic treatments: clinical and immunological evidence from three patient cases*. Cancer Immunol Immunother, **58**:1297–306

[327] Peggs, K.S., Quezada, S.A., Chambers, C.A., Korman, A.J. & Allison, J.P. (2009) *Blockade of CTLA-4 on both effector and regulatory T cell compartments contributes to the antitumor activity of anti-CTLA-4 antibodies*. J Exp Med, **206**:1717–25

[328] Shields, R.L., Namenuk, A.K., Hong, K., Meng, Y.G., Rae, J., Briggs, J., Xie, D., Lai, J., Stadlen, A., Li, B., Fox, J.A. & Presta, L.G. (2001) *High resolution mapping of the binding site on human IgG1 for Fc gamma RI, Fc gamma RII, Fc gamma RIII, and FcRn and design of IgG1 variants with improved binding to the Fc gamma R*. J Biol Chem, **276**:6591–604

[329] Presta, L.G. (2008) *Molecular engineering and design of therapeutic antibodies*. Curr Opin Immunol, **20**:460–70

[330] Rodriguez-Palmero, M., Hara, T., Thumbs, A. & Hunig, T. (1999) *Triggering of T cell proliferation through CD28 induces GATA-3 and promotes T helper type 2 differentiation in vitro and in vivo*. Eur J Immunol, **29**:3914–24

[331] Beyersdorf, N., Hanke, T., Kerkau, T. & Hunig, T. (2006) *CD28 superagonists put a break on autoimmunity by preferentially activating CD4+CD25+ regulatory T cells*. Autoimmun Rev, **5**:40–5

[332] Beelar, V.P., Zimmerman, H.J. & Manchester, B. (1949) *Prozone phenomenon in the serodiagnosis of syphilis; a clinical study*. Am J Med Sci, **217**:658–65